SUBSONIC WIND-TUNNEL WALL CORRECTIONS ON A WING WITH A CLARK Y-14 AIRFOIL

A Masters Project

Presented to

The Faculty of the Department of

Mechanical and Aerospace Engineering

San Jose State University

In Partial Fulfillment

Of the Requirements for a Degree

Master of Science

In

Aerospace Engineering

By

Tommy James Blackwell

May 2011

The Designated Masters Project Committee Approves the Masters Project Titled

SUBSONIC WIND-TUNNEL WALL CORRECTIONS ON A WING WITH A CLARK Y-14 AIRFOIL

by

Tommy J. Blackwell

APPROVED FOR THE DEPARTMENT OF AEROSPACE ENGINEERING

SAN JOSÉ STATE UNIVERSITY

May 2011

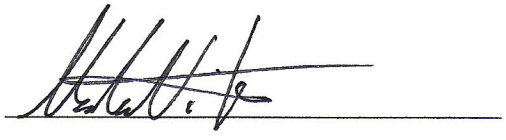

Dr. Nikos Mourtos — Department of Aerospace Engineering

Dr. Periklis Papadopoulos — Department of Aerospace Engineering

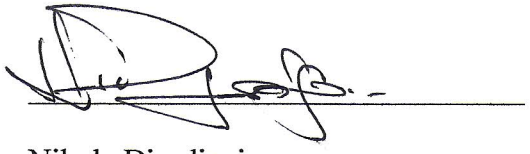

Nikola Djordjevic — Lockheed Martin Space Systems Company Aero / Fluids / Performance Manager

ABSTRACT

As our civilization relies more heavily on aircrafts and rockets, the use of wind-tunnels has increasing been integrated as an important aeronautical tool in their design. Even though wind-tunnels are great scientific tools, they do have their flaws. Based on the specific wind-tunnel design, one of the main negatives is that wind-tunnels cannot simulate free-flight conditions without having to correct the data for wall effects and other flow phenomena.

Both two and three-dimensional flows need to have corrections applied that are unique to that wind-tunnels design. For two dimensional flows, corrections that can be obtain are for the $\Delta\alpha,\ \Delta c_l,\ and\ \Delta c_{m_{\frac{1}{4}}}$ with direct corrections available for V, q, Re, $\alpha,\ c_l,\ and\ c_{m_{\frac{1}{4}}}$. The corrections are developed from the buoyancy, solid and wake blockages, and streamline curvature corrections. For tree-dimensional flows, corrections can be obtain are $\Delta\alpha,\ \Delta c_l,\ \Delta c_{m_{\frac{1}{4}}}$, $\Delta\alpha_i\ and\ \Delta C_{Di}$. These corrections depend on the methods applied to the two-dimensional cases along with the method of images.

The experiments contained in this project are utilizing an AEROLAB wind-tunnel along with a ClarkY-14 airfoil and wing. The wind-tunnel was set up to have inlet velocities of 6, 30, 68 and 102 mph and outlet atmospheric environmental conditions. The data collected with the correction factors applied was then compared with free-flight CFD models to compare corrections effectiveness

ACKNOWLEDGEMENTS

I would like to take the opportunity to thank Dr. Mourtos and Dr. Papadopoulos for their support throughout this project. Their assistance has been invaluable during the process of finishing this project. I would also like to thank San Jose State University for the use of their wind tunnel facility.

A special thanks goes to my mom, dad and family, who have stood by me with encouragement and moral support. Also to my Aunt Helen and Jim Lyons, who provided editing assistance, I thank you so much for your time and effort.

Finally, I thank Hai Le, Albert Rios and Paul Linggi for being a sounding board and encouragement throughout the project.

Table of Contents

List of Figures

List of Variables

Abbreviation	Description
c	Chord
h	Test Section Height
S	Planform Area
ΔD_B	Change in Drag due to Buoyancy
Λ	Body Shape Factor
t	Body Thickness
LE	Leading Edge
TE	Trailing Edge
ω	Induced velocity
α_{eff}	Effective Angle of Attack
α_i	Induced Angle of Attack
$\Delta\alpha_i$	Change in Induced Angle of Attack
α	Angle of Attack
α_c	Corrected Angle of Attack
α_u	Uncorrected Angle of Attack
c_d	Coefficient of Drag for an Airfoil
c_{du}	Uncorrected Coefficient of Drag for an Airfoil
c_{dc}	Corrected Coefficient of Drag for an Airfoil
c_{d0}	Coefficient of Drag at 0 Lift Condition
C_D	Coefficient of Drag for a Wing
C_{Du}	Uncorrected Coefficient of Drag for a Wing

C_{Dc}	Corrected Coefficient of Drag for a Wing
C_{Di}	Coefficient of Induced Drag
ΔC_{Di}	Change in the Coefficient of Induced Drag
C_l	Coefficient of Lift for an Airfoil
C_{lu}	Uncorrected Coefficient of Lift for an Airfoil
C_{lc}	Corrected Coefficient of Lift for an Airfoil
C_L	Coefficient of Lift for a Wing
C_{Lu}	Uncorrected Coefficient of Lift for a Wing
C_{Lc}	Corrected Coefficient of Lift for a Wing
Re	Reynolds Number
Re_u	Uncorrected Reynolds Number
Re_c	Corrected Reynolds Number
Re_{cr}	Critical Reynolds Number
C_m	Moment Coefficient for an Airfoil
C_{mu}	Uncorrected Moment Coefficient for an Airfoil
C_{mc}	Corrected Moment Coefficient for an Airfoil
$C_{m_{\frac{1}{4}c}}$	Corrected Moment Coefficient for an Airfoil at $\frac{1}{4}$ Chord
$C_{m_{\frac{1}{4}u}}$	Uncorrected Moment Coefficient for an Airfoil at $\frac{1}{4}$ Chord
C_M	Moment Coefficient for a Wing
C_{Mu}	Uncorrected Moment Coefficient for a Wing
C_{Mc}	Corrected Moment Coefficient for a Wing
N	Normal Force
A	Axial Force

C_N	Normal Force Coefficient
C_p	Pressure Coefficient
C_{pu}	Uncorrected Pressure Coefficient
C_{pc}	Corrected Pressure Coefficient
q_∞	Dynamic Pressure
q_u	Uncorrected Dynamic Pressure
q_c	Corrected Dynamic Pressure
P_t	Total Pressure
P	Pressure
P_s	Static Pressure
P_∞	Freestream Pressure
Γ	Vortex Strength
M	Pitching Moment
M_u	Pitching Moment on Upper Surface
M_l	Pitching Moment on Lower Surface
ρ_∞	Density
V	Velocity
V_∞	Freestream Velocity
V_u	Uncorrected Velocity
V_c	Corrected Velocity
B	Tunnel Width
b	Wing Span
r	Vortex Spacing

$\Delta\omega$	Change in Induced Velocity
a	Cylinder Radius
u	Local Velocity
C	Test Section Cross-sectional Area
δ	Boundary Layer Thickness
δ^*	Boundary Layer Displacement
δ^*_{TBL}	Turbulent Boundary Layer Displacement
δ^*_{LBL}	Laminar Boundary Layer Displacement
$\frac{dp}{dl}$	Static Pressure Curve Slope
$\frac{dl}{dx}$	Wing Lift Curve Slope
S_x	Airfoil Cross-Sectional Area
l	Length of Leading Edge
λ_2	Body Shape for 2D Bodies
λ_3	Body Shape for 3D Bodies
μ	Doublet Strength
l_{tc}	Length of Test Section
$\frac{l}{t}$	Fineness Ratio
P_0	Initial Pressure
x_{cr}	Distance where the flow transitions
c_{model}	Model Chord
v_{model}	Model Volume
ϵ_{sb}	Solid Blockage
ϵ_{wb}	Wake Blockage

ϵ_{total}	Total Blockage
Q	Mass Flow Rate
h_s	Spacing between sources
Y_w	Wake Width
ω_v	Induced Velocity in the Vertical Direction

Chapter 1: Introduction

1.1 Background

1.1.1 Development of Wind-Tunnels

The first attempt to simulate steady, controllable air flow used mountain slopes and valley's where the wind was usually steady with minimal trees and other turbulence landscape features. These early attempts were met with limited success and depended on weather conditions which at the time, were hard to predict hour to hour much less a few days out from a test date. In the early 1700's, Benjamin Robins' whirling arm device (Figure 1.1) produced air velocities of only a few feet per second for testing models and was the only device at the time that could achieve those marginal from what could be found naturally.

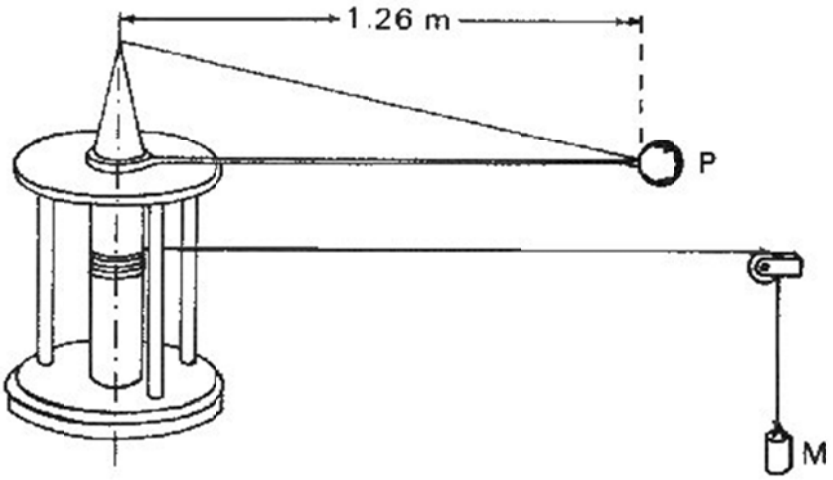

Figure 1.1 - Benjamin Robins' Whirling Arm where a mass was dropped which rotated the arm. (NASA, 2005)

The whirling arm device did not produce a reliable flow of air for testing and caused turbulence from the model going through its own wake. (NASA,2005) During the mid-1700's, Sir George

Cayley used a whirling arm that could produce velocities of 10 to 20 feet per second but was not modified in any way to correct for the model going through its own wake. (Theodorsen, 1933) Over the years since Robins' first whirling arm, they had gotten bigger and able to produce faster velocities to the point that researchers were able to obtain tip velocities in excess of 100 mph. Since the times of Leonardo da Vinci and Sir Isaac Newton as well as Benjamin Robins and Sir George Cayley, engineers realized that there was a need for a device to create and maintain a steady, controllable flow of air. It wasn't till the 1870's that the Aeronautical Society of Great Britain began development of the first enclosed wind tunnel that could maintain a steady, controlled air flow. The society invented, designed and operated with the help of Francis Herbert Wenham, who is credited with many aeronautical fundamental discoveries including the measurement of lift-to-drag ratios and the importance of a high aspect ratio. (NASA,2005) Along with other experiments that were completed using the new technology, Osborne Reynolds demonstrated that the airflow pattern over a scale model would be the same as for a full-scale model if certain parameters were the same with the scaled and full–scale model. The flow parameter became known as the Reynolds Number which is a description for all fluid-flow situations, including the shapes of flow pattern, the ease of heat transfer and the onset of turbulence. However there are limitations on the conditions in which dynamic similarity are based upon the Reynolds Number alone. (Theodorsen, 1933) With the advent of the Reynolds Number, the wind-tunnel became a more powerful research tool which allowed the Wright brothers to test their variously designed airfoils which revolutionized manned flight. Since the Wright brothers, the use of wind-tunnels has exploded and the science of aerodynamics was born.

Wind-tunnels are often limited to the volume and the speed of airflow which could be delivered by the flow environment and power plant respectively. The wind-tunnels used by the Germans during WWII are an interesting example of the difficulties associated with extending the useful range of large wind-tunnels. To overcome the limit in volume that kept large wind-tunnels from operating effectively, the Germans used caves which were excavated to be even larger to store air which could be diverted to their wind-tunnels when needed. The caves allowed for an increase in air volume which in turn allowed the research labs to explore the high-speed regimes and greatly accelerated the number of aircraft advances that German held over the Allies. By the end of the war, Germany had three different supersonic wind-tunnels that were able to sustain velocities of Mach 4.4. (NASA, 2005) Since the time of the war, metal vessels which can hold very high pressure and handle higher volumes of air where developed and are used as a substitute to the German design. Later research focused on more powerful power plants, turbine blade design, tunnel shape and test section design. Wind-tunnels and other types of tunnels were the best aerodynamic research tool until computer power increased enough for the development of CFD (Computational Fluid Dynamics) programs to take over for the expensively run wind-tunnels. Even with CFD solvers being used, wind-tunnels still have their place in research today.

1.1.2 Wind-Tunnel Design

The design of wind-tunnels can be open-circuit or closed-circuit. Open-circuit tunnels (Figure 1.2) can also be “suckdown” or “blower” tunnels. A “Suckdown” tunnel is open to the atmosphere (open-circuit) and has the axial fan or centrifugal blower downstream of the test section which sucks the fluid through the test section. A “Blower” tunnel is also open to the

atmosphere but has the axial fan or centrifugal blower upstream of the test station and blows the fluid through the test station. Open-circuit tunnels have the advantage of being less expensive to build but come at the cost of requiring more power to operate and the model can only be subjected to ambient conditions.

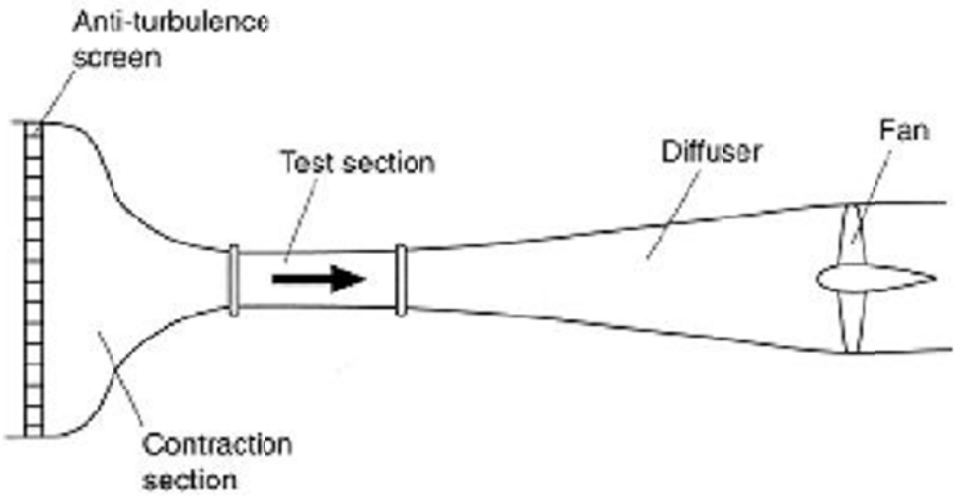

Figure 1.2 - Example of open-circuit wind-tunnel (Kasravi, 2010)

Closed-circuit tunnels (Figure 1.3) are closed to the outside atmosphere with an axial fan or multi-stage axial compressor (supersonic tunnels) to create the fluid stream. Two advantages over the open-circuit tunnels are that the atmospheric conditions in the tunnel can be controlled and this type of tunnel avoids the loss of returning air's momentum. Closed-circuit tunnels also have more uniform flow through the test section than open-circuit tunnels but great attention needs to be concentrated on the design of the entrance to the test section to maintain uniform flow. The control over the conditions and flow in the tunnel comes with the cost of being very expensive to build. (Pankhurst, 1952)

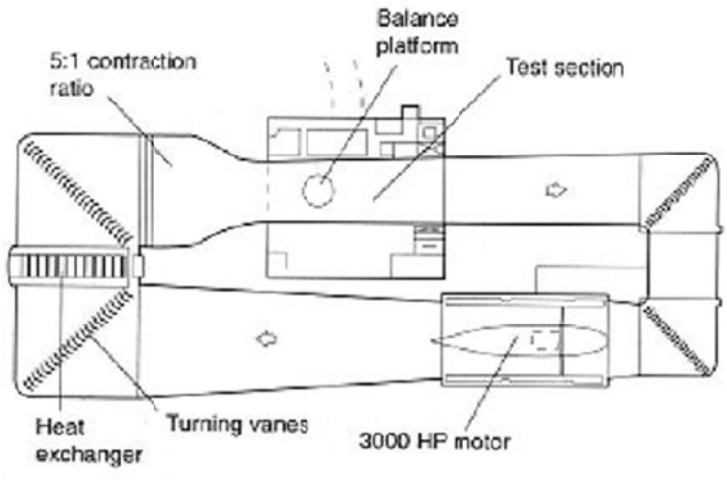

Figure 1.3 - Example of closed-circuit wind-tunnel (Kasravi, 2010)

The fluid flow created by the fans blowing into the test section is highly turbulent due to the motion of the blades on the fan. The turbulence can be dissipated by adding closely-spaced vertical and horizontal vanes which smooth out the fluid before it enters the test section. "Suckdown" tunnels do not have this issue since the fan is positioned behind the test section and downstream of the fluid flow. In closed-circuit tunnels, the fan or turbine is located on the opposite side of the tunnel from the test section which allows the fluid flow to encounter several vane sets to straighten the fluid flow before it reaches the test section. The vane set allow for the flow to be "sucked" or "blown" down the tunnel with the fluid flow entering the test section in a laminar state. The tunnel itself is usually circular due to the effects of viscosity of a fluid flow through a square cross section. The fluid flow through a square cross section will have flow constriction in the corners of the square tunnel which will cause turbulent flow. The inside face of the tunnel walls are made as smooth as possible to reduce surface drag and turbulence.

1.1.3 Wall Effects

The test section of most wind tunnels is rectangular while the tunnel itself is circular which causes its own design issues. The inlet must keep the flow laminar during the transition from circular to rectangular. Since there will always be some turbulence entering the test section, this must be accounted for when analyzing the model data. The model in the test section is usually kept in the center of the test section to reduce interaction with the test section wall boundary layer but this cannot always be obtained due to test section design or placement of the model itself. (Figure 1.4a and b) The test section and model create a host of other issues that will need to be corrected and factored out in order for the model data to be accurate and useful.

Figure 1.4a - Example of model maintained on the centerline of test section. (NASA, 2005)

Figure 1.4b - Example of model mounted on test section wall. (NASA, 2005)

In the book, "Low-Speed Wind Tunnel Testing", the author produces a list of issues produced by the existence of the walls in the test section. The issues one needs to consider are listed below; (Pope, 1984)

- In a closed test section, a lateral constraint to the flow pattern about a body is known as "solid blockage" and causes an increase of dynamic pressure, increasing all forces and moments at a given angle of attack. In an open test section, the effect of "solid blockage" is usually negligible since the flow is allowed to expand in a normal matter.
- In closed test sections, a lateral constraint to the flow pattern about the wake is known as "wake blockage." The "wake blockage" effect increases the wake size which in turn increases the drag on the model. In an open test section, the effect of "wake blockage" is usually negligible since the flow is allowed to expand in a normal matter.
- In closed test section, the angle of attack near the wingtips of a model with a large span is increased excessively, making the tip stall start early. The effect of an open jet is opposite

where the tips are unstalled. In both cases the effect is diminished to the point of negligibility by keeping model span less than .8 of the tunnel width

- An alteration to the normal curvature of the flow about a wing so that the wing moment coefficient, wing lift and angle of attack are increased in a closed wind tunnel and is decreased with an open jet.
- The normal downwash is altered so that the measured lift and drag are in error. The closed jet makes the lift too large and the drag too small at a given geometric angle of attack. An open jet has just the opposite effect.

The normal downwash is altered so that behind the wing is the measured tail setting and static stability are in error In a closed jet, the model has too much stability and an excessively high wake location. In an open jet, the stability effect is large.

- The normal flow pattern is altered so that the hinge moments are too large in a closed test section and too small in an open test section.
- The normal flow is altered about an asymmetrically loaded wing such that the boundary effects become asymmetric and the observed rolling and yawing moments are in error.
- The flow is altered by a thrusting propeller such that a given thrust occurs at a speed lower than it would be in free-flowing air when in a closed test section. With the propeller braking, the effect is opposite. Wake effects such as these are negligible when a free jet is employed.

In most instances, corrections for all the above will not be used at once. With these corrections listed above, extraneous corrections are needed due to wind tunnel design which includes angularity of flow, local variations in velocity, tare, and interference.

1.1.4 Wall Effect Corrections

Wall effects that need to be corrected depend on the model that is placed in the tunnel. With an airfoil spanning the test section, wall to wall, 2D wall effect corrections will be utilized. Other shapes that are not considered 2D will employ 3D wall effect corrections.

A. The Method of Images

The method of images approach allows for the flow pattern about the wing to be closely simulated mathematically by replacing the wing with a system of vortices composed of a lifting line vortex and a pair of trailing vortices. (Theodorsen, 1933) Similarly, a solid body may be represented by a source-sink system and a wake by source. The simulation of a course, sink, doublet or vortex behind the boundary to be represented. “Solid boundaries are formed by the addition of an image system which produces a zero streamline matching the solid boundary.

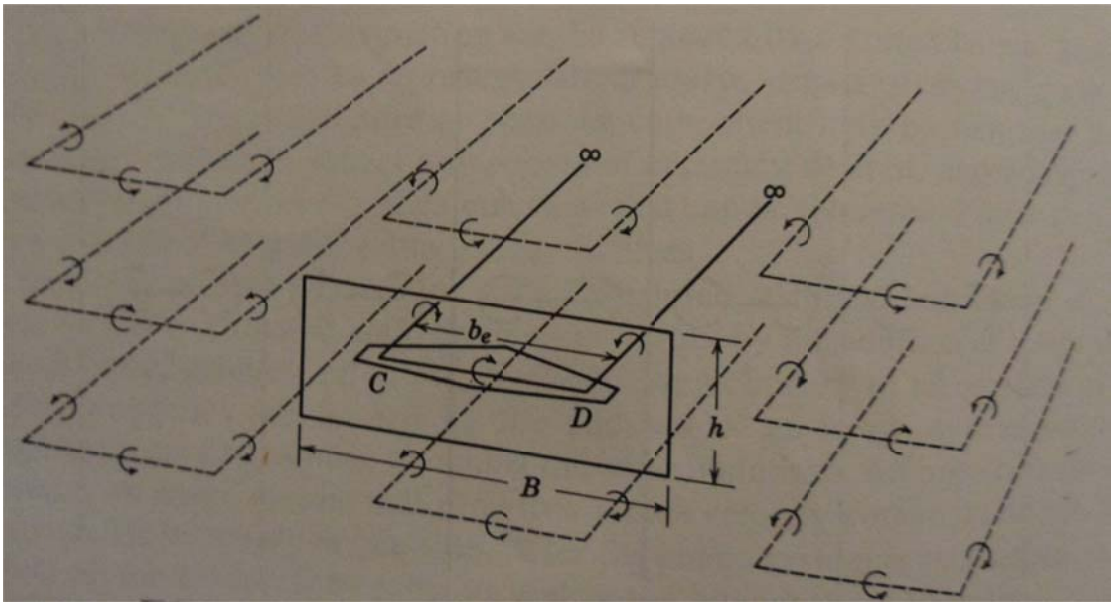

Figure 1.5 - Example of 3D image system utilizing lifting line and a pair of trailing vortices. (Pope, 1984)

An open boundary requires an image system that produces a zero velocity potential line which matches the boundary. (Pope, 1984) After the image system is established, a closed rectangular test section becomes a doubly infinite system of vortices. This method can be used to determine the corrected values for the induced drag coefficient, induced angle of attack and the induced velocities. In the book written by Gustafson, he discusses the need, in both the inviscid and viscous flow, that the normal boundary condition for the solid walls to set the system of images correctly. This will ensure you have an accurate solution when calculating the correction factors. (Gustafson and Sethian, 1991)

B. Buoyancy Correction

Like the other correction factors needed to analyze the data returned from wind tunnel testing, the buoyancy correction is need for all parts of an aircraft, especially the fuselage. While the fuselage experiences significantly higher drag due to buoyancy force than a wing or airfoil, the

development of the correction factor for a wing or airfoil is still necessary. As the flow passes an immersed body in a wind tunnel test section, the flow would like to expand beyond the walls of the test section. In order to conserve mass, the flow therefore must accelerate. This interaction between the test section walls and the flow near the test section is referred to as horizontal buoyancy, and is defined (Hahn, 2004) as

$$\Delta D_B = -\frac{6h^2}{\pi}\Lambda\sigma\frac{dp}{dx} \tag{1.1}$$

where

$$\sigma = \frac{\pi^2}{48}\left(\frac{c}{h}\right)^2 \tag{1.2}$$

Values of Λ can be found in figure 1.6. The derivative of pressure with respect to x was provided as some pressure. The horizontal buoyancy must be subtracted from the drag of the model before analysis can commence. Some wind tunnels have slightly expanding walls to mitigate the buoyancy force that is projected onto the body in the flow field. (Pope, 1984)

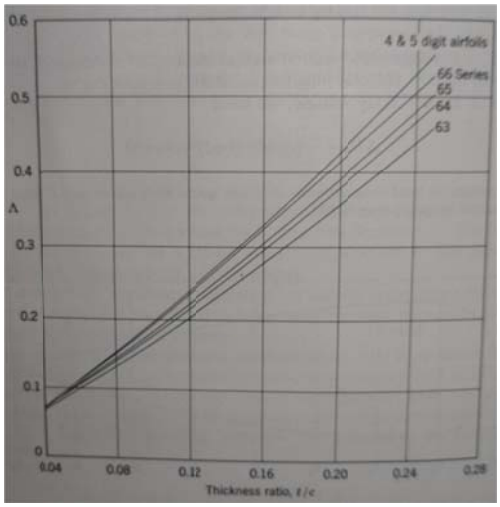

Figure 1.6 - Shape factor to determine Λ (Pope, 1984)

C. Wake Blockage Corrections

Any real body without suction-type boundary layer control will have a wake behind it and this wake will have a mean velocity lower than the free stream. The velocity outside the wake in a closed tunnel must be higher than free stream in order that a constant volume of fluid may pass through the test section. Maskell's theory of wake blockage in closed tunnels was originally intended for use with aircraft models. The theory applies to large blockages arising in the testing of bluff models, particularly those mounted on the floor. "Maskell has derived expressions for the correction of force and pressure coefficients measured in a closed wind tunnel on bluff models subject to separated flow. For symmetrical models, normal to the wind direction, the relationships given" (Gould, 1970) are shown in equation 1.2.

$$\frac{C_D}{C_{D_c}} = \frac{q_c}{q} = \frac{1-C_p}{1-C_{p_c}} = 1 + nC_D\frac{S}{C} \tag{1.3}$$

These relationships are the key to developing the corrected values for wake blockage and can be verified through experimental methods using a flat plate.

D. Solid Blockage Corrections

The presence of a model in the test section reduces the area through which the air can flow and by continuity and Bernoulli's equation increases the velocity of the air as it flows over the model. This increase of velocity is called solid blockage. "Its effect is a function of model thickness, thickness distribution, model size and is independent of the camber." (Herriot, 1950) To determine the blockage correction for a symmetrical body at zero attack, it is only necessary to consider only the basic profile of the airfoil. The wing can be represented by a series of finite

lines of sources and sinks. The lines will thin down at the extreme tip and the planform will not be exactly rectangular. The actual wing is represented quite well by this method and enables a calculation to be made of the induced velocity along the tunnel axis by images of the wing. The velocity induced by the images which represents the effect of the tunnel walls on the velocity at the model is known as the solid-blockage correction.

Chapter 2: Clark Y-14 Airfoil and Wing

2.1 Development of Airfoils and Wings

The earliest serious work on the development of airfoil sections began in the late 1800's. Although it was known that flat plates would produce lift when set at an angle of incidence, some suspected that shapes with curvature, which more closely resembled bird wings would produce more lift or do so more efficiently. H.F. Phillips patented a series of airfoil shapes in 1884 after testing them in one of the earliest wind tunnels in which "artificial currents of air (were) produced from induction by a steam jet in a wooden trunk or conduit." (Theodorsen, 1933) Octave Chanute writes in 1893, "...it seems very desirable that further scientific experiments be made on concavo-convex surfaces of varying shapes, for it is not impossible that the difference between success and failure of a proposed flying machine will depend upon the sustaining effect between a plane surface and one properly curved to get a maximum of 'lift'." (Theodorsen, 1933)

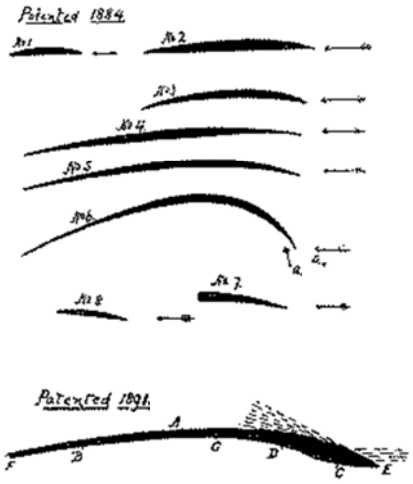

Figure 2.1 - Early patented airfoil shapes by H.F. Phillips (CTIE, 2004)

At nearly the same time, Otto Lilienthal had similar ideas. (Lilienthal, 2000) Lilienthal had a clear interest in the physical basis of flight: He wanted to fly. He realized quickly and correctly that the knowledge of his time was absolutely insufficient for his aim. So he put his main aim aside for decades in order to concentrate on an extensive aerodynamic measurement program. After more than 20 years of experiments in physics without a single practical attempt to fly, Lilienthal summarized his knowledge in the book "Bird flight as the basis of aviation" in 1889. Lilienthal describes the technique of flight as a stomping ground for amateurs, "emotion-mechanics" and only a few specialists (Lilienthal, 2000). His book is for all of them. It is a popular book about physics which guides in a clear line of thought to from Lilienthal' achieved newest state of research. The book is still a standard for the research of bird flight today. Lilienthal combined theoretical and technical skills and skills in craft and athletics in a very special way which enabled him to become the first flying human. He worked out the theoretical stock-in-trade for human flight, constructed a suitable flying apparatus and built it mostly by himself. He had the physical constitution, courage and dexterity in order to test his flying apparatus. He was designer and testing pilot in one person. So it was easier for him to improve his construction during the testing period. The diversity of Lilienthal`s skills, the broadness of his interests and his interdisciplinary approach are certainly essential reasons for his success.

No one equaled him in the power to draw new recruits to the cause; no one equaled him in fullness and desire of understanding of the principles of flight; no one did so much to convince the world of the advantages of curved wing surfaces; and no one did so much to transfer the problem of human flight to the open air where it belonged.

As a missionary, he was wonderful. He presented the cause of human flight to his readers so earnestly, so attractively, and so convincingly that it was difficult for anyone to resist the

temptation to make an attempt at it himself, … he was without question the greatest of the precursors, and the world owes to him a great debt. With these words in 1912, Wilbur Wright described the man who was the most important influence on practical flying and flight theory before the Wright brothers: the German engineer, Otto Lilienthal.

Airfoils used by the Wright Brothers closely resembled Lilienthal's sections: thin and highly cambered. (Lilienthal, 2000) This was quite possibly because early tests of airfoil sections were done at an extremely low Reynolds number, where such sections behave much better than thicker ones. The erroneous belief that efficient airfoils had to be thin and highly cambered was one reason that some of the first airplanes were biplanes. The use of such sections gradually diminished over the next decade. A wide range of airfoils were developed, based primarily on trial and error. Some of the more successful sections such as the Clark Y and Gottingen 398 were used as the basis for a family of sections tested by the NACA in the early 1920's. (NASA, 2005)

In 1939, Eastman Jacobs at the NACA in Langley, designed and tested the first laminar flow airfoil sections. These shapes had extremely low drag and the section shown here achieved a lift to drag ratio of about 300. A modern laminar flow section, used on sailplanes, illustrates that the concept is practical for some applications. It was not thought to be practical for many years after Jacobs demonstrated it in the wind tunnel. Even now, the utility of the concept is not wholly accepted and the "Laminar Flow True-Believers Club" meets each year at the homebuilt aircraft fly-in. One of the reasons that modern airfoils look quite different from one another and designers have not settled on the one best airfoil is that the flow conditions and design goals change from one application to the next. On the right are some airfoils designed for low Reynolds numbers. Unusual airfoil design constraints can sometimes arise, leading to some unconventional shapes. The airfoil here was designed for an ultra-light sailplane requiring very

high maximum lift coefficients with small pitching moments at high speed. One possible solution: a variable geometry airfoil with flexible lower surface.

Today, airfoils are continuously re-evaluated in order to meet the growing demand in commercial, military, and scientific applications. Drag can be reduced to save on fuel costs; lift can be increased to enable lower speed flight; profiles can be redesigned to accommodate heat transfer at high speeds. In these applications, airfoils are optimized for performance and economy at specific operating conditions defined by altitude, temperature, and velocity. The main consideration in airfoil design is the relative velocity of the airfoil. For this reason, airfoils for subsonic, transonic, supersonic, and hypersonic flow conditions exhibit strikingly different design philosophies (John. D. Anderson). High speed airfoils may have less camber to reduce skin friction drag and low speed airfoils will tend to have more camber in order to maximize lift. Different airfoils are defined by various parameters such as leading edge (LE), trailing edge (TE), thickness (t), chord (c), and camber, as seen in Figure 2.2.

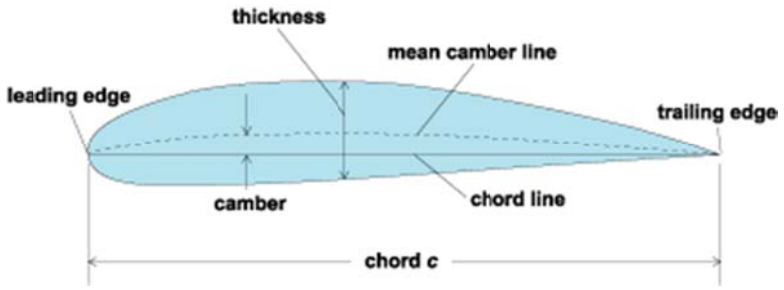

Figure 2.2 - Airfoil Nomenclature (NASA, 2005)

2.2 Development of the Clark Y-14

Clark Y-14 is the name of a particular airfoil profile, widely used in general purpose aircraft designs, and much studied in aerodynamics over the years. The profile was designed in 1922 by Virginius E. Clark. The airfoil has a thickness of 11.7 percent and is flat on

the lower surface from 30 percent of chord back. The flat bottom simplifies angle measurements on propellers, and makes for easy construction of wings on a flat surface. The Clark Y is appealing thanks to its high camber, which produces a very good lift-to-drag ratio.

Figure 2.3 - Clark Y Airfoil

The Lockheed Vega is one example of the Clark Y used in practice. For many applications the Clark Y has been adequate; it gives reasonable overall performance in respect of its lift-to-drag ratio, and has gentle and relatively benign stall characteristics. But the flat lower surface is sub-optimal from an aerodynamic perspective, and it is rarely used in new designs. The Spirit of St. Louis and the Piper Cub use the Clark Y.

2.3 Characterizing the Clark Y-14

The Clark Y-14 was chosen for this project due to the airfoil being a general purpose design that can be used for its superb control at low Reynolds numbers. An additional feature of this wing is that its lower surface is parallel to its chord, enabling the use of an inclinometer to change the angle of attack directly if needed. For this project, the Clark Y-14 airfoil is characterized under low-speed operating conditions. A full airfoil is mounted vertically in the SJSU wind tunnel to obtain 2D flow conditions and pressure distributions over the chord as well as measure the wake. In addition to the 2D characterization, a Clark Y-14 wing is used for 3D characterization. The Wing is mounted to a sting balance, in a horizontal position, to measure the reaction forces directly. The data obtained from both the 2D and 3D experiments will be analyzed in order to

obtain values for the coefficients; C_L, C_D, C_M and C_N. Wind tunnel wall corrections for the SJSU tunnel are combined with the test data to develop corrected data more similar to free space conditions. These results will then be compared with the theoretical and excepted data values for any given angle of attack. The analysis will be building a more rigorous model of the Clark Y-14's behavior under low speed conditions.

2.3.1 Aerodynamic Forces

The aerodynamic forces acting on a body may be described by lift, drag and pitching moment. Lift is the net vertical force and drag is the net horizontal force with respect to the direction of motion. The pitching moment reflects the tendency of the airfoil or wing to pitch about a given reference point. These quantities are derived from the normal force and axial force acting on the airfoil by equations 2.1 and 2.2;

$$L = N\cos\alpha - A\sin\alpha \tag{2.1}$$

$$D = A\cos\alpha + N\sin\alpha \tag{2.2}$$

The normal force (N) is defined as the force perpendicular to the airfoil chord and the axial force (A) that is acting parallel to the chord. It can be seen in the equations for the lift force (L) and the drag force (D)are both derived from the same normal and axial force. However, the angle of attack (α) determines how much of the normal and axial forces transfer into the lift and how transfer into the drag forces. The pitching moment may be expressed by an integral of the net moments acting on the airfoil (Equation 2.3).

$$M = \int_{LE}^{TE} dM_u + \int_{LE}^{TE} dM_L \tag{2.3}$$

In Equation 2.3, the differential moments are taken with respect to a given reference and then integrated from the leading edge to the trailing edge. A graphical representation of these forces is shown in Figure 2.4.

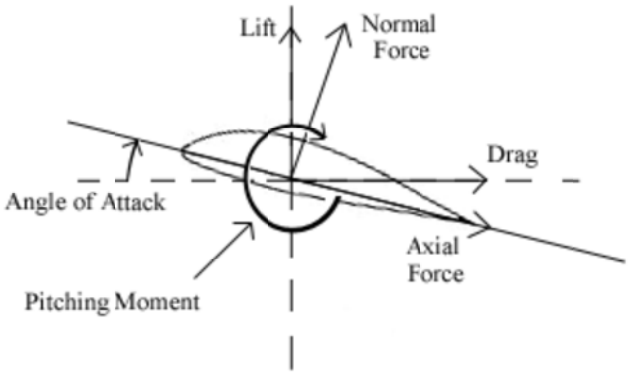

Figure 2.4 - Aerodynamic Forces (Anderson, 2007)

2.3.2 Low-Speed Aerodynamics

In low-speed flows, several idealizations can be applied when the free stream velocity is under Mach .3 to help simplify the fluid dynamics analysis. One assumption that can be made from the idealization of the flow is that density remains constant (no compressibility of the fluid) since the density varies by only a few percent from a velocity range of 0 to 300 mph (Anderson, 2007) Another idealization is the flow is inviscid. Inviscid flows are flows that neglect the viscous effects that occur in any flow such as fraction, thermal conduction and diffusion. Using this assumption relies on having a higher Reynolds number because viscous effects have a significant effect at low Reynolds numbers. These effects are known to be minimal for low-speed air flows and this idealization is well supported by current theory. (Anderson, 2007) The flow is assumed to be steady and the body forces acting on the working fluid were assumed to be minor compared to dynamic effects. These idealized conditions are sufficient to allow the use of Bernoulli's equation (Equation 2.4), in the low-speed flow analysis.

Bernoulli's equation may also be derived from the momentum equation by considering a differential control volume and applying the assumptions made previously. The resulting equation shows that the sum of the local pressure (p) and the dynamic pressure (q), (Equation 2.5), is constant throughout a given flow. From this Equation, the local velocities may be computed from knowledge of upstream data and local pressure so that all of the flow characteristics may be obtained.

$$p + \frac{1}{2}\rho V^2 = constant = p + q_\infty \tag{2.4}$$

$$q_\infty = \frac{1}{2}\rho V_\infty^2 \tag{2.5}$$

Effects of the wind tunnel walls may be ignored by applying the inviscid flow approximation. By doing so, the flow may be assumed to be uniform except over the airfoil/wing. Uniform flow simplifies the control volume analysis and allows the consideration of a full length airfoil as a 2D profile. The assumption of uniform flow is justified due to the smooth wind, the filtered flow and the controlled entry into the test section.

2.3.3 Characterizing Airfoil Performance

Airfoil performance may be characterized by quantities such as the lift, drag or pitching moment produced under different operating conditions. These aerodynamic forces are often computed from the total pressure over the planform area and are then normalized by the dynamic pressure in order to produce non-dimensional quantities. For example, the lift, drag and normal coefficients may be expressed as Equation 2.6, 2.7 and 2.8 respectively. The pitching moment must also be normalized by the chord length in order to produce a non-dimensional moment coefficient as in Equation 2.9.

$$C_l = \frac{D}{\frac{1}{2}\rho_\infty V_\infty^2 A} \tag{2.6}$$

$$C_d = \frac{D}{\frac{1}{2}\rho_\infty V_\infty^2 A} \tag{2.7}$$

$$C_n = \frac{F_n}{\frac{1}{2}\rho_\infty V_\infty^2 A} = \frac{p}{q_\infty} \tag{2.8}$$

$$C_m = \frac{\int \Delta p(x) dc}{q_\infty c} = \frac{M}{\frac{1}{2}\rho_\infty V_\infty^2 Ac} \tag{2.9}$$

$$Re = \frac{\rho_\infty V_\infty d}{\mu_\infty} \tag{2.10}$$

These non-dimensional quantities are functions of the Reynolds number (Equation 2.10) and the angle of attack. The Reynolds influence may be seen by the inclusion of the density (ρ_∞)and the velocity (V_∞) terms while the angle of attack influence is implied through the force, moment and area terms. Thus, in order to appreciate the full range of responses of a given airfoil, it is necessary to consider a range of Reynolds numbers and angles of attack. Variation in the Reynolds number produces different lift curves, while variations in the angle of attack will alter the lift-drag ratio.

2.3.4 Characterizing Wing Performance

Wing performance can be characterized much the same way as an airfoil's performance.

2.4 Obtaining Airfoil Characteristics from Data

2.4.1 Airfoil control Volume Analysis

One method of obtaining the lift, drag and pitching moment coefficients of interest is to analyze a control volume over the surface of the airfoil. In this method, localized pressure measurements are taken in a plane in the chord wise direction on both the upper and lower surfaces to obtain a pressure distribution. (Figure 2.5) The difference in the pressure distributions may then be integrated in order to obtain an expression for the net pressure acting over the surface.

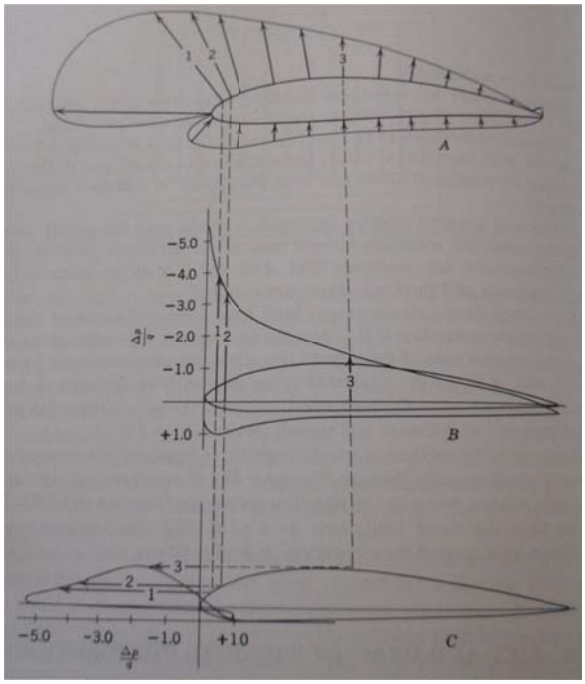

Figure 2.5 - Pressure distribution over an airfoil (Pope, 1984)

In the pressure distribution shown in Figure 2.5, the arrows pointing towards the wingspan represents a positive gage pressure while the upper pressure distribution shows outward pointing arrows to show negative gage pressure. This is clarified in the two plots shown below the pressure distribution diagram. It can be seen that the normalized gage pressure is lowest near the leading edge where the velocity is the highest. This observation confirms the behavior predicted by Bernoulli's equation. However, a limitation of this arrangement is that the summation of pressure data fails to detect the axial forces acting on the airfoil and the skin friction is unaccounted for in this method.

2.4.2 Test Section Control Volume Analysis

An alternative method of measuring drag force is to perform a control volume analysis over a streamline bounded control volume. By applying conservation of momentum to this control volume, it can be deduced that the body within the control volume contributed to a loss of

momentum. The effects may be visualized by marking the inlet and outlet velocity profiles as shown in Figure 2.6. The inlet flow is uniform while the outlet flow will have a non-uniform shape due to localized loss of momentum. This loss of momentum is known as the drag

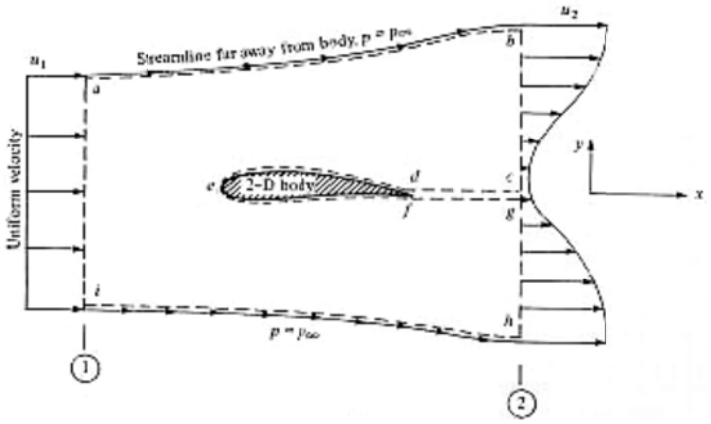

Figure 2.6 - Control volume on a 2D body (Anderson, 2007)

produced by the airfoil and may be indirectly calculated by solving the velocity profiles at either end of the control volume. Alternatively, through the use of Bernoulli's equation, localized pressure measurements in the wake may be used instead. A non-dimensional analysis considering normalized pressure was then used to solve for the coefficient of drag. This type of arrangement will provide sufficient data to calculate the drag coefficient but differential forces were not measured and thus lift and moment cannot be evaluated from this data.

2.4.3 Wing Direct Force Measurement

A more realistic method of predicting airfoil performance is to consider a finite length wingspan mounted in the center of the test section. The 3D airfoil (wing) uses a sting balance that measures the axial and normal reaction force imposed on the sting-airfoil structure due to the flow. The

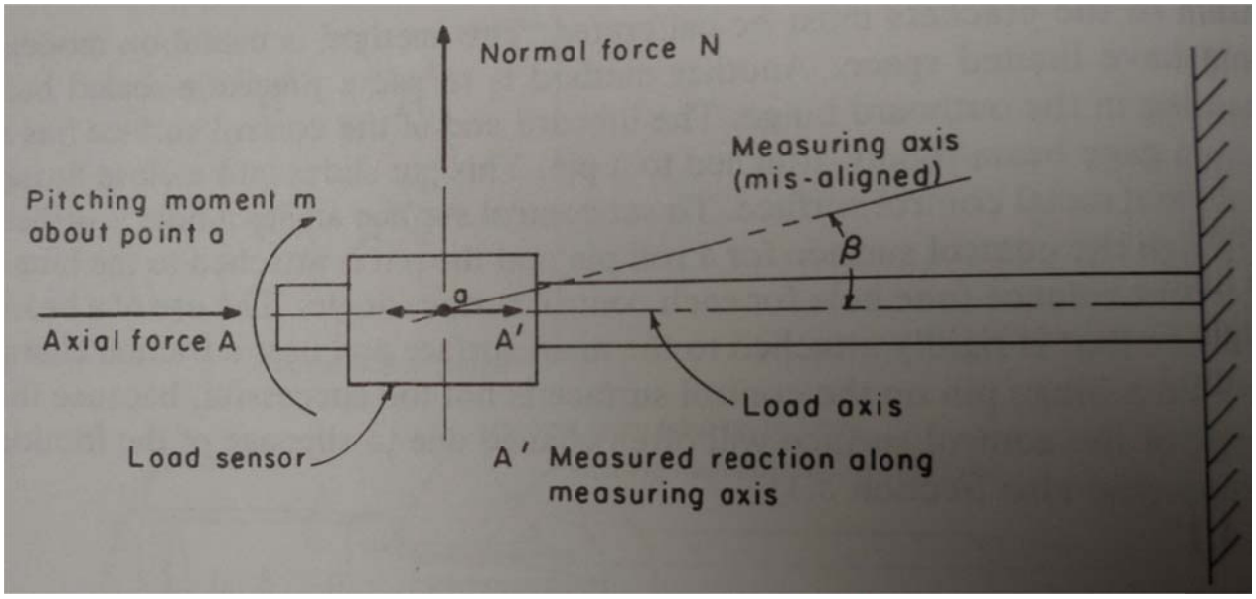

Figure 2.7: Schematic of Forces on Sting balance (Pope, 1984)

reduced constraints allow the airfoil to respond with the full six degrees of freedom and the finite width of the airfoil will allow rotational flow over the sides of the wing.

Chapter 3: AEROLAB Low-Speed Wind Tunnel

3.1 General AEROLAB Wind Tunnel Specifications

The San Jose State University wind tunnel (Figure 3.1) was designed by AEROLAB and is specifically made for the educational environment. The wind tunnel is an open circuit or "Eiffel" tunnel with a 12x12x12-inch test section where a force balance or table mounted models can be used to obtain a variety of aerodynamics data.

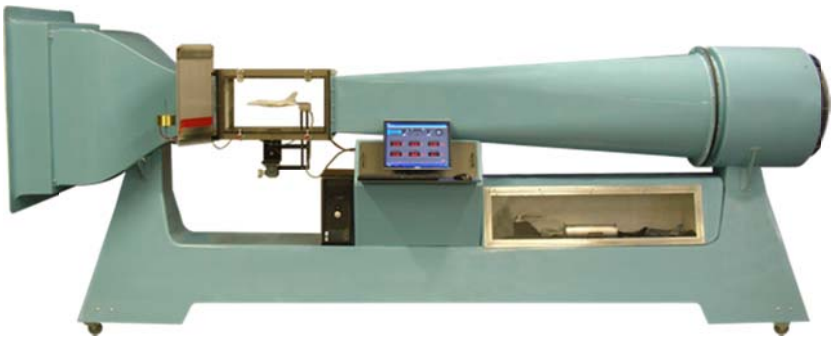

Figure 3.1 - AEROLAB Educational Wind Tunnel (AEROLAB, 2007)

The maximum velocity that can be created is around 145 mph with a clear channel with near-infinite adjustability above 10 mph with the 9 blade fan which is constructed of reinforced-fiberglass. The blades are rated to a maximum rotational speed of 3437 rpm but maximum rotational speed in the wind tunnel is 2345 rpm. The fan is mounted directly to the shaft of a 10HP motor which is controlled by heavy-duty variable frequency drive.

The tunnel ductings are composed of four major duct components which are the contraction, the test section, the diffuser and then fan housing. A proprietary 9^{th}-order polynomial defines the contraction contour. The contraction ratio (inlet area to outlet area) is 9.5:1 which allows the tunnel to achieve high performance and low turbulence level at low speeds. Along with the

contraction ratio, the shallow-angle (6º total-included divergence angle based on cross sectional area) helps eliminate diffuser effects especially when large models are being tested (AEROLAB, 2007). Another contributing factor to the high performance of this tunnel is that flow conditioning uses hexagonal matrixes which are 4 inches long and .25 inches wide to straighten the flow. The hexagonal matrixes do little to eliminate small eddies, although the tunnel is equipped with two turbulence-reducing screens immediately downstream of the hexagonal matrixes. They are made of 0.009 inch stainless steel wire spaced at 20 wires per inch. Small eddies in the air are broken into yet smaller eddies by the screens. Comparatively speaking, smaller eddies dissipate faster than larger eddies.

3.2 Test Section and Instrumentation

The test section of the AEROLAB wind tunnel is 12x12x12-inch (Figure 3.2) and is equipped with diverging walls that diverge 0.0625 inches from the test section inlet to the outlet. The diverging walls mitigate the test section buoyancy effect resulting from the growing boundary layer thickness.

Figure 3.2 - AEROLAB Wind Tunnel Test Section (AEROLAB, 2007)

The test section is also equipped with a manually-operated yaw table for models needing to be mounted to the floor of the test section usually for pressure models. These models can be

connected to a 24-tube multi-manometer that does not require the DAC or to the two solid-state differential pressure transducers. When using the 24-tube multi-manometer, it only required reading of the change of pressure from the tubes manually. The vertical glass tubes provide pressure measurement as well as visualization. Along the bottom, these tubes connect to an anodized aluminum reservoir. The reservoir remains at atmospheric pressure because the lid does not make a perfect seal. To use models that require pressure transducers, a data acquisition (DAC) system is supplied and is used with the pressure transducers and the sting balance. Also, there is a "sting" Force/Moment Balance that is mounted to the top of the MPS (Motion Positioning System) vertical arms. The wind tunnel's three-component sting balance is mounted on a parallelogram-type model positioning system. The model positioning system was designed specifically for the EWT sting balance. It was dimensioned such that changes in pitch angle have little effect on model height – the forward tip of the balance remains essentially stationary as pitch angle is changed, therefore keeping the test model centered in the airflow. The pitch angle range is +/- 20°. Prior to shipment, the balance was calibrated (first order only) at AEROLAB.

The maximum load ranges are:

Normal Force (Side Force):	25 lbs. (111.2 N)
Axial Force:	10 lbs. (44.5 N)
Pitching Moment (Yawing Moment):	50 inch-lbs. (5.65 N-m)

The use of the DAC is controlled by a program written in LabVIEW to control all tunnel functions. This program is connected and used to control the two solid-state differential pressure transducers and a three-component sting Force/Moment balance.

3.3 Clark Y-14 Airfoil and Wing Models

The wind tunnel comes with a variety of models but the two models used to develop the correction factors for the wind tunnel were the Clark Y-14 airfoil and wing. The Airfoil (Figure 3.3) is mounted vertically to the yaw table and spans the test section. The 18 flush-mounted pressure tabs are connected to the pressure transducer array or can be connected to the 24-tube multi-manometer. For this project, the pressure tabs are connected to the DAC to have the test runs recorded through LabVIEW.

Figure 3.3 - Clark Y-14 Airfoil (AEROLAB, 2007)

The Clark Y-14 wing (Figure 3.4) can be mounted on sting balance only and has adjustable slats and flaps for a wide variety of experiments that can be performed. The wing is 9.875 inches long and has a span of 3.5 inches. For the purpose of this project, the wing will be left in a clean configuration which entails the slats and flaps being left un-deployed.

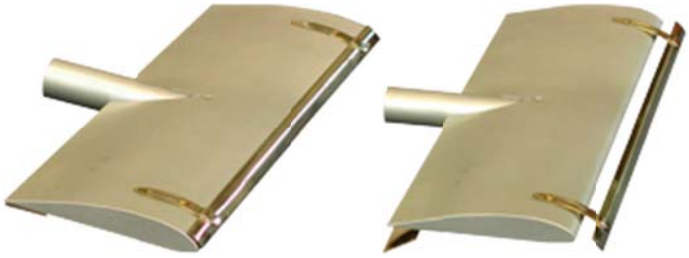

Figure 3.4 - Clark Y-14 Wing with and without Flaps and slats deployed (AEROLAB, 2007)

Chapter 4: Two-Dimensional Wall Corrections for the Clark Y-14 Airfoil

For an airfoil, there are several corrections that need to be performed to more accurately model free-flight conditions. The four main wall corrections for an airfoil are buoyance, wake blockage, solid blockage and streamline curvature. The buoyance corrections will have an additive component to the drag force while the wake and solid blockage component are dimensionless but are used in the correction for the streamline curvature. The streamline curvature corrections are the most important for correcting airfoil data corrections for $\Delta\alpha$, Δc_L, Δc_m and includes the parameters; V_c, q_c, Re_c, α_c, c_{lc}, $c_{m\frac{1}{4}c}$ and c_{d0}. The velocities tested in the wind-tunnel are 6.5, 30, 68 and 102 MPH and the Reynolds numbers are 100,000, 500,000, 1,200,000 and 1,800,000 respectively. Data and calculations for this chapter can be found in Appendix B

4.1 Buoyancy Correction

4.1.1 Theory

Closed-throat wind-tunnels have a variation of static pressure along the axis of the test section. The variation of static pressure is due to a thickening of the boundary layer as the flow progresses through the test section. As the flow approaches the end of the test section, the pressure progressively becomes more negative. With the pressure turning more negative down the length of the test section, the model tends to be sucked down the test section. The amount of buoyancy is usually insignificant for wings and airfoils but the correction becomes more important for fuselages and nacelles. The buoyancy corrections can be applied in the two-dimensional or three-dimensional space. For the two-dimensional case, the cross-section area is

shown in figure 4.1 and the static pressure variation along the test section length is graphed in figure 4.2 as an example. It should be noted that for every velocity change, the static pressure gradient through the test section will change. The static pressure can be determined experimentally by measuring the pressure distribution over the airfoil or wing or by utilizing equation 4.1 to determine the slope.

$$\frac{dp}{dl} = -k\frac{\frac{\rho}{2}V^2}{B} \tag{4.1}$$

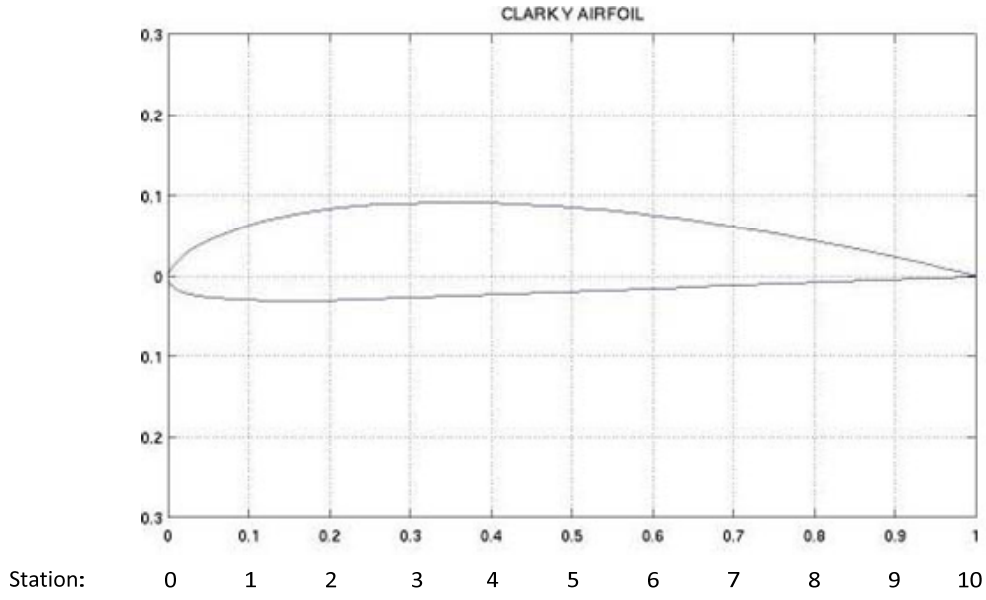

Figure 4.1 - Cross-sectional area in percentage of length

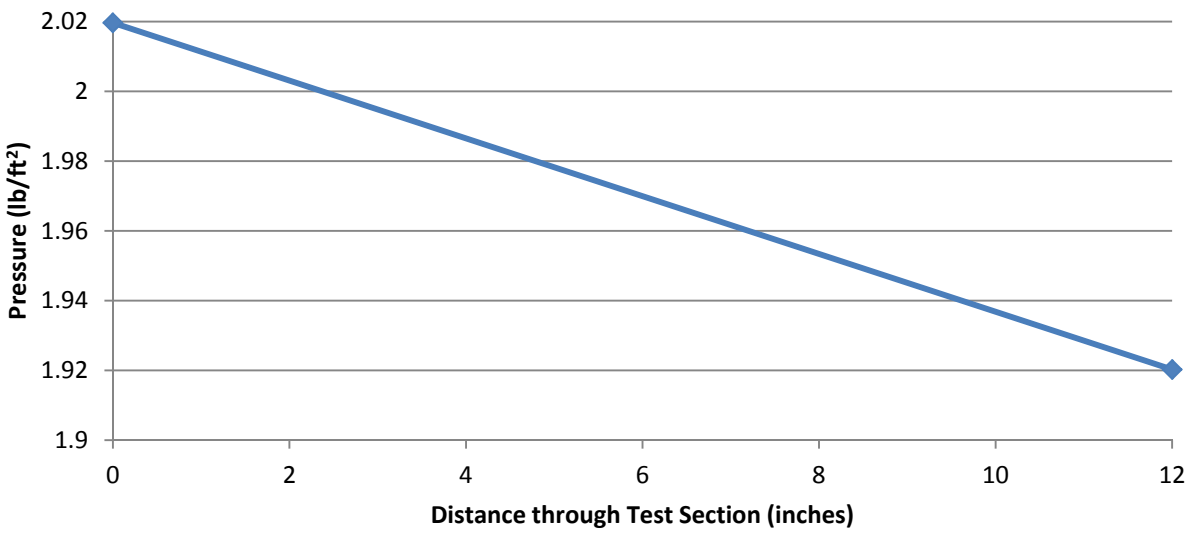

Figure 4.2 – Static Pressure Gradient in the test section for a velocity of 6.5 MPH

Wind tunnel designers employ slanted vertical walls along the test section length to mitigate the effects of the buoyancy force on the model. The walls slightly widen from the narrowest point at the mouth of the test section and opens to a determined width through calculations and then verification of the results to ensure the test section exit has not over expanded.

4.1.2 Approach

It can be seen that the variation of the static pressure in figure 4.2 from any two given station along the airfoil is linear and therefore the pressure differential acts on the average area. The resulting drag force for that segment of the airfoil is

$$\Delta D_B = (p_2 - p_3)(\tfrac{S_2+S_3}{2}) \tag{4.2}$$

Equation 4.2 can be solved by plotting the local static pressure against the cross-section area as in figure 4.2 and the area under the curve is found to be the buoyancy. If the static pressure gradient is a straight line, equation 4.2 simplifies to

$$\Delta D_B = -\sum S_x \left(\frac{dp}{dl}\right) dl \tag{4.3}$$

Graphing the static pressure gradient shows that the test section is effectively shrinking and this can be illustrated by viewing streamlines transiting down the test-section. As the streamlines approach the end of the test section, they are closer together than when entering the test section. The squeezing effect should be accounted for in the corrected equation and added to the pressure gradient effect. The total drag increment per span length with the included squeezing effect is

$$\Delta D_B = -\frac{\pi}{2}\lambda_2 t^2 \frac{dp}{dl} \tag{4.4}$$

where $\lambda_2$can be found from figure 4.3. Without experimental data to find the values for the body shape, ΔD_B can be determined easier by replacing $\lambda_2 t^2$ with $\frac{1}{4}\Lambda c^2$. With the substitution of $\frac{1}{4}\Lambda c^2$, ΔD_B becomes

$$\Delta D_B = -\frac{\pi}{8}\Lambda c^2 \frac{dp}{dl} = -\frac{6h^2}{\pi}\Lambda\sigma\frac{dp}{dl} \tag{4.5}$$

where $\sigma = \left(\frac{\pi^2}{48}\right)\left(\frac{c}{h}\right)^2$; $\Lambda = \frac{16}{x}\int_0^1 \frac{y}{c}\left[(1-P)(1+\frac{dy}{dx})\right]^{\frac{1}{2}} d\frac{x}{c}$, Λ can also be determined by Figure 5.4.

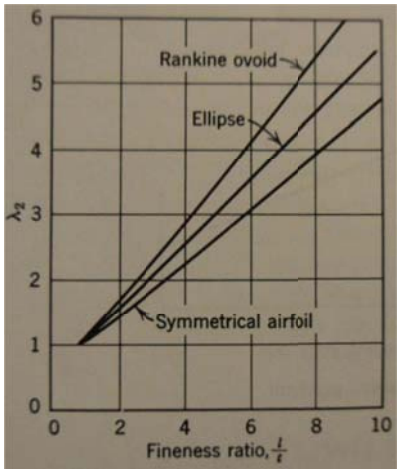

Figure 4.3 - Body shape factor for different shapes (Pope, 1984)

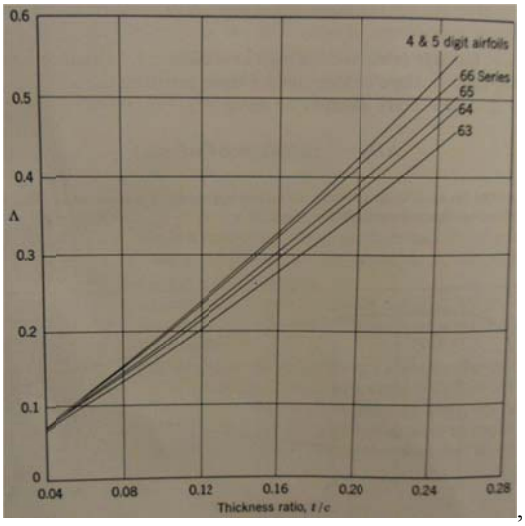

Figure 4.4 - Plot of thickness ratios for a category of airfoils vs. Λ (Pope, 1984)

A more rigorous approach is necessary if the pressure gradient is not given where the use of the Bernoulli's and continuity equations are needed. The pressure gradient can be determined by using Bernoulli's equation (Equation 4.6) and the continuity equation (Equation 4.7) by knowing the velocity and pressure at the entrance of the wind tunnel. The velocity and pressure can be then determined at the test section entrance and exit.

$$P_1 + \frac{1}{2}\rho V_1^2 = P_1 + \frac{1}{2}\rho V_2^2 \tag{4.6}$$

$$\rho_1 V_1 A_1 = \rho_2 V_2 A_2 \tag{4.7}$$

To begin, the Re_c will need to be determined for a given V_∞ for the experiment. Re_{cr} for a flat plate, which taking one side of the test section can be assumed, is 500,000. For Re < 500,000, the flow is considered to be laminar and for Re > 500,000, the flow is considered to be turbulent. The Reynolds number for a length is found by

$$Re_c = \frac{\rho_\infty V_\infty c}{\mu_\infty} \tag{4.8}$$

Once the Reynolds number is found for the test section length, the determination if the flow is laminar or turbulent can be made. If the flow is laminar the test section length, the boundary layer displacement can be found directly from

$$\delta^*_{LBL} = \frac{1.72x}{Re_c^{.5}} \tag{4.9}$$

The exit velocity is needed at the test section exit which depends on the cross-sectional area at the exit. The cross-sectional area is dependent on the boundary layer displacement. Since the boundary layer displacement has been found, the effective area at the exit can also be found by

$$A_{2\,eff} = (c - \delta^*_{LBL}) \tag{4.10}$$

For the case where flow turns turbulent before exiting the test section, the x_{cr} will need to be found to determine the boundary layer displacement. (Figure 4.3)

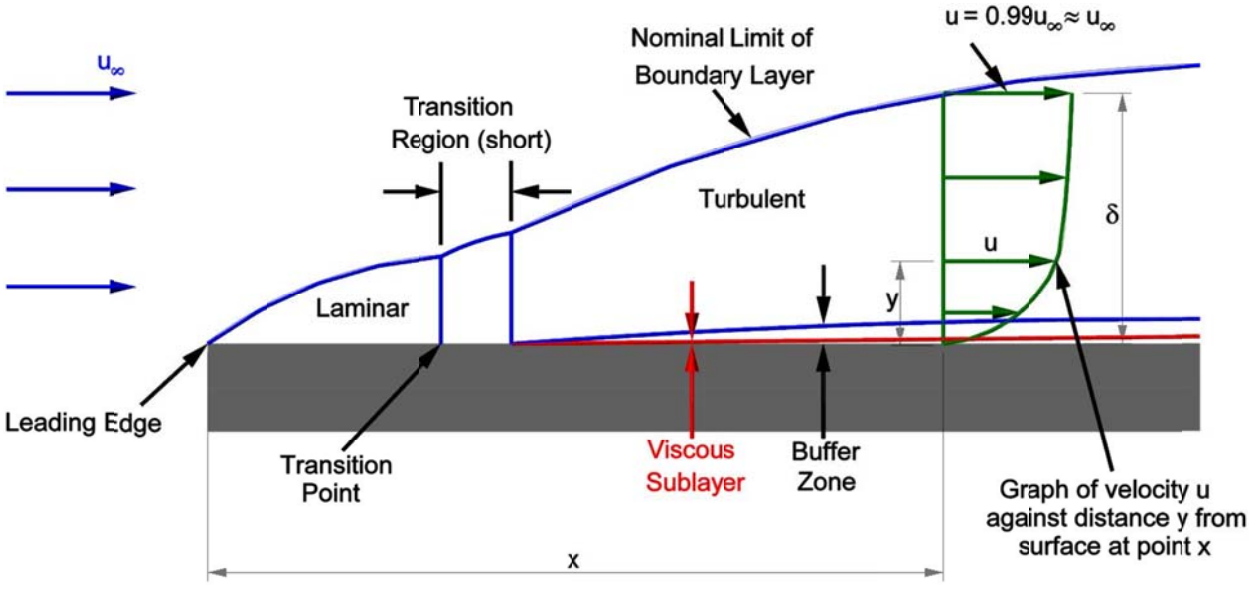

Figure 4.5 – Laminar and turbulent boundary layer over a flat plate (CFD Online, 2009)

The transition point, x_{cr}, is determined by using the critical Reynolds number for a flat plate in

$$x_{cr} = \frac{Re_{cr}\mu_{\infty}}{\rho_{\infty}V_{\infty}} \tag{4.11}$$

With the transition point found, the laminar boundary layer displacement can be found at that point by using equation 4.9. The laminar boundary layer displacement at the transition point can also be assumed to be the thickness of the turbulent boundary layer displacement. With that assumption,

$$\delta^*_{LBL} = \delta^*_{TBL} = \frac{.046x_{eq}}{Re^{.2}_{x\,eq}} \tag{4.12}$$

Solving for $x_{eq,}$ the starting point of turbulent boundary layer can be found by subtracting x_{eq} from x_{cr}. Since the turbulent boundary layer start point has been identified, equation 4.12 can be used to find the turbulent boundary layer displacement at the test section exit by replacing x_{eq} in the equation with the length of the turbulent boundary layer. Using equation 4.10 and replacing $\delta^*_{LBL}$with δ^*_{TBL}, the effective exit area can be found.

The test section exit area can now be used in equation 4.7 but the other parameters also need to be found. Some assumptions need to be made to simplify the problem 1) by ignoring the losses through the contraction of the inlet of the test section, 2) ignoring the losses through the flow screen at the wind-tunnel entrance, 3) assuming incompressible flow and the pressure at the entrance of the test section is actually lower than the pressure calculated at the test section entrance. The known parameters for equation 4.6 are $P_0, \rho_{\infty}\ and\ V_0$ which are assumed to be STD and V_0 is 0 $\frac{ft}{sec}$.

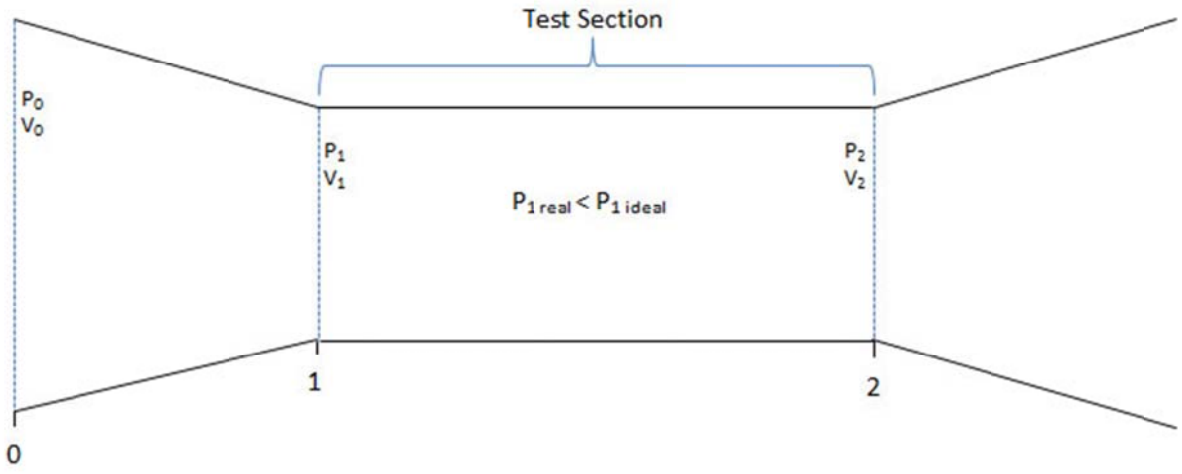

Figure 4.6 – Test section diagram for calculation of P_2 and V_2

Since the boundary conditions at the entrance of the wind-tunnel are known, equation 4.6 can be utilized to find P_1 at station 1 but realize P_1 is actually less than P_1. (Figure 4.6) V_1 is also known since it is measured at station 1 with the DAC. All variables are now known for station 0 and 1 but unknown for station 2. V_2 at station 2 will need to be calculated by equation 4.7 and the cross-sectional area that was calculated for section 2, the test section exit by the process of determining the boundary layer displacement. (Figure 4.7) The last variable that needs to be found is P_2 which can be easily calculated by equation 4.6. Once all six variables have been calculated, the longitudinal static pressure gradient can be found for any free-stream velocity.

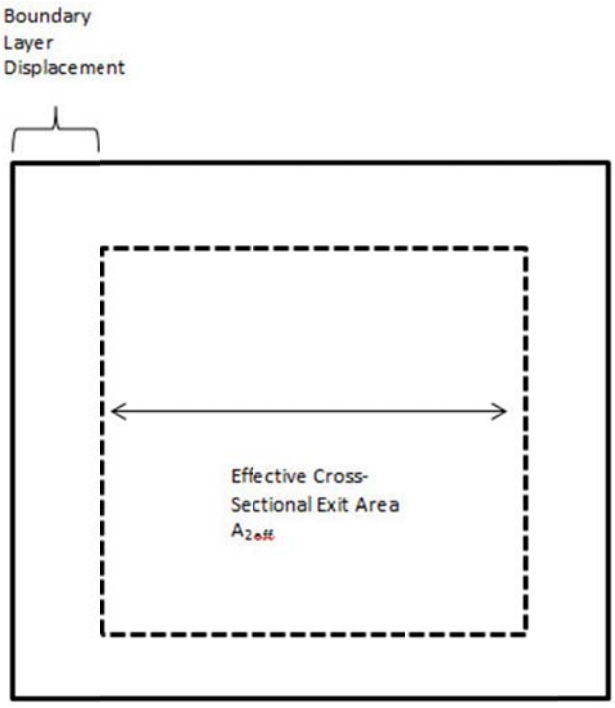

Figure 4.7 – Effective cross-sectional exit area of the test section with the boundary layer displacement removed

By using the P_1 and P_2, the longitudinal static pressure gradient is calculated by

$$\frac{dp}{dl} = \frac{P_2 - P_1}{l} \tag{4.13}$$

This process can be repeated as many times as needed to obtain a $\frac{dp}{dl}$ curve for the wind-tunnel.

A code to complete this task is shown in Appendix A and can be used to output a range of $\frac{dp}{dl}$ to excel file. Now that the pressure gradient through the test section is known, this allows for the application of a simplified equation for the buoyancy correction (Equation 4.14) for an airfoil.

$$\Delta D_b = -\left(\frac{dp}{dl}\right)(body\ volume) \tag{4.14}$$

4.1.3 Results

To determine the 2D buoyancy correction, the cross-sectional exit area of the test section is shown in figure 4.8.

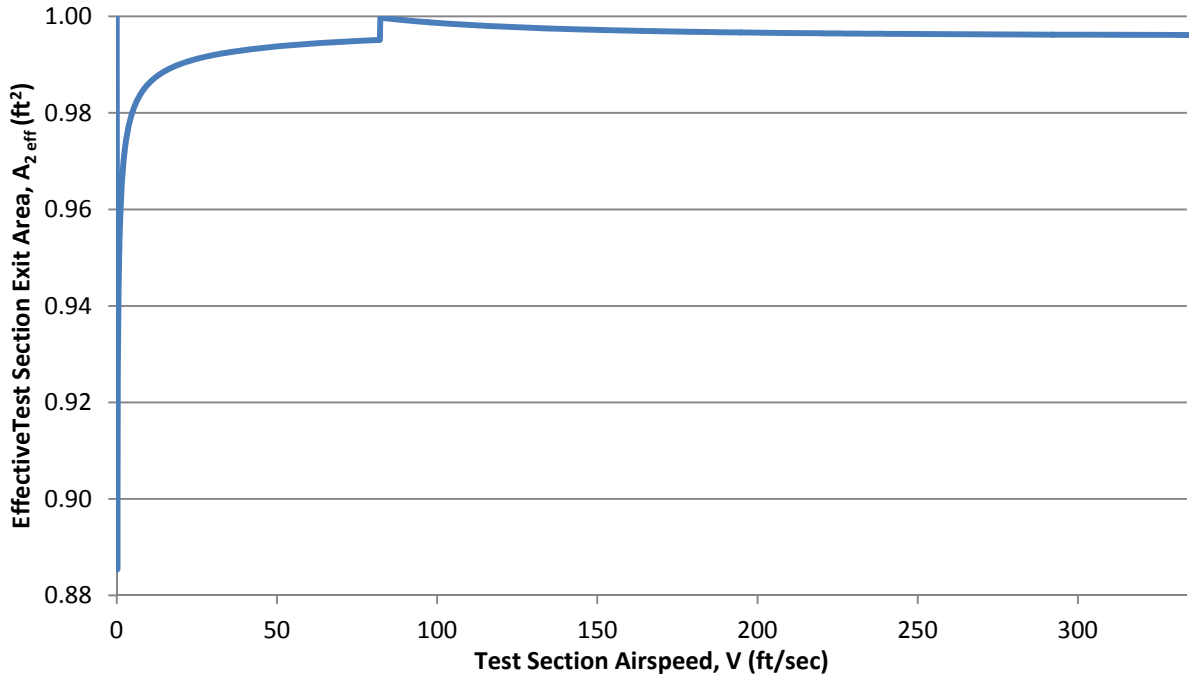

Figure 4.8 – Effective cross-sectional area at exit of test section for various airspeeds

Equation 4.14 is used along with equation 4.6 and 4.6 to determine the static pressure gradient through the test section (Figure 4.9).

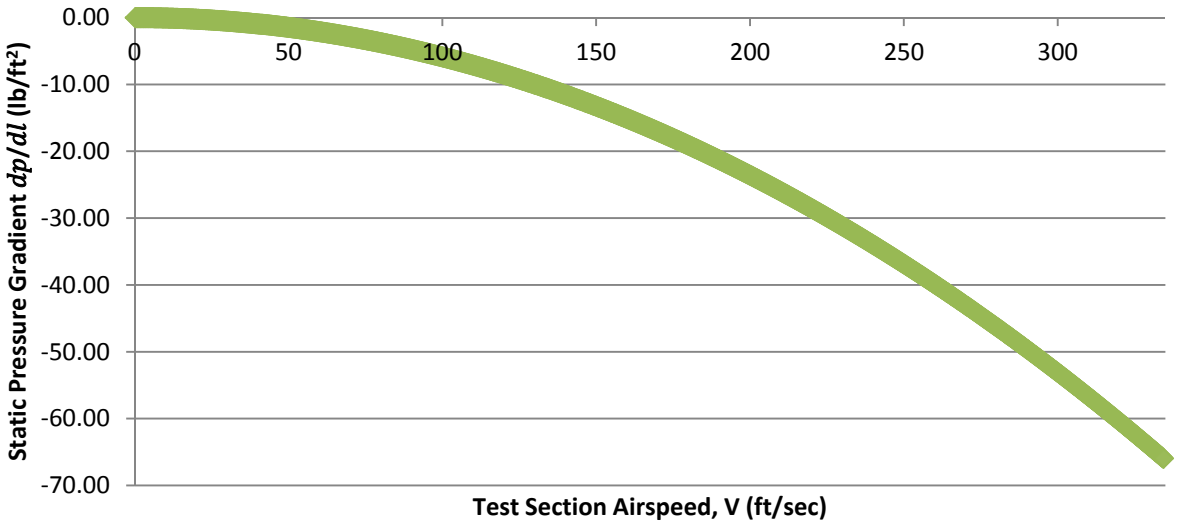

Figure 4.9 - Static pressure gradient through the test section from 0 to 334 $\frac{ft}{sec}$

The airfoil has a model volume of .0068 ft^3 by recreating an exact model of the airfoil in SolidWorks. The 2D buoyancy correction, as shown on the chart below, was calculated for a velocity range of 0 – 334 $\frac{ft}{sec}$ and is plotted in figure 5.6. The maximum velocity plotted corresponds to $M = .3$ at sea level.

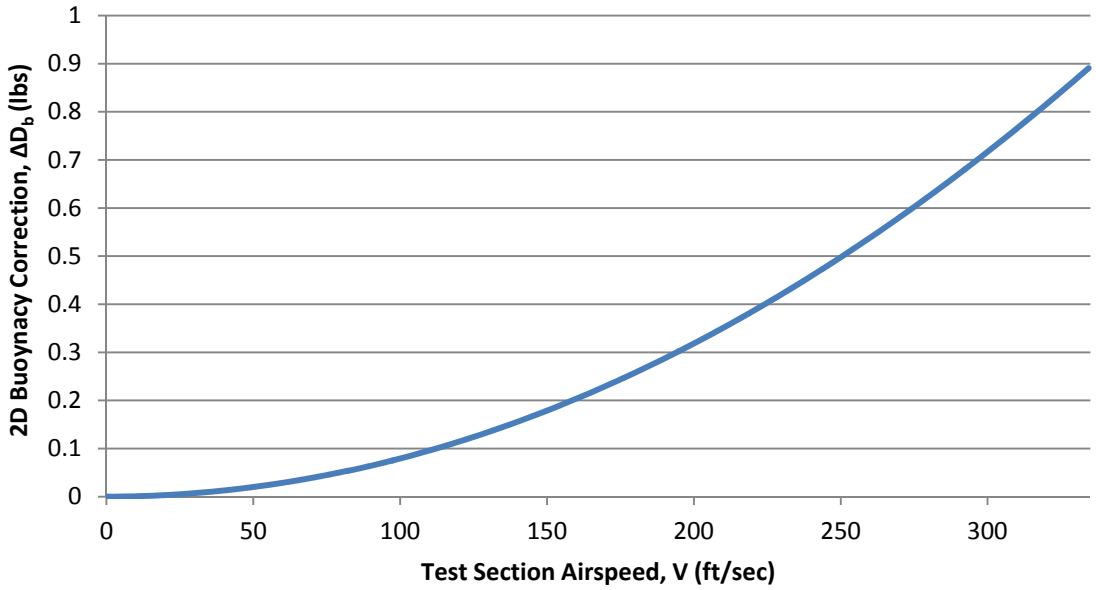

Figure 4.10 - 2D Buoyancy Correction for 0 – 334 $\frac{ft}{sec}$

4.1.4 Discussion

As seen in figure 4.10, the buoyancy drag contributes very little to the overall drag on the airfoil. The largest amount of drag for what is considered "low speed" is approximately .9 lbs. per span length and could be omitted from the wall corrections if a high degree of fidelity is not required. With the assumptions that the boundary layer starts at station 1 in figure 4.6, this creates a certain amount of error in the calculations. Since the boundary layer actually starts at the entrance of the wind-tunnel, by the time the flow reaches the test section entrance, it could already be turbulent. The assumption was made because the exact equation used to create the inlet is not known nor the actually roughness of the inner surface. Also, the wind-tunnel has a flow straightening system at the entrance. The entering air first passes through a matrix of parallel passages that are shaped as a hexagonal matrix, like a "honeycomb". The honeycomb cells are 4 inches long and serve to straighten the flow – to eliminate most flow angularity. The "honeycomb" matrix does little to

eliminate small eddies and it is hard to account for these eddies which effects on the boundary layer thickness. The tunnel is equipped with two turbulence-reducing screens immediately downstream of the honeycomb and even though they help keep the flow straight, it is hard to calculate the screens effects on the boundary layer.

The effective cross-sectional exit area of the test section is affected by the wind-tunnel inlet conditions. The effective area is more susceptible to the inlet conditions at very low speeds as seen in figure 4.8. At approximately 90 ft/sec, the test section exit turns from laminar to turbulent which reduces the boundary layer displacement and which causes the pressure gradient slope to decrease slightly. Once the flow turns turbulent in the test section, the effective cross-sectional exit area stabilizes and at approximately 140 ft/sec, the area becomes equal to .9962 ft^2 for M < 3.

4.2 Solid Blockage Correction

4.2.1 Theory

With a two-dimensional model in the test section, the flow is semi-blocked and the flow area is reduced. In order for continuity and Bernoulli's equation to be satisfied, the flow must increase in velocity to maintain the same mass flow rate through the test section. The increase of velocity is considered solid blockage and is a function of model thickness, thickness distribution and model size. The camber of the airfoil is independent of the solid blockage. "The solid blockage velocity increment at the model is much less (about ¼) than the increment one obtains from the direct area reduction." (Pope, 1984) The streamlines furthest from the model are also impacted by the increment velocity since they are displaced more due to the confines of the test section.

4.2.2 Approach

In solving solid-blockage problems, it is important to determine the axial velocity. One case to examine is where a circular cylinder is placed into a two-dimensional test section. The circular cylinder can be simulated as doublet of certain strength and is contained by an infinite vertical series of doublets of the same strength. Using this simulation of doublets, the axial velocity can be found by

$$\frac{\Delta V}{V_u} = \frac{a^2}{h^2} \tag{4.15}$$

Since the velocity produced by a doublet varies inversely with the square of the distance from the doublet, then doubly infinite doublet series may be summed as

$$\in_{sb} = \left(\frac{\Delta V}{V_u}\right)_{total} = 2\sum_1^{\infty} \frac{1}{n^2}\frac{a^2}{h^2} = \left(\frac{\pi^2}{3}\right)\left(\frac{a^2}{h^2}\right) \tag{4.16}$$

To use a 2-ft diameter cylinder in a tunnel that is 10-ft high would have a solid blockage that would cause the flow velocity to be increased by 3.3% over the true free-stream velocity. In the case of an airfoil, the solid-blockage velocity increment (Glauert, 1933) is show be

$$\in_{sb} = \left(\frac{\Delta V}{V_u}\right)_{total} = \left(\frac{\pi^2}{3}\right)\left(\frac{\lambda_2}{4}\right)\left(\frac{t^2}{h^2}\right) = .822\lambda_2\frac{t^2}{h^2} \tag{4.17}$$

where values of $\lambda_2$can be found in figure 4.9. Another variation to determine the solid-blockage

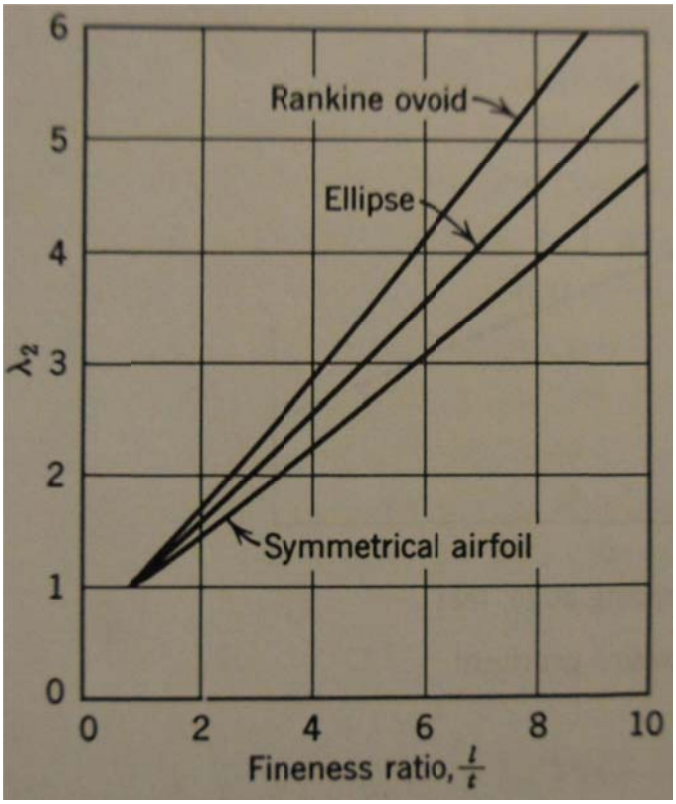

Figure 4.11 – Plot of λ_2 vs. Fineness ratio $\frac{l}{t}$

on an airfoil is from a report that uses some factors associated with the buoyancy correction (Allen and Vincenti, 1944). The following result is from their work where

$$\in_{sb} = \Lambda\sigma \tag{4.18}$$

where $\sigma = \left(\frac{\pi^2}{48}\right)\left(\frac{c}{h}\right)^2$; $\Lambda = 4\lambda_2\frac{t^2}{c^2}$. A simpler equation for the solid-blockage correction for a two-dimensional tunnel is given by

$$\in_{sb} = \frac{K_1(model\ volume)}{C^{\frac{3}{2}}} \tag{4.19}$$

where K_1 is .74 for a wing spanning the tunnel test section horizontally and K_1 is .52 for a span that is spanning vertically and a good approximation for an airfoil model volume is

$$v_{model} = .7(t)(c_{model})(b) \tag{4.20}$$

The approximation of the airfoil model volume is only appropriate at a 0 angle of attack. For any other angle of attack, the model thickness becomes

$$t = c * \sin(\alpha) + .49 \tag{4.21}$$

where the .49 is the thickness of the airfoil due to the chord line of the Clark Y-14 being the bottom edge of the airfoil. The model chord becomes

$$c_{model} = c * \cos(\alpha) \tag{4.22}$$

and the model span remains unaffected. The variable, C, can be used but if greater accuracy is desired, the geometric area of the exit of the test section should be used less the boundary layer displacement thickness around the perimeter. The boundary layer displacement can be calculated by using the process in section 4.1. But if an approximation is adequate, the approximation of the displacement thickness is .6 of the boundary layer thickness, since the boundary layer turns turbulent at some point in the test section. The boundary layer thickness can be found by

$$\delta = \int_0^Y \frac{u}{V_\infty} dy \tag{4.23}$$

For an example of boundary layer thicknesses, wind tunnels with the general size of 7x10-ft have displacement thicknesses of $\frac{1}{2} - \frac{3}{4}$ inch.

4.2.3 Results

For the 2D solid blockage correction, equation 4.19 is used to determine the correction factor for the solid blockage. Since the airfoil is mounted vertically in the wind tunnel, a K_1 value of .52 was used. C is the effective area at the exit of the test section and figure 4.8 can be used to find the effective area for a plotted velocity. The model volume is estimated with equations 4.20, 4.21, 4.22 and is plotted in figure 4.12. With the model volume and test section exit effective area

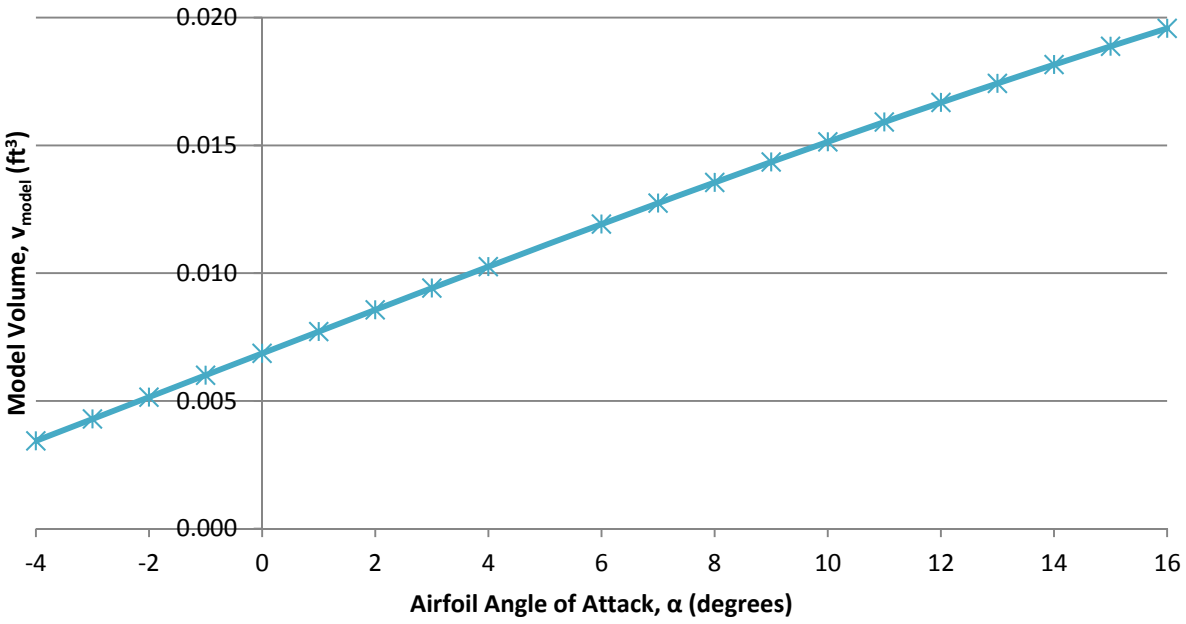

Figure 4.12 – Model volume plotted with airfoil angle attack

calculated for angle of attacks from -4 to 16 degrees, the solid blockage is calculated and plotted in figure 4.13a. A more detailed view of solid blockage curve is plotted in figure 4.13b.

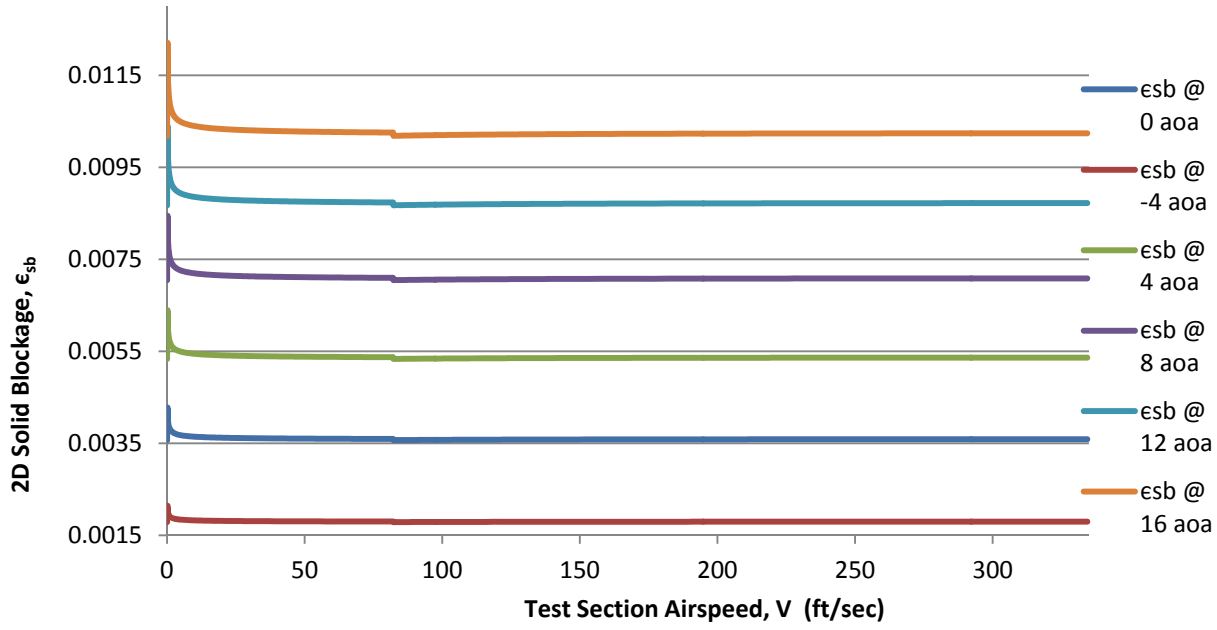

Figure 4.13a – Solid Blockage for the Clark Y-14 for M < .3

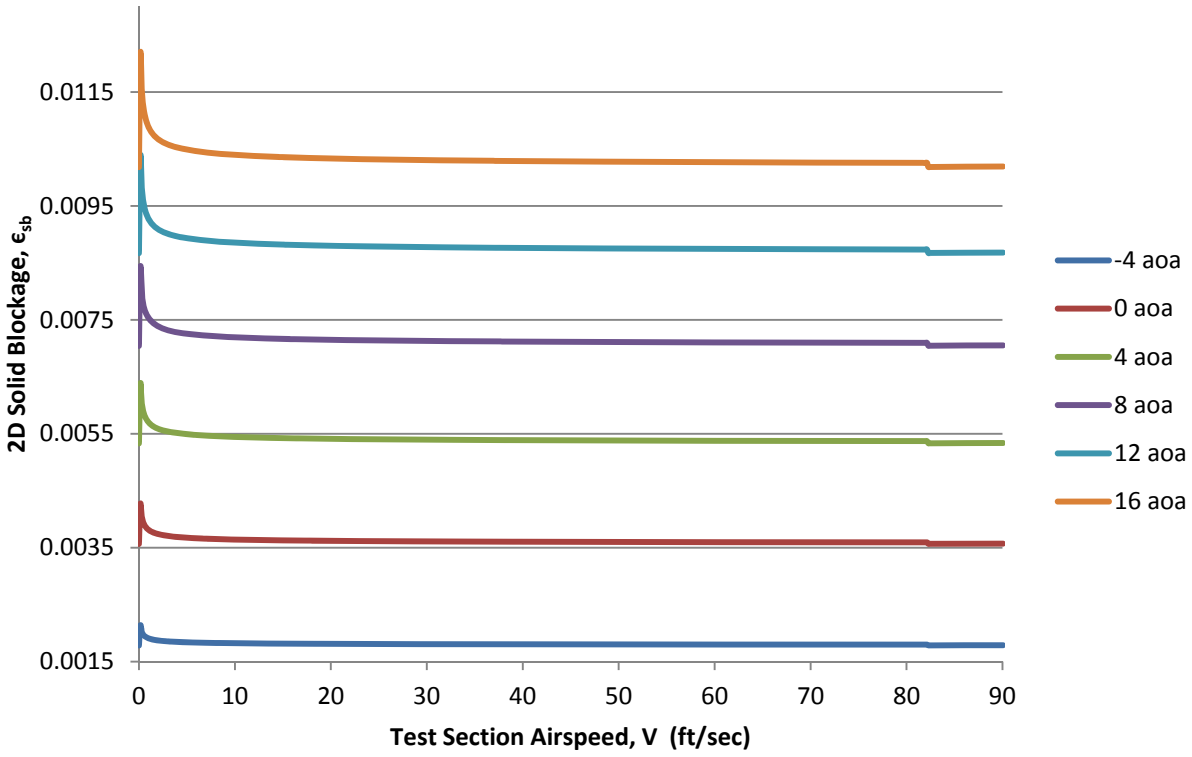

Figure 4.13b – Solid Blockage for the Clark Y-14 for V <90 ft/sec

4.2.4 Discussion

The two-dimensional solid blockage is a dimensionless quantity and increases with angle of attack as seen in figure 4.12 and 4.13. The plot shows the solid blockage at very low speeds jumps dramatically but continues in a decreasing slope as the flow speed increases. At a velocity of approximately 83 feet per second, the boundary layer turns turbulent at the exit of the test section and causes the solid blockage to drop and stay flat for the remainder of the velocities used in calculations.

A fundamental source of error in the solid blockage used in section 4.2.2 is the simulation of the body by doublet system to develop the equations. It may be possible to circumvent the error if the pressure at the tunnel wall is measured with the model in place and then with the model

removed. The resultant velocity increment can be computed and the image system theory can be used to compute the ratio between blockage at the wall and at the tunnel centerline. The AEROLAB wind tunnel has two holes in the walls of the test section used for pitot tube insertion to measure pressure. When the pitot tube is not installed, the holes are left open and can actually lead to a reduction in the solid blockage since pressure can be naturally increased or decreased depending on tunnel conditions.

4.3 Wake Blockage Correction

4.3.1 Theory

All bodies create a wake with the fluid they are moving through and bodies in wind tunnels are not exempt. The law of continuity states the velocity outside the wake in a closed tunnel must be higher than the free stream velocity in order for a constant volume of fluid to flow through the test section. (Figure 4.14) The velocity in the mainstream will be higher due to Bernoulli's principle. Bernoulli's principle states that a pressure gradient derived because of the boundary layer growth along the model induces a velocity increment on the model. Wake blockage may be neglected for the case of open top and bottom of the test section. The natural tendency for the

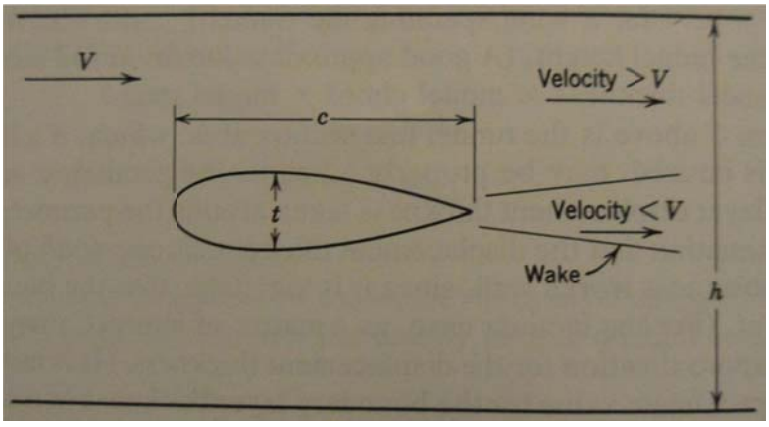

Figure 4.14: Diagram of the velocity profiles in a test section with wake. (Pope, 1984)

wake is toward the axial symmetry which permits a single correction.

4.3.2 Approach

In order to calculate the wake effect due to the model, we must first simulate the wake and the tunnel boundaries. For the two-dimensional case, a line source is needed to be placed at the wing's trailing edge with some hypothetical different colored fluid which can mark the wake region. The region to be emitted (Q) may be determined by

$$D = \rho Q V \tag{4.24}$$

To preserve continuity, a sink must be placed at least 4 body lengths downstream. This simulation of the wake must be contained between the upper and lower surface of the test section walls by an infinite vertical row of sink-source combinations. The sources will not produce an axial velocity on the model but the sinks will induce a horizontal velocity in the amount of

$$\Delta V = \frac{\frac{Q}{h_s}}{2} \tag{4.25}$$

where h_s is the spacing between sources. The one-half in equation 4.25 is due to half of the sink velocity increment will be felt upstream and downstream. The incremental velocity is produced at the model due to the walls and it should be added to the measured velocity. A handy equation for the incremental velocity is

$$\in_{wb} = \frac{\Delta V}{V_u} = \tau c_{du} \tag{2.26}$$

where $\tau = \frac{\frac{c}{h_s}}{4}$. Maskell's two-dimensional method calculates the wake blockages correction by

$$\in_{wb} = \frac{\Delta V}{V_u} = \frac{\frac{c}{h_s}}{2} c_{du} \tag{2.27}$$

To be able to utilize equation 2.27, the c_{du} must be known or be able to be calculated. One method for calculating the c_{du} is by

$$c_d = \frac{1}{c}\int_0^c (c_{p,u}\frac{dy_u}{dx} - c_{p,l}\frac{dy_l}{dx})dx + \frac{1}{c}\int_0^c (c_{f,u} + c_{f,l})\,dx \tag{2.28}$$

This method requires that the shear stresses from the upper and lower surfaces of the airfoil to be measured. The AEROLAB wind-tunnel is incapable of measuring the shear stresses and with only the c_p available, only the pressure drag can be measured which is a very small part of the total drag. The shear stresses on the surface of the airfoil dominate the additive component of the drag. An alternate method is to calculate the c_{du} from the wake that is created behind the airfoil.

$$c_d = \frac{Y_w}{c} - \frac{\int q dy}{q_\infty c} \tag{2.29}$$

This method does not have the additive component of skin friction drag but is more accurate when using only pressure. To measure the wake, a "wake" rake is placed behind the airfoil as in figure 4.15. The "wake" rake measures the pressure across 18 pressure ports, these pressures are

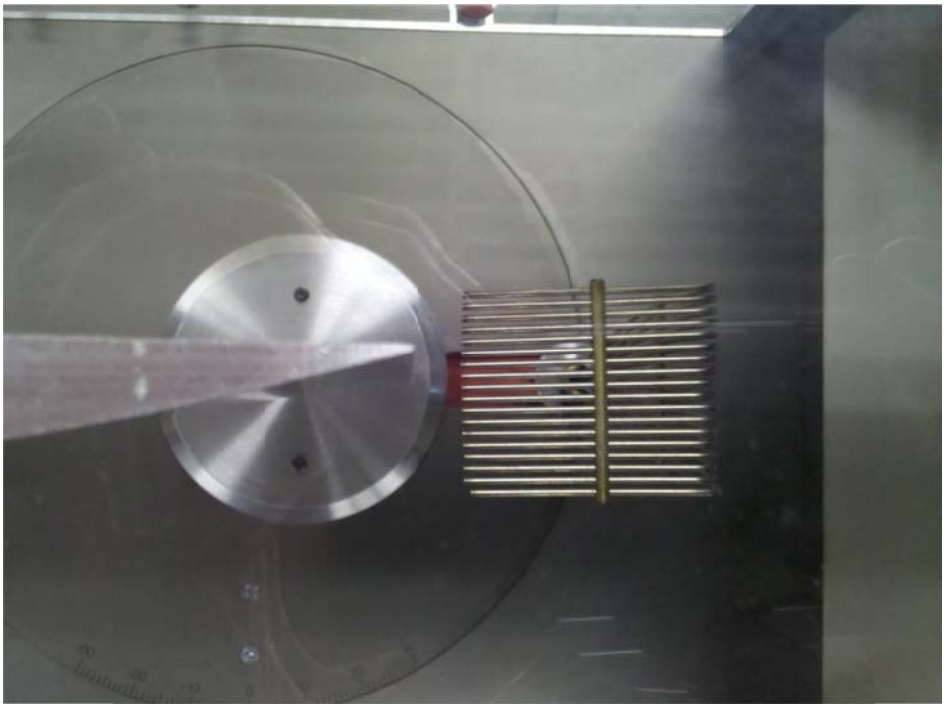

Figure 4.15 – "Wake" rake behind the Clark Y-14 airfoil

then converted to dynamic pressures by

$$q = P_t - P_s \tag{4.30}$$

Once the dynamic pressures across the rake have been calculated, a plot of the q is needed to visually see where the wake is located. Taking the q's that are in the wake, apply equation 4.31

$$area\ of\ increment\ x = \frac{q_1+q_2}{2}(\Delta x) \tag{4.31}$$

where the Δx is the distance between the pressure ports to find the area under the curve for each q value and the area can then be summed to satisfy the $\int q\ dy$ in equation 2.29. After the integration has been completed, the rest of the equation becomes trivial to calculate the c_d.

4.3.3 Results

Figures 4.16 through 4.18 were plotted with the calculated data from using equation 2.29.

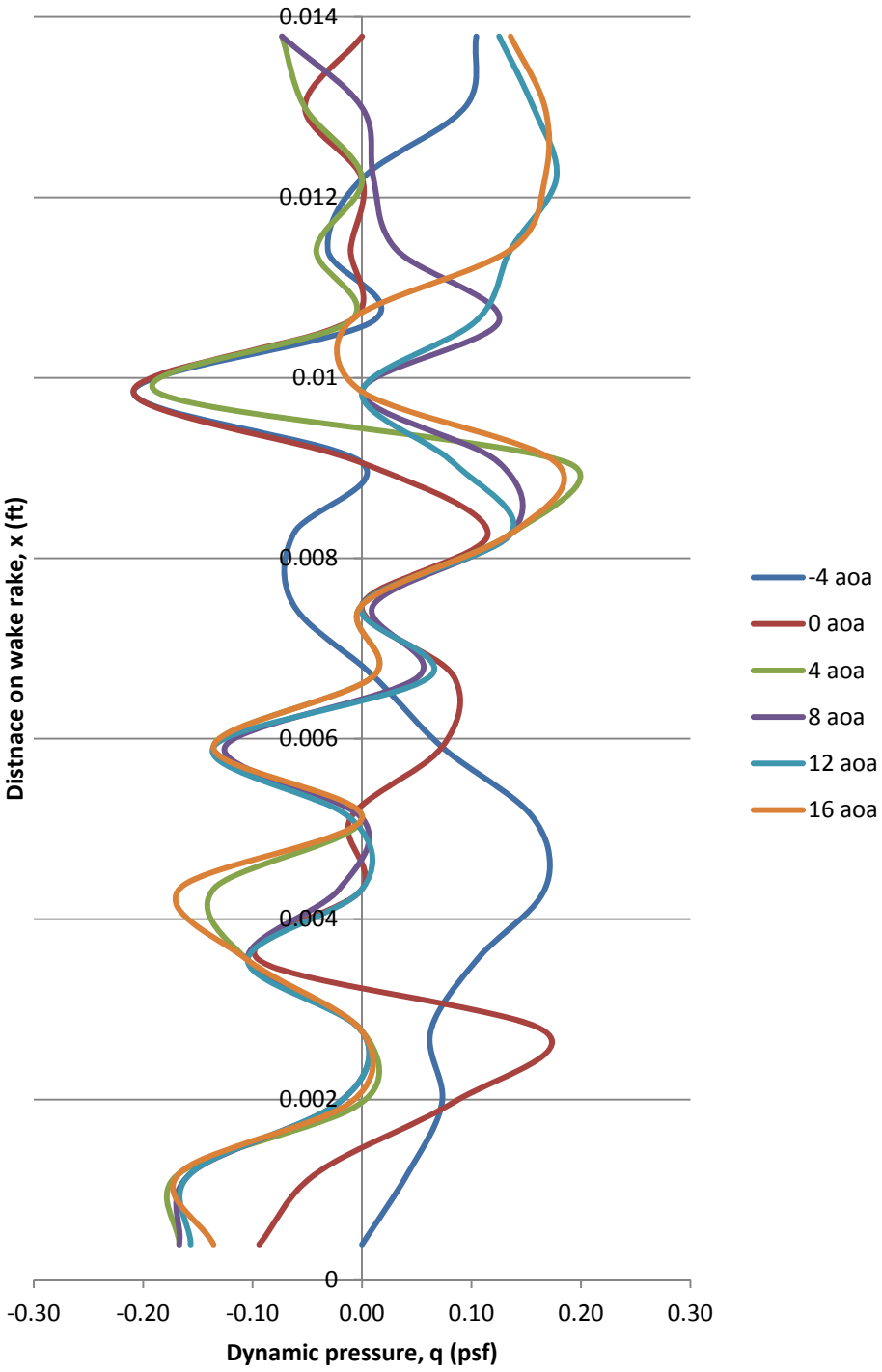

Figure 4.16 – Profile of wake at 6.5MPH

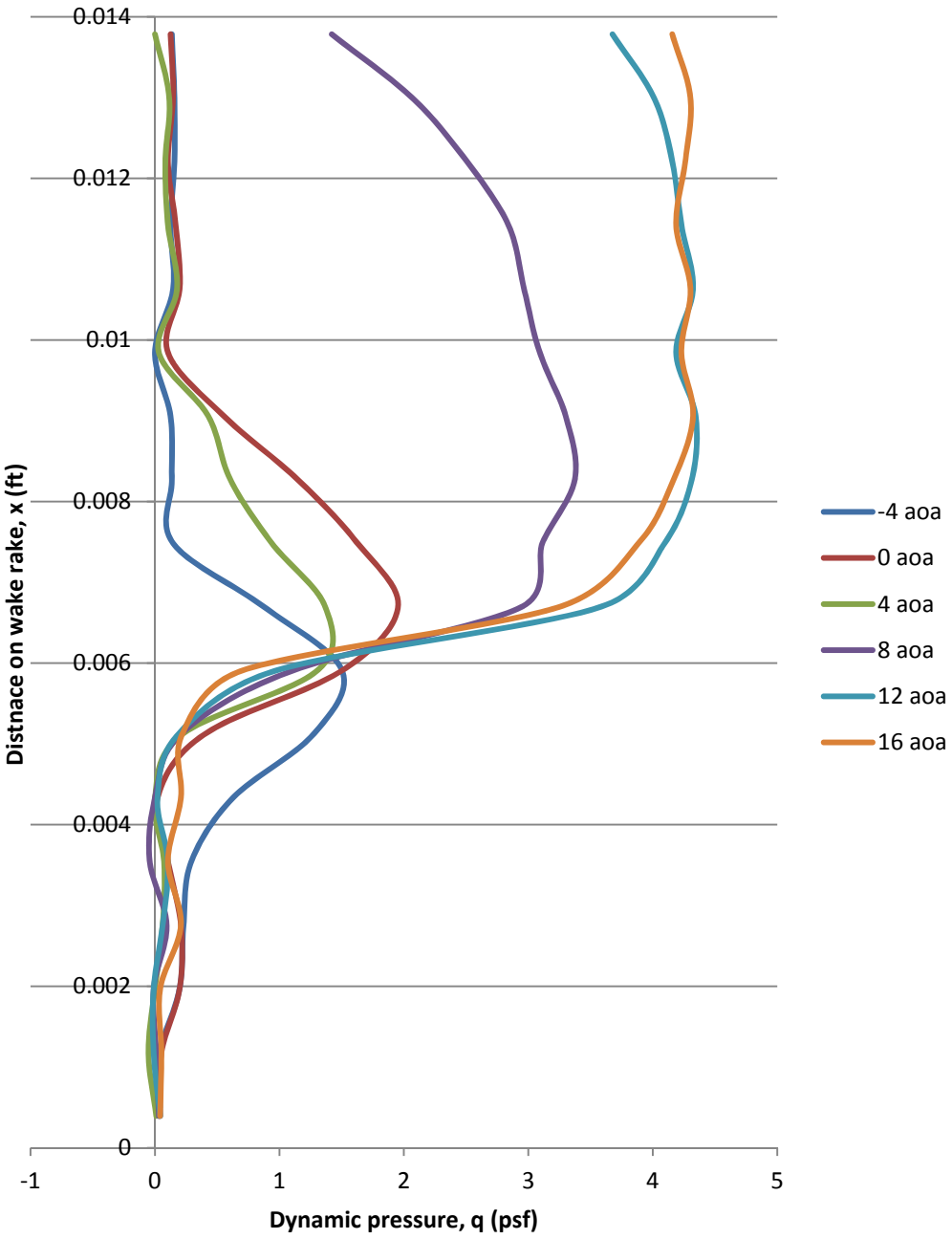

Figure 4.17 – Profile of wake at 30 MPH

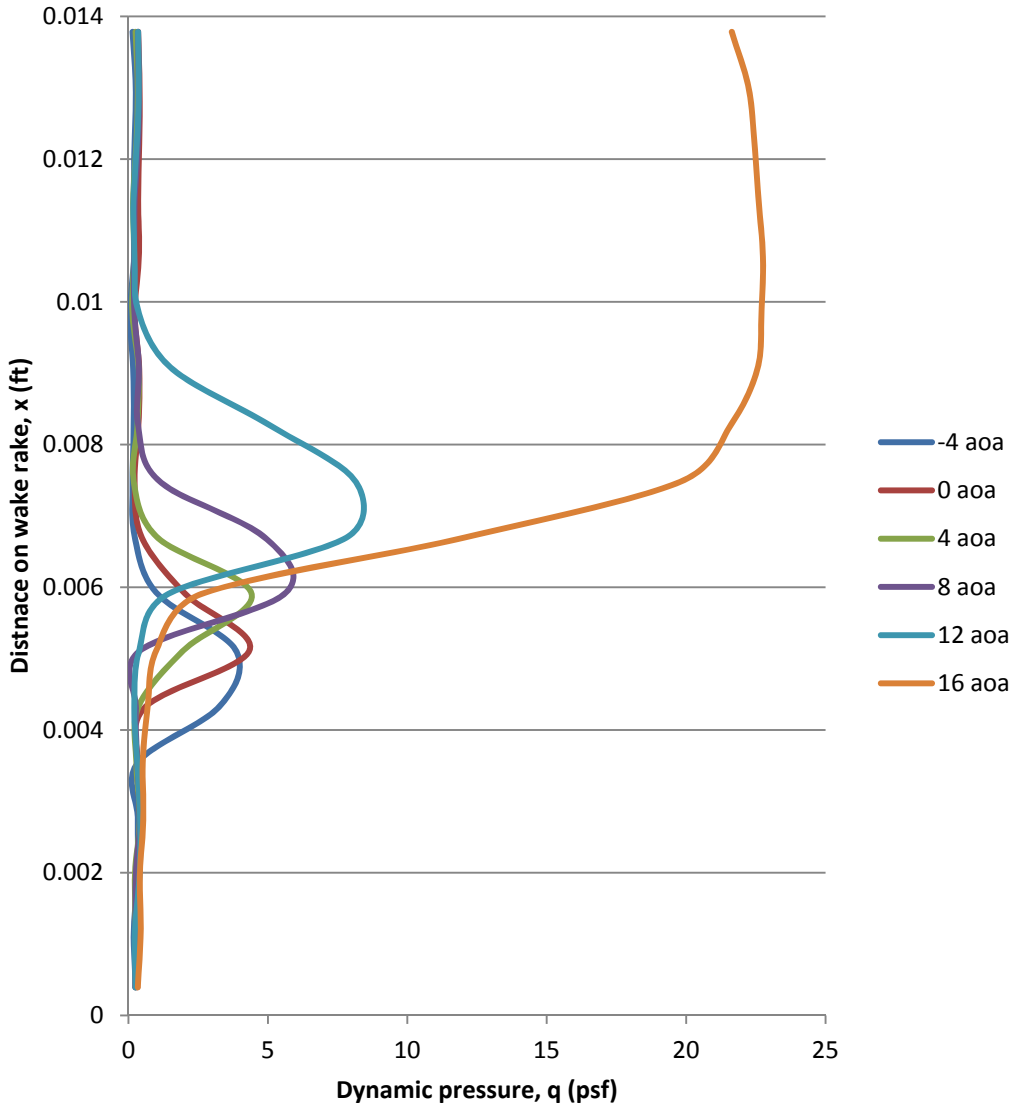

Figure 4.18 – Profile of wake at 68 MPH

Figure 4.19 is developed from the calculated c_d of the pressure data corresponding to equation 4.30.

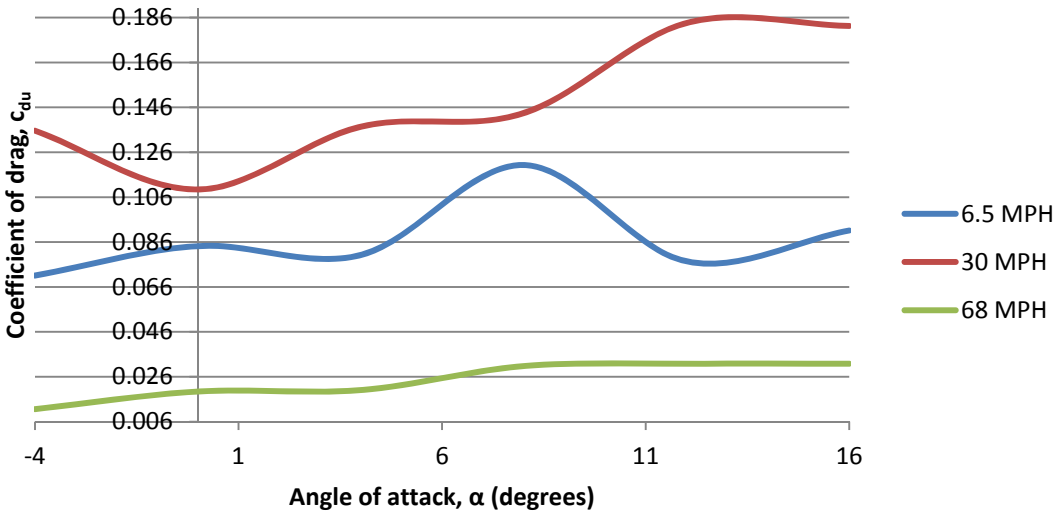

Figure 4.19 – Plot of the coefficient of drag vs. angle of attack

Figure 4.20 is plotted with the calculated wake blockage from equation 2.27.

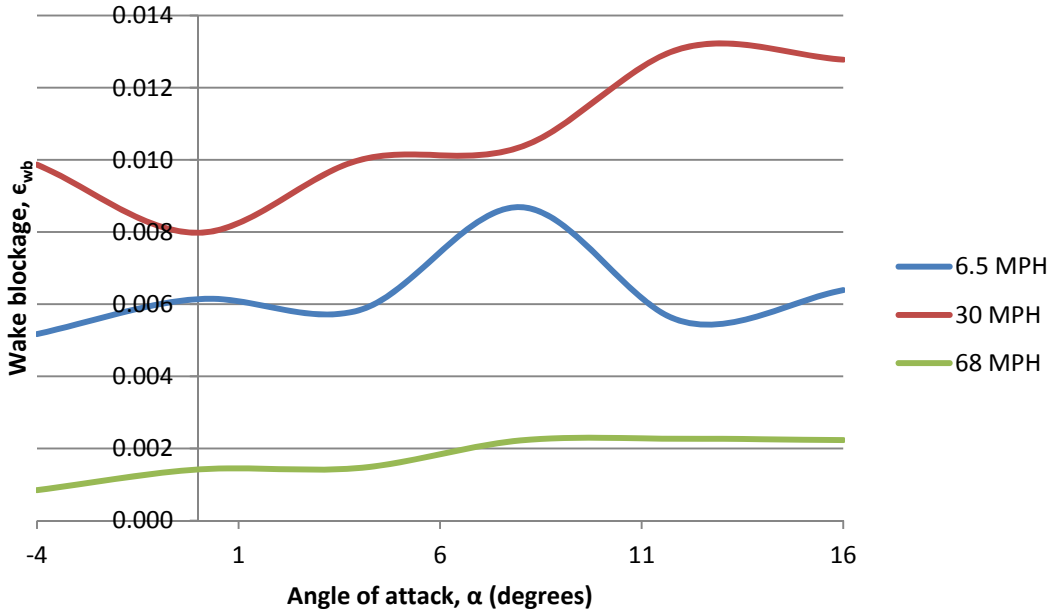

Figure 4.20 – Plot of the wake blockage vs. angle of attack

4.3.4 Discussion

The wake blockage for a two-dimensional shape depends heavily on the coefficient of drag and it is important to have complete data relating to the drag (skin friction and pressure). Without all the components for the drag, it is hard to calculate the correct wake blockage. It is also difficult to get a complete picture of the drag without developing an equation to model the pressures to integrate in equations 2.28 and 2.29. This point is illustrated in figure 4.19 where the c_d is greater for the case of the 30 MPH flow compared with the 6.5 MPH flow but both are higher for the 68 MPH flow. This is confusing because it would be expected that the c_d would slowly increase with flow speed to a certain point.

In figure 4.16, flow through the test section is so slow that that pressure sensors have a difficult time measuring any pressure change over the noise created by the senor itself. Figure 4.17 shows a more expect profile shape as the flow velocity increases. It can be seen that the flow is becoming steadier and when the test section velocity is increased to 68 MPH, the wake profile becomes very smooth and easily distinguishable from the normal flow conditions. Due to tunnel limitations, a 102 MPH run could not be performed due to the wake and solid blockage becoming so great, that it would "choke" the tunnel flow, and possibly damage some of the equipment.

Also, a consideration needs to be made that the wake rake did not measure the entire wake and therefore, the wake correction is left incomplete. This issue will lead to an incorrect c_d from being calculated. Since two of the main contributors of the wake blockage come from the wake calculations, the error could be significant.

4.4 Streamline Curvature Correction

4.4.1 Theory

For the streamlines, the presence of the ceiling and the floor prevents the normal curvature of the free flow that occurs about any lifting body, and relative to the straightened flow, the body appears to have more camber than it actually has. This is usually on the order of 1% for customary sizes. Accordingly, the airfoil in a closed wind tunnel has too much lift and moment force about the quarter chord at any given angle of attack as well as the angle of attack being too large itself. This effect is not limited to cambered airfoils but to any lifting body that produces a general curvature in the airstream.

To gain insight into the streamline curvature effect, it must be assumed that the airfoil in question is small and may be approximated by a single vortex at its quarter-chord point. The image system necessary to contain this vortex between the floor and ceiling consists of a vertical row of vortices about and below the real vortex. The image system extends to infinity both above and below and has alternating signs according to the section about the method of images that will be discussed in a later section. With the method of images, it can be seen that by considering the first image pair as shown in figure 4.22, it is apparent that the vortices induce no horizontal velocity since the horizontal components cancel but the vertical components add induced velocity.

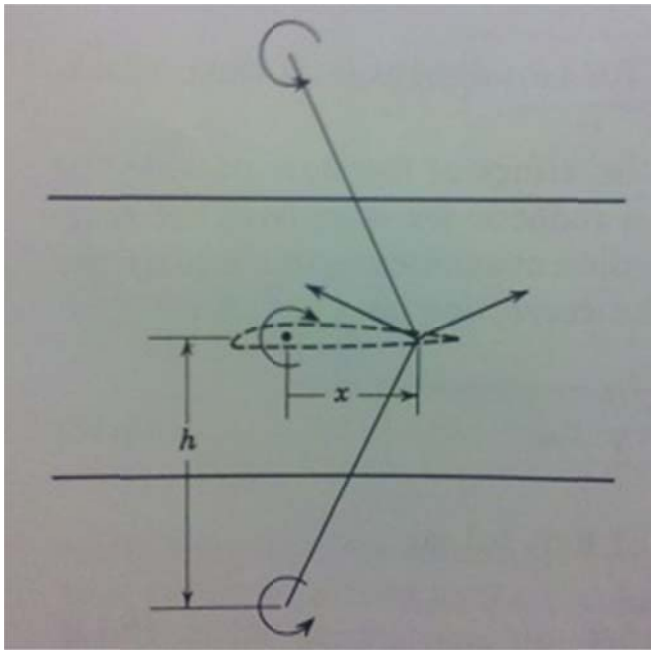

Figure 4.21 – Image system needed for the streamline curvature correction (Pope, 1984)

From simple vortex theory, the vertical velocity at a distance x from the lifting line will be

$$\omega_v = \frac{\Gamma}{2\pi}\frac{x}{h^2+x^2} \tag{4.31}$$

Substitution of reasonable values for x and h into the above equation reveals that the boundary-induced upwash angle varies almost linearly along the chord, and hence the stream curvature is essentially circular.

The chordwise load for an airfoil with circular camber may be considered to be a flat plate loading plus an elliptically shaped loading. The magnitude of the flat plate loaded is determined from the product of the slope of the lift curve and the boundary-induced increase in the angle of the tangent at the half-chord point because for a circular camber the curve at this point is parallel to the line connecting the ends of the camber line. The load is properly computed as an angle of attack correction.

4.4.2 Approach

To complete the corrections for the streamlines, the airfoil will need to be assumed to be a flat plate. A correction for the angle of attack is developed by

$$\Delta\alpha = (\frac{6\sigma}{\pi^2})c_l \tag{4.32}$$

where

$$\sigma = (\frac{\pi^2}{48})(\frac{c}{h})^2 \tag{4.33}$$

assuming that $(\frac{c}{h})^2$ is small compared to h^2 which is the first image pair. The second pair of vortices being twice as far away, will be roughly one-fourth as effective and the third pair, one-ninth. So that so that for the images above and below the real wing, we have

$$\Delta\alpha_{sc} = (\frac{1}{2\pi})\sigma c_l \tag{4.34}$$

The additive lift correction is

$$\Delta c_{l\,sc} = -2\pi(\frac{1}{2}\pi)\sigma c_l \tag{4.35}$$

and the additive moment correction is

$$\Delta c_{m_{\frac{1}{2}}sc} = (\frac{-\sigma}{4})\Delta c_{l\,sc} \tag{4.36}$$

The complete low-speed wall effects for two-dimensional wind-tunnel testing are located below if only the corrected term is needed. The data with the subscript u are uncorrected data and bases on free-stream, clear tunnel q, with the exception of drag which must have the buoyancy correction due to the longitudinal static-pressure gradient removed before final correcting.

The velocity correction is

$$V = V_u(1 + \varepsilon_{total}) \tag{4.37}$$

The dynamic pressure is

$$q = q_u(1 + 2\epsilon_{total}) \tag{4.38}$$

The Reynolds number is

$$Re = Re_u(1 + \epsilon_{total}) \tag{4.39}$$

The angle of attack is

$$\alpha = \alpha_u + \frac{57.3\sigma}{2\pi}(c_{lu} + 4c_{m_{\frac{1}{4}}u}) \tag{4.40}$$

where $c_{m_{\frac{1}{4}}u}$ comes from the moment force measured during wing-tunnel testing. The measure of $c_{m_{\frac{1}{4}}u}$ is from the wing testing and needs to have its own correction due the moment force being taken at a different spot than at the quarter-chord point. In figure 4.22, it can seen that the actual point of force measurement is located behind the quarter-chord and the equation to

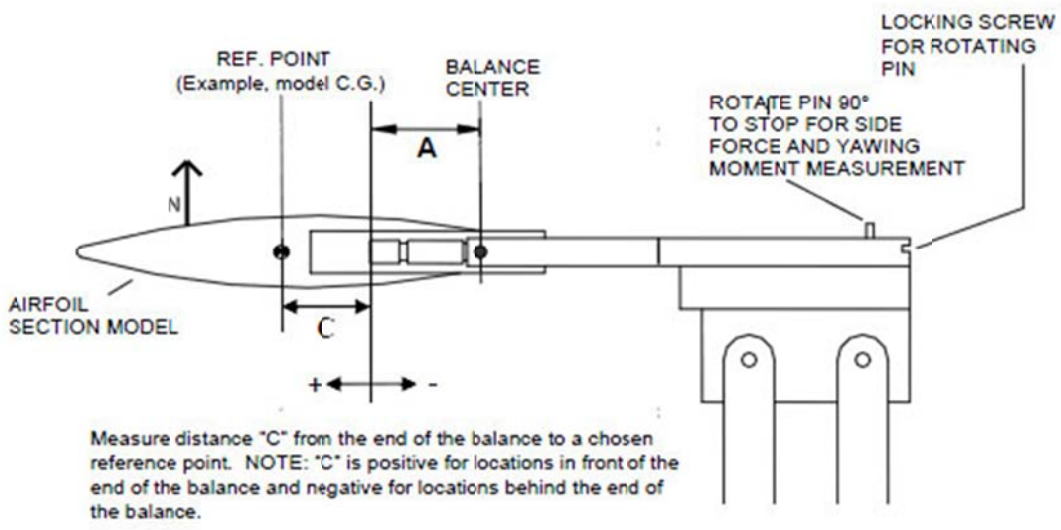

Figure 4.22 – Translation of moment to quarter-chord point on the Clark Y-14 (AEROLAB)

translate it to the quarter-chord point is

$$M_{\frac{c}{4}} = \left(\frac{M}{N} - (A + C)\right)N \tag{4.41}$$

where A is 1.135 inches for this wind-tunnel. With the $M_{\frac{c}{4}}$ determined, find $M_{\frac{c}{4}}'$ by

$$M'_{\frac{c}{4}} = \frac{M_{\frac{c}{4}}}{b} \tag{4.42}$$

$M'_{\frac{c}{4}}$ is used to calculate $c_{m_{\frac{c}{4}}}$

$$c_{m_{\frac{c}{4}}} = \frac{M'_{\frac{c}{4}}}{q_\infty c^2} \tag{4.43}$$

The coefficient of lift is

$$c_l = c_{lu}(1 - \sigma - 2\varepsilon_{total}) \tag{4.44}$$

where the coefficient of lift is derived from the pressure distribution over the wing. The pressure distribution is calculated by

$$c_p = \frac{P_s - (P_t - q_\infty)}{q_\infty} \tag{4.45}$$

Once the c_p has been determined, summing the area under the curve created by the $c_p$on the upper and lower surface of the airfoil, gives the c_l for a particular angle of attack and velocity. The coefficient of moment is

$$c_{m_{\frac{1}{4}}} = c_{m_{\frac{1}{4}u}}(1 - 2\varepsilon_{total}) \tag{4.46}$$

The coefficient of drag at 0 lift angle is

$$c_{d0} = c_{d0\,u}(1 - 3\varepsilon_{sb} - 2\varepsilon_{wb}) \tag{4.47}$$

4.4.3 Results

The results below are created from equations 4.34 -4.46.

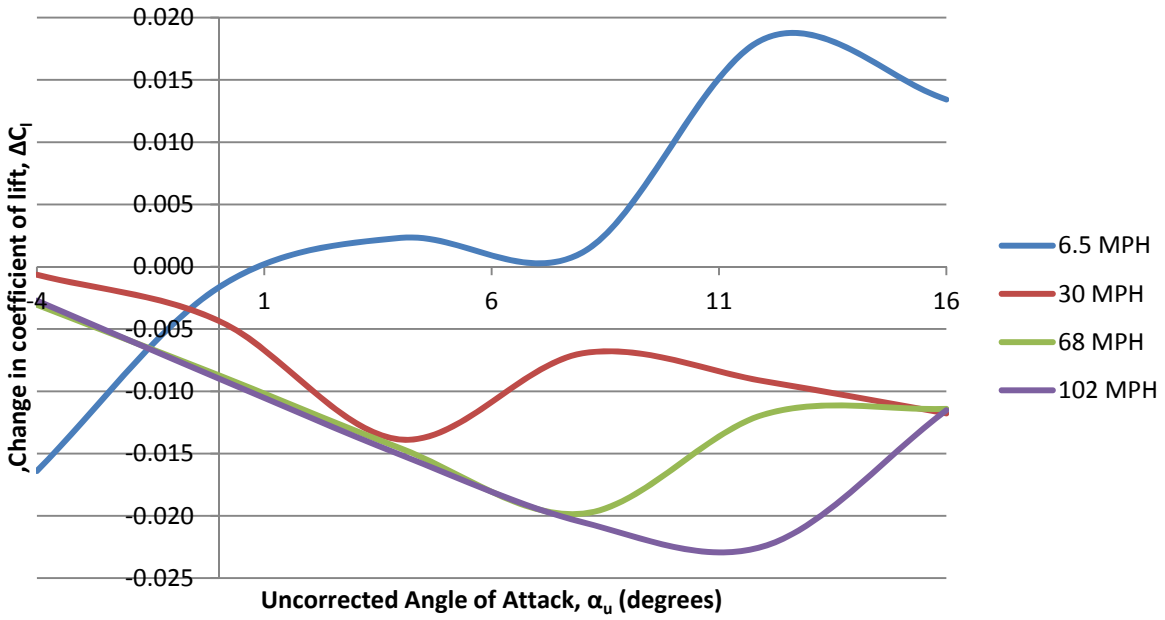

Figure 4.23 – Plot of ΔC_l vs. uncorrected angle of attack

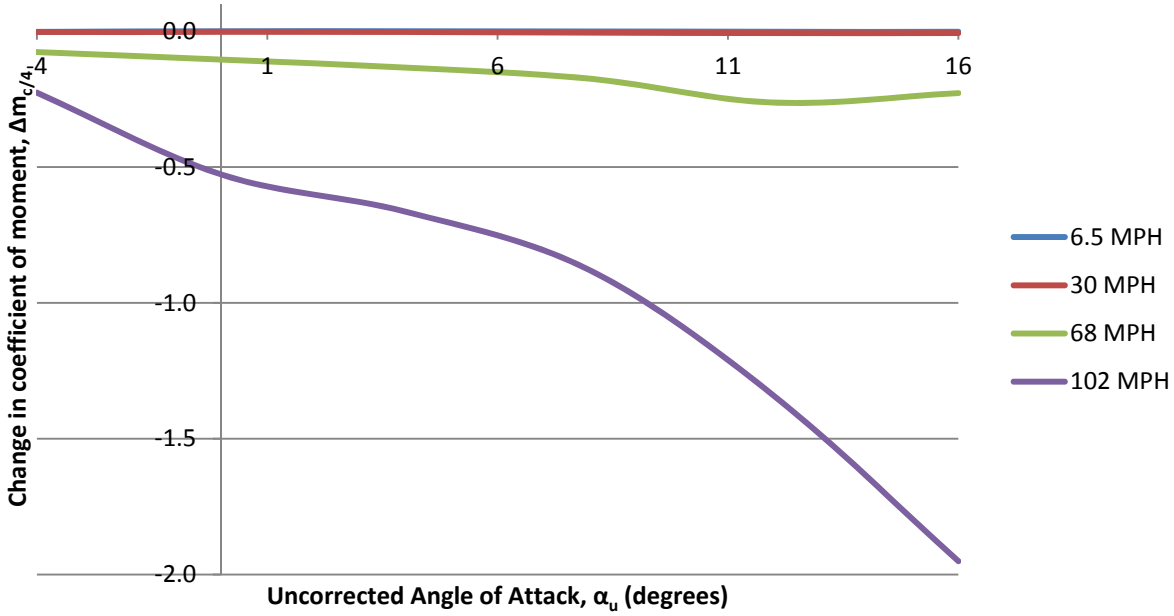

Figure 4.24 – Plot of $\Delta m_{c/4}$ vs. uncorrected angle of attack

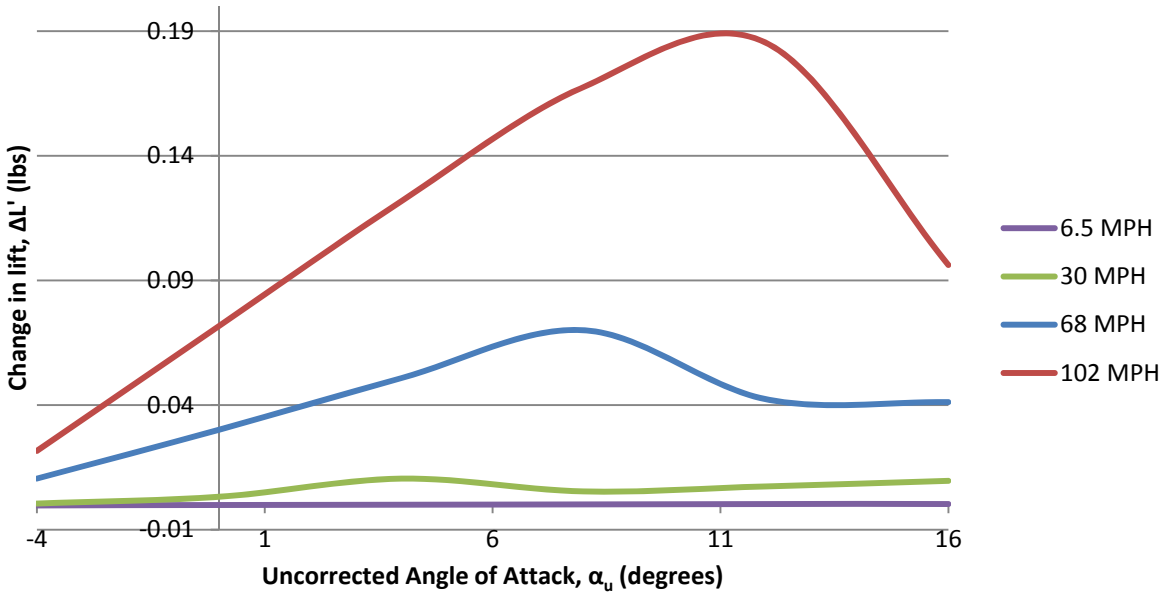

Figure 4.25 – Plot of ΔL' vs. uncorrected angle of attack

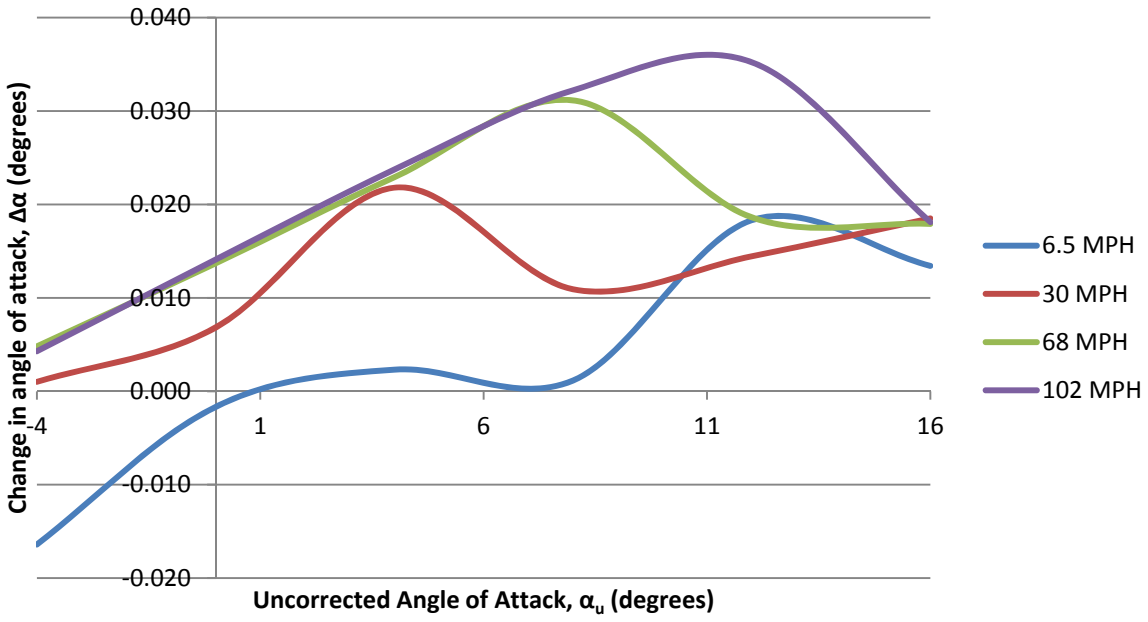

Figure 4.26 – Plot of Δα vs. uncorrected angle of attack

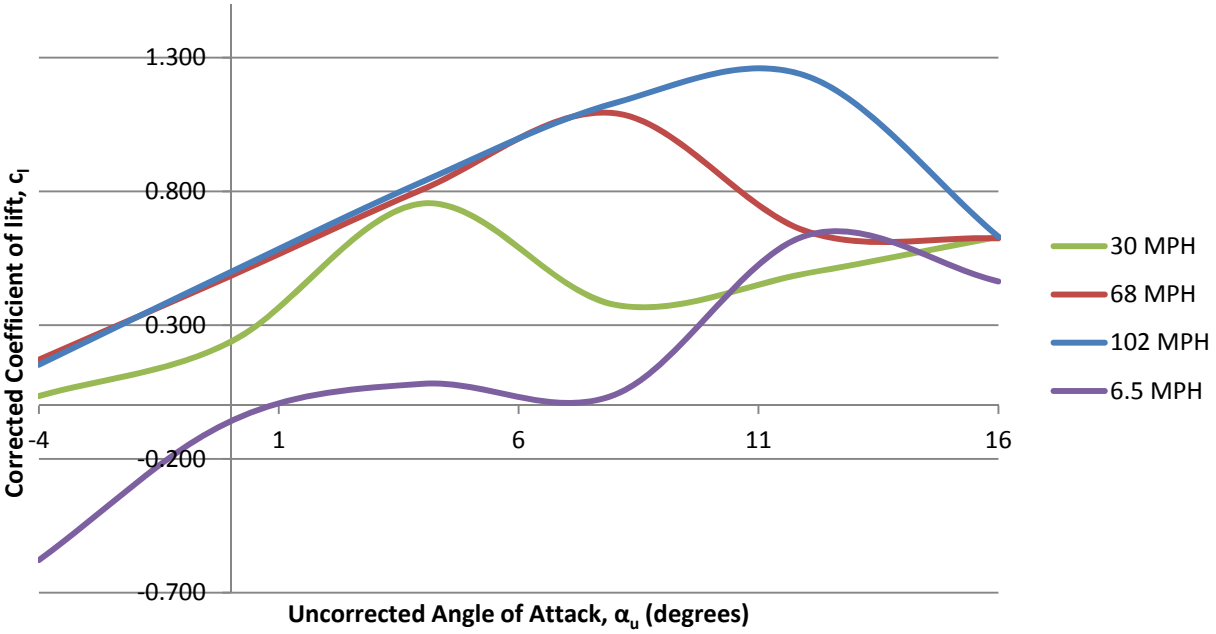

Figure 4.27– Plot of corrected C_l vs. uncorrected angle of attack

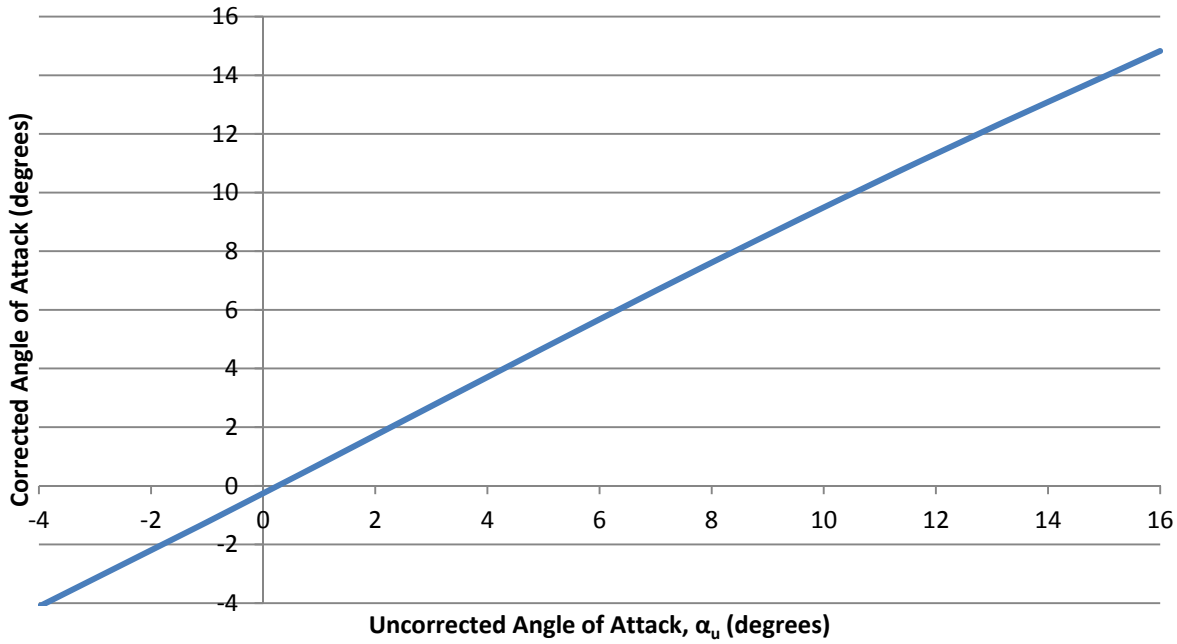

Figure 4.28 – Plot of corrected angle of attack vs. uncorrected angle of attack

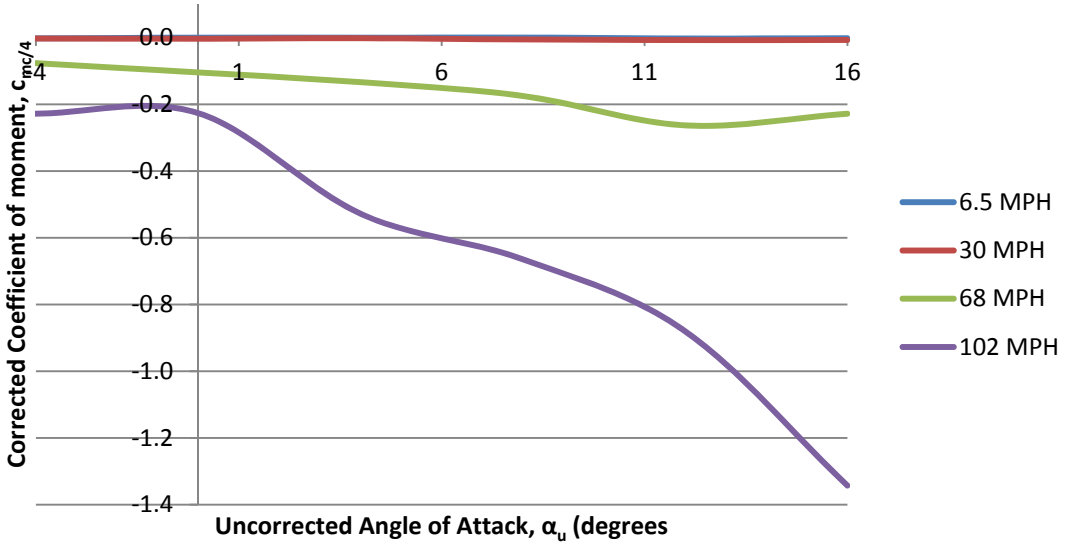

Figure 4.29 – Plot of corrected coefficient of moment vs. uncorrected angle of attack

The profile drag was created at the zero lift position of -3.5 degrees angle of attack and is in Table 1.

Uncorrected Velocity, V_U (ft/s)	Uncorrected Angle of Attack, α_u (degrees)	Uncorrected Coefficient of Drag, C_{d0u}	Corrected Coefficient of Drag, C_{d0}
9.53	-3.46	0.080	0.08
44.00	-3.67	0.150	0.15
99.73	-3.51	0.010400	0.0104

Table 1 – Uncorrected and corrected C_{d0}

4.4.4 Discussion

The correction mainly depends on the calculated c_l and the c_l comes from the pressure distribution over the airfoil. The airfoil has pressure ports from the 0 chord line position to the 80% of the chord line. The last 20% of the pressure distribution is not included due to any pressure readings after the 80% chord length. This introduces an element of error into the

calculations for total C_p and filters through to the calculation of total c_l. The corrected angle of attack vs. uncorrected angle of attack is as expected in that the figure 4.25 shows for any uncorrected angle of attack; the corrected angle of attack is lower. Also the Δc_l has a negative slope for most test sections airspeeds and behaves as expected. All the 6.5 MPH cases produced erratic results due to the flow speed itself and the very low Reynolds number plays an important role in the results. The corrected coefficient of moment is negative as expected but again, the 6.5 MPH case shows 0 correction factor required.

The C_{d0} calculations introduce the most error of all the corrections. The correction depends on the solid blockage and the wake blockage which as discussed previously, the wake blockage has a large error rate. The error is then multiplied by 3 times due to the equation used to calculate it. Another source of error is coming from the plotting of the c_l vs. c_d to determine the initial C_{d0} to correct. From published data for the Clark Y-12 and Clark Y-15, the correction is two orders of magnitude higher than it should be. Also the wake calculated for the c_d is incomplete at high angles of attack due to the wake rake not being long enough to capture the whole wake.

Chapter 5: Three-Dimensional Wall Corrections for the Clark Y-14 Wing

For a wing, there are several corrections that need to be performed to more accurately model free-flight conditions when data is collected from a wind tunnel. The four main wall corrections for an airfoil is buoyance, wake blockage, solid blockage and streamline curvature. The buoyancy corrections will have an additive component to the drag force while the wake and solid blockage component are dimensionless but are used in the correction for the streamline curvature. The streamline curvature corrections are the most important for correcting wing data and includes the corrections for $\Delta\alpha$, ΔC_L, ΔC_m and ΔC_{Di}. The velocities used in testing in the wind-tunnel are 6.5, 30, 68 and 102 MPH and the Reynolds numbers are 100,000, 500,000, 1,200,000 and 1,800,000 respectively. The data and calculations are located in Appendix C.

5.1 Buoyancy Correction

5.1.1 Theory

Closed-throat wind-tunnels have a variation of static pressure along the axis of the test section. The variation of static pressure is due to a thickening of the boundary layer as the flow progresses through the test section. As the flow approaches the end of the test section, the pressure progressively becomes more negative. With the pressure turning more negative down the length of the test section, the model tends to be sucked down the test section. The amount of buoyancy is usually insignificant for wings and airfoils but the correction becomes more important for fuselages and nacelles. The buoyancy corrections can be applied in a three-dimensional space. The philosophy behind the three-dimensional buoyancy correction is the same as the two-dimensional.

5.1.2 Approach

The approach to the three-dimensional case is very similar to the two-dimensional one. The process can be followed in section 4.1.2 down to equation 4.14. At the point, the buoyancy correction becomes

$$\Delta D_B = \frac{\pi}{4}\lambda_3 t^3 \frac{dp}{dl} \tag{5.1}$$

The λ_3 is determined by finding the fineness ratio of the shape being tested and in this case, the Clark Y-14 wing. The fineness ratio is calculated by the length of the shape being tested divided by the maximum thickness of the shape. The ratio is used to find the λ_3 by figure 5.1.

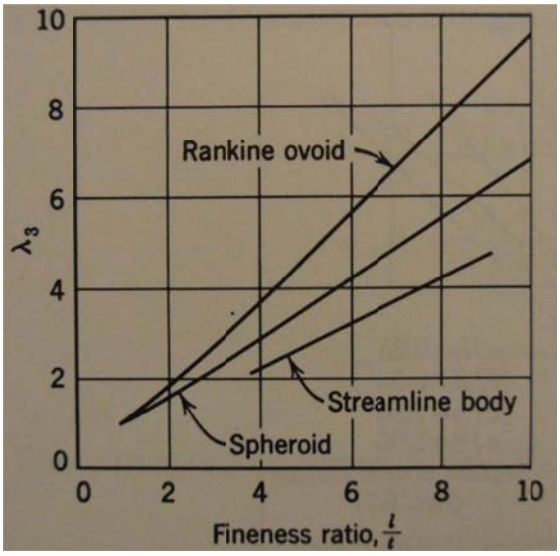

Figure 5.1 – Values of λ_3 vs. fineness ratio (Pope, 1984)

5.1.3 Results

The buoyancy correction was calculated using equation 5.1 and using the methods in section 4.1.2 to determine the pressure gradient through the test section. The buoyancy correction is plotted in figure 5.2 for M < .3.

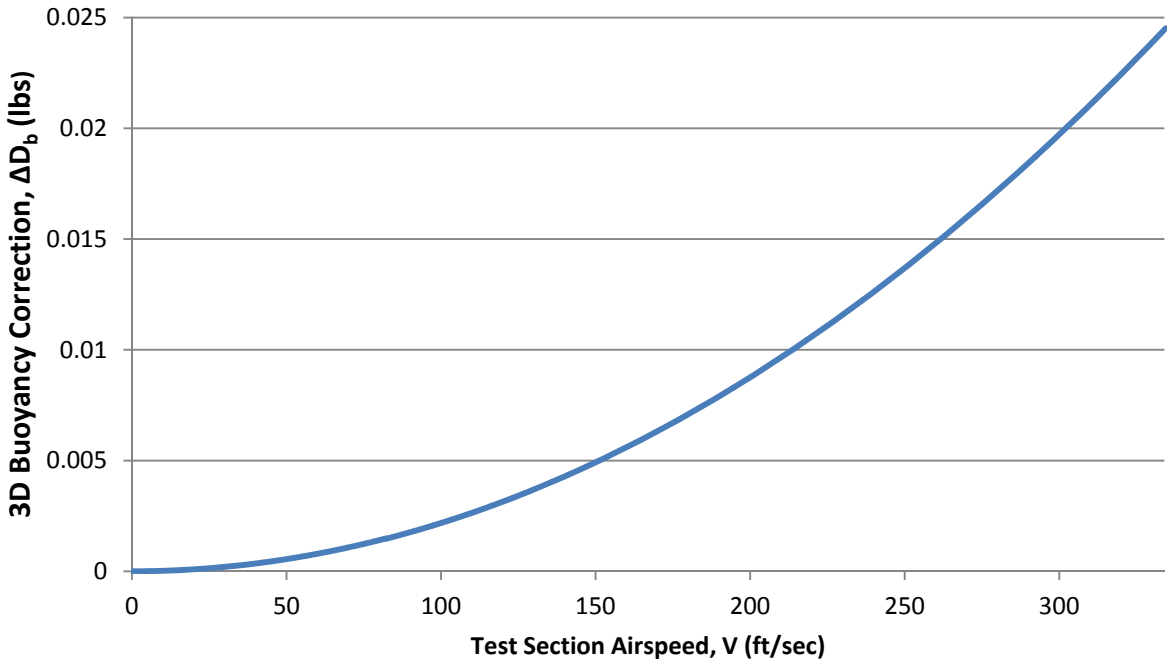

Figure 5.2 – Plot of the buoyancy correction vs. the test section airspeed

5.1.4 Discussion

The buoyancy for the wing is lower than that of the airfoil. This could be due to the airfoil covering the entire berth of the test section where the wing is only 80% of the test section berth. The calculated drag due to the buoyancy is a really small component of the overall drag. This small component is so small that it could be left out of the correction altogether and still represent less than .1% of the error in drag force.

5.2 Solid Blockage Correction

5.2.1 Theory

With a three-dimensional model in the test section, the flow is semi-blocked and the flow area is reduced. In order for continuity and Bernoulli's equation to be satisfied, the flow must increase in velocity to maintain the same mass flow rate through the test section. The increase of velocity

is considered solid blockage and is a function of model thickness, thickness distribution and model size. The camber of the airfoil is independent of the solid blockage. “The solid blockage velocity increment at the model is much less (about ¼) than the increment one obtains from the direct area reduction.” (Pope, 1984) The streamlines furthest from the model are also impacted by the increment velocity since they are displaced more due to the confines of the test section.

5.2.2 Approach

The solid blockage correction for a three-dimensional body follows the same procedures as in section 4.2.2. The approach for solid-blockage of a wing defined by Thom’s short-form equation is

$$\frac{\Delta V_{sb}}{V_u} = \in_{sb} = \frac{k(wing\ volume)}{C^{\frac{3}{2}}} \tag{5.2}$$

where k is .90 for a wing and .96 for a body of revolution. Solid-blockage for a wing-body system is a combination of simply the sum of each component as determined from their respective equations. This will give you the total solid blockage for the entire system.

5.2.3 Results

Applying equation 5.2 to the Clark Y-14 wing and using a k value of .90, the solid blockage is plotted in figure 5.3 for test section velocities of M < .3. The cross-sectional area was derived from the process used in 4.1 and those C values were used in the solid blockage for a wing.

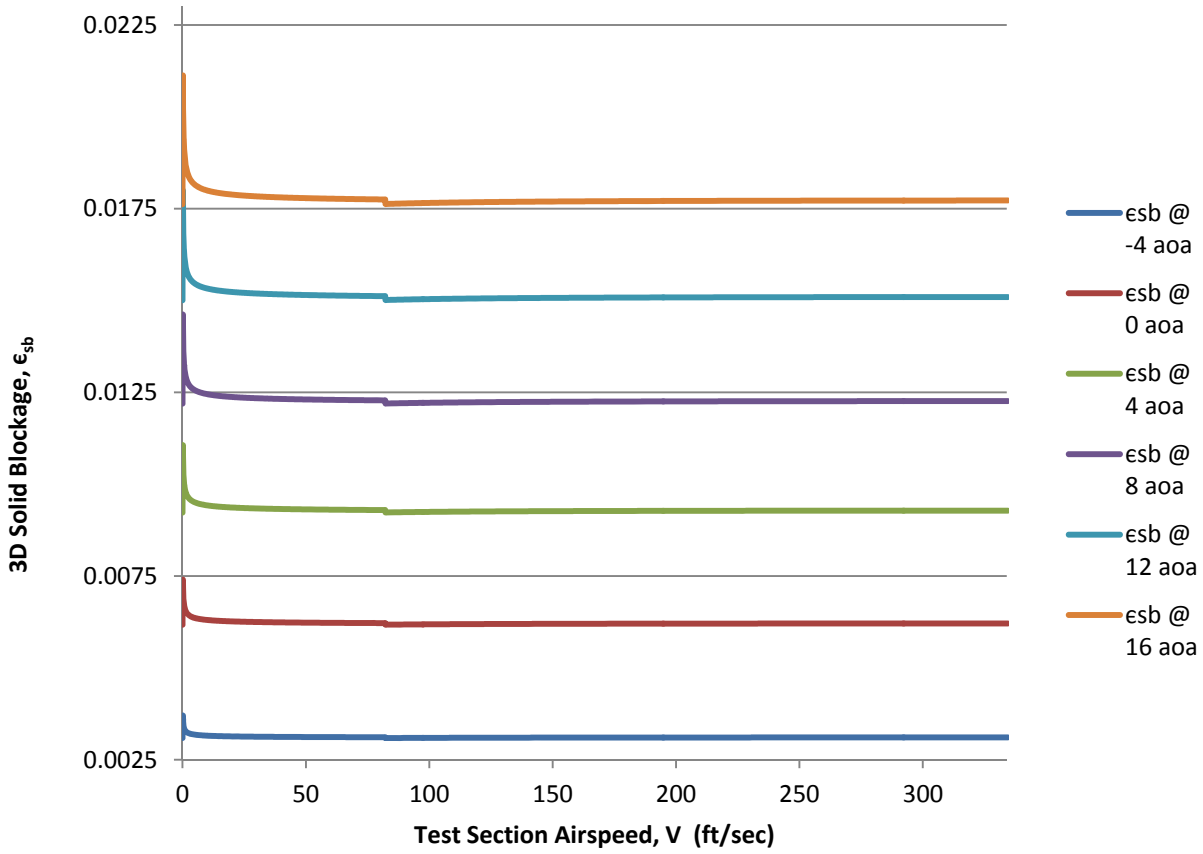

Figure 5.3 – Plot of the solid blockage for the Clark Y-14 wing

5.2.4 Discussion

The solid blockage is greater for the wing compared with the airfoil's solid blockage in section 4.2. This makes sense because the wing blocks more area in the flow as the angle of attack increases than an airfoil. But wing's solid blockage follows the same pattern as the airfoil as the velocity increases.

5.3 Wake Blockage Correction

5.3.1 Theory

All bodies, two-dimensional and three-dimensional, create wake with the fluid they are moving through and bodies in wind tunnels are not exempt. The law of continuity states the velocity outside the wake in a closed tunnel must be higher than the free stream velocity in order for a constant volume of fluid to flow through the test section. For the three-dimensional case, Maskell's three-dimensional method is utilized. The Maskell's method accounts for the effects of momentum outside the wake when separated flow occurs. This added effect from the momentum is added by the lateral wall constraint on the wake and results in lower wake and model base pressure than what would occur in the free flow condition. (Maskell, 1965) Maskell demonstrates that wake blockage yields results similar to their higher speed counter parts on the same model. The natural tendency for the wake is toward the axial symmetry which permits a single correction.

5.3.2 Approach

The wake blockage correction for streamline flow follows the loci for the two-dimensional case in section 4.3.2 as far as the wake is simulated by a source of strength

$$Q = \frac{D}{\rho V} \tag{5.3}$$

which is matched for continuity by adding a downstream sink of the same strength. However for the three-dimensional case, the image system consists of a doubly infinite course-sink system space a tunnel height apart vertically and a tunnel width apart horizontally. The axial velocity induced at the model by the image source system is again zero, and due to the image sink system is

$$\epsilon_{wb} = \frac{\Delta V}{V_u} = \frac{S}{4C} C_{Du} \tag{5.4}$$

The increased drag due to the pressure gradient may be subtracted by removing the wing wake pressure draw by

$$\Delta C_{Dw} = \frac{K_1 \tau_1 (wing\ volume)}{C^{\frac{3}{2}}} C_{Du} \tag{5.5}$$

where K_1 is derived from figure 5.4

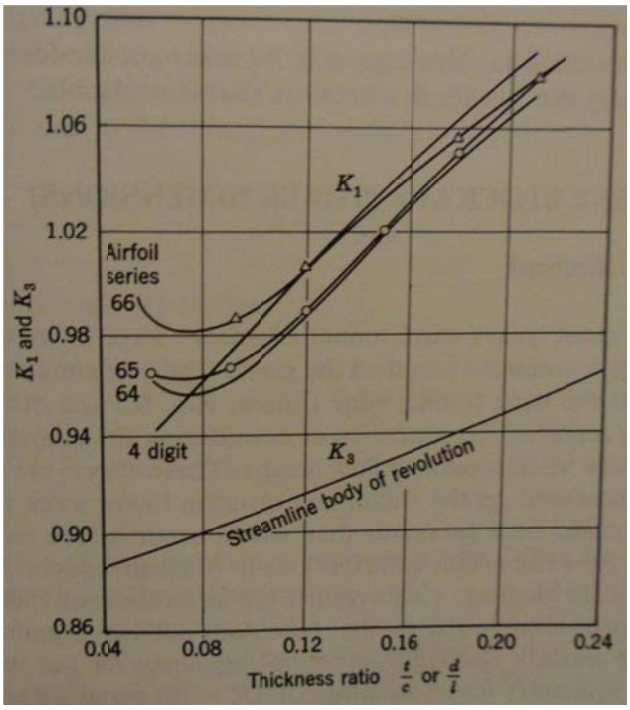

Figure 5.4 – Values of K_3 and K_3 for a number of bodies

The C_{du} for the wing is calculated by using the force data generated by test completed in the AEROLAB wind-tunnel. The force data is generated by the 3-component force/moment sting balance. The normal and axial forces measured by the sting balance had equation 2.2 applied to convert the raw data to a drag force. To convert the drag to into its coefficient form, apply

$$C_{Du} = \frac{D}{q_\infty S} \tag{5.6}$$

Using the C_{Du} calculated from the wind-tunnel data, the wake blockage and change to the C_D due to the wake can be found.

5.3.3 Results

The calculated C_{Du} is shown in figure 5.5 and the ϵ_{WB} is shown is figure 5.6.

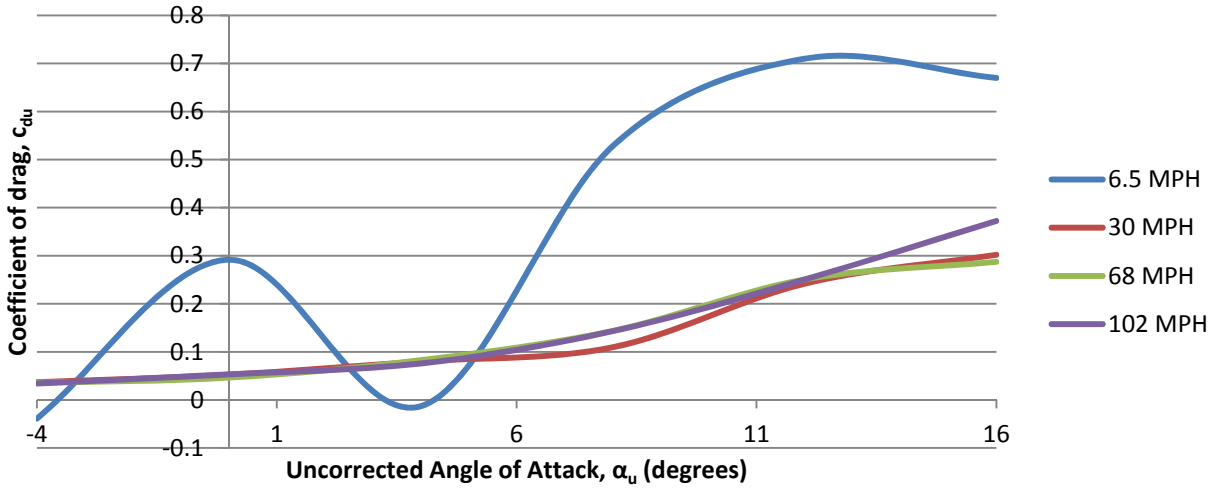

Figure 5.5 – Plot of the angle of attack vs. the coefficient of drag

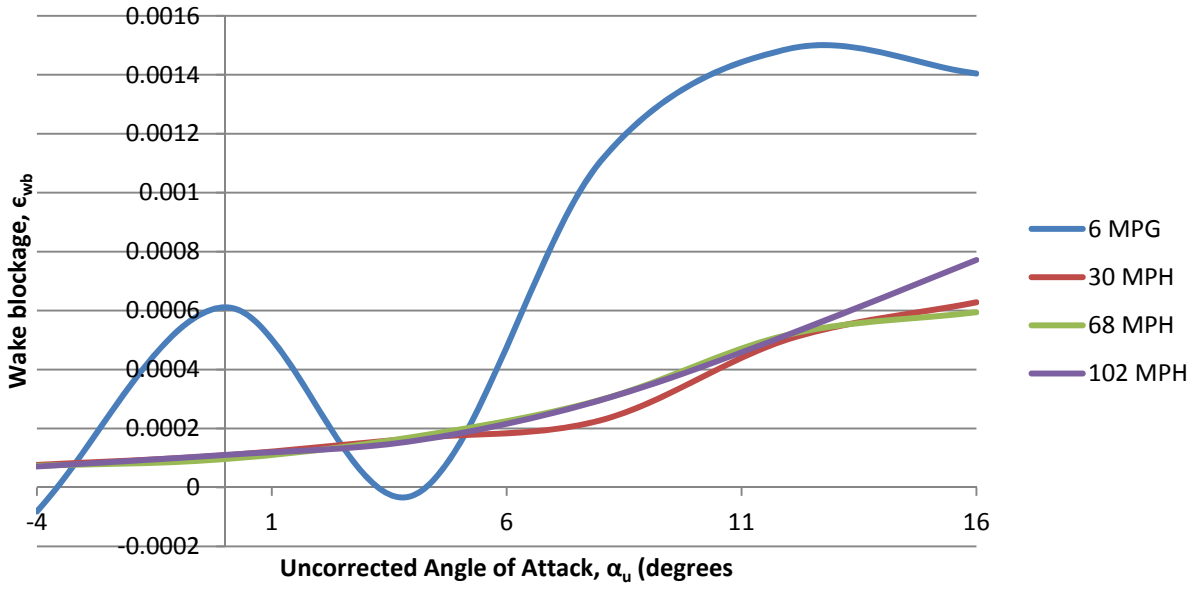

Figure 5.6 – Plot of the angle of attack vs. wake blockage

5.3.4 Discussion

When comparing figures 5.5 and 5.6 to each other, it can be seen that the two plots are highly coupled together. The coefficient of drag is the dominating factor in the wake blockage correction. The correction for the coefficient of drag could not be completed due to the Clark Y-14 not being graphed in figure 5.4 even though the thickness ratio is known for the Clark Y-14. Being able to determine the correction factor for the coefficient of the drag is extremely important and without it, the drag cannot be corrected.

5.4 Method of Images

5.4.1 Theory

Method of images has many applications in modern engineering from aerospace to electrical. Method of images can be used in any application where the item of interest is located inside a field. In electrical engineering, one example of its use is to determine a conductor's change in an electromagnetic field whereas in aerospace, method of images can be used to determine the downwash on a wing or airfoil in a wind-tunnel. A wing being flown in nature close to the ground can have method of images applied to determine the downwash. Downwash is defined as a small velocity component in the downward direction at the wing and is caused by the wing-tip vortices downstream of the wing. The wing-tip vortices induce a small downward velocity component in the neighborhood of the wing by the vortices "dragging" the surrounding air around them and this motion induces a small downward velocity component on the wing. (Anderson, 2007) The downwash then combines with the V_∞ to produce a local relative wind that the wing encounters. The downwash caused by these wing-tip vortices become very important when the wing is located in a confined space such as a wind-tunnel. When the airflow is confined by the walls of the wind-tunnel, downwash produces a higher induced velocity (ω) on the wing

which creates a moment on the wing. Figure 4.1 illustrates what occurs when the induced velocity from the downwash acts upon a finite wing. The moment created on the wing by the induced velocity introduces the induced angle of attack (α_i) component to the wing. While pilots only care about the effective angle of attack (α_{eff}), engineers care greatly about the induced angle of attack. The induced angle of attack adds to the effective angle of attack to equal the geometric angle of attack (α). The induced angle of attack reduces the local angle of attack the wing encounters but adds to the drag (D) the wing experiences in the form of induced drag (d_i). The induced drag is defined as a component of the

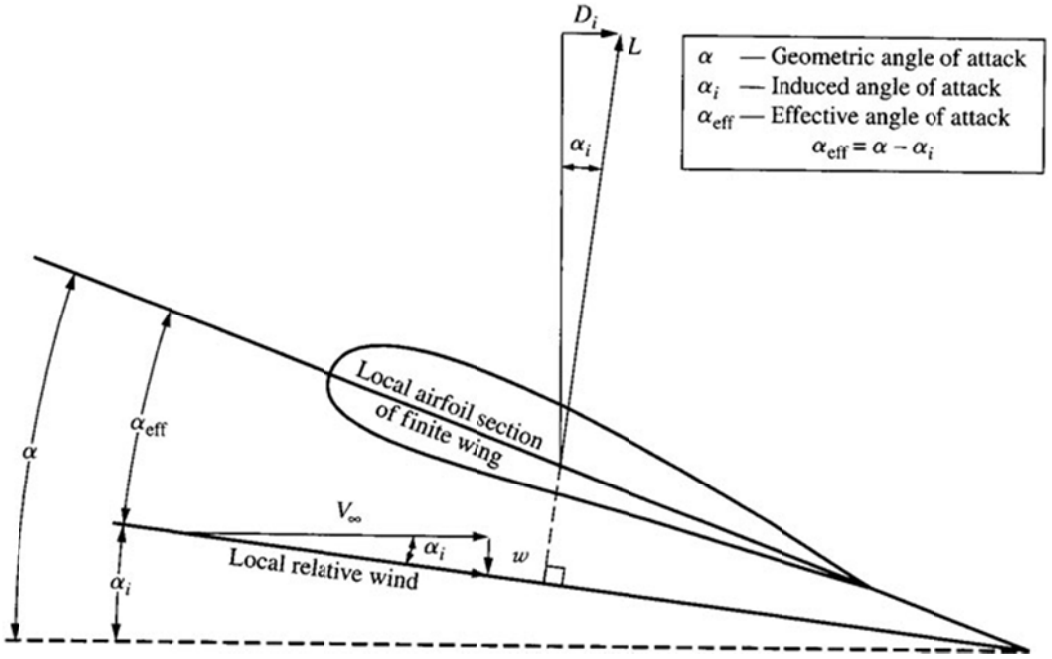

Figure 5.7 - The effects of downwash on a finite wing to produce induced drag (Anderson, 2007)

total drag on the wing due to the downwash of the airstream passing over it. The induced drag can be approximated by equating the L multiplied by the tangent of the induced angle of attack. (Anderson, 2007) Because of the confined space of the wind-tunnel, the downwash affects the wing more than if it was unconfined, hence the need for a correction of the induced drag

gathered from wind-tunnel data. An application of method of images is to correct for the inflated induced drag on the wing due to the wind tunnel walls. To apply this method, the wing can be replaced with a vortex system composed of a lifting line vortex and a pair of trailing vortices. A solid body, like a wing, can be represented by a source-sink system where the body is located and the wake can be represented by a source. (Pope, 1984) Using this vortex system can produce accurate results to any degree necessary. The solid boundary of the wing is formed by the production of a zero streamline matching the solid boundary. After the image system is established for the wing, the system can be applied for a closed rectangular wind-tunnel. It should be noted that the two-dimensional application of method of images only applies if the downwash is needed along the lifting line and the three-dimensional application is necessary to get induced upwash after the wing, the streamline curvature effect or the correction for the wing with a lot of sweepback. (Pope, 1984)

To setup the image system, take the image and replicate the opposite sign of the image system as demonstrated in figure 5.8 where one vortex A is bound by two walls 1 and 2. To correctly setup

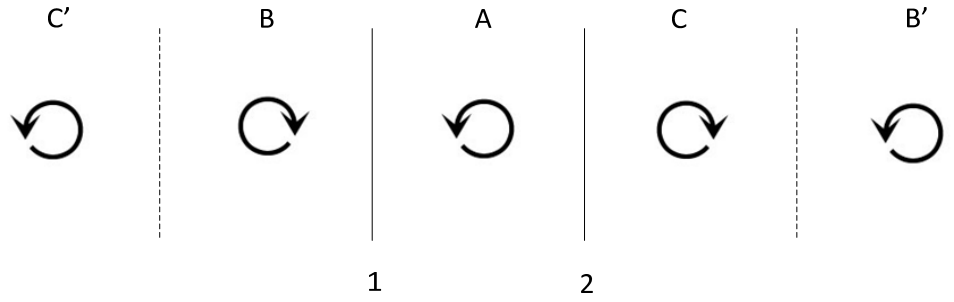

Figure 5.8 - Single vortex arrangement for simulation with vertical boundaries

the images, second vortex is created that is assigned the opposite sign of A to wall 1 which is vortex B. Vortex C is the same sign as B and created opposite side of wall 2. The higher the order of accuracy needed, more images are needed in the system in order for the system to be

balanced. With the addition of vortex B and C, there images need to be created with vortex B' and C'. Vortex B' is added to the opposite side of vortex B and is assigned the opposite sign of vortex B. The same concept is applied to vortex C and all additional vortices needed for the desired accuracy. For the case of a rectangular test section of a wind-tunnel, figure 5.10

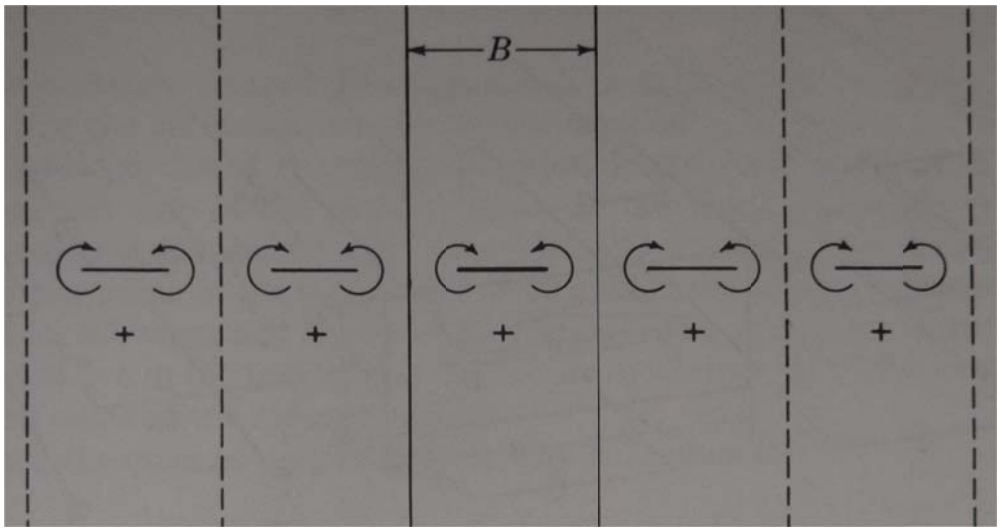

Figure 5.9 - Vortex image system for the horizontal simulation of wing in a rectangular test section (Pope, 1984)

demonstrates the vertical walls component and figure 5.9 demonstrates the horizontal walls and

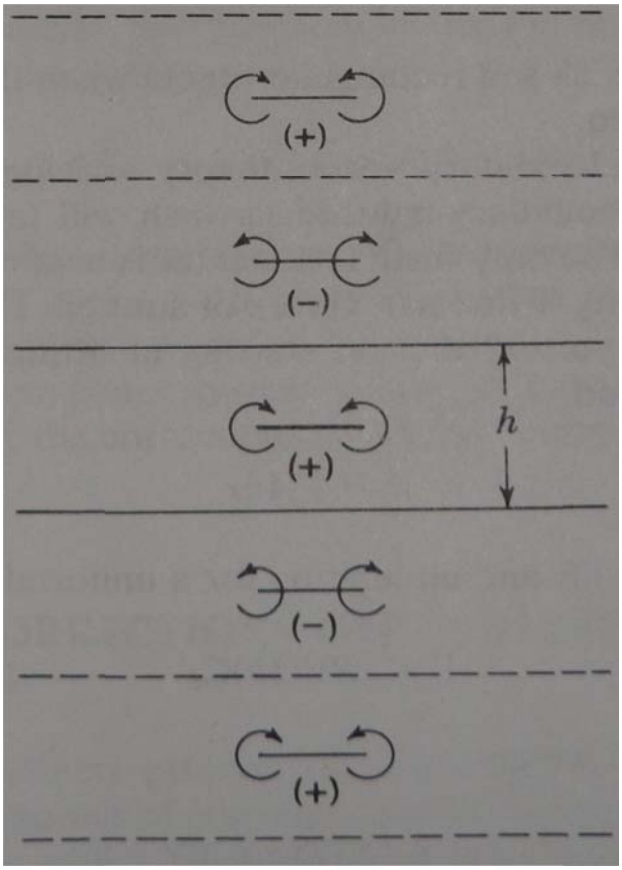

Figure 5.10 - Vortex image system for the vertical simulation of wing in a rectangular test section (Pope, 1984)

shows the image system becomes a doubly infinite system of vortices. (Pope, 1984) For a wing in a closed rectangular test section where the three-dimensional quantities are required is shown in figure 1.5.

5.4.2 Approach

With the use of elementary vortex theory and the expression for the induced velocity due to the vortex strength (Γ) at a distance (r) from each bound vortex. The expression applies to a semi-infinite vortex starting at the lifting line and trailing to infinity in the aft direction. The induced velocity is

$$\omega = \frac{\Gamma}{4\pi r} \tag{5.7}$$

and combined with the strength of a vortex equation which is formed from the relationship between the circulation for a uniformly loaded wing and lift is

$$\Gamma = (\frac{SV_\infty}{2b})C_L \tag{5.8}$$

produces;

$$\omega = (\frac{SV_\infty}{8\pi rb})C_L \tag{5.9}$$

For each image of the vortex where the vortex applies a downwash on the wing, the induced velocity is calculated. Since the positive direction is considered the down direction, the calculated induced velocity is subtracted from the induced velocity calculated for the wing simulated in the test section.

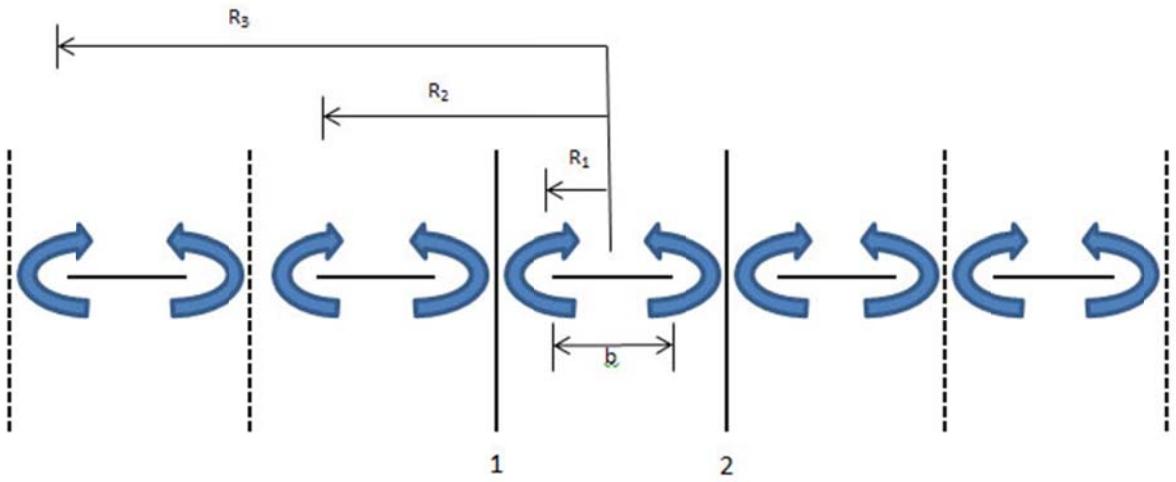

Figure 5.11 – Vortices image setup to calculate the induced velocity

The wing in free flight produces an induced velocity on itself and that is found by

$$\alpha_i = \frac{\omega}{V} = \frac{\frac{SV}{8\pi Rb}}{V} C_L \tag{5.10}$$

The coefficient of lift for the wing is found by using the axial and normal forces measured in the tunnel by the sting balance, then applying equation 2.1 to get the lift. Once the lift is calculated for the wing, the C_L is found by

$$C_L = \frac{L}{q_\infty S} \tag{5.11}$$

The correction to the angle of attack comes from the summing of equation 5.10 of all the images but does not include the wing itself. When the sum of the change of the angle of attack is added the induced angle of attack that the wing experiences in free flight, the total induced angle of attack is found for in the tunnel.

$$\Delta\alpha_i = \sum \frac{\omega}{V} \tag{5.12}$$

Now the corrected $C_L$needs to be introduced to determine the ΔC_{Di} to calculate the corrected C_{Di}. Since the cosine of the angle between the lift and lift component created in the wind-tunnel is one, the

$$C_L \cong C_{L\,c} \tag{5.13}$$

The induced drag coefficient can be written as

$$C_{Di} = \propto_i C_L \tag{5.14}$$

and the change in the induced drag caused by the boundary induced downwash becomes

$$\Delta C_{Di} = \Delta\alpha_i C_{L\,c} \tag{5.15}$$

This method will need to be modified to calculate the downwash on bigger models over the 80% cross section length of the test section width.

5.4.3 Results

Using the method of images, figures 5.12 and 5.13 were plotted against the angle of attack for the correction factor of $\Delta\alpha$ and Δc_{di}, respectively.

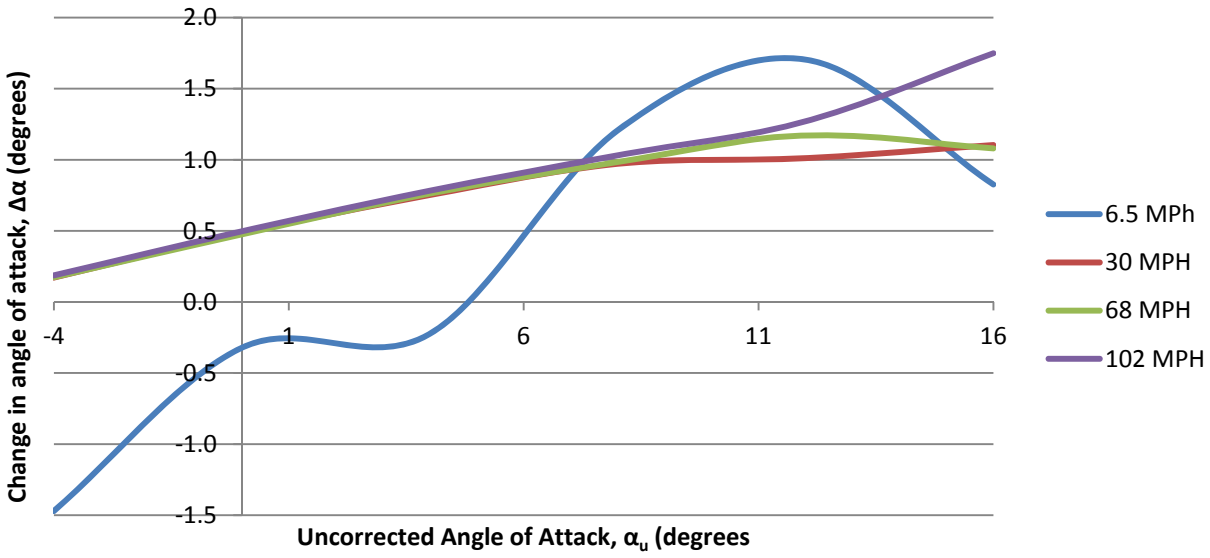

Figure 5.12 – Plot of Δα vs. the α_u

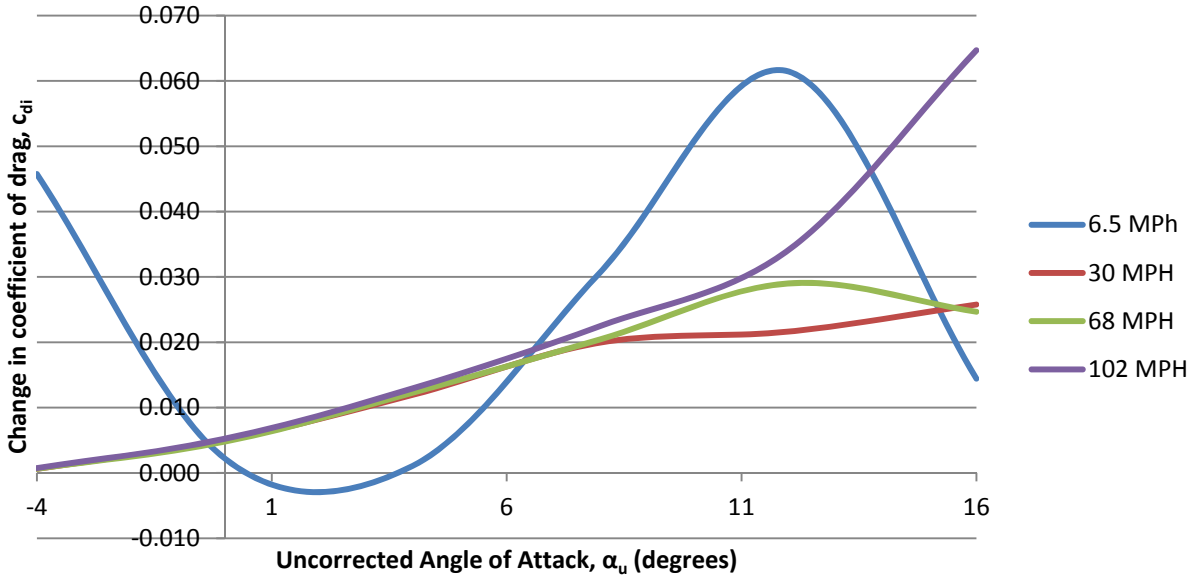

Figure 5.13 – Plot of Δc_{di} vs. the α_u

5.4.4 Discussion

The method of images is an accurate way of determining corrections utilizing the image methodology. As seen from these plots, the run at 6.5 MPH, gives the most problematic data but

other runs seem to align with each other except at high angles of attack. At high angles of attack, the correction becomes larger and is expected based on the method used to develop the correction equations.

5.5 Streamline Curvature Correction

5.5.1 Theory

The corrections for the streamline curvature for three-dimensional testing follows the same as for protocol the two-dimensional case in that they are concerned with the variation of the boundary-induced upwash along the chord. Once again the variation turns out to be essentially a linear increase in angle so that the streamlines curvature effects may be treated as the loading on a a circular arc airfoil. Similarly, the loading is treated as a flat-plate effect based on the flow angle change between the quarter and half chord, and an elliptic load based on the flow angle change between the half and three-quarters chord but for the three-dimensional case, the image system is vastly different from the simple system for two dimensions.

The three-dimensional image system as in figure 1.5 where basically it consists of the real wing with its bound vortex and its trailing vortices. The vertical boundary is simulated by the infinite system of horseshoe vortices and the horizontal boundaries by the infinite lateral system. Linking the two systems are the infinite diagonal system. The effect of the doubly infinite image system at the lifting line of the real wing is the main boundary upwash effect. Mostly the area of interest is in the change of the upwash along the chord and along the span as well.

5.5.2 Approach

The total additive correction for the angle of attack is

$$\Delta\alpha_c = \frac{c}{4}(\Delta\alpha_i) \tag{5.16}$$

The additive lift correction is

$$\Delta C_{L\,c} = -\Delta\alpha_c(a) \tag{5.17}$$

where a is the wing lift curve slope which is plotted from the data collected from wind-tunnel test on the Clark Y-14 wing.

The additive correction to the moment coefficient is

$$\Delta C_{m\,c} = -\Delta C_{L\,c}(.25) \tag{5.18}$$

5.5.3 Results

The wing lift slope curves were created for each Reynolds number and is shown in figure 5.14 - 5.17.

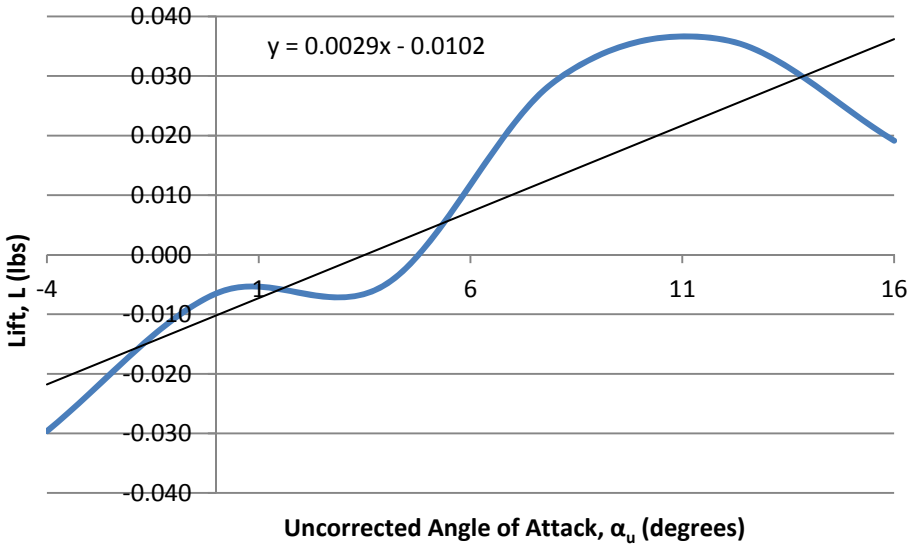

Figure 5.14 – Wing lift slope curves for 6.5 MPH

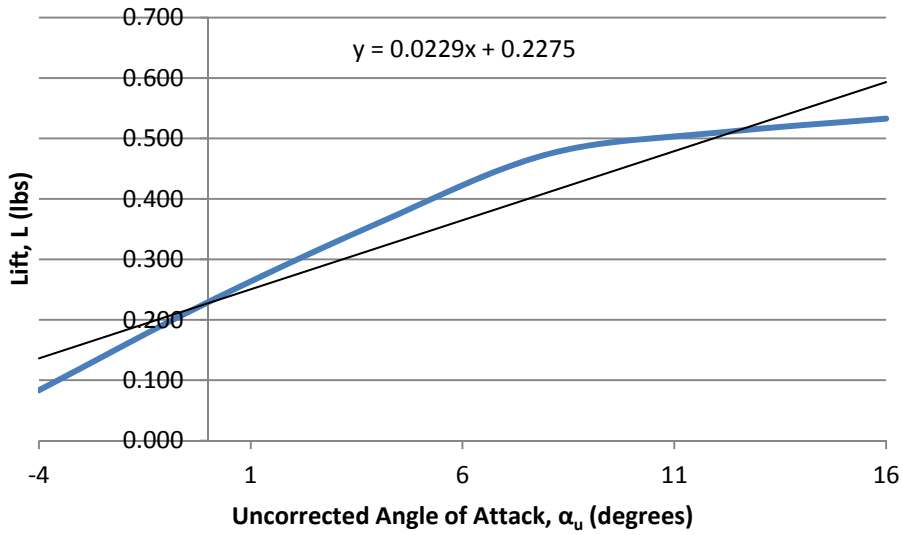

Figure 5.15 – Wing lift slope curves for 30 MPH

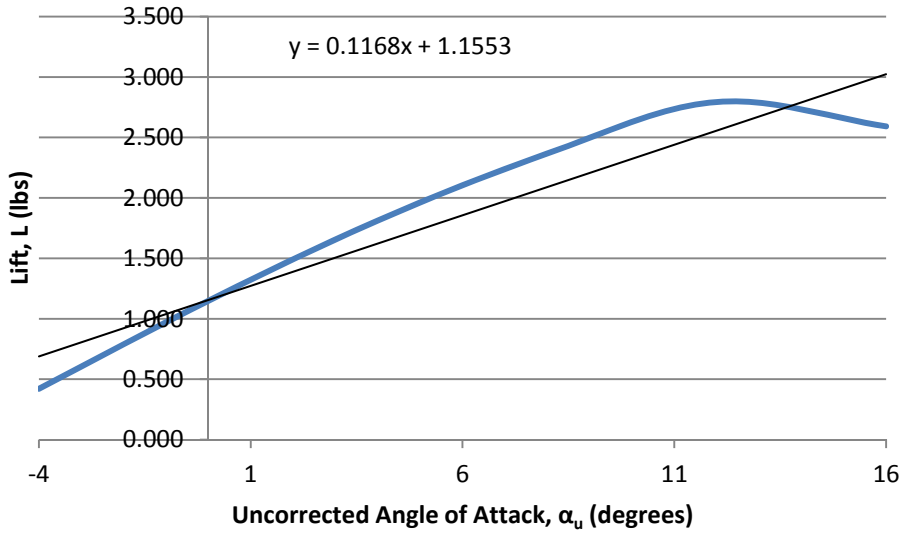

Figure 5.16 – Wing lift slope curves for 68 MPH

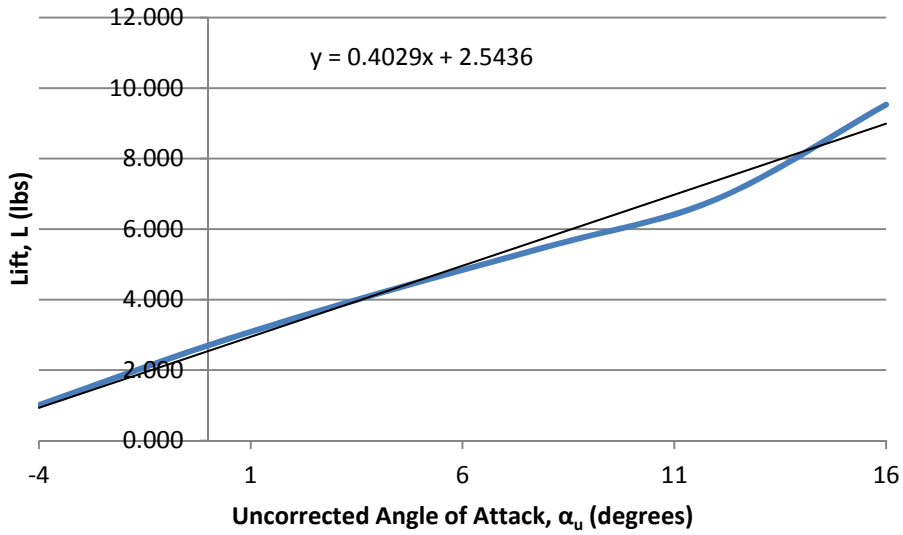

Figure 5.14 – Wing lift slope curves for 102 MPH

Figure 5.18 – 5.20 are derived from the corrections discussed in this section.

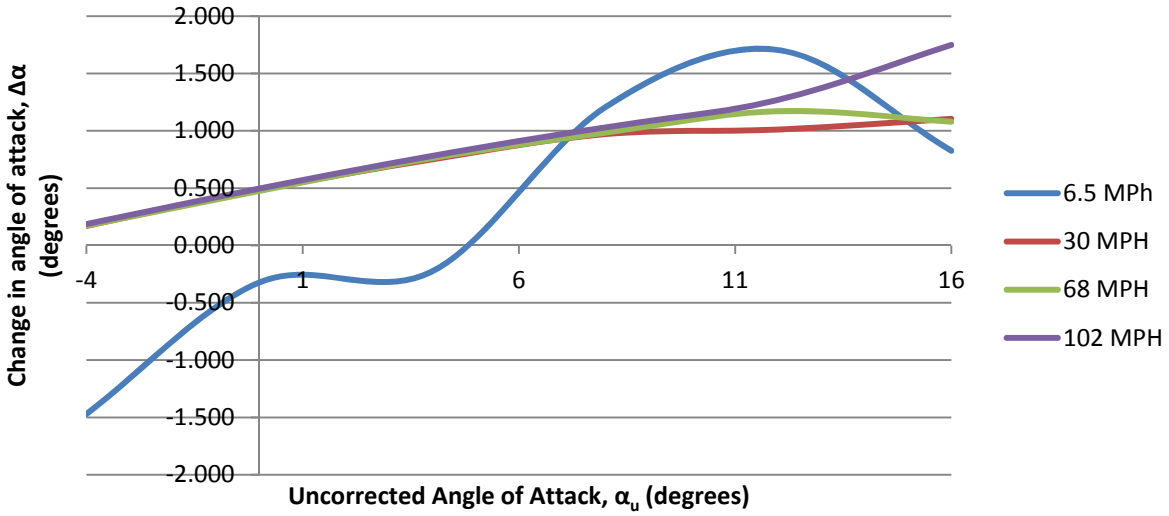

Figure 5.18 – Plot of the change in the angle of attack vs. uncorrected angle of attack

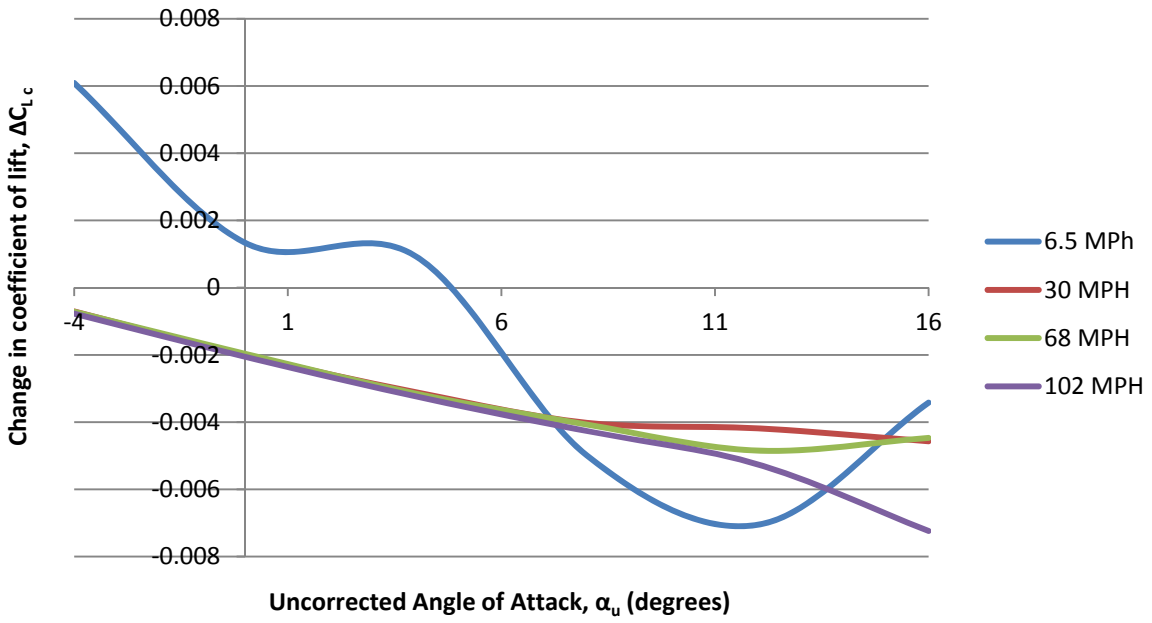

Figure 5.19 – Plot of the change in coefficient of lift vs. uncorrected angle of attack

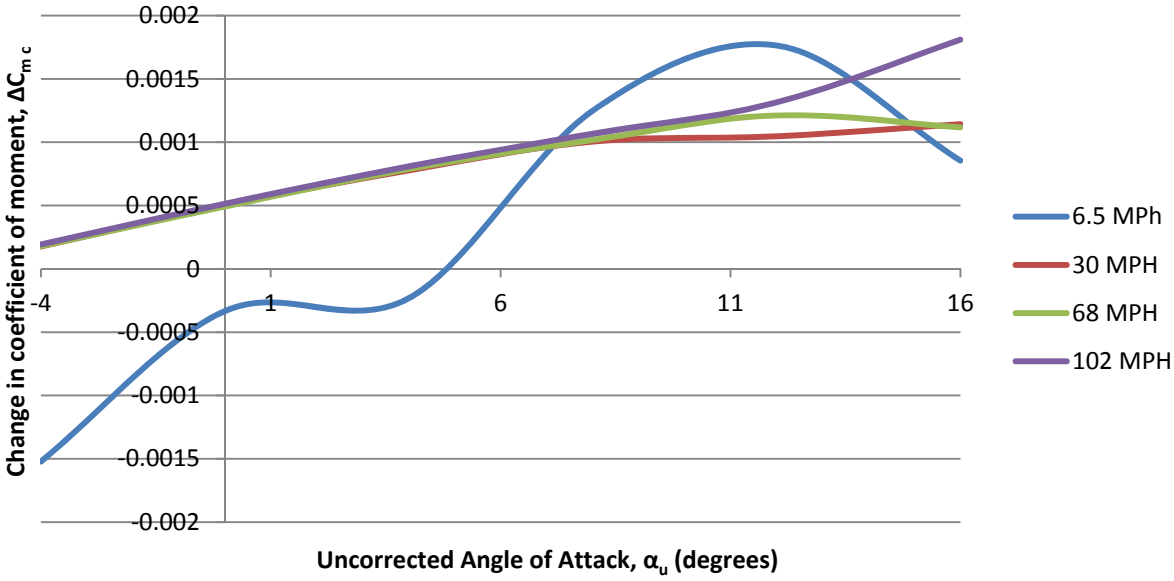

Figure 5.20 – Plot of the change in moment coefficient vs. uncorrected angle of attack

Chapter 6: Computational Fluid Dynamics of the Clark Y-14 Airfoil

6.1 Grids

Two grids were created to simulate the fluid flow inside the wind-tunnel and another to model the ClarkY-14 in free flight conditions. The free flight grid was created in Pointwise and is constructed by orthogonality (Figure 6.1). The airfoil is import from SolidWorks where a one-step structured grid is placed around the Clark Y-14 Airfoil. The grid was stepped out to 10 body lengths around the airfoil.

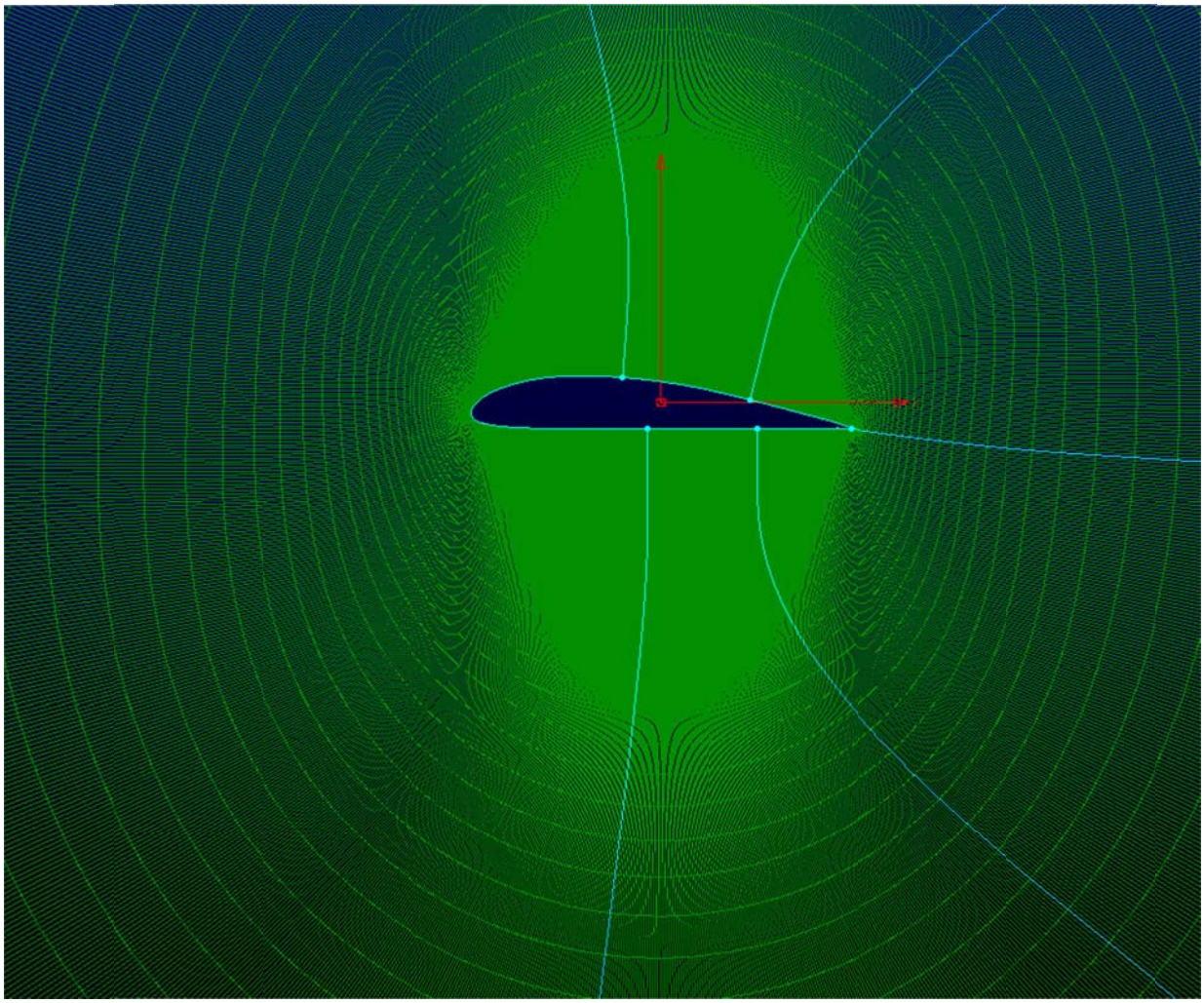

Figure 6.1 – Orthogonal grid around the Clark Y-14 Airfoil

After the grid is formed around the airfoil, the main domain is divided into 5 smaller domains. All five down have the volume setting set to fluid with the biggest domain outside boundary being set as the inlet. All the remaining domains will have their outside boundary set to pressure outlets. The last boundary condition to be set is the boundary around the airfoil needs to be set to wall. The grid is now ready to be exported to Fluent.

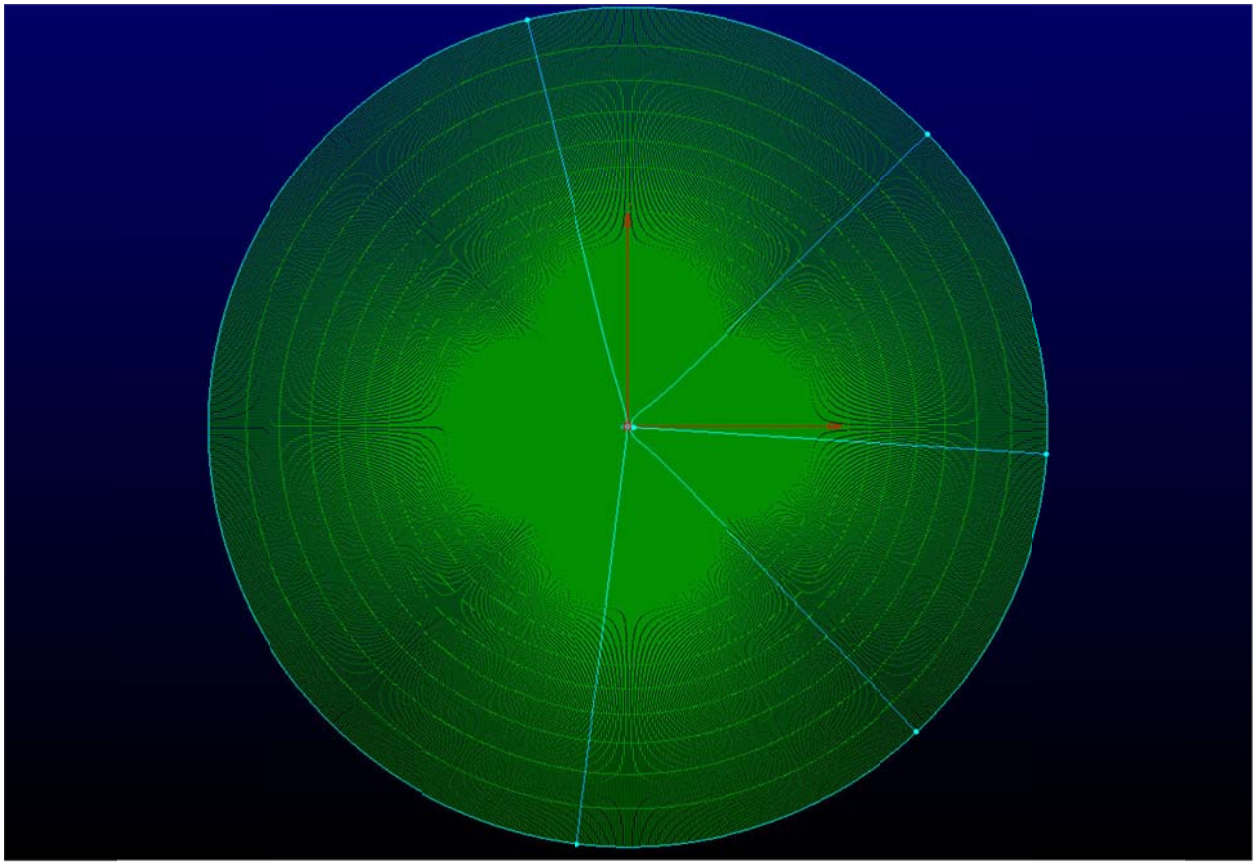

Figure 6.2 – Free flight grid with 5 sub-domains for the Clark Y-14

The next grid to be created is for the airfoil inside the tunnel but instead of the grid being 2D, it will be 3D due to an bug in the software that will not allow this grid type to be exported to Fluent properly. This grid also be constructed out of an orthogonal grid located around the airfoil but not stepped out to 10 body lengths. The step out should be in a multiple of 8+1. The grid in figure 6.3 was stepped out 57 steps. The orthogonal grid is then divided up 6 sub-domains.

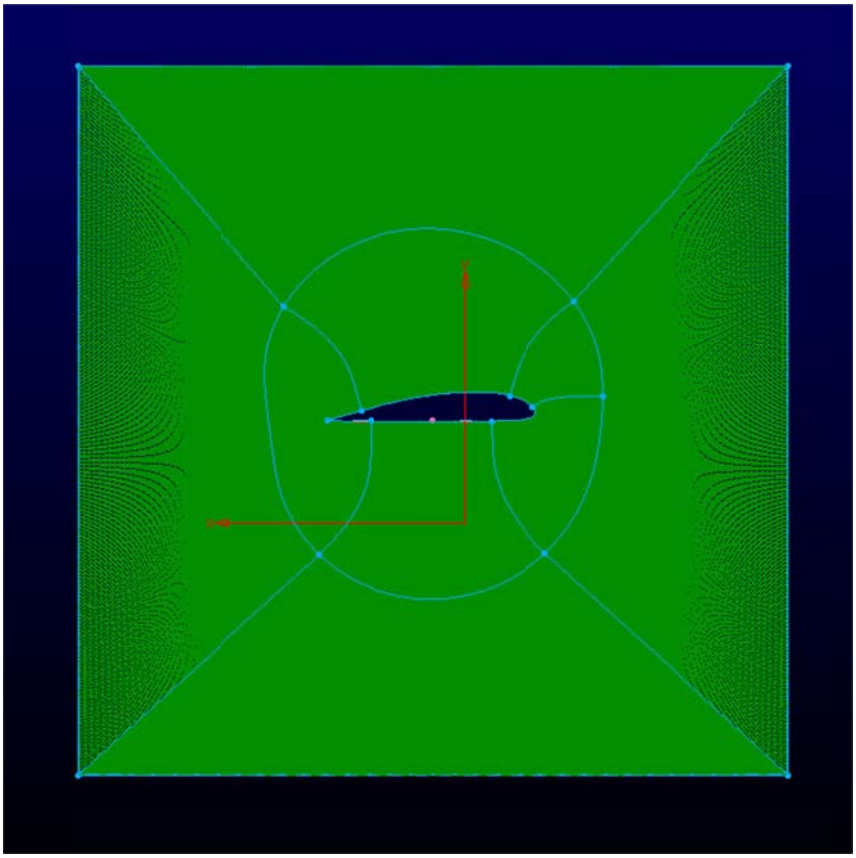

Figure 6.3 – Grid modeling the flow inside the wind-tunnel with the Clark Y-14

From the boundary of the orthogonal grid, a new structured out to the boundaries of the test section. All domains in figure 6.3 are assigned the volume condition of fluid. The boundary conditions are also setup as the velocity inlet on the right side of the grid and a pressure outline on the left. The upper and lower boundaries are set as walls as their boundary conditions as well as the airfoil. Once the setup is complete, the grid is exported to Fluent.

6.2 Setup

The setup for the grids is performed in Fluent where the grid was sized to the correct dimensions of chord of 3.5 inches. After the grid is scaled, the boundary conditions are checked to ensure they were properly imported into Fluent. The residuals were set for convergence at 1e-07. The flow conditions are set at inviscid with air selected at the medium.

6.3 Results

In figures 6.4 – 6.9, the static pressure is plotted in the contour map for the Clark Y-14 at angle of attacks of -4, 0, 4, 8, 12, and 16 at a free-stream velocity of 149.64 ft/sec..

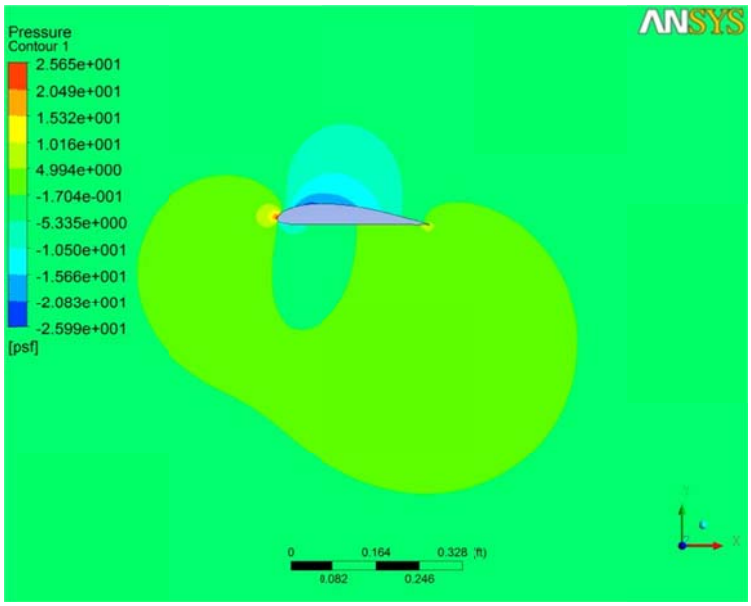

Figure 6.4 – CFD Results for the Clark Y-14 at -4 aoa

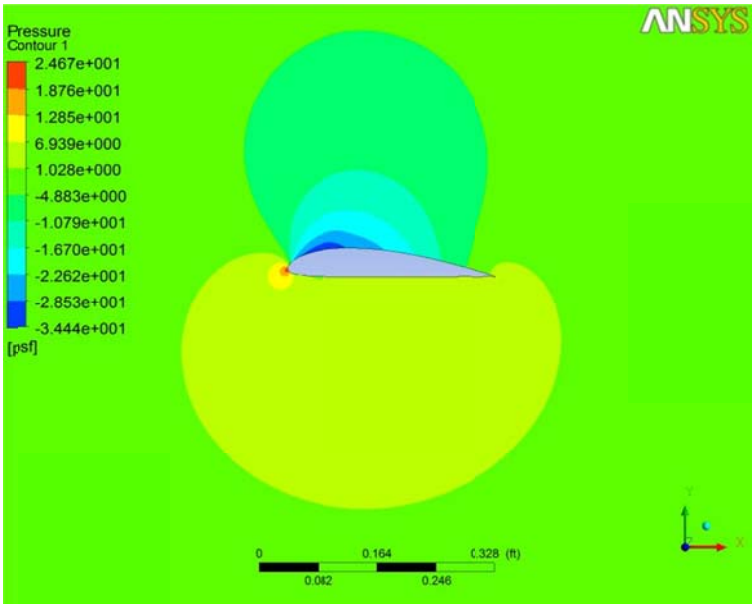

Figure 6.5 – CFD Results for the Clark Y-14 at 0 aoa

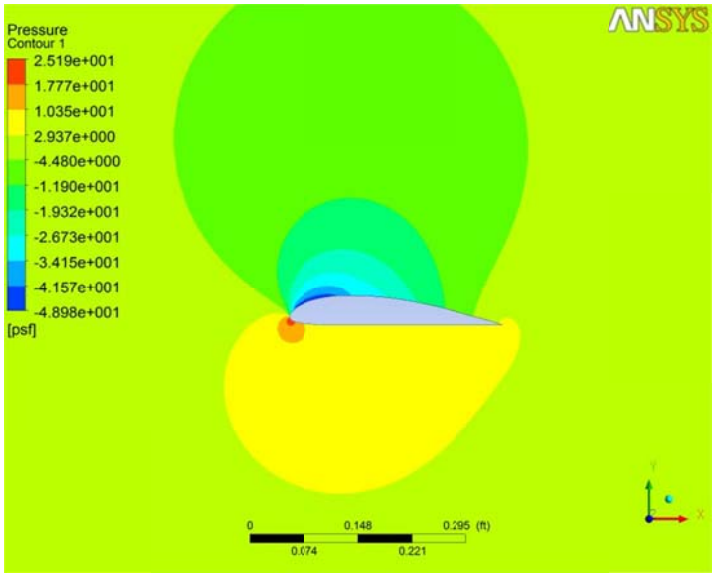

Figure 6.6 – CFD Results for the Clark Y-14 at 4 aoa

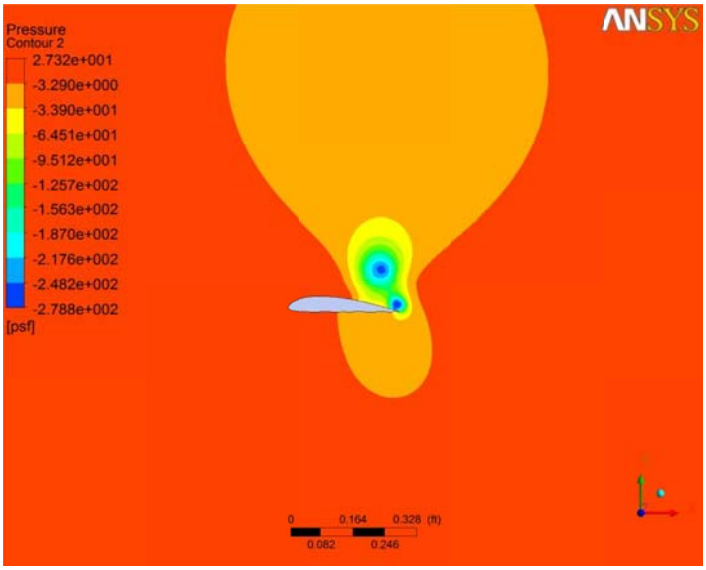

Figure 6.7 – CFD Results for the Clark Y-14 at 8 aoa

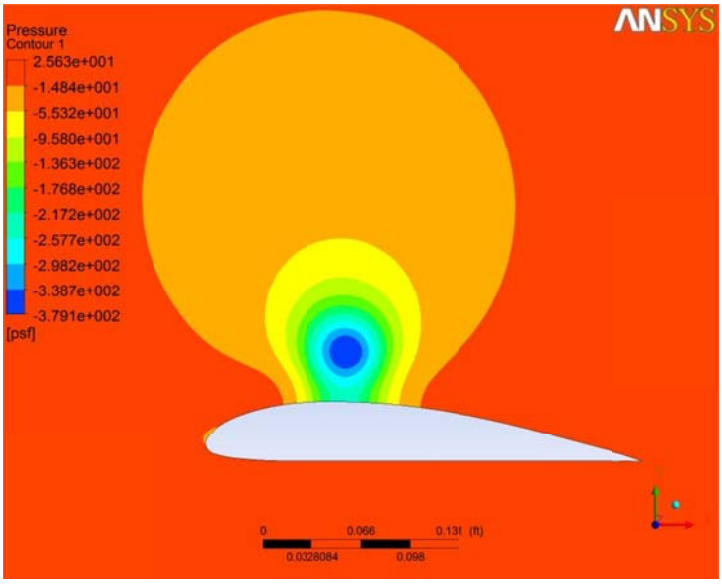

Figure 6.8 – CFD Results for the Clark Y-14 at 12 aoa

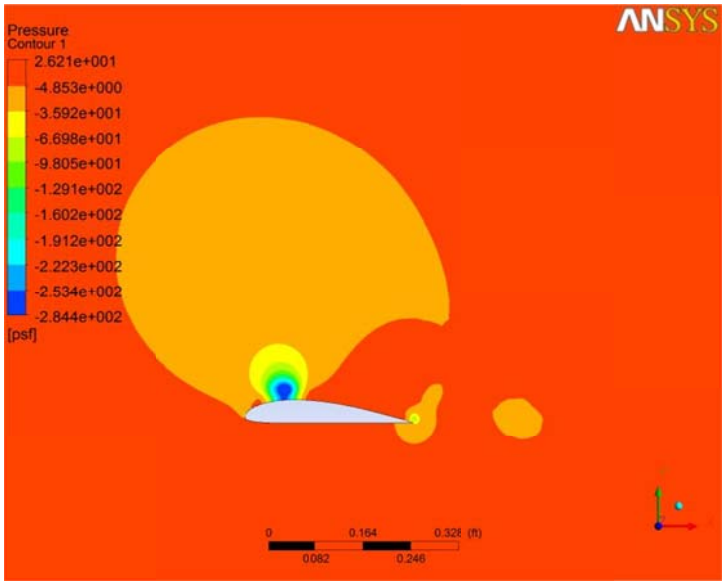

Figure 6.9 – CFD Results for the Clark Y-14 at 16 aoa

In figures 6.10 – 6.15, the C_p over the airfoil is plotted and is used to calculate the coefficient of lift over the airfoil at angles of attack of -4, 0, 4, 8, 12 and 16 and a flow velocity of 149.64 ft/sec.

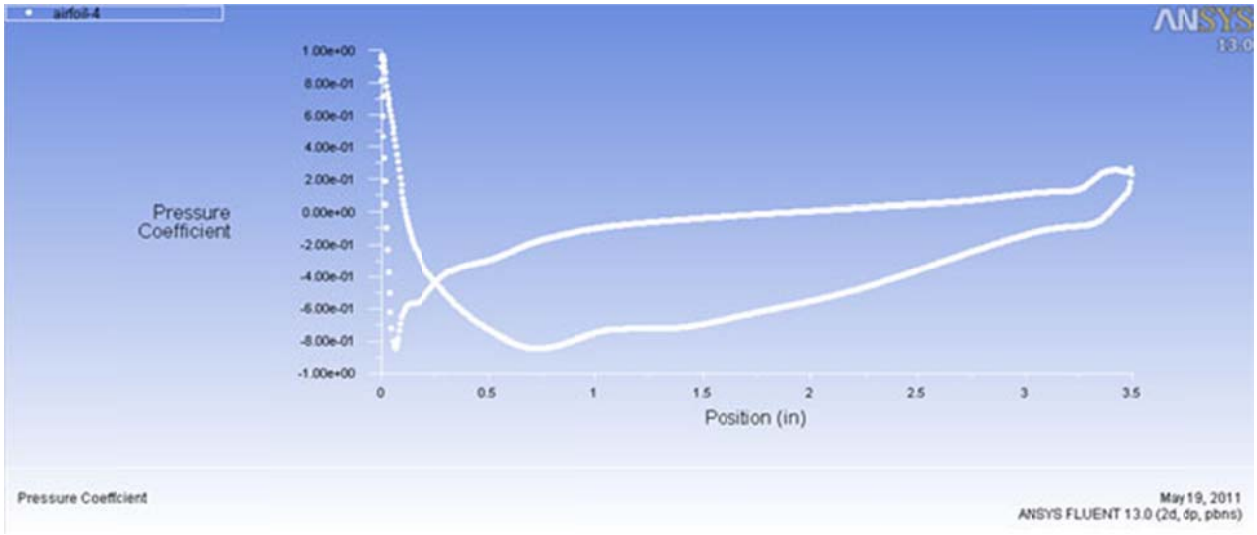

Figure 6.10 –Plot of the C_p over the Clark Y-14 at -4 aoa

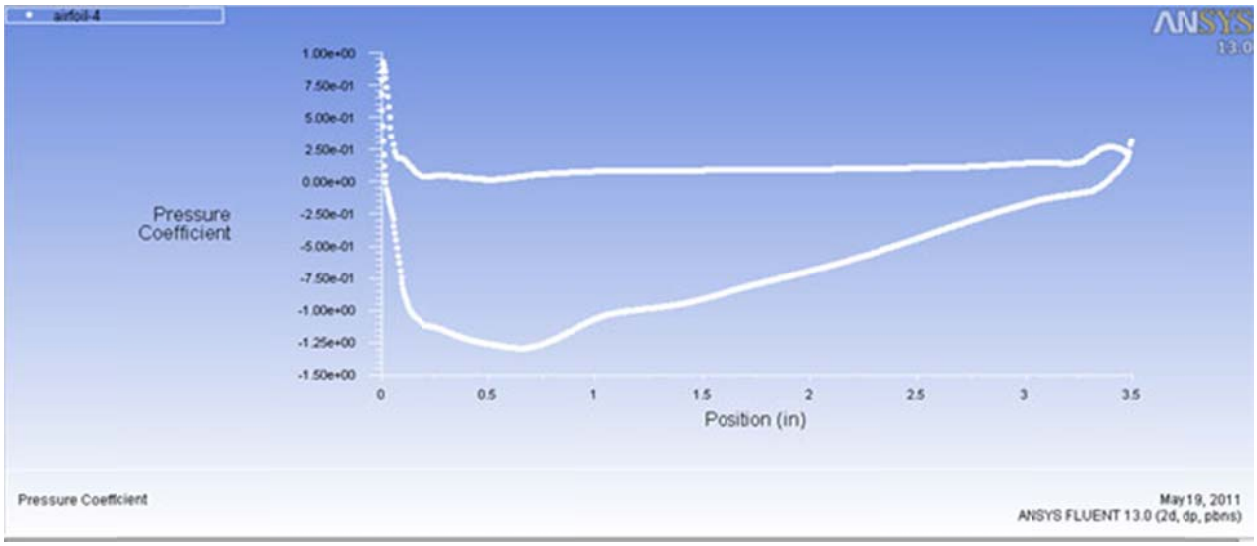

Figure 6.11 –Plot of the C_p over the Clark Y-14 at 0 aoa

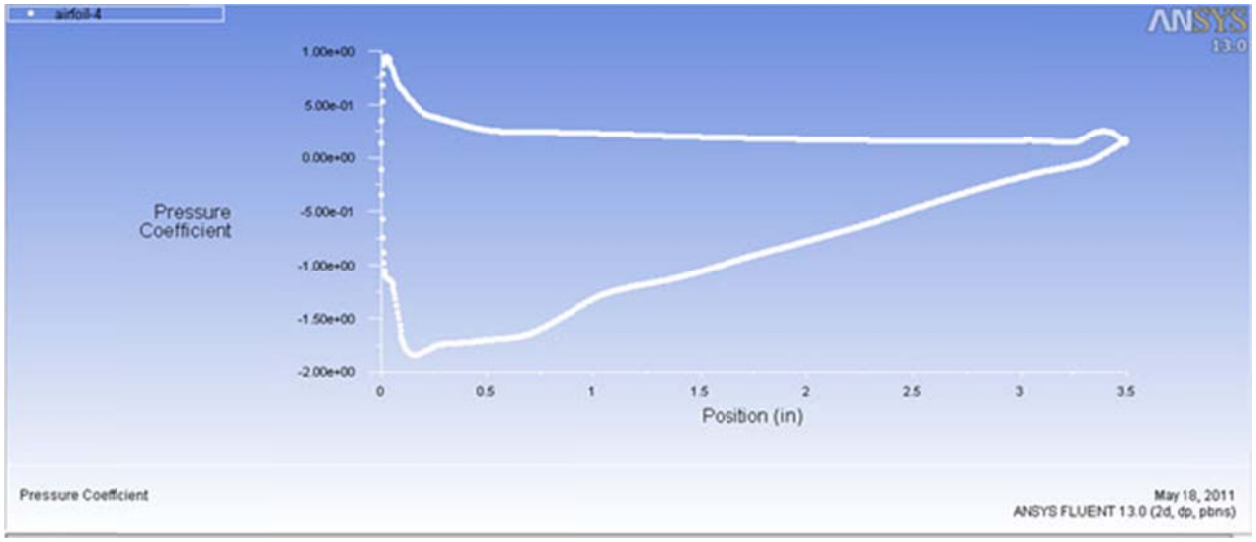

Figure 6.12 –Plot of the C_p over the Clark Y-14 at 4 aoa

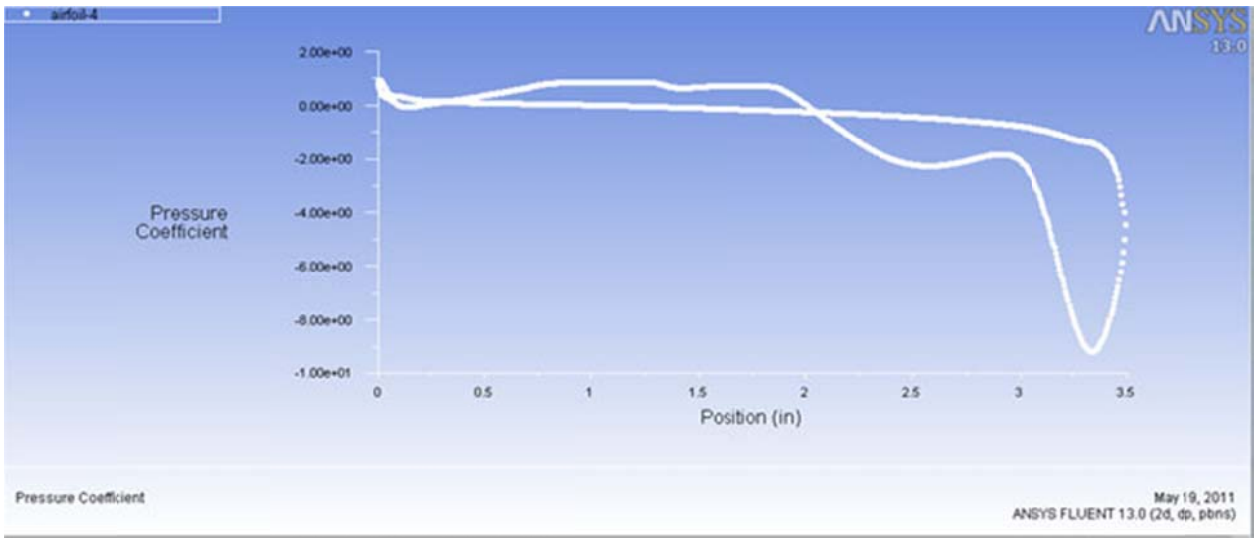

Figure 6.13 –Plot of the C_p over the Clark Y-14 at 8 aoa

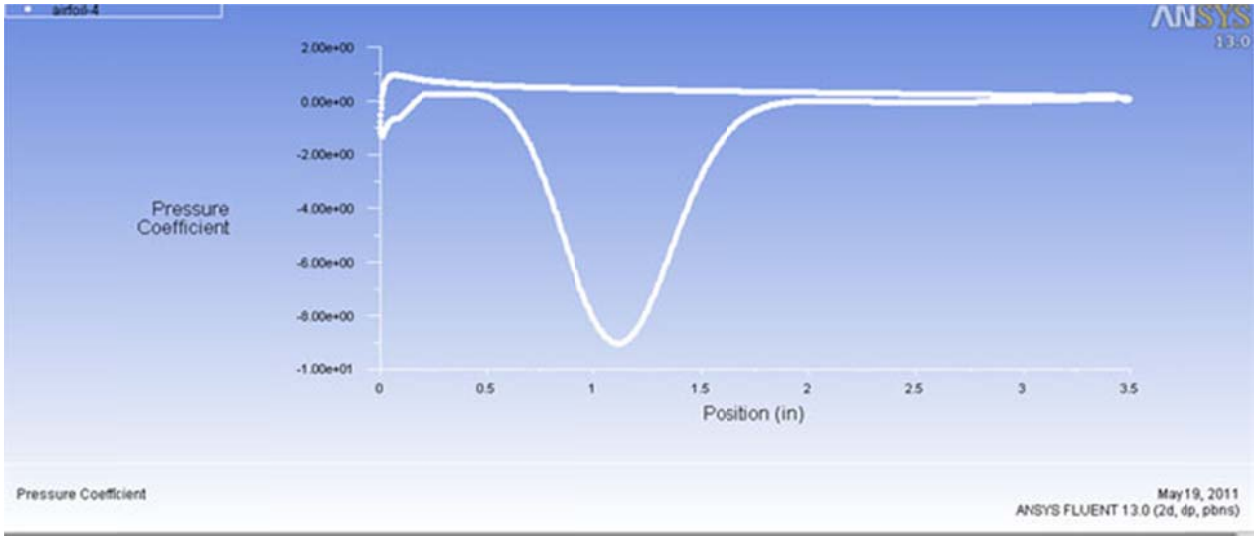

Figure 6.14 –Plot of the C_p over the Clark Y-14 at 12 aoa

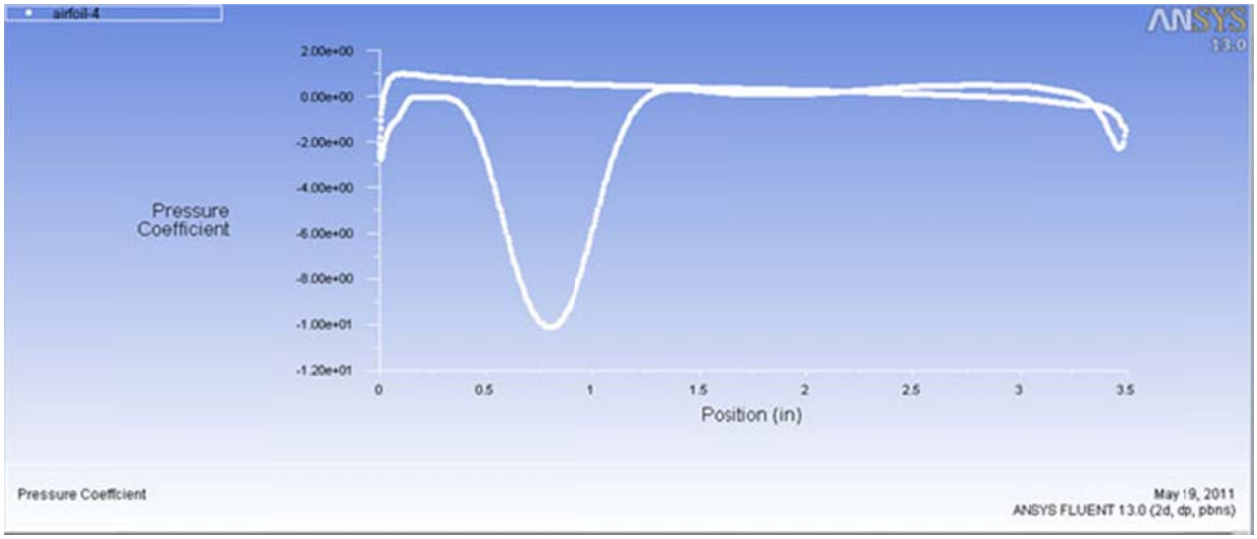

Figure 6.15 –Plot of the C_p over the Clark Y-14 at 16 aoa

In figures 6.16 – 6.18, the coefficient of lift is graphed for -4, 0, 4, 8, 12 and 16 for corrected, uncorrected, expected and CFD results.

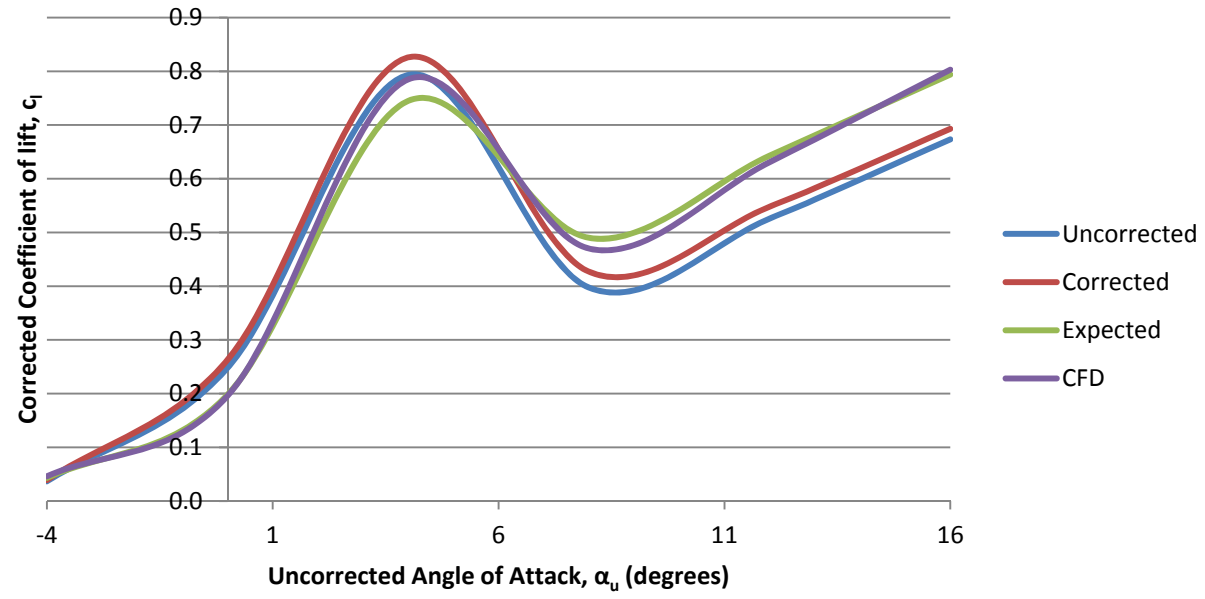

Figure 6.16 – Plot of the C_l at a velocity of 44 ft/sec comparing uncorrected, corrected, expected and CFD results

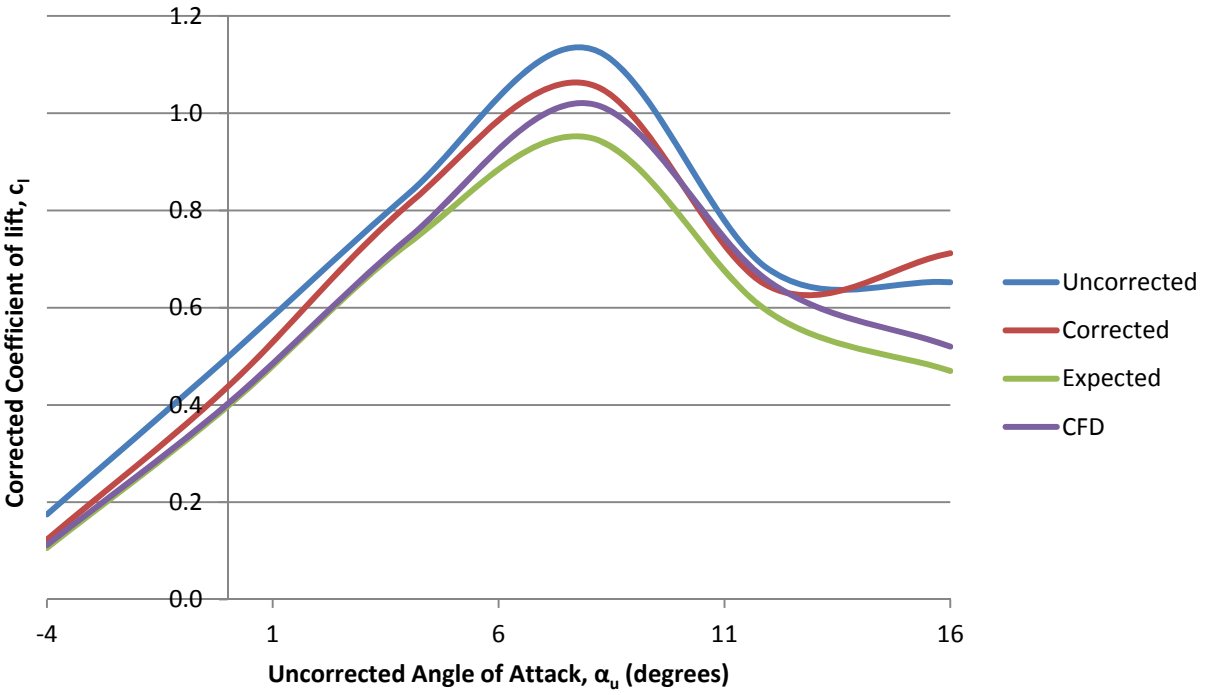

Figure 6.17 – Plot of the C_l at a velocity of 99.73 ft/sec comparing uncorrected, corrected, expected and CFD results

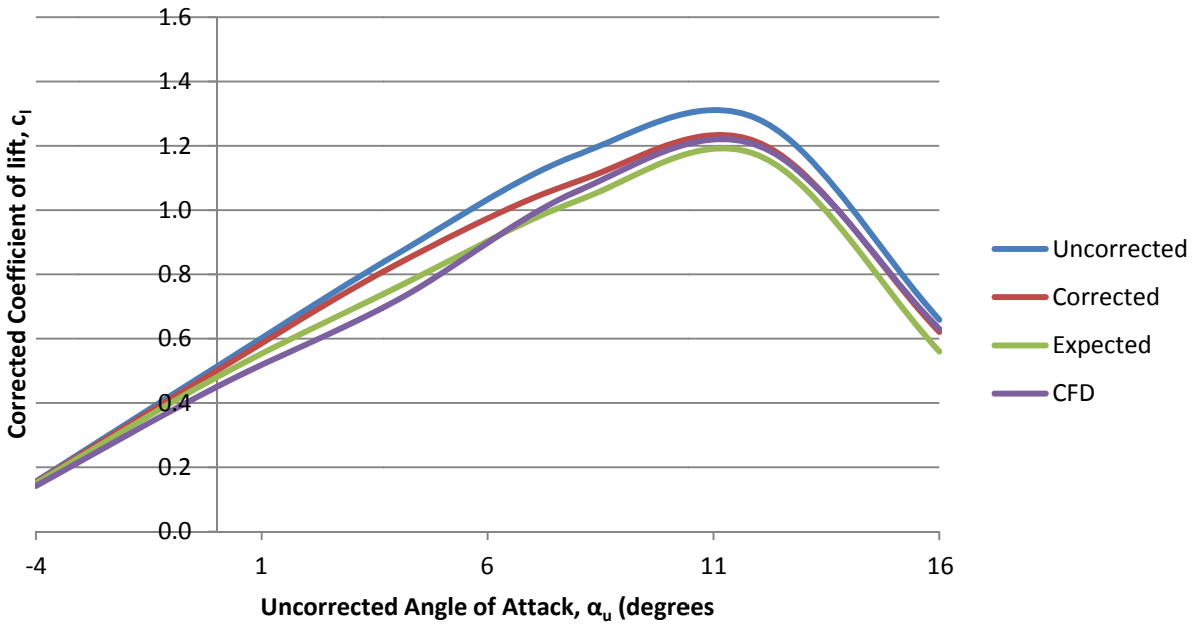

Figure 6.18 – Plot of the C_l at a velocity of 149.64 ft/sec comparing uncorrected, corrected, expected and CFD results

In figures , The streamlines are shown for only one velocity of 149.64 ft/sec at varies angles of attack.

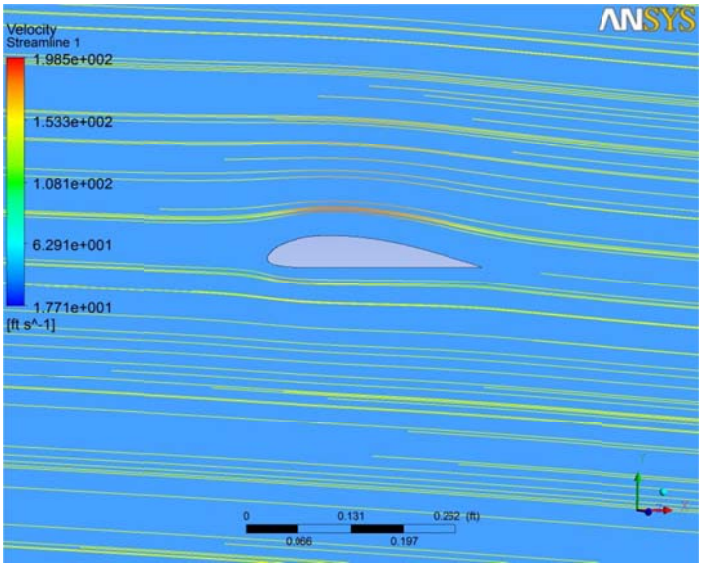

Figure 6.19 – Streamlines over the Clark Y-14 at -4 aoa

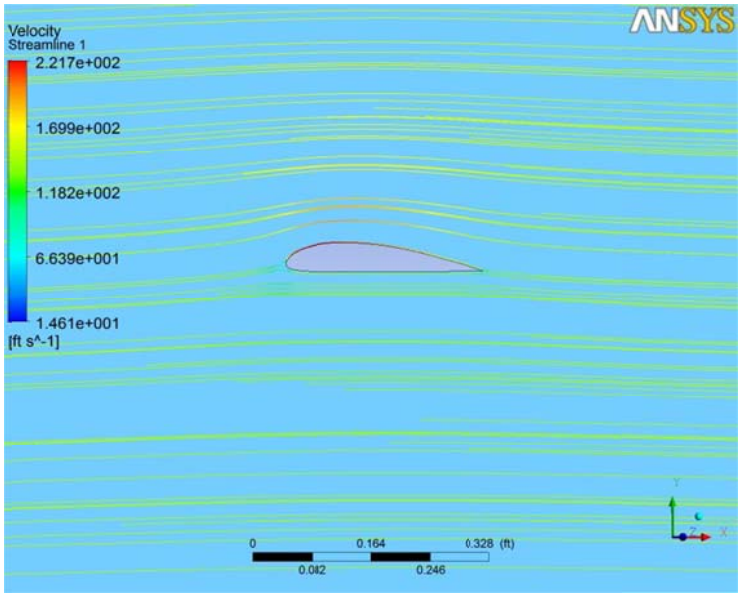

Figure 6.20 – Streamlines over the Clark Y-14 at 0 aoa

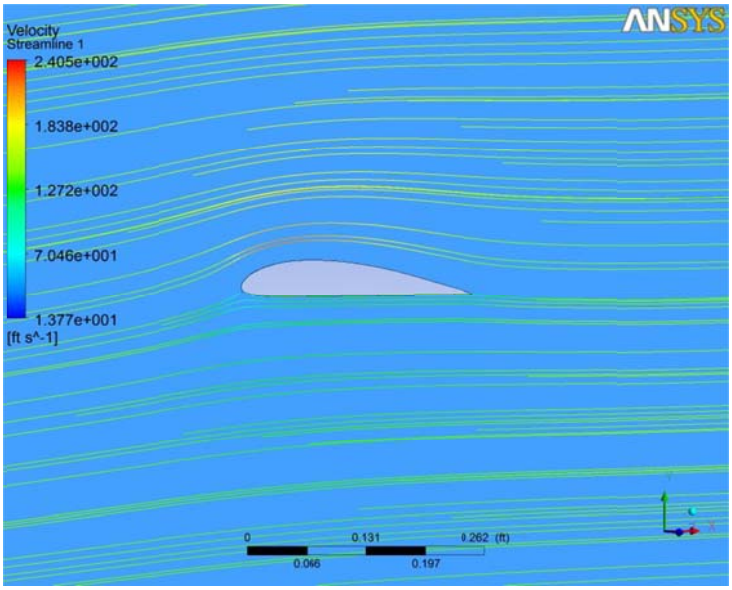

Figure 6.21 – Streamlines over the Clark Y-14 at 4 aoa

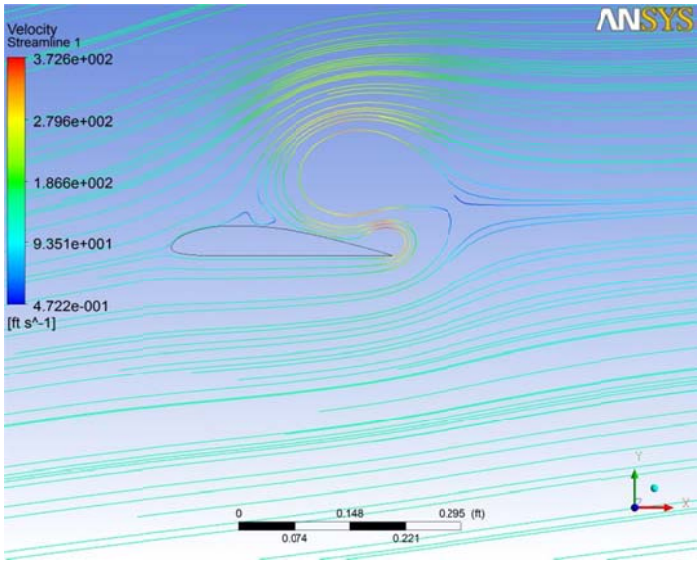

Figure 6.22 – Streamlines over the Clark Y-14 at 8 aoa

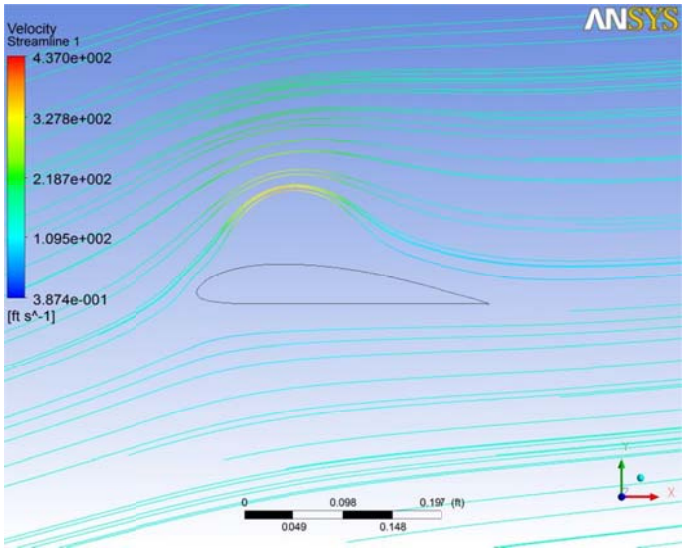

Figure 6.23 – Streamlines over the Clark Y-14 at 12 aoa

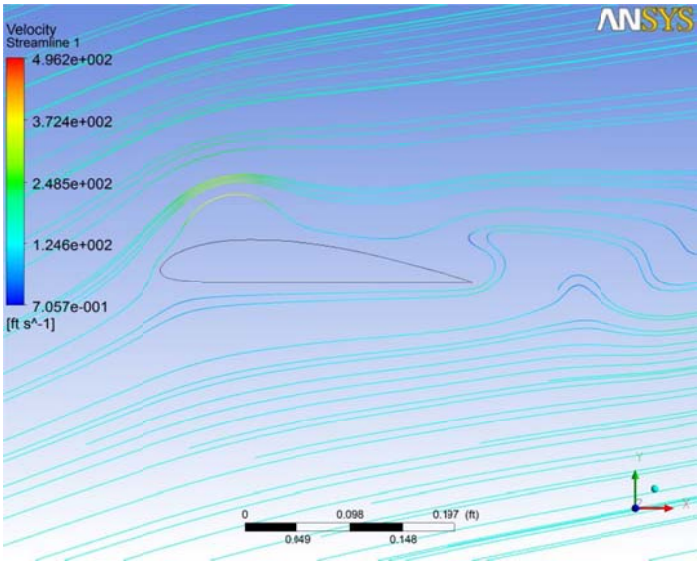

Figure 6.24 – Streamlines over the Clark Y-14 at 16 aoa

6.4 Discussion

The CFD was successful at plotting the c_p over the Clark Y-14 for 9.533, 44.000, 99.732 and 149.642 ft/sec at -4, 0, 4, 8, 12 and 16 degrees of angle of attack. In figures 6.4 – 6.9 shows the static pressure as the angle of attack increases. It can be seen that as the angle of attack increases, the static pressure shifts over the airfoil as the airfoil stalls. The c_p is used to calculate the c_l as in section 4.4 for use in comparing the data to corrected and expected results. In figures 6.16 – 6.18, the graphs show how the correction factors compare with the CFD result and the expected values. The graphs show that corrected c_l is close to the expected values where the CFD is very close to the corrected results. For the CFD cases for the a velocity of 9.533, 44.00 and 99.73 ft/sec, the CFD results are in Appendix C but mainly represents what is shown in figures 6.4 – 6.15.

Chapter 7: Conclusion

As our civilization relies more heavily on aircrafts and rockets, the use of wind-tunnels has increasing been integrated as an important aeronautical tool in their design. Even though wind-tunnels are great scientific tools, they do have their flaws. Based on the specific wind-tunnel design, one of the main negatives is that wind-tunnels cannot simulate free-flight conditions without having to correct the data for wall effects and other flow phenomena.

Both two and three-dimensional flows need to have corrections applied that are unique to that wind-tunnels design. For two dimensional flows, corrections that can be obtain are for the $\Delta\alpha,\ \Delta c_l,\ and\ \Delta c_{m_{\frac{1}{4}}}$ with direct corrections available for V, q, Re, $\alpha,\ c_l,\ and\ c_{m_{\frac{1}{4}}}$. The corrections are developed from the buoyancy, solid and wake blockages, and streamline curvature corrections. For tree-dimensional flows, corrections can be obtain are $\Delta\alpha,\ \Delta c_l,\ \Delta c_{m_{\frac{1}{4}}}$, $\Delta\alpha_i\ and\ \Delta C_{Di}$. These corrections depend on the methods applied to the two-dimensional cases along with the method of images.

The CFD can be a cheaper solution to wind-tunnels but as seen in the results throughout chapter 6, require an almost perfect grid. This can be very expensive due to grid building, setup and supercomputer time to the point the cost match that of wind-tunnels. Wind Tunnel testing and the corrections developed for that specific tunnel that are easily applied to any model, keep tunnels operating and a competitive source of aeronautical information.

Works Cited

Abbott, I. (1959). Theory of Wing Sections. New York City: Dover Publications.

American Institute of Aeronautics and Astronautics (AIAA). (2004). NACA 0012 Airfoil Aerodynamics Analysis. Reston: Hahn, Philip.

Anderson, J. D. (2007). Fundamentals of Aerodynamics , 4th Edition. New York City: McGraw-Hill.

Kasravi, K. (2010). Tec452 body Structures I. Retrieved from http://www.kasravi.com/cmu/tec452/aerodynamics/WindTunnel.html

Lilienthal, O. (2000). Birdflight as the Basis of Aviation. Hummelstown: Markowski International Publishers

Monash University. (2004). Flying Wings: An Anthology: Horatio F. Phillips. Retrieved from http://wwwctie.monash.edu.au/hargrave/phillis.html

National Aeronautics and Space Administration (NASA). (2005). Wind Tunnel History. Retrieved from http://www.grc.nasa.gov/WWW/K-12/WindTunnel/History.html

National Aeronautics and Space Administration (NASA). (1950). Blockage Corrections for Three-Dimensional – Flow Closed –Throat Wind (TR 643). Washington DC: U.S. Government Printing Office.

National Aeronautics and Space Administration (NASA). (1944). Wall Interference in a Two-Dimensional – Flow Wind Tunnel with Considerations of the Effects of Compressibility (TR 612). Washington DC: U.S. Government Printing Office.

Pankhurst, R. C. (1952). Wind Tunnel Technique. London: Pitman

Pope, A. (1984). Low-Speed Wind Tunnel Testing. New York City: John Wiley & Sons.

Society for Industrial and Applied Mathematics. (1991). Vortex Methods and Vortex Motion. Philadelphia: Gustafson, K. E, Sethian, J. A.

Appendix A

```
/* This program determines the Pressure Gradient through the SJSU Wind Tunnel Test
Section.*/

#define _CRT_SECURE_NO_DEPRECATE
#include <stdio.h>
#include <math.h>
#define VISCOCITY 0.000000382f
#define DENSITY 0.002325f
#define PRESSURE 2.1162f
#define VELOCITY_ZERO 0.0f
#define AREA_ONE 1.0f

double reynoldsNumber(double velocity, double cord_length) {
	return (DENSITY * velocity * cord_length) / VISCOCITY;
}

double criticalPoint(double velocity, double cord_length, double reynolds_number) {
	return ((reynolds_number * VISCOCITY) / (DENSITY * velocity));
}

double laminarBoundaryDisplacement(double velocity, double cord_length) {
	return (1.72f * cord_length)/pow(reynoldsNumber(velocity,cord_length),0.5);
}

double turbulentBoundaryDisplacement(double velocity, double cord_length, double
reynolds_number) {
	return (0.046f * cord_length)/pow(reynolds_number,0.2);
}

int
	main(void)
{
	double reynolds_number = 0.0f;
	double velocity = 0.0f;
	double cord_length = 1.0f;
	double critical_point = 0.0f;
	double boundary_displacement=0.0;
	double effective_area = 0.0;
	double pressure_one = 0.0f;
	double velocity_two = 0.0f;
	double pressure_two = 0.0f;
	double ts_length = 0.0f;
```

```
	double pressure_grad = 0.0f;
	double starting_velocity = 0.0;
	double ending_velocity = 0.0;
	double velocity_increment = 0.0;
	double velocity_mph = 0.0;

	int dummy;
	FILE *file;

	file = fopen("C:\\data.csv","w+");

	printf("Enter the starting velocity (MPH) of the flow over flat plate > ");
	scanf_s("%lf", &starting_velocity);
	printf("Enter the ending velocity (MPH) of the flow over the flat plate > ");
	scanf_s("%lf", &ending_velocity);
	printf("Enter the velocity increment (MPH) > ");
	scanf_s("%lf", &velocity_increment);

	fprintf(file,"MPS,FPS,Reynolds Number,Cross-Sectional Test Section Area (ft),Pressure
Gradient\n");
	for (velocity_mph = starting_velocity;velocity_mph <= ending_velocity;
velocity_mph+= velocity_increment) {
		velocity = velocity_mph * 1.46666666666667;

		reynolds_number = reynoldsNumber(velocity,cord_length);



		//printf("Reynolds Number -> %lf\n", reynolds_number);
		critical_point = criticalPoint(velocity,cord_length,500000);
		//printf("Critical Point (ft) -> %lf\n", critical_point);
		if (reynolds_number < 500000.0f) {
			//printf("Reynolds Number < 500000 - Laminar\n");

			boundary_displacement =
laminarBoundaryDisplacement(velocity,cord_length);
			effective_area = pow((cord_length - boundary_displacement),2.0);
			//printf("Laminar Boundary Displacement (ft) ->
%lf\n",boundary_displacement);
			//printf("Effective Area (ft^2) -> %lf\n\n", effective_area);
		}
		else {
			double delta_x = 0.0;
			double turbulent_start_point = 0.0;
			double new_start_point = 0.0;
			double new_laminar_boundary_displacement = 0.0;
```

```
                        double turbulent_boundary_displacement = 0.0;
                        //printf("Reynolds Number >= 500000 - Turbulent\n");
                        boundary_displacement =
laminarBoundaryDisplacement(velocity,critical_point);
                        delta_x = pow((boundary_displacement * pow(((DENSITY * velocity) /
VISCOCITY),0.2) / 0.46),1.25);
                        //printf("Delta X (ft) -> %lf\n",delta_x);
                        turbulent_start_point = critical_point - delta_x;

                        new_start_point = cord_length - turbulent_start_point;
                        //printf("New Start Point Turbulent Boundary Distplacement (ft) ->
%lf\n",new_start_point);
                        turbulent_boundary_displacement =
turbulentBoundaryDisplacement(velocity,new_start_point, reynolds_number);
                        //printf("Turbulent Boundary Displacement (ft) ->
%lf\n",turbulent_boundary_displacement);
                        effective_area = pow(cord_length -
turbulent_boundary_displacement,2.0);
                        //printf("Effective Area (ft^2) -> %lf\n\n",effective_area);

                }

                pressure_one = PRESSURE - .5 * DENSITY * pow((velocity),2);
                //printf("Pressure at Test Section Entrance (lb/ft^2) -> %lf\n",pressure_one);

                velocity_two = (velocity * AREA_ONE) / effective_area;
                //printf("Test Section Exit Velocity (ft/sec) -> %lf\n",velocity_two);

                pressure_two = pressure_one - .5 * DENSITY * pow((velocity_two),2);
                //printf("Pressure at Test Section Exit (lb/ft^2) -> %lf\n",pressure_two);

                //printf("Enter Test Section Axial Length (ft) >");
                //scanf_s("%lf", &ts_length);
                ts_length = 1.0;
                pressure_grad = (pressure_two - pressure_one) / ts_length;
                //printf("Pressure Gradient through the Test Section (lb/ft^3) ->
%lf\n\n",pressure_grad);



        fprintf(file,"%lf,%lf,%lf,%lf,%lf\n",velocity_mph,velocity,reynolds_number,effective_ar
ea,pressure_grad);

        }
        printf("DONE.\n");
        fclose(file);
```

```
        scanf_s("%d",&dummy);
        return (0);
}
```

Appendix B

2D Airfoil Data (Pressure)

count	q [psf]	V_ref [mph]	Alpha [deg]	P 1 [mbar]	P 2 [mbar]	P 3 [mbar]	P 4 [mbar]	P 5 [mbar]	P 6 [mbar]	P 7 [mbar]	P 8 [mbar]	P 9 [mbar]	P 10 [mbar]	P 11 [mbar]	P 12 [mbar]	P 13 [mbar]	P 14 [mbar]	P 15 [mbar]	P 16 [mbar]	P 17 [mbar]	P 18 [mbar]	P 19 [mbar]	1 mbar = 2.0885433 psf 1 mph = 1.466667 fps 1 sq. ft = 144 psi in
1	0	2	0	10 16.1	10 16.4	10 16.2	10 16.1	10 16.3	10 15.9	10 16.2	10 16	10 16.3	10 16.3	10 16.4	10 15.9	10 16.2	10 16.3	10 16.3	10 15.8	10 16.2	10 16.3	10 16	
2	0	3	0	10 16.1	10 16.4	10 16.3	10 16.1	10 16.3	10 15.8	10 16.2	10 16	10 16.3	10 16.3	10 16.3	10 15.9	10 16.2	10 16.3	10 16.3	10 15.8	10 16.2	10 16.3	10 16	
3	0	4	0	10 16.1	10 16.4	10 16.3	10 16.1	10 16.3	10 15.9	10 16.2	10 16	10 16.3	10 16.3	10 16.3	10 15.9	10 16.2	10 16.3	10 16.3	10 15.8	10 16.2	10 16.3	10 16	
4	0	4	0	10 16.1	10 16.3	10 16.2	10 16.1	10 16.3	10 15.8	10 16.2	10 16	10 16.3	10 16.2	10 16.4	10 15.9	10 16.2	10 16.3	10 16.3	10 15.8	10 16.2	10 16.3	10 16	
5	0	3	0	10 16.1	10 16.4	10 16.2	10 16.1	10 16.3	10 15.8	10 16.2	10 16	10 16.3	10 16.3	10 16.4	10 15.9	10 16.2	10 16.3	10 16.3	10 15.8	10 16.2	10 16.3	10 16	
6	0.1	4	0	10 16.	10 16.	10 16.	10 16.	10 16.	10 15.	10 16.	10 16	10 16.	10 16.	10 16.	10 15.	10 16.	10 16.	10 16.	10 15.	10 16.	10 16.	10 16	

				1	4	2	1	3	8	2		3	2	4	9	2	3	3	8	2	3	
				10	10	10	10	10	10	10		10	10	10	10	10	10	10	10	10	10	
				16.	16.	16.	16.	16.	15.	16.	10	16.	16.	16.	15.	16.	16.	16.	15.	16.	16.	10
7	0	3	0	1	4	2	1	3	8	2	16	3	3	4	9	2	3	3	8	2	3	16
				10	10	10	10	10	10	10		10	10	10	10	10	10	10	10	10	10	
				16.	16.	16.	16.	16.	15.	16.	10	16.	16.	16.	15.	16.	16.	16.	15.	16.	16.	10
8	0	2	0	1	4	2	1	3	8	2	16	3	3	3	9	2	3	3	8	2	3	16
				10	10	10	10	10	10	10		10	10	10	10	10	10	10	10	10	10	
				16.	16.	16.	16.	16.	15.	16.	10	16.	16.	16.	15.	16.	16.	16.	15.	16.	16.	10
9	0	3	0	1	4	3	1	3	8	2	16	3	2	3	9	2	3	3	8	2	3	16
				10	10	10	10	10	10	10		10	10	10	10	10	10	10	10	10	10	10
				16.	16.	16.	16.	16.	15.	16.	10	16.	16.	16.	15.	16.	16.	16.	15.	16.	16.	15.
10	0	4	0	1	4	2	1	3	8	2	16	3	3	3	9	2	3	3	8	2	3	9
				10	10	10	10	10	10	10		10	10	10	10	10	10	10	10	10	10	10
				16.	16.	16.	16.	16.	15.	16.	10	16.	16.	16.	15.	16.	16.	16.	15.	16.	16.	15.
11	0	4	0	1	4	2	1	3	8	2	16	3	3	3	9	2	3	3	8	2	3	9
				10	10	10	10	10	10	10		10	10	10	10	10	10	10	10	10	10	
				16.	16.	16.	16.	16.	15.	16.	10	16.	16.	16.	15.	16.	16.	16.	15.	16.	16.	10
12	0.1	5	0	1	4	3	1	3	8	2	16	3	2	3	9	2	3	3	8	2	3	16
				10	10	10	10	10	10	10		10	10	10	10	10	10	10	10	10	10	
				16.	16.	16.	16.	16.	15.	16.	10	16.	16.	16.	15.	16.	16.	16.	15.	16.	16.	10
13	0.1	5	0	1	4	3	1	3	8	2	16	3	2	4	9	2	3	3	8	2	3	16
				10	10	10	10	10	10	10		10	10	10	10	10	10	10	10	10	10	10
				16.	16.	16.	16.	16.	15.	16.	10	16.	16.	16.	15.	16.	16.	16.	15.	16.	16.	15.
14	0	2	0	1	3	3	1	3	8	2	16	3	2	3	9	2	3	3	8	2	3	9
				10	10	10	10	10	10	10		10	10	10	10	10	10	10	10	10	10	
				16.	16.	16.	16.	16.	15.	16.	10	16.	16.	16.	15.	16.	16.	16.	15.	16.	16.	10
15	0	2	0	1	4	3	1	3	8	2	16	3	2	3	9	2	3	3	8	2	3	16
				10	10	10	10	10	10	10		10	10	10	10	10	10	10	10	10	10	10
				16.	16.	16.	16.	16.	15.	16.	10	16.	16.	16.	15.	16.	16.	16.	15.	16.	16.	15.
16	0	2	0	1	4	3	1	3	8	2	16	3	2	3	9	2	3	3	8	2	3	9
					10	10	10	10	10	10		10	10	10	10	10	10	10	10	10	10	10
				10	16.	16.	16.	16.	15.	16.	10	16.	16.	16.	15.	16.	16.	16.	15.	16.	16.	15.
17	0	3	0	16	4	2	1	3	8	2	16	3	2	3	9	2	3	3	8	2	3	9

					10	10	10	10	10	10		10	10	10	10	10	10	10	10	10	10	10	
				10	16.3	16.2	16.1	16.2	15.8	16.2	10	16.3	16.2	16.3	15.9	16.2	16.3	16.3	15.8	16.2	16.3	15.9	
18	0	3	0	16							16												
				10	10	10	10	10	10	10		10	10	10	10	10	10	10	10	10	10	10	
				16.	16.	16.	16.	16.	15.	16.	10	16.	16.	16.	15.	16.	16.	16.	15.	16.	16.	15.	
19	0	4	0	1	4	2	1	3	8	2	16	3	2	3	9	2	3	3	8	2	3	9	
				10	10	10	10	10	10	10		10	10	10	10	10	10	10	10	10	10	10	
				16.	16.	16.	16.	16.	15.	16.	10	16.	16.	16.	15.	16.	16.	16.	15.	16.	16.	15.	
20	0	1	0	1	4	2	1	3	8	2	16	3	2	3	9	2	3	3	8	2	3	9	
					10			10															
				10	16.	10	10	16.	10	10		10	10	10	10	10	10	10	10	10	10	10	
	0.0	3.1		16.	38	16.	16.	29	15.	16.	10	16.	16.	16.	15.	16.	16.	16.	15.	16.	16.	15.	Av
	15	5	0	09	5	24	1	5	81	2	16	3	24	33	9	2	3	3	8	2	3	96	g
				21	21	21	21	21	21	21		21	21	21	21	21	21	21	21	21	21	21	
				22.	22.	22.	22.	22.	21.	22.	21	22.	22.	22.	21.	22.	22.	22.	21.	22.	22.	21.	
				14	76	46	16	57	56	37	21.	58	46	64	75	37	58	58	54	37	58	87	
				8	4	1	9	6	3	8	96	7	1	9	1	8	7	7	2	8	7	7	psf
		4.6																					
		20																					
		00																					FP
		1																					S

Airfoil Station	1	2	3	4	5	6	7	8	9	10	11	12	13	14	15	16	17	18	19
% of Chord	0.8	0.7	0.6	0.5	0.4	0.3	0.2	0.1	0.075	0	0.075	0.1	0.2	0.3	0.4	0.5	0.6	0.7	0.8
Distance	2.8	2.45	2.1	1.75	1.4	1.05	0.7	0.35	0.262	0	0.262	0.35	0.7	1.05	1.4	1.75	2.1	2.45	2.8

from LE								5		5																	
count	q [psf]	V_ref [mph]	Alpha [deg]	P 1 [mbar]	P 2 [mbar]	P 3 [mbar]	P 4 [mbar]	P 5 [mbar]	P 6 [mbar]	P 7 [mbar]	P 8 [mbar]	P 9 [mbar]	P 10 [mbar]	P 11 [mbar]	P 12 [mbar]	P 13 [mbar]	P 14 [mbar]	P 15 [mbar]	P 16 [mbar]	P 17 [mbar]	P 18 [mbar]	P 19 [mbar]	1 mbar = 2.08854 3 1 mph = 1.46667 1 sq. ft = 144	psf psf psi
1	0.1	5	0	10 16	10 16.3	10 16.2	10 16.1	10 16.2	10 15.8	10 16.2	10 15.9	10 16.3	10 16.2	10 16.2	10 15.8	10 16.1	10 16.2	10 16.2	10 15.7	10 16.1	10 16.2	10 15.9		
2	0.1	5	0	10 16	10 16.3	10 16.3	10 16.1	10 16.2	10 15.8	10 16.2	10 16	10 16.3	10 16.3	10 16.2	10 15.9	10 16.1	10 16.2	10 16.2	10 15.7	10 16.1	10 16.2	10 15.9		
3	0.1	7	0	10 16	10 16.3	10 16.3	10 16.1	10 16.2	10 15.8	10 16.2	10 16	10 16.3	10 16.3	10 16.3	10 15.8	10 16.1	10 16.2	10 16.2	10 15.7	10 16.1	10 16.2	10 15.9		
4	0.1	6	0	10 16	10 16.3	10 16.2	10 16	10 16.2	10 15.8	10 16.2	10 16	10 16.3	10 16.3	10 16.2	10 15.8	10 16.1	10 16.2	10 16.2	10 15.7	10 16.1	10 16.2	10 15.9		
5	0.1	7	0	10 16	10 16.4	10 16.2	10 16	10 16.2	10 15.8	10 16.2	10 16	10 16.3	10 16.2	10 16.3	10 15.8	10 16.1	10 16.2	10 16.2	10 15.7	10 16.1	10 16.2	10 15.9		
6	0.1	5	0	10 16	10 16.3	10 16.2	10 16	10 16.2	10 15.8	10 16.2	10 16	10 16.3	10 16.2	10 16.3	10 15.8	10 16.1	10 16.2	10 16.2	10 15.7	10 16.1	10 16.2	10 15.9		
7	0.2	8	0	10 16	10 16.3	10 16.2	10 16	10 16.2	10 15.8	10 16.2	10 15.9	10 16.3	10 16.2	10 16.2	10 15.8	10 16.1	10 16.2	10 16.2	10 15.7	10 16.1	10 16.2	10 15.9		

				10	10	10		10	10	10		10	10	10	10	10	10	10	10	10	10	10
				16.	16.	16.	10	16.	15.	16.	10	16.	16.	16.	15.	16.	16.	16.	15.	16.	16.	15.
8	0.1	7	0	1	3	2	16	2	8	2	16	3	2	3	9	1	2	2	7	1	2	9
					10	10		10	10	10	10	10	10	10	10	10	10	10	10	10	10	10
				10	16.	16.	10	16.	15.	16.	15.	16.	16.	16.	15.	16.	16.	16.	15.	16.	16.	15.
9	0.1	7	0	16	3	2	16	2	7	2	9	3	2	3	8	1	2	2	7	1	2	9
					10	10		10	10	10		10	10	10	10	10	10	10	10	10	10	10
				10	16.	16.	10	16.	15.	16.	10	16.	16.	16.	15.	16.	16.	16.	15.	16.	16.	15.
10	0.1	5	0	16	3	2	16	2	8	2	16	3	2	3	8	1	2	2	7	1	2	9
					10	10		10	10	10		10	10	10	10	10	10	10	10	10	10	10
				10	16.	16.	10	16.	15.	16.	10	16.	16.	16.	15.	16.	16.	16.	15.	16.	16.	15.
11	0.1	6	0	16	3	2	16	2	8	2	16	3	3	2	8	1	2	2	7	1	2	9
				10	10	10		10	10	10	10	10	10	10	10	10	10	10	10	10	10	10
				16.	16.	16.	10	16.	15.	16.	15.	16.	16.	16.	15.	16.	16.	16.	15.	16.	16.	15.
12	0.1	6	0	1	3	2	16	2	8	2	9	3	3	3	8	1	2	2	7	1	2	9
					10	10		10	10	10	10	10	10	10	10	10	10	10	10	10	10	10
				10	16.	16.	10	16.	15.	16.	15.	16.	16.	16.	15.	16.	16.	16.	15.	16.	16.	15.
13	0.1	6	0	16	3	2	16	2	8	1	9	3	3	3	8	1	2	2	7	1	2	9
					10	10		10	10	10		10	10	10	10	10	10	10	10	10	10	10
				10	16.	16.	10	16.	15.	16.	10	16.	16.	16.	15.	16.	16.	16.	15.	16.	16.	15.
14	0.2	8	0	16	3	2	16	2	8	2	16	3	3	3	9	1	2	2	7	1	2	9
					10	10		10	10	10		10	10	10	10	10	10	10	10	10	10	10
				10	16.	16.	10	16.	15.	16.	10	16.	16.	16.	15.	16.	16.	16.	15.	16.	16.	15.
15	0.1	7	0	16	3	2	16	2	8	2	16	3	3	2	8	1	2	2	7	1	2	9
				10	10	10		10	10	10	10	10	10	10	10	10	10	10	10	10	10	10
				16.	16.	16.	10	16.	15.	16.	15.	16.	16.	16.	15.	16.	16.	16.	15.	16.	16.	15.
16	0.1	7	0	1	3	2	16	2	8	2	9	3	3	3	8	1	3	2	7	1	2	9
					10	10		10	10	10	10	10	10	10	10	10	10	10	10	10	10	10
				10	16.	16.	10	16.	15.	16.	15.	16.	16.	16.	15.	16.	16.	16.	15.	16.	16.	15.
17	0.1	7	0	16	3	2	16	2	8	1	9	3	3	2	8	1	2	2	7	1	2	9
					10	10		10	10	10	10	10	10	10	10	10	10	10	10	10	10	10
				10	16.	16.	10	16.	15.	16.	15.	16.	16.	16.	15.	16.	16.	16.	15.	16.	16.	15.
18	0.1	7	0	16	3	2	16	2	8	1	9	3	2	2	8	1	2	2	7	1	2	9
19	0.1	7	0	10	10	10	10	10	10	10	10	10	10	10	10	10	10	10	10	10	10	10

				16	16.3	16.2	16	16.2	15.8	16.2	15.9	16.3	16.3	16.3	15.8	16.1	16.3	16.2	15.7	16.1	16.2	15.9	
				10	10	10		10	10	10	10	10	10	10	10	10	10	10	10	10	10	10	
20	0.1	7	0	10 16	16.3	16.2	10 16	16.2	15.8	16.2	15.9	16.3	16.3	16.3	15.8	16.1	16.2	16.2	15.7	16.2	16.2	15.9	
				10	10		10		10	10					10					10			
	0.11	6.5	0	16.015	16.305	10 16.215	10 16.015	10 16.215	10 15.795	16.185	10 15.955	10 16.363	10 16.2626	10 16.2626	10 15.815	10 16.161	10 16.2121	10 16.222	10 15.757	10 16.105	10 16.222	10 15.959	Avg
				21	21	21	21	21	21	21	21	21	21	21	21	21	21	21	21	21	21	21	
				21.99	22.59	22.39	21.99	22.378	21.532	22.346	21.856	22.587	22.503	22.503	21.574	22.169	22.399	22.378	21.334	22.179	22.378	21.751	psf
		9.533336																					FPS
				-0.42401	-0.51894	0.430397	-0.61387	-0.80374	0.715199	0.715199	0.050662	1	1.379735	-0.32907	-0.61387	-0.80898	-0.70881	-0.80898	-0.80898	-0.80374	-0.80898	-0.13921	Cp
				10	10	10	10	10	10	10	10	10	10	10	10	10	10	10	10	10	10	10	
21	2.4	31	0	14.7	14.9	14.8	14.5	14.6	14.2	14.6	14.7	15.4	15.8	14.3	10 14	14.3	10 15	10 15	14.5	14.9	15.1	14.8	
				10	10	10	10	10	10	10	10	10	10	10	10	10	10		10		10	10	
22	2.3	30	0	14.7	14.9	14.8	14.5	14.7	14.2	14.6	14.7	15.5	15.8	14.4	14.1	14.3	15.1	10 15	14.5	10 15	15.1	14.8	
				10	10	10	10	10	10	10	10	10	10	10		10	10		10		10	10	
23	2.2	30	0	14.7	14.9	14.8	14.5	14.7	14.2	14.6	14.7	15.5	15.8	14.4	10 14	14.3	10 15	10 15	14.5	10 15	15.1	14.8	
				10	10	10	10	10	10	10	10	10	10	10		10			10		10	10	
24	2.4	30	0	14.7	14.9	14.8	14.5	14.7	14.2	14.6	14.7	15.5	15.8	14.4	10 14	14.3	10 15	10 15	14.5	10 15	15.1	14.8	

				10	10	10	10	10	10	10	10	10	10	10	10	10	10	10		10	10
				14.	14.	14.	14.	14.	14.	14.	14.	15.	15.	14.	14.	14.	15.	15.	14.	10	15.	14.
25	2.3	30	0	7	9	8	5	7	2	6	7	5	8	4	1	3	1	1	5	15	1	8
				10	10	10	10	10	10	10	10	10	10	10	10	10			10		10	10
				14.	14.	14.	14.	14.	14.	14.	14.	15.	15.	14.	14.	14.	10	10	14.	10	15.	14.
26	2.2	30	0	6	9	8	5	7	2	6	7	5	8	4	1	3	15	15	5	15	1	8
				10	10	10	10	10	10	10	10	10	10	10	10	10	10	10	10		10	10
				14.	14.	14.	14.	14.	14.	14.	14.	15.	15.	14.	14.	14.	15.	15.	14.	10	15.	14.
27	2.3	30	0	6	9	8	5	7	2	6	7	5	8	3	1	3	1	1	5	15	1	8
				10		10	10	10	10	10	10	10	10	10	10	10	10		10		10	10
				14.	10	14.	14.	14.	14.	14.	14.	15.	15.	14.	14.	14.	15.	10	14.	10	15.	14.
28	2.3	30	0	7	15	8	5	7	2	6	7	5	8	3	1	3	1	15	5	15	1	8
				10	10	10	10	10	10	10	10	10	10	10	10	10	10	10	10		10	10
				14.	14.	14.	14.	14.	14.	14.	14.	15.	15.	14.	14.	14.	15.	15.	14.	10	15.	14.
29	2.3	30	0	7	9	8	5	7	2	6	7	5	8	4	1	3	1	1	5	15	1	8
				10	10	10	10	10	10	10	10	10	10	10	10	10			10		10	10
				14.	14.	14.	14.	14.	14.	14.	14.	15.	15.	14.	14.	14.	10	10	14.	10	15.	14.
30	2.3	30	0	7	9	8	5	7	2	6	7	5	8	4	1	3	15	15	5	15	1	8
				10	10	10	10	10	10	10	10	10	10	10	10	10			10	10	10	10
				14.	14.	14.	14.	14.	14.	14.	14.	15.	15.	14.	14.	14.	10	10	14.	14.	15.	14.
31	2.3	30	0	6	9	8	5	7	2	6	7	5	8	4	1	3	15	15	5	9	1	8
				10	10	10	10	10	10	10	10	10	10	10	10	10			10		10	10
				14.	14.	14.	14.	14.	14.	14.	14.	15.	15.	14.	14.	14.	10	10	14.	10	15.	14.
32	2.3	30	0	6	9	8	5	7	2	6	7	5	8	4	1	3	15	15	5	15	1	8
				10	10	10	10	10	10	10	10	10	10	10	10	10	10		10		10	10
				14.	14.	14.	14.	14.	14.	14.	14.	15.	15.	14.	14.	14.	15.	10	14.	10	15.	14.
33	2.3	30	0	7	9	8	5	7	2	6	7	5	8	4	1	3	1	15	5	15	1	8
				10	10	10	10	10	10	10	10	10	10	10	10	10	10		10	10	10	10
				14.	14.	14.	14.	14.	14.	14.	14.	15.	15.	14.	14.	14.	15.	10	14.	14.	15.	14.
34	2.3	30	0	7	9	8	5	7	2	6	7	4	8	4	1	3	1	15	5	9	1	8
				10	10	10	10	10	10	10	10	10	10	10		10			10		10	10
				14.	14.	14.	14.	14.	14.	14.	14.	15.	15.	14.	10	14.	10	10	14.	10	15.	14.
35	2.4	30	0	6	9	8	5	7	2	6	7	5	8	3	14	3	15	15	5	15	1	8
36	2.4	30	0	10	10	10	10	10	10	10	10	10	10	10	10	10	10	10	10	10	10	10

				14.7	14.9	14.8	14.5	14.7	14.2	14.6	14.7	15.5	15.8	14.4	14	14.3	15.1	15	14.5	15	15.1	14.8	
				10	10	10	10	10	10	10	10	10	10	10		10	10		10	10	10	10	
37	2.3	30	0	14.7	14.9	14.8	14.5	14.7	14.2	14.6	14.7	15.5	15.8	14.4	10 14	14.3	15.1	10 15	14.5	14.9	15.1	14.8	
				10	10	10	10	10	10	10	10	10	10	10		10			10		10	10	
38	2.3	30	0	14.6	14.9	14.8	14.5	14.6	14.2	14.5	14.7	15.5	15.8	14.3	10 14	14.3	15	10 15	14.5	10 15	15.1	14.8	
				10	10	10	10	10	10	10	10	10	10	10		10	10		10		10	10	
39	2.4	31	0	14.6	14.9	14.8	14.5	14.7	14.2	14.6	14.7	15.5	15.8	14.3	10 14	14.3	15.1	10 15	14.5	10 15	15.1	14.8	
				10	10	10	10	10	10	10	10	10	10	10		10	10		10	10	10	10	
40	2.4	30	0	14.7	14.9	14.8	14.5	14.6	14.2	14.6	14.6	15.5	15.8	14.3	10 14	14.2	15.1	10 15	14.5	14.9	15.1	14.8	
				10	10			10		10	10			10	10	10		10		10			
				14.10	14.10	10	10	14.10	10	14.10	14.10	10	10	14.10	14.10	14.10	10	15.10	10	14.10	10	10	
	2.32	30.1	0	14.665	14.905	14.8	14.5	14.685	14.2	14.595	14.695	15.49	15.8	14.365	14.055	14.295	15.06	15.015	14.55	14.975	15.1	14.8	Avg
				21	21	21	21	21	21	21	21	21	21	21	21	21	21	21	21	21		21	
				19.172	19.673	19.454	18.827	19.214	18.201	19.026	19.235	20.895	21.542	18.545	17.898	18.399	19.997	19.903	18.827	19.819	21.08	19.454	psf
		44.1466																					FPS
				-0.28283	-0.33235	-0.29634	-0.40437	-0.44938	-0.44938	-0.44888	-0.10474	-0.27081	0.603897	-0.76896	-0.66093	-0.71495	-0.11629	-0.15688	-0.17033	-0.10279	-0.08028	-0.04427	Cp
				10	10	10	10	10	10	10	10	10	10	10	10			10	10	10	10	10	
41	9.5	61	0	10.3	10.2	09.9	09.3	09.3	08.8	09.1	10.3	12.8	14.6	08.2	08.4	10 11	10 11	11.2	10.9	11.4	11.7	11.5	

				10	10	10	10	10	10	10	10	10	10	10	10	10	10	10	10	10	10
				10.	10.	09.	09.	09.	08.	09.	10.	12.	14.	08.	08.	11.	11.	11.	10.	11.	11.	11.
42	9.5	61	0	3	2	8	3	3	8	1	4	9	6	2	5	1	1	2	9	5	7	5
				10	10	10	10	10	10	10	10	10	10	10	10	10		10	10	10	10	10
				10.	10.	09.	09.	09.	08.	09.	10.	12.	14.	08.	08.	11.	10	11.	10.	11.	11.	11.
43	9.3	60	0	3	2	9	3	3	8	1	4	9	6	2	5	1	11	3	9	4	7	5
				10	10	10	10	10	10	10	10	10	10	10	10	10	10	10	10	10	10	10
				10.	10.	09.	09.	09.	08.	09.	10.	12.	14.	08.	08.	11.	11.	11.	10.	11.	11.	11.
44	9.4	61	0	3	2	9	3	3	8	1	4	8	6	2	5	1	1	2	9	4	7	6
				10	10	10	10	10	10	10	10	10	10	10	10	10	10	10	10	10	10	10
				10.	10.	09.	09.	09.	08.	09.	10.	12.	14.	08.	08.	11.	11.	11.	10.	11.	11.	11.
45	9.5	61	0	3	2	9	4	3	8	1	4	9	6	2	5	1	1	3	9	5	7	5
				10	10	10	10	10	10	10	10	10	10	10	10	10	10	10	10	10	10	10
				10.	10.	09.	09.	09.	08.	09.	10.	12.	14.	08.	08.	11.	11.	11.	10.	11.	11.	11.
46	9.4	61	0	3	2	9	4	3	8	2	4	8	6	2	5	1	1	3	9	4	7	5
				10	10	10	10	10	10	10	10	10	10	10	10	10		10	10	10	10	10
				10.	10.	09.	09.	09.	08.	09.	10.	12.	14.	08.	08.	11.	10	11.	10.	11.	11.	11.
47	9.5	61	0	3	2	9	3	3	8	1	3	9	6	2	4	1	11	2	9	4	7	5
				10	10	10	10	10	10	10	10	10	10	10	10	10	10	10	10	10	10	10
				10.	10.	09.	09.	09.	08.	09.	10.	12.	14.	08.	08.	11.	11.	11.	10.	11.	11.	11.
48	9.3	60	0	3	2	9	4	3	8	1	4	9	6	2	5	1	1	2	9	4	7	6
				10	10	10	10	10	10	10	10	10	10	10	10	10		10	10	10	10	10
				10.	10.	09.	09.	09.	08.	09.	10.	12.	14.	08.	08.	11.	10	11.	10.	11.	11.	11.
49	9.4	61	0	3	2	9	4	3	8	1	4	9	6	2	5	1	11	2	9	4	7	5
				10	10	10	10	10	10	10	10	10	10	10	10	10		10	10	10	10	10
				10.	10.	09.	09.	09.	08.	09.	10.	12.	14.	08.	08.	11.	10	11.	10.	11.	11.	11.
50	9.4	61	0	3	2	8	3	3	8	1	3	9	6	1	4	1	11	2	8	4	7	5
				10	10	10	10	10	10	10	10	10	10	10	10	10		10	10	10	10	10
				10.	10.	09.	09.	09.	08.	09.	10.	12.	14.	08.	08.	11.	10	11.	10.	11.	11.	11.
51	9.6	61	0	2	2	8	3	3	8	1	3	8	6	2	4	1	11	2	9	4	7	5
				10	10	10	10	10	10	10	10	10	10	10	10	10		10	10	10	10	10
				10.	10.	09.	09.	09.	08.	09.	10.	12.	14.	08.	08.	11.	10	11.	10.	11.	11.	11.
52	9.4	61	0	3	2	8	3	3	8	1	3	8	6	2	4	1	11	2	8	4	7	5
53	9.5	61	0	10	10	10	10	10	10	10	10	10	10	10	10	10	10	10	10	10	10	10

				10.3	10.2	09.8	09.3	09.2	08.8	09.1	10.3	12.8	14.6	08.2	08.4	11.1	11	11.2	10.8	11.4	11.7	11.5	
				10	10	10	10	10	10	10	10	10	10	10	10	10		10	10	10	10	10	
54	9.5	61	0	10.2	10.2	09.8	09.3	09.3	08.8	09.1	10.3	12.8	14.6	08.1	08.4	11.1	10	11.2	10.8	11.4	11.7	11.5	
				10	10	10	10	10	10	10	10	10	10	10	10			10	10	10	10	10	
55	9.4	61	0	10.3	10.2	09.8	09.3	09.3	08.7	09.1	10.3	12.8	14.6	08.2	08.4	10.11	10	11.2	10.9	11.4	11.7	11.5	
				10	10	10	10	10	10	10	10	10	10	10	10			10	10	10	10	10	
56	9.6	61	0	10.3	10.2	09.8	09.3	09.3	08.8	09.1	10.3	12.8	14.6	08.1	08.5	10.11	10	11.2	10.8	11.4	11.7	11.5	
				10	10	10	10	10	10	10	10	10	10	10	10			10	10	10	10	10	
57	9.4	60	0	10.2	10.2	09.8	09.3	09.2	08.8	09.1	10.3	12.8	14.6	08.1	08.4	10.11	10	11.2	10.9	11.5	11.7	11.5	
				10	10	10	10	10	10	10	10	10	10	10	10	10		10	10	10	10	10	
58	9.4	61	0	10.3	10.2	09.8	09.3	09.3	08.8	09.1	10.3	12.8	14.6	08.2	08.5	11.1	10	11.2	10.8	11.4	11.7	11.5	
				10	10	10	10	10	10	10	10	10	10	10	10	10	10	10	10	10	10	10	
59	9.4	61	0	10.3	10.2	09.9	09.3	09.3	08.8	09.1	10.3	12.8	14.7	08.2	08.5	11.1	11.1	11.2	10.9	11.5	11.7	11.5	
				10	10	10	10	10	10	10	10	10	10	10	10	10	10	10	10	10	10	10	
60	9.4	61	0	10.3	10.2	09.9	09.4	09.3	08.8	09.1	10.4	12.9	14.6	08.2	08.5	11.1	11.1	11.2	10.9	11.5	11.7	11.5	
				10			10		10	10			10		10		10	10		10			
	9.44	60.85	0	10.28	10.2	09.85	09.32	09.29	08.79	09.15	10.34	12.84	14.60	08.18	08.45	11.08	11.03	11.21	10.87	11.42	11.7	11.51	Avg
				21	21	21	21	21	21		21		21	21	21	21		21	21	21	21	21	
				10.02	09.84	09.11	08.01	07.94	06.91	21 07.56	10.13	21 15.36	19.04	05.62	06.20	11.68	21 11.59	11.96	11.24	12.40	12.97	12.58	
				4	7	6	9	6	2		9		7	8	2	4		6	6	5	9	3	psf
		89.2466																					FPS

		9																				
				-	-	-	-	-	-	-	-	0.2	0.6	-	-	-	-	-	-	-	-	0.0	
				0.2	0.3	0.4	0.4	0.5	0.5	0.5	0.2	34	38	0.8	0.6	0.1	0.1	0.1	0.0	0.0	0.0	15	
				84	68	13	98	49	52	69	52	49	26	03	47	32	64	25	90	56	17	46	
				32	39	75	93	81	03	73	24	6	6	14	16	77	85	03	73	44	72	4	Cp
				10								10	10			10	10	10	10	10		10	
	27.	10		01.	99	99	99	99	99	99	99	06.	11.	99	99	00.	00.	01.	01.	02.	10	03.	
61	7	4	0	5	8.5	7.7	6.4	5.9	5.3	5.5	9.6	5	3	1.9	3.5	1	9	6	6	5	03	2	
				10								10	10				10	10	10	10		10	
	27.	10		01.	99	99	99	99	99	99	99	06.	11.	99	99	10	00.	01.	01.	02.	10	03.	
62	3	3	0	5	8.5	7.6	6.4	5.9	5.3	5.5	9.6	5	3	1.9	3.5	00	9	6	6	5	03	2	
				10								10	10			10	10	10	10	10	10	10	
	26.	10		01.	99	99	99	99	99	99	99	06.	11.	99	99	00.	00.	01.	01.	02.	03.	03.	
63	9	3	0	6	8.5	7.7	6.5	6	5.3	5.6	9.7	6	3	2	3.6	1	9	6	7	6	1	2	
				10								10	10			10		10	10	10		10	
	26.	10		01.	99	99	99	99	99	99	99	06.	11.	99	99	00.	10	01.	01.	02.	10	03.	
64	6	2	0	6	8.6	7.8	6.5	6	5.4	5.7	9.7	6	3	2	3.6	1	01	6	7	5	03	2	
				10								10	10			10	10	10	10	10		10	
	26.	10		01.	99	99	99	99	99	99	99	06.	11.	99	99	00.	00.	01.	01.	02.	10	03.	
65	7	2	0	5	8.5	7.7	6.4	5.9	5.3	5.5	9.6	5	3	2	3.6	1	9	6	6	5	03	2	
				10								10	10				10	10	10	10		10	
	26.	10		01.	99	99	99	99	99	99	99	06.	11.	99	99	10	00.	01.	01.	02.	10	03.	
66	9	3	0	5	8.5	7.7	6.4	5.9	5.3	5.6	9.6	5	3	1.9	3.4	00	9	6	6	5	03	2	
				10								10	10			10		10	10	10		10	
	26.	10		01.	99	99	99	99	99	99	99	06.	11.	99	99	00.	10	01.	01.	02.	10	03.	
67	8	2	0	5	8.5	7.7	6.4	5.9	5.3	5.6	9.7	6	3	1.9	3.5	1	01	6	7	5	03	2	
				10								10	10			10		10	10	10		10	
	26.	10		01.	99	99	99	99	99	99	99	06.	11.	99	99	00.	10	01.	01.	02.	10	03.	
68	2	1	0	6	8.6	7.8	6.5	6	5.4	5.7	9.7	6	2	2	3.6	1	01	7	7	6	03	2	
				10								10	10			10		10	10	10	10	10	
	26.	10		01.	99	99	99	99	99	99	99	06.	11.	99	99	00.	10	01.	01.	02.	03.	03.	
69	9	3	0	6	8.6	7.8	6.6	6	5.4	5.7	9.8	6	3	2	3.6	1	01	7	7	6	1	2	
70	26.	10	0	10	99	99	99	99	99	99	99	10	10	99	99	10	10	10	10	10	10	10	

	4	2		01.6	8.6	7.8	6.5	6	5.4	5.6	9.7	06.6	11.3	2	3.5	00.1	00.9	01.7	01.7	02.5	03	03.2
				10								10	10			10		10	10	10		10
	26.5	102	0	01.6	99 8.5	99 7.8	99 6.5	99 6	99 5.4	99 5.6	99 9.7	06.6	11.3	99 2	99 3.6	00.1	10 01	01.6	01.6	02.5	10 03	03.2
				10								10	10			10		10	10	10	10	10
72	26.8	102	0	01.6	99 8.5	99 7.8	99 6.5	99 6	99 5.4	99 5.7	99 9.8	06.6	11.3	99 2	99 3.6	00.1	10 01	01.7	01.7	02.6	03.1	03.3
				10								10	10			10		10	10	10	10	10
73	26.6	102	0	01.7	99 8.7	99 7.8	99 6.6	99 6.1	99 5.5	99 5.8	99 9.8	06.6	11.3	99 2.2	99 3.7	00.2	10 01	01.7	01.8	02.6	03.1	03.3
				10								10	10			10		10	10	10		10
74	26.3	101	0	01.6	99 8.6	99 7.8	99 6.5	99 6	99 5.5	99 5.7	99 9.8	06.6	11.3	99 2.1	99 3.7	00.2	10 01	01.7	01.7	02.5	03	03.2
				10								10	10			10	10	10	10	10	10	10
75	27.2	103	0	01.6	99 8.5	99 7.8	99 6.5	99 5.9	99 5.3	99 5.6	99 9.7	06.6	11.3	99 2	99 3.6	00.1	00.9	01.6	01.7	02.5	03.1	03.2
				10								10	10			10		10	10	10	10	10
76	26.5	102	0	01.6	99 8.6	99 7.7	99 6.5	99 5.9	99 5.4	99 5.6	99 9.7	06.6	11.3	99 2.1	99 3.7	00.1	10 01	01.7	01.7	02.6	03.1	03.3
				10								10	10			10		10	10	10	10	10
77	26.8	102	0	01.6	99 8.6	99 7.8	99 6.6	99 6.1	99 5.5	99 5.7	99 9.8	06.6	11.3	99 2.1	99 3.7	00.2	10 01	01.7	01.7	02.6	03.1	03.3
				10								10	10			10	10	10	10	10	10	10
78	26.9	103	0	01.6	99 8.6	99 7.9	99 6.6	99 6.1	99 5.5	99 5.8	99 9.8	06.7	11.4	99 2.3	99 3.8	00.2	01.1	01.8	01.8	02.7	03.2	03.4
				10								10	10			10		10	10	10	10	10
79	27	103	0	01.7	99 8.7	99 7.9	99 6.6	99 6.1	99 5.5	99 5.7	99 9.8	06.6	11.3	99 2.1	99 3.7	00.2	10 01	01.8	01.7	02.6	03.1	03.3
				10								10	10			10	10	10	10	10		10
80	26.2	101	0	01.6	99 8.5	99 7.7	99 6.5	99 5.9	99 5.3	99 5.6	99 9.7	06.6	11.3	99 1.9	99 3.5	00.1	00.9	01.6	01.6	02.5	03	03.2
	26.76	102.3	0	10 01.	99 8.5	99 7.7	99 6.5	99 5.9	99 5.3	99 5.6	99 9.7	10 06.	10 11.	99 2.0	99 3.6	10 00.	10 00.	10 01.	10 01.	10 02.	10 03.	10 03.	Av g

				585	6	65		8	85	4	15	585	3	2		115	965	66	68	55	05	235			
				2091.8544	2085.5366	2083.8766	2081.234	2080.1467	2078.9055	2079.4377	2087.9488	2102.2966	2112.1444	2071.8777	2075.1777	2088.7844	2090.5559	2092.01	2092.052	2093.869	2094.913	2095.3	psf		
		150.04																					FPS		
				-0.13207	-0.39119	-0.44192	-0.52973	-0.58553	-0.59411	-0.60465	-0.2271	0.241771	0.614447	-0.89733	-0.74045	-0.25539	-0.19685	-0.14261	-0.10203	-0.06534	-0.03413	0.006849	Cp		
count	q [psf]	V_ref [mph]	Alpha [deg]	P 1 [mbar]	P 2 [mbar]	P 3 [mbar]	P 4 [mbar]	P 5 [mbar]	P 6 [mbar]	P 7 [mbar]	P 8 [mbar]	P 9 [mbar]	P 10 [mbar]	P 11 [mbar]	P 12 [mbar]	P 13 [mbar]	P 14 [mbar]	P 15 [mbar]	P 16 [mbar]	P 17 [mbar]	P 18 [mbar]	P 19 [mbar]	1 mbar = 1 mph = 1 sq. ft =	2.0885433 1.466667 144	psf psf in
1	0.1	7	0	1016	1016.2	1016.1	1015.9	1016.1	1015.7	1016.1	1015.9	1016.1	1016.2	1016.2	1015.8	1016	1016.2	1016.1	1015.6	1016.1	1016.2	1015.9			
2	0.1	6	0	1016	1016.2	1016.1	1015.9	1016.1	1015.7	1016.1	1015.9	1016.1	1016.2	1016.2	1015.7	1016	1016.2	1016.2	1015.6	1016.1	1016.2	1015.9			
3	0.1	7	0	1016	1016.3	1016.1	1016	1016.1	1015.7	1016.1	1015.9	1016.2	1016.2	1016.2	1015.8	1016	1016.2	1016.2	1015.7	1016	1016.2	1015.9			
4	0	4	0	1016	1016.3	1016.1	1016	1016.1	1015.7	1016.1	1015.9	1016.2	1016.2	1016.2	1015.8	1016	1016.2	1016.2	1015.7	1016	1016.2	1015.9			

					3	1		1	7	1	9	1	2	2	7		2	2	7	1	2	9
					10	10		10	10	10	10	10	10	10	10		10	10	10	10	10	10
				10	16.	16.	10	16.	15.	16.	15.	16.	16.	16.	15.	10	16.	16.	15.	16.	16.	15.
5	0.1	6	0	16	3	2	16	1	7	1	9	2	2	2	7	16	2	2	7	1	2	9
					10	10		10	10	10	10	10	10	10	10		10	10	10	10	10	10
				10	16.	16.	10	16.	15.	16.	15.	16.	16.	16.	15.	10	16.	16.	15.	16.	16.	15.
6	0.1	6	0	16	3	2	16	1	7	1	9	2	2	2	8	16	2	2	7	1	2	9
					10	10	10	10	10	10	10	10	10	10	10		10	10	10	10	10	10
				10	16.	16.	15.	16.	15.	16.	15.	16.	16.	16.	15.	10	16.	16.	15.	16.	16.	15.
7	0.1	6	0	16	3	1	9	1	7	1	9	1	2	2	8	16	2	2	6	1	2	9
					10	10		10	10	10	10	10	10	10	10		10	10	10	10	10	10
				10	16.	16.	10	16.	15.	16.	15.	16.	16.	16.	15.	10	16.	16.	15.	16.	16.	15.
8	0.1	7	0	16	3	1	16	1	7	1	8	1	2	2	7	16	2	2	6	1	2	9
					10	10		10	10	10	10	10	10	10	10		10	10	10	10	10	10
				10	16.	16.	10	16.	15.	16.	15.	16.	16.	16.	15.	10	16.	16.	15.	16.	16.	15.
9	0.1	5	0	16	2	1	16	1	7	1	8	1	2	2	8	16	2	2	6	1	2	9
					10	10		10	10	10	10	10	10	10	10		10	10	10	10	10	10
				10	16.	16.	10	16.	15.	16.	15.	16.	16.	16.	15.	10	16.	16.	15.	16.	16.	15.
10	0.1	5	0	16	3	2	16	1	7	1	9	1	2	2	8	16	2	2	7	1	1	9
					10	10		10	10	10	10	10	10	10	10		10	10	10	10	10	10
				10	16.	16.	10	16.	15.	16.	15.	16.	16.	16.	15.	10	16.	16.	15.	16.	16.	15.
11	0.1	7	0	16	3	1	16	2	7	1	9	2	2	2	8	16	2	2	7	1	2	9
					10	10		10	10	10	10	10	10	10	10		10	10	10	10	10	10
				10	16.	16.	10	16.	15.	16.	15.	16.	16.	16.	15.	10	16.	16.	15.	16.	16.	15.
12	0.1	6	0	16	3	1	16	1	7	1	9	2	2	2	8	16	2	2	6	1	2	9
					10	10		10	10	10	10	10	10	10	10	10	10	10	10	10	10	10
				10	16.	16.	10	16.	15.	16.	15.	16.	16.	16.	15.	16.	16.	16.	15.	16.	16.	15.
13	0.1	6	0	16	2	2	16	2	7	1	9	2	2	2	8	1	2	2	7	1	2	9
					10	10		10	10	10	10	10	10	10	10		10	10	10	10	10	10
				10	16.	16.	10	16.	15.	16.	15.	16.	16.	16.	15.	10	16.	16.	15.	16.	16.	15.
14	0.1	6	0	16	3	1	16	1	7	1	8	2	2	2	8	16	2	2	7	1	2	9
					10	10		10	10	10	10	10	10	10	10	10	10	10	10	10	10	10
				10	16.	16.	10	16.	15.	16.	15.	16.	16.	16.	15.	16.	16.	16.	15.	16.	16.	15.
15	0.1	5	0	16	3	2	16	1	7	1	9	2	2	2	8	1	2	2	7	1	2	9

					10	10		10	10	10	10	10	10	10	10	10	10	10	10	10	10	10	
				10	16.	16.	10	16.	15.	16.	15.	16.	16.	16.	15.	16.	16.	16.	15.	16.	16.	15.	
16	0.1	5	0	16	3	2	16	2	7	1	9	2	2	2	8	1	2	2	7	1	2	9	
					10	10		10	10	10	10	10	10	10	10		10	10	10	10	10	10	
				10	16.	16.	10	16.	15.	16.	15.	16.	16.	16.	15.	10	16.	16.	15.	16.	16.	15.	
17	0.1	6	0	16	3	2	16	2	7	1	8	2	2	2	8	16	2	2	6	1	2	9	
					10	10		10	10	10	10	10	10	10	10		10	10	10	10	10	10	
				10	16.	16.	10	16.	15.	16.	15.	16.	16.	16.	15.	10	16.	16.	15.	16.	16.	15.	
18	0.1	7	0	16	3	2	16	2	7	1	9	2	2	2	8	16	2	2	7	1	2	9	
					10	10		10	10	10	10	10	10	10	10		10	10	10	10	10	10	
				10	16.	16.	10	16.	15.	16.	15.	16.	16.	16.	15.	10	16.	16.	15.	16.	16.	15.	
19	0.1	7	0	16	3	1	16	2	7	1	9	2	2	2	8	16	2	2	7	1	2	9	
					10	10		10	10	10	10	10	10	10	10	10	10	10	10	10	10	10	
				10	16.	16.	10	16.	15.	16.	15.	16.	16.	16.	15.	16.	16.	16.	15.	16.	16.	15.	
20	0.1	7	0	16	2	2	16	2	7	1	9	2	2	2	8	1	2	1	7	1	2	9	
					10	10	10	10				10							10	10	10		
					16.	16.	15.	16.	10	10	10	16.	10	10	10	10	10	10	15.	16.	16.	10	
	0.0	6.0		10	27	14	98	13	15.	16.	15.	16	16.	16.	15.	16.	16.	16.	66	09	19	15.	Av
	95	5	0	16	5	5	5	5	7	1	88	5	2	2	78	02	2	19	5	5	5	9	g
					21	21	21	21	21	21	21	21	21	21	21	21	21	21		21	21	21	
				21	22.	22.	21.	22.	21.	22.	21.	22.	22.	22.	21.	22.	22.	22.	21	22.	22.	21.	
				21.	53	26	92	24	33	16	70	30	37	37	50	00	37	35	21.	15	36	75	
				96	4	3	9	2	4	9	9	5	8	8	1	2	8	7	26	9	7	1	psf
		8.8																					
		73																					
		33																					FP
		5																					S
				-	-	-	-	-	-	-	-	-	0.1	-	-	-	-	-	-	-	-	-	
				0.9	1.4	1.0	1.5	2.5	1.4	1.1	1.6	1.9	20	1.8	1.6	2.9	1.1	1.4	1.9	1.3	1.3	0.3	
				78	18	88	28	17	18	98	38	67	61	58	38	57	98	18	67	08	08	19	
				62	31	54	24	55	31	47	16	93	3	01	16	24	47	31	93	39	39	08	Cp
				10	10	10	10	10	10	10	10	10	10	10	10	10	10	10	10	10	10	10	
21	2.3	30	0	14.	14.	14.	14.	14.	14.	14.	14.	14.	16.	14.	14.	14.	15	15	14.	14.	15	14.	

				5	8	7	5	7	1	3	2	9	1	7	4	8			5	9		7
				10	10	10	10	10		10	10		10	10	10	10			10	10		10
				14.	14.	14.	14.	14.	10	14.	14.	10	16.	14.	14.	14.	10	10	14.	14.	10	14.
22	2.3	30	0	5	8	6	5	6	14	3	2	15	1	7	4	8	15	15	5	9	15	7
				10	10	10	10	10		10	10	10	10	10	10	10			10	10		10
				14.	14.	14.	14.	14.	10	14.	14.	14.	16.	14.	14.	14.	10	10	14.	14.	10	14.
23	2.3	30	0	5	8	7	4	6	14	2	3	9	1	7	4	8	15	15	5	9	15	7
				10	10	10	10	10		10	10	10	10	10	10	10			10	10	10	10
				14.	14.	14.	14.	14.	10	14.	14.	14.	16.	14.	14.	14.	10	10	14.	14.	15.	14.
24	2.4	31	0	5	7	6	4	6	14	2	2	9	1	7	4	8	15	15	5	9	1	7
				10	10	10	10	10		10	10		10	10	10	10			10	10		10
				14.	14.	14.	14.	14.	10	14.	14.	10	16.	14.	14.	14.	10	10	14.	14.	10	14.
25	2.3	30	0	5	7	7	4	7	14	3	2	15	1	7	4	8	15	15	5	9	15	7
				10	10	10	10	10		10	10		10	10	10	10			10	10		10
				14.	14.	14.	14.	14.	10	14.	14.	10	16.	14.	14.	14.	10	10	14.	14.	10	14.
26	2.2	29	0	5	7	6	4	6	14	3	3	15	1	7	4	8	15	15	5	9	15	8
				10	10	10	10	10		10	10	10	10	10	10	10			10	10		10
				14.	14.	14.	14.	14.	10	14.	14.	14.	16.	14.	14.	14.	10	10	14.	14.	10	14.
27	2.3	30	0	5	8	6	4	6	14	2	2	9	1	7	4	8	15	15	5	9	15	7
				10	10	10	10	10		10	10	10	10	10	10	10			10	10		10
				14.	14.	14.	14.	14.	10	14.	14.	14.	16.	14.	14.	14.	10	10	14.	14.	10	14.
28	2.3	30	0	5	7	6	4	6	14	2	2	9	1	7	4	8	15	15	6	9	15	8
				10	10	10	10	10	10	10	10		10	10	10	10			10	10		10
				14.	14.	14.	14.	14.	14.	14.	14.	10	16.	14.	14.	14.	10	10	14.	14.	10	14.
29	2.3	30	0	5	7	6	4	6	1	3	2	15	1	7	4	8	15	15	5	9	15	7
				10	10	10	10	10		10	10	10	10	10	10	10			10	10		10
				14.	14.	14.	14.	14.	10	14.	14.	14.	16.	14.	14.	14.	10	10	14.	14.	10	14.
30	2.3	30	0	5	7	6	4	6	14	2	2	9	1	7	4	8	15	15	5	9	15	7
				10	10	10	10	10		10	10	10	10	10	10	10			10	10		10
				14.	14.	14.	14.	14.	10	14.	14.	14.	16.	14.	14.	14.	10	10	14.	14.	10	14.
31	2.3	30	0	5	7	6	4	6	14	2	2	9	2	7	4	8	15	15	5	9	15	8
				10	10	10	10	10		10	10	10	10	10	10	10			10	10	10	10
				14.	14.	14.	14.	14.	10	14.	14.	14.	16.	14.	14.	14.	10	10	14.	14.	15.	14.
32	2.3	30	0	5	7	6	4	6	14	2	2	9	1	7	4	8	15	15	5	9	1	8

				10	10	10	10	10		10	10	10	10	10	10	10			10	10		10	
				14.5	14.7	14.6	14.4	14.6	10 14	14.2	14.2	14.9	16.2	14.7	14.4	14.8	10 15	10 15	14.5	14.9	10 15	14.7	
33	2.4	30	0	10	10	10	10	10		10	10	10	10	10	10	10			10	10		10	
				14.5	14.7	14.6	14.4	14.6	10 14	14.2	14.2	14.9	16.2	14.7	14.4	14.8	10 15	10 15	14.5	14.9	10 15	14.7	
34	2.4	31	0	10	10	10	10	10		10	10	10	10	10	10	10			10	10		10	
				14.5	14.7	14.6	14.4	14.6	10 14	14.2	14.2	14.9	16.1	14.7	14.4	14.8	10 15	10 15	14.5	14.9	10 15	14.7	
35	2.3	30	0	10	10	10	10	10		10	10	10	10	10	10	10			10	10		10	
				14.5	14.7	14.6	14.4	14.6	10 14	14.2	14.2	14.9	16.1	14.7	14.4	14.8	10 15	10 15	14.5	14.9	10 15	14.7	
36	2.3	30	0	10	10	10	10	10		10	10	10	10	10	10	10			10	10		10	
				14.5	14.7	14.7	14.4	14.6	10 14	14.2	14.2	14.9	16.1	14.7	14.4	14.8	10 15	10 15	14.5	14.9	10 15	14.7	
37	2.5	31	0	10	10	10	10	10		10	10	10	10	10	10	10			10	10	10	10	
				14.5	14.7	14.6	14.4	14.7	10 14	14.3	14.2	14.9	16.1	14.7	14.4	14.8	10 15	10 15	14.5	14.9	15.1	14.8	
38	2.3	30	0	10	10	10	10	10		10	10	10	10	10	10	10			10	10		10	
				14.5	14.7	14.7	14.4	14.6	10 14	14.3	14.2	14.9	16.1	14.7	14.4	14.8	10 15	10 15	14.5	14.9	10 15	14.7	
39	2.4	30	0	10	10	10	10	10	10 14	10 14	10 14		10 16	10 14	10 14	10 14	10 15	10 15	10 14	10 14	10 15	10 14	
40	2.3	30	0	5	7	7	4	7	1	3	2	15	1	7	4	8	15	1	5	15	1	8	
				10	10	14.5	10	10	10 14	10 14	10 14	10 14	10 16	10 14	10 14	10 14		10 15	10 14	10 14	10 15	10 14	
	2.325	30.1	0	14.5	14.72	63 5	14.41	14.62	01 5	14.24	14.21	92 5	11 5	14.7	14.4	14.8	10 15	00 5	50 5	90 5	15.02	73 5	Avg
				21	21	21	21	21	21	21	21	21		21	21	21	21	21	21	21	21	21	
				18.827	19.287	19.109	18.639	19.078	17.814	18.284	18.222	19.715	21 22.2	19.245	18.618	19.454	19.872	19.882	18.838	19.673	19.913	19.318	psf
		44.14																					FPS

		668																					
				-0.42829	-0.49567	-0.44177	-0.51812	-0.50465	-0.61245	-0.76066	-0.60795	-0.23516	0.887713	-0.46423	-0.34745	-0.25762	-0.16779	-0.1633	-0.1633	-0.1633	-0.14982	-0.10042	Cp
41	12	69	0	1009.4	1008.1	1007	1006.5	1006.1	1005.2	1004.8	1005.6	1008.1	1016	1009.2	1009.2	1010.1	1010.5	1010.6	1010.2	1010.6	1010.8	1010.6	
42	12	69	0	1009.5	1008.1	1007	1006.5	1006.2	1005.2	1004.9	1005.6	1008.1	1016	1009.2	1009.3	1010.2	1010.5	1010.6	1010.2	1010.7	1010.8	1010.6	
43	11.8	68	0	1009.5	1008.2	1007.1	1006.5	1006.2	1005.2	1004.9	1005.7	1008.2	1016	1009.3	1009.3	1010.2	1010.5	1010.6	1010.2	1010.7	1010.8	1010.6	
44	11.7	68	0	1009.5	1008.2	1007.1	1006.6	1006.2	1005.2	1004.9	1005.7	1008.2	1016	1009.3	1009.3	1010.2	1010.5	1010.6	1010.2	1010.7	1010.8	1010.6	
45	12	69	0	1009.5	1008.2	1007.1	1006.5	1006.2	1005.2	1004.9	1005.7	1008.2	1016	1009.3	1009.3	1010.2	1010.5	1010.6	1010.2	1010.6	1010.8	1010.6	
46	11.7	68	0	1009.4	1008.2	1007	1006.5	1006.2	1005.2	1004.9	1005.7	1008.1	1016	1009.3	1009.2	1010.2	1010.5	1010.6	1010.2	1010.6	1010.8	1010.6	
47	12.1	69	0	1009.4	1008.1	1007	1006.5	1006.1	1005.2	1004.8	1005.7	1008.1	1016	1009.3	1009.3	1010.1	1010.5	1010.6	1010.2	1010.7	1010.8	1010.6	
48	11.9	68	0	1009.5	1008.2	1007	1006.5	1006.2	1005.2	1004.9	1005.7	1008.1	1016	1009.3	1009.3	1010.2	1010.5	1010.6	1010.2	1010.6	1010.8	1010.6	
49	11.9	68	0	1009.4	1008.2	1007	1006.5	1006.2	1005.2	1004.9	1005.7	1008.1	1016	1009.3	1009.3	1010.2	1010.5	1010.6	1010.1	1010.6	1010.8	1010.6	

				10	10		10	10	10	10	10	10		10	10	10	10	10	10	10	10	10	
	11.			09.	08.	10	06.	06.	05.	04.	05.	08.	10	09.	09.	10.	10.	10.	10.	10.	10.	10.	
50	9	68	0	5	1	07	5	2	2	9	7	1	16	3	3	2	5	6	2	6	8	6	
				10	10	10	10	10	10	10	10	10		10	10	10	10	10	10	10	10	10	
				09.	08.	07.	06.	06.	05.	04.	05.	08.	10	09.	09.	10.	10.	10.	10.	10.	10.	10.	
51	12	69	0	5	1	1	5	2	2	9	7	1	16	3	3	2	6	6	2	7	8	7	
				10	10	10	10	10	10		10	10		10	10	10	10	10	10	10	10	10	
				09.	08.	07.	06.	06.	05.	10	05.	08.	10	09.	09.	10.	10.	10.	10.	10.	10.	10.	
52	12	68	0	5	2	1	6	3	3	05	8	2	16	4	3	2	6	7	2	7	9	6	
				10	10	10	10	10	10		10	10		10	10	10	10	10	10	10	10	10	
	11.			09.	08.	07.	06.	06.	05.	10	05.	08.	10	09.	09.	10.	10.	10.	10.	10.	10.	10.	
53	8	68	0	5	2	1	6	3	3	05	8	2	16	3	3	2	5	6	2	7	8	6	
				10	10	10	10	10	10	10	10	10		10	10	10	10	10	10	10	10	10	
	11.			09.	08.	07.	06.	06.	05.	04.	05.	08.	10	09.	09.	10.	10.	10.	10.	10.	10.	10.	
54	8	68	0	5	2	1	5	2	2	9	7	2	16	4	3	2	5	6	2	7	9	6	
				10	10	10	10	10	10	10	10	10		10	10	10	10	10	10	10	10	10	
				09.	08.	07.	06.	06.	05.	04.	05.	08.	10	09.	09.	10.	10.	10.	10.	10.	10.	10.	
55	12	68	0	5	2	1	5	2	2	9	7	1	16	3	3	2	5	6	2	7	9	6	
				10	10	10	10	10	10		10	10		10	10	10	10	10	10	10	10	10	
	11.			09.	08.	07.	06.	06.	05.	10	05.	08.	10	09.	09.	10.	10.	10.	10.	10.	10.	10.	
56	8	68	0	5	2	1	6	2	3	05	8	2	16	4	3	2	6	6	2	7	9	7	
				10	10	10	10	10	10		10	10		10	10	10	10	10	10	10	10	10	
	11.			09.	08.	07.	06.	06.	05.	10	05.	08.	10	09.	09.	10.	10.	10.	10.	10.	10.	10.	
57	6	67	0	5	2	1	6	3	3	05	8	2	16	4	3	2	6	7	2	7	9	7	
				10	10	10	10	10	10		10	10		10	10	10	10	10	10	10	10	10	
	11.			09.	08.	07.	06.	06.	05.	10	05.	08.	10	09.	09.	10.	10.	10.	10.	10.	10.	10.	
58	8	68	0	5	3	2	6	3	3	05	8	2	16	4	3	2	5	7	3	7	9	6	
				10	10	10	10	10	10		10	10		10	10	10	10	10	10	10	10	10	
	11.			09.	08.	07.	06.	06.	05.	10	05.	08.	10	09.	09.	10.	10.	10.	10.	10.	10.	10.	
59	8	68	0	5	2	2	6	2	3	05	8	2	16	4	3	2	6	7	2	7	9	7	
				10	10	10	10	10	10		10	10		10	10	10	10	10	10	10	10	10	
	11.			09.	08.	07.	06.	06.	05.	10	05.	08.	10	09.	09.	10.	10.	10.	10.	10.	10.	10.	
60	8	68	0	5	2	2	6	3	3	05	8	2	16	4	4	2	6	7	3	7	9	7	
	11.	68.	0	10	10	10	10	10	10	10	10	10	10	10	10	10	10	10	10	10	10	10	Av

	87	2		09.48	08.18	07.08	06.54	06.2155	05.2355	04.9255	05.7255	08.1555	16	09.3255	09.2955	10.19	10.53	10.6255	10.2055	10.67	10.84	10.6255	g
				21 08.343	21 05.628	21 03.33	21 02.202	21 01.524	20 99.477	20 98.829	21 00.55	21 05.575	21 21.96	21 08.019	21 07.956	21 09.826	21 10.536	21 10.734	21 09.857	21 10.828	21 11.183	21 10.734	psf
		100.0267																					FPS
				-0.16304	-0.44368	-0.61172	-0.68221	-0.77359	-0.86069	-0.98385	-0.80795	-0.43312	0.957772	-0.23254	-0.16216	-0.05724	-0.01547	0.001476	0.015552	0.026989	0.039305	0.061299	Cp
61	26.6	102	0	1000.6	998.8	995.2	994	992.9	991.4	990.1	992.3	997.7	1015.8	1000.3	1000.8	1002.6	1003.3	1003.5	1003.2	1003.8	1004	1004	
62	26.7	102	0	1000.7	998.9	995.3	994.2	993.1	991.6	990.3	992.5	997.8	1015.8	1000.4	1000.9	1002.6	1003.3	1003.5	1003.3	1003.8	1004	1004	
63	26.8	102	0	1000.7	998.9	995.3	994.2	993.1	991.5	990.2	992.4	997.6	1015.7	1000.3	1000.8	1002.6	1003.2	1003.5	1003.1	1003.7	1003.9	1003.8	
64	27.5	104	0	1000.5	998.7	995	993.9	992.7	991.2	989.9	992.1	997.4	1015.8	1000.2	1000.6	1002.4	1003.1	1003.4	1003	1003.6	1003.8	1003.7	
65	27.4	104	0	1000.4	998.6	994.9	993.8	992.8	991.2	989.9	992.2	997.5	1015.8	1000.2	1000.7	1002.5	1003.2	1003.4	1003.1	1003.7	1004	1003.9	
66	26.1	101	0	1000.6	998.9	995.2	994.1	993	991.5	990.2	992.4	997.7	1015.8	1000.4	1000.8	1002.6	1003.2	1003.5	1003.2	1003.7	1004	1004	

				10									10	10	10	10	10	10	10	10		10
	26.	10		00.	99	99	99	99	99	99	99	99	15.	00.	00.	02.	03.	03.	03.	03.	10	03.
67	3	1	0	7	8.9	5.3	4.1	3.1	1.5	0.3	2.4	7.7	8	4	9	6	3	5	2	8	04	9
				10									10	10	10	10	10	10	10	10		10
	27.	10		00.	99	99	99	99	99	99	99	99	15.	00.	00.	02.	03.	03.	03.	03.	10	03.
68	1	3	0	6	8.9	5.2	4.1	3	1.4	0.2	2.4	7.6	8	4	8	6	3	5	2	8	04	9
				10									10	10	10	10	10	10	10	10	10	10
	26.	10		00.	99	99	99	99	99	99	99	99	15.	00.	00.	02.	03.	03.	03.	03.	03.	03.
69	8	2	0	6	8.9	5.2	4.1	3	1.4	0.2	2.3	7.6	8	3	7	5	2	4	1	6	9	8
				10									10	10	10	10	10	10	10	10		
		10		00.	99	99	99	99	99	99	99	99	15.	00.	00.	02.	03.	03.	03.	03.	10	10
70	27	3	0	5	8.7	5	3.9	2.8	1.3	0	2.2	7.6	8	3	8	5	2	4	2	7	04	04
				10									10	10	10	10	10	10	10	10	10	
	26.	10		00.	99	99	99	99	99	99	99	99	15.	00.	00.	02.	03.	03.	03.	03.	04.	10
71	5	2	0	7	8.9	5.3	4.2	3.1	1.6	0.4	2.5	7.8	8	4	9	6	3	5	3	8	1	04
				10									10	10	10	10	10	10	10	10		10
		10		00.	99	99	99	99	99	99	99	99	15.	00.	00.	02.	03.	03.	03.	03.	10	03.
72	26	1	0	8	9	5.4	4.3	3.3	1.8	0.5	2.7	7.9	8	5	9	7	3	6	2	8	04	9
				10									10	10	10	10	10	10	10	10	10	10
	26.	10		00.	99	99	99	99	99	99	99	99	15.	00.	00.	02.	03.	03.	03.	03.	03.	03.
73	9	2	0	7	8.8	5.2	4.1	2.9	1.4	0.1	2.3	7.6	8	3	7	5	2	5	1	7	9	9
				10									10	10	10	10	10	10	10	10		
	26.	10		00.	99	99	99	99	99	99	99	99	15.	00.	00.	02.	03.	03.	03.	03.	10	10
74	5	2	0	5	8.8	5.1	4	2.9	1.4	0.2	2.3	7.6	8	3	8	6	2	5	2	7	04	04
				10									10	10	10	10	10	10	10	10		10
	26.	10		00.	99	99	99	99	99	99	99	99	15.	00.	00.	02.	03.	03.	03.	03.	10	03.
75	5	2	0	7	8.9	5.3	4.2	3.1	1.5	0.3	2.4	7.7	8	4	9	6	3	5	2	8	04	9
				10									10	10	10	10	10	10	10	10	10	
	26.	10		00.	99	99	99	99	99	99	99	99	15.	00.	00.	02.	03.	03.	03.	03.	04.	10
76	8	2	0	6	8.8	5.2	4.1	3	1.5	0.2	2.4	7.7	8	5	9	6	3	5	3	8	1	04
				10									10	10	10	10	10	10	10	10		10
		10		00.	99	99	99	99	99	99	99	99	15.	00.	00.	02.	03.	03.	03.	03.	10	03.
77	27	3	0	7	9	5.4	4.3	3.2	1.7	0.4	2.5	7.8	8	5	9	7	3	5	2	8	04	9
78	27.	10	0	10	99	99	99	99	99	99	99	99	10	10	10	10	10	10	10	10	10	10

	4	4		00.5 10	8.7	5.1	4	2.9	1.3	0	2.2	7.5	15.8 10	00.2 10	00.7 10	02.5 10	03.1 10	03.4 10	03 10	03.6 10	03.8	03.7							
79	26.5	102	0	00.5 10	99 8.8	99 5.1	99 4	99 3	99 1.4	99 0.2	99 2.4	99 7.7	15.8 10	00.3 10	00.8 10	02.5 10	03.3 10	03.4 10	03.2 10	03.8 10	10 04 10	10 04 10							
80	27	103	0	00.5 10	99 8.7	99 5.1	99 3.9	99 2.8	99 1.3	99 0	99 2.2	99 7.5	15.8 10	00.2	00.7	02.5 10	03.1 10	03.4	03.1	03.6	03.9	03.8 10							
	26.77	102.35	0	00.60 5 20 89.807	99 8.83 20 86.1	99 5.19 20 78.498	99 4.075 20 76.169	99 2.985 20 73.892	99 1.445 20 70.676	99 0.18 20 68.034	99 2.355 20 72.577	99 7.65 20 83.635	15.795 21 21.532	10 00.34 20 89.254	10 00.8 20 90.214	02.565 20 93.901	03.235 20 95.3	10 03.47 20 95.791	10 03.17 20 95.164	10 03.73 20 96.334	10 03.97 20 96.835	03.905 20 96.699	Avg psf						
		150.113 4																					FPS						
				-0.208 11	-0.369 61	-0.642 28	-0.718 35	-0.818 6	-0.900 91	-1.003 03	-0.844 74	-0.455 04	0.965 282	-0.247 51	-0.178 07	-0.063 78	-0.019 31	-0.000 97	0.014 632	0.027 115	0.038 037	0.059 492	Cp						
count	q [psf]	V_ref [mph]	Alpha [deg]	P 1 [mbar]	P 2 [mbar]	P 3 [mbar]	P 4 [mbar]	P 5 [mbar]	P 6 [mbar]	P 7 [mbar]	P 8 [mbar]	P 9 [mbar]	P 10 [mbar]	P 11 [mbar]	P 12 [mbar]	P 13 [mbar]	P 14 [mbar]	P 15 [mbar]	P 16 [mbar]	P 17 [mbar]	P 18 [mbar]	P 19 [mbar]	1 mbar = 1 mm	2.0 88 54 3 1.4 66	psf fp					
1	0.1	6	0	10 15.	10 16.	10 16.	10 15.	10 16.	10 15.	10 16.	10 15.	10 16.	10 16.	10 16.	10 15.	10 16	10 16.	10 16.	10 15.	10 16	10 16.	10 15.							

				9	2	1	9	1	7	1	8	1	2	2	8		2	1	6		1	8	ph = 1	667	s
				10	10	10	10	10	10		10	10	10	10	10		10	10	10		10	10	sq.		p s
				15.	16.	16.	15.	16.	15.	10	15.	16.	16.	16.	15.	10	16.	16.	15.	10	16.	15.	ft	144	i
2	0.1	6	0	9	2	1	9	1	7	16	8	1	2	2	8	16	2	2	7	16	2	8	=		n
				10	10	10	10	10	10		10	10	10	10	10		10	10	10		10	10			
				15.	16.	16.	15.	16.	15.	10	15.	16.	16.	16.	15.	10	16.	16.	15.	10	16.	15.			
3	0.1	7	0	9	2	1	9	1	7	16	8	2	2	2	7	16	2	1	6	16	1	8			
				10	10	10	10	10	10		10	10	10	10	10		10	10	10		10	10			
				15.	16.	16.	15.	16.	15.	10	15.	16.	16.	16.	15.	10	16.	16.	15.	10	16.	15.			
4	0.1	7	0	9	2	1	9	1	7	16	8	1	2	2	8	16	2	1	7	16	1	8			
				10	10	10	10	10	10		10	10	10	10	10		10	10	10		10	10			
				15.	16.	16.	15.	16.	15.	10	15.	16.	16.	16.	15.	10	16.	16.	15.	10	16.	15.			
5	0.1	7	0	9	2	1	9	1	7	16	8	1	2	2	8	16	2	1	6	16	1	8			
				10	10	10	10	10	10		10	10	10	10	10		10	10	10		10	10			
				15.	16.	16.	15.	16.	15.	10	15.	16.	16.	16.	15.	10	16.	16.	15.	10	16.	15.			
6	0.1	7	0	9	2	1	9	1	7	16	8	1	2	2	8	16	2	1	6	16	1	8			
				10	10	10	10	10	10		10	10	10	10	10		10	10	10		10	10			
				15.	16.	16.	15.	16.	15.	10	15.	16.	16.	16.	15.	10	16.	16.	15.	10	16.	15.			
7	0.1	6	0	9	2	1	9	1	7	16	8	1	2	2	8	16	2	2	6	16	1	8			
				10	10	10	10	10	10		10	10	10	10	10		10	10	10		10	10			
				15.	16.	16.	15.	16.	15.	10	15.	16.	16.	16.	15.	10	16.	16.	15.	10	16.	15.			
8	0.1	7	0	9	2	1	9	1	7	16	8	1	2	2	8	16	2	2	6	16	1	8			
				10	10	10	10	10	10		10	10	10	10	10		10	10	10		10	10			
				15.	16.	16.	15.	16.	15.	10	15.	16.	16.	16.	15.	10	16.	16.	15.	10	16.	15.			
9	0.1	7	0	9	2	1	9	1	7	16	8	1	2	2	8	16	2	2	6	16	1	8			
				10	10	10	10	10	10	10	10	10	10	10	10		10	10	10		10	10			
				15.	16.	16.	15.	16.	15.	16.	15.	16.	16.	16.	15.	10	16.	16.	15.	10	16.	15.			
10	0.1	7	0	9	2	1	9	1	7	1	8	1	2	2	8	16	2	2	7	16	1	8			
				10	10	10	10	10	10	10	10	10	10	10	10		10	10	10		10	10			
				15.	16.	16.	15.	16.	15.	16.	15.	16.	16.	16.	15.	10	16.	16.	15.	10	16.	15.			
11	0.1	6	0	9	2	1	9	1	7	1	8	1	2	2	8	16	2	2	7	16	1	8			
12	0.2	8	0	10	10	10	10	10	10	10	10	10	10	10	10	10	10	10	10	10	10	10			

				15.9	16.2	16.1	15.9	16.1	15.7	16.1	15.8	16.1	16.2	16.2	15.8	16	16.2	16.1	15.6	16	16.1	15.8	
				10	10	10	10	10	10	10	10	10	10	10	10		10	10	10		10	10	
13	0.1	7	0	15.9	16.2	16.1	15.9	16.1	15.7	16.1	15.8	16.1	16.2	16.2	15.8	10 16	16.2	16.1	15.6	10 16	16.1	15.8	
				10	10	10	10	10	10	10	10	10	10	10	10		10	10	10		10	10	
14	0.1	7	0	15.9	16.2	16.1	15.9	16.1	15.7	16.1	15.8	16.1	16.2	16.2	15.8	10 16	16.2	16.1	15.6	10 16	16.1	15.8	
				10	10	10	10	10	10	10	10	10	10	10	10		10	10	10		10	10	
15	0.1	6	0	15.9	16.2	16.1	15.9	16.1	15.7	16.1	15.8	16.1	16.2	16.2	15.7	10 16	16.2	16.1	15.6	10 16	16.1	15.8	
				10	10	10	10	10	10	10	10	10	10	10	10	10	10	10	10		10	10	
16	0.1	7	0	15.9	16.2	16.1	15.9	16.1	15.7	16.1	15.8	16.1	16.2	16.2	15.8	16.1	16.2	16.1	15.6	10 16	16.1	15.8	
				10	10	10	10	10	10	10	10	10	10	10	10		10	10	10		10	10	
17	0.1	7	0	15.9	16.2	16.1	15.9	16.1	15.7	16.1	15.8	16.1	16.2	16.2	15.8	10 16	16.2	16.2	15.6	10 16	16.1	15.8	
				10	10	10	10	10	10	10	10	10	10	10	10		10	10	10		10	10	
18	0.1	6	0	15.9	16.2	16.1	15.9	16.1	15.7	16.1	15.8	16.1	16.2	16.2	15.7	10 16	16.2	16.2	15.6	10 16	16.1	15.8	
				10	10	10	10	10	10		10	10	10	10	10		10	10	10		10	10	
19	0.1	6	0	15.9	16.2	16.1	15.9	16.1	15.7	16.1	15.8	16.1	16.2	16.2	15.7	10 16	16.2	16.1	15.6	10 16	16.1	15.8	
				10	10	10	10	10	10		10	10	10	10	10		10	10	10		10	10	
20	0.2	8	0	15.9	16.2	16.1	15.9	16.1	15.7	16.1	15.8	16.1	16.2	16.2	15.7	10 16	16.2	16.1	15.6	10 16	16.1	15.8	
				10	10	10	10	10	10	10	10	10	10	10	10	10	10	10	10		10	10	
	0.11	6.75	0	15.9	16.2	16.1	15.9	16.1	15.7	16.05	15.8	16.105	16.2	16.2	15.775	10 16.005	16.2	16.14	15.62	10 16	16.15	15.8	Avg
				21	21	21	21	21	21	21	21	21	21	21		21	21	21	21		21	21	
				21.75 1	22.37 8	22.16 9	21.75 1	22.16 9	21.33 4	22.06 5	21.54 2	22.17 9	22.37 8	22.37 8	21.49	21.97 1	22.37 8	22.25 3	21.16 6	21.96	22.17 9	21.54 2	psf

		9.900002																			FPS
				-2.60748	-2.51255	-1.61558	-2.79735	-2.70242	-1.08854	-1.84801	-2.79735	-2.70242	-0.24053	-1.46828	-1.37334	-2.70242	-0.89898	-2.03737	-2.41762	-2.70242	-2.03737	Cp
				10	10		10	10	10	10	10	10		10	10	10	10	10	10	10	10	10	
21	2.4	31	0	14.7	14.7	10	13.7	13.9	13.4	13.6	13.2	13.7	10	15.4	14.9	15.1	15.2	15.2	14.7	15.1	15.1	14.8	
				10	10		10	10	10	10	10	10		10	10	10	10	10	10	10	10	10	
22	2.4	31	0	14.7	14.7	10	13.7	13.9	13.4	13.6	13.2	13.7	10	15.4	14.9	15.2	15.2	15.2	14.7	15.1	15.2	14.8	
				10	10		10	10	10	10	10	10		10	10	10	10	10	10	10	10	10	
23	2.3	30	0	14.7	14.7	10	13.8	13.9	13.5	13.6	13.2	13.7	10	15.4	14.9	15.2	15.3	15.2	14.7	15.1	15.2	14.8	
				10	10		10	10	10	10	10	10		10	10	10	10	10	10	10	10	10	
24	2.4	31	0	14.7	14.7	10	13.7	13.9	13.4	13.6	13.2	13.7	10	15.4	14.9	15.1	15.3	15.2	14.7	15.1	15.2	14.9	
				10	10		10	10	10	10	10	10		10	10	10	10	10	10	10	10	10	
25	2.5	31	0	14.7	14.7	10	13.7	13.9	13.4	13.5	13.2	13.7	10	15.4	14.9	15.1	15.3	15.2	14.7	15.1	15.2	14.8	
				10	10		10	10	10	10	10	10		10	10	10	10	10	10	10	10	10	
26	2.4	30	0	14.7	14.7	10	13.8	13.9	13.4	13.6	13.2	13.7	10	15.4	14.9	15.1	15.2	15.2	14.7	15.1	15.2	14.8	
				10	10		10	10	10	10	10	10		10	10	10	10	10	10	10	10	10	
27	2.5	31	0	14.7	14.7	10	13.7	13.9	13.5	13.5	13.2	13.7	10	15.4	14.9	15.2	15.3	15.2	14.7	15.1	15.2	14.8	
				10	10		10	10	10	10	10	10		10	10	10	10	10	10	10	10	10	
28	2.5	31	0	14.7	14.7	10	13.8	13.9	13.5	13.5	13.2	13.7	10	15.4	14.9	15.2	15.3	15.2	14.7	15.1	15.2	14.8	
29	2.5	31	0	10	10	10	10	10	10	10	10	10	10	10	10	10	10	10	10	10	10	10	

				14.7	14.7	14	13.7	13.9	13.5	13.5	13.2	13.7	16	15.4	14.9	15.2	15.3	15.2	14.7	15.1	15.2	14.8
				10	10		10	10	10	10	10	10	10	10	10	10	10	10	10	10	10	10
30	2.4	31	0	14.7	14.7	10 14	13.8	13.9	13.4	13.5	13.2	13.7	15.9	15.4	14.9	15.1	15.2	15.2	14.7	15.1	15.2	14.9
				10	10		10	10	10	10	10	10		10	10	10	10	10	10	10	10	10
31	2.6	32	0	14.7	14.7	10 14	13.7	13.9	13.4	13.5	13.2	13.6	16	15.4	14.9	15.1	15.2	15.2	14.7	15.1	15.2	14.8
				10	10		10	10	10	10	10	10		10	10	10	10	10	10	10	10	10
32	2.5	31	0	14.7	14.7	10 14	13.7	13.9	13.4	13.5	13.2	13.7	16	15.4	14.9	15.1	15.2	15.2	14.7	15.1	15.2	14.8
				10	10		10	10	10	10	10	10		10	10	10	10	10	10	10	10	10
33	2.4	31	0	14.7	14.7	10 14	13.7	13.9	13.4	13.5	13.2	13.6	16	15.4	14.9	15.1	15.2	15.2	14.7	15.1	15.1	14.8
				10	10		10	10	10	10	10	10		10	10	10	10	10	10	10	10	10
34	2.5	31	0	14.7	14.7	10 14	13.7	13.9	13.4	13.5	13.2	13.6	16	15.4	14.9	15.1	15.2	15.2	14.7	15.1	15.2	14.8
				10	10		10	10	10	10	10	10		10	10	10	10	10	10	10	10	10
35	2.4	31	0	14.7	14.7	10 14	13.7	13.9	13.4	13.5	13.2	13.7	16	15.4	14.9	15.1	15.2	15.2	14.7	15.1	15.2	14.8
				10	10		10	10	10	10	10	10		10	10	10	10	10	10	10	10	10
36	2.5	31	0	14.7	14.8	10 14	13.7	13.9	13.4	13.5	13.2	13.7	16	15.4	14.9	15.1	15.2	15.2	14.7	15.1	15.2	14.8
				10	10		10	10	10	10	10	10		10	10	10	10	10	10	10	10	10
37	2.4	31	0	14.7	14.7	10 14	13.7	13.9	13.4	13.5	13.2	13.6	16	15.4	14.9	15.1	15.2	15.2	14.7	15.1	15.1	14.8
				10	10		10	10	10	10	10	10		10	10	10	10	10	10	10	10	10
38	2.5	31	0	14.7	14.7	10 14	13.7	13.9	13.4	13.5	13.2	13.6	16	15.4	14.9	15.1	15.3	15.2	14.7	15.1	15.1	14.8
				10	10		10	10	10	10	10	10		10	10	10	10	10	10	10	10	10
39	2.5	32	0	14.7	14.7	10 14	13.7	13.9	13.4	13.5	13.2	13.6	16	15.5	14.9	15.1	15.3	15.2	14.7	15.1	15.2	14.9
				10	10		10	10	10	10	10	10		10	10	10	10	10	10	10	10	10
40	2.4	30	0	14.7	14.7	14	13.7	13.9	13.5	13.5	13.2	13.7	16	15.4	14.9	15.2	15.3	15.2	14.7	15.1	15.2	14.8

				7	7		8	9	4	6	2	7		4	9	2	3	2	7	1	2	8	
					10		10						10	10			10					10	
				10	14.		13.	10	10	10	10	10	15.	15.	10	10	15.	10	10	10	10	14.	
	2.4	30.		14.	70	10	72	13.	13.	13.	13.	13.	99	40	14.	15.	24	15.	14.	15.	15.	81	Av
	5	95	0	7	5	14	5	9	42	53	2	67	5	5	9	13	5	2	7	1	18	5	g
				21	21	21	21	21	21	21	21	21		21	21	21	21	21	21		21	21	
				19.	19.	17.	17.	17.	16.	16.	16.	17.	21	20.	19.	20.	20.	20.	19.	21	20.	19.	
				24	25	78	20	57	57	80	11	09	21.	71	66	14	38	28	24	20.	24	48	
				5	5	3	9	4	2	1	2	4	95	7	3	3	3	9	5	08	8	5	psf
		45.																					
		39																					
		33																					FP
		4																					S
				-	-	-	-	-	-	-	-	-	0.7	0.2	0.1	0.0	0.1	0.0	0.0	0.0	0.0	0.0	
				0.1	0.4	0.9	1.0	1.0	1.0	1.2	1.3	1.2	91	11	47	87	00	62	62	62	45	23	
				84	32	09	24	41	37	76	86	41	14	46	53	86	64	28	28	28	23	92	
				93	14	53	61	66	4	09	91	99	6	8	3	1	8	7	7	7	7	6	Cp
				10	10	10	10	10	10	10			10	10	10	10	10	10	10	10	10	10	
	11.			09.	08.	07.	05.	04.	03.	02.	10	10	14.	12.	11.	11.	11.	11.	10.	11.	11.	10.	
41	8	68	0	1	3	3	3	7	5	5	02	03	8	4	4	6	6	4	8	2	2	9	
				10	10	10	10	10	10	10			10	10	10	10	10	10	10	10	10	10	
	12.			09.	08.	07.	05.	04.	03.	02.	10	10	14.	12.	11.	11.	11.	11.	10.	11.	11.	10.	
42	1	69	0	1	3	3	3	6	5	5	02	03	8	4	4	6	6	4	9	2	2	9	
				10	10	10	10	10	10	10	10	10	10	10	10	10	10	10	10	10	10	10	
	11.			09.	08.	07.	05.	04.	03.	02.	02.	03.	14.	12.	11.	11.	11.	11.	10.	11.	11.	10.	
43	8	68	0	1	3	3	3	7	5	6	1	1	8	4	4	6	6	4	9	2	2	9	
				10	10	10	10	10	10	10			10	10	10	10	10	10	10	10	10	10	
	12.			09.	08.	07.	05.	04.	03.	02.	10	10	14.	12.	11.	11.	11.	11.	10.	11.	11.	10.	
44	1	69	0	1	3	3	3	6	5	5	02	03	8	4	4	5	6	4	9	2	2	9	
				10	10	10	10	10	10	10			10	10	10	10	10	10	10	10	10	10	
	11.			09.	08.	07.	05.	04.	03.	02.	10	10	14.	12.	11.	11.	11.	11.	10.	11.	11.	10.	
45	8	68	0	1	3	3	3	6	5	5	02	03	8	4	4	5	6	4	9	2	2	9	
46	12.	69	0	10	10	10	10	10	10	10	10	10	10	10	10	10	10	10	10	10	10	10	

	3			09.1	08.2	07.2	05.3	04.6	03.5	02.5	02	03	14.8	12.4	11.4	11.5	11.5	11.4	10.9	11.2	11.2	10.8
					10	10	10	10	10	10	10		10	10	10	10	10	10	10	10	10	10
	11.			10	08.	07.	05.	04.	03.	02.	01.	10	14.	12.	11.	11.	11.	11.	10.	11.	11.	10.
47	8	68	0	09	2	2	2	5	4	4	9	03	8	4	4	5	6	4	9	2	2	9
				10	10	10	10	10	10	10	10	10	10	10	10	10	10	10	10	10	10	10
	11.			09.	08.	07.	05.	04.	03.	02.	02.	03.	14.	12.	11.	11.	11.	11.	10.	11.	11.	10.
48	9	68	0	1	3	3	3	7	5	6	1	1	8	4	4	5	6	4	9	2	2	9
				10	10	10	10	10	10	10			10	10	10	10	10	10	10	10	10	10
	12.			09.	08.	07.	05.	04.	03.	02.	10	10	14.	12.	11.	11.	11.	11.	10.	11.	11.	10.
49	1	69	0	1	3	3	3	6	5	5	02	03	8	4	4	5	6	4	9	2	2	9
					10	10	10	10	10	10	10		10	10	10	10	10	10	10	10	10	10
	12.			10	08.	07.	05.	04.	03.	02.	01.	10	14.	12.	11.	11.	11.	11.	10.	11.	11.	10.
50	2	69	0	09	2	2	2	6	4	4	9	03	8	4	4	5	5	4	8	1	2	9
					10	10	10	10	10	10	10	10	10	10	10	10	10	10	10	10	10	10
	11.			10	08.	07.	05.	04.	03.	02.	01.	02.	14.	12.	11.	11.	11.	11.	10.	11.	11.	10.
51	9	68	0	09	2	2	2	4	3	3	8	8	8	4	3	5	5	4	7	1	1	7
				10				10			10	10	10	10	10	10	10	10	10			10
	12.			08.	10	10	10	04.	10	10	01.	02.	14.	12.	11.	11.	11.	11.	10.	10	10	10.
52	5	70	0	8	08	07	05	2	03	02	5	5	7	2	2	4	4	2	6	11	11	6
				10	10	10	10		10	10	10	10	10	10	10	10	10	10	10			10
	12.			08.	07.	06.	04.	10	02.	01.	01.	02.	14.	12.	11.	11.	11.	11.	10.	10	10	10.
53	5	70	0	7	8	8	8	04	9	8	3	3	7	2	2	3	4	2	6	11	11	6
				10	10	10	10		10	10	10	10	10	10	10	10	10	10	10	10		10
	12.			08.	07.	06.	04.	10	02.	01.	01.	02.	14.	12.	11.	11.	11.	11.	10.	10.	10	10.
54	5	70	0	7	8	8	8	04	8	8	3	3	7	2	2	3	3	2	6	9	11	6
				10	10	10	10		10	10	10	10	10	10	10	10	10	10	10	10	10	10
	12.			08.	07.	06.	04.	10	02.	01.	01.	02.	14.	12.	11.	11.	11.	11.	10.	10.	10.	10.
55	7	70	0	7	8	8	8	04	8	8	3	3	7	2	1	3	3	2	6	9	9	6
				10	10	10	10		10	10	10	10	10	10	10	10	10	10	10	10	10	10
				08.	07.	06.	04.	10	02.	01.	01.	02.	14.	12.	11.	11.	11.	11.	10.	10.	10.	10.
56	13	71	0	7	8	7	7	04	7	7	2	2	7	2	2	3	3	1	6	9	9	6
	12.			10	10	10	10	10	10	10	10	10	10	10	10	10	10	10	10	10	10	10
57	6	70	0	08.	07.	06.	04.	03.	02.	01.	01.	02.	14.	12.	11.	11.	11.	11.	10.	10.	10.	10.

				7	8	7	7	9	7	7	2	2	7	2	1	2	3	1	6	9	9	6	
				10	10	10	10	10	10	10	10	10	10	10	10	10	10	10	10	10	10	10	
	12.7			08.6	07.7	06.7	04.6	03.9	02.7	01.6	01.1	02.1	14.7	12.2	11.1	11.2	11.3	11.1	10.6	10.9	10.9	10.6	
58		70	0																				
				10	10	10	10	10	10	10	10	10	10	10	10	10	10	10	10	10	10	10	
	12.9			08.6	07.8	06.7	04.7	03.9	02.7	01.6	01.1	02.2	14.7	12.2	11.1	11.3	11.3	11.2	10.6	10.9	10.9	10.5	
59		71	0																				
				10	10	10	10	10	10	10	10	10	10	10	10	10	10	10	10	10	10	10	
	12.8			08.6	07.8	06.7	04.6	03.9	02.6	01.6	01.1	02.1	14.7	12.2	11.1	11.2	11.3	11.1	10.5	10.9	10.9	10.5	
60		71	0																				
							10			10	10		10			10				10	10		
				08.89	10	10	05.03	10	10	02.14	01.64	10	14.75	10	10	11.41	10	10	10	11.06	11.07	10	
	12.3	69.3		5	08.06	07.04	5	04.32	03.15	5	5	02.66	5	12.31	11.28	5	11.46	11.29	10.74	5	5	10.74	Avg
				21	21	21	20	20	20	20	20	20		21	21	21	21	21	21	21	21	21	
				07.12	05.37	03.24	99.05	97.56	95.12	93.02	91.97	94.09	21	14.25	12.10	12.38	12.47	12.12	10.97	11.65	11.67	10.97	
				1	7	7	9	6	2	3	9	9	19.36	3	2	4	8	3	4	3	4	4	psf
		101.64																					FPS
				-	-	-	-	-	-	-	-	-	0.747	0.317	0.215	0.187	0.178	0.149	0.140	0.128	0.112	0.113	
				0.221	0.413	0.562	0.778	1.033	1.149	1.386	1.437	1.316	84	40	52	50	16	30	81	07	79	64	
				71	59	16	84	36	67	54	48	08	7	3	3	6	7	1	1	6	4	3	Cp
				10										10	10	10	10	10	10	10	10	10	
		103		00.2	99	99	99	98	98	98	98	98	10	07.5	05.8	05.8	05.6	05.3	04.6	04.9	04.8	04.4	
62	27		0		7.7	5.1	2.8	9.5	7.3	4.6	3.8	5.7	13										
				10										10	10	10	10	10	10	10	10	10	
	26.8	102		00.1	99	99	99	98	98	98	98	98	10	07.4	05.7	05.7	05.4	05.2	04.5	04.8	04.7	04.3	
63			0		7.6	4.9	2.7	9.4	7.1	4.4	3.6	5.6	13										
	27.2	103		99	99	99	99	98	98	98	98	98	10	10	10	10	10	10	10	10	10	10	
64			0	9.8	7.4	4.6	2.4	9	6.7	4	3.2	5.2	12.	07.	05.	05.	05.	05.	04.	04.	04.	04.	

													9	3	6	6	4	1	5	7	7	3
													10	10	10	10	10	10	10	10	10	10
	27.	10		99	99	99	99	98	98	98	98	98	12.	07.	05.	05.	05.	05.	04.	04.	04.	04.
65	1	3	0	9.9	7.4	4.7	2.4	9	6.8	4	3.3	5.3	9	3	6	6	4	1	5	7	7	3
													10	10	10	10	10	10	10	10	10	10
	27.	10		99	99	99	99	98	98	98	98	98	12.	07.	05.	05.	05.	05.	04.	04.	04.	04.
66	6	4	0	9.9	7.4	4.7	2.4	9	6.7	4	3.2	5.2	9	3	6	6	3	1	4	7	6	2
													10	10	10	10	10	10	10	10	10	10
	27.	10		99	99	99	99	98	98	98	98	98	12.	07.	05.	05.	05.	05.	04.	04.	04.	04.
67	5	4	0	9.8	7.4	4.6	2.3	8.9	6.7	3.8	3.1	5.1	9	3	6	6	4	1	5	7	7	3
													10	10	10	10	10	10	10	10	10	10
	27.	10		99	99	99	99	98	98	98	98	98	12.	07.	05.	05.	05.	05.	04.	04.	04.	04.
68	3	3	0	9.9	7.5	4.7	2.5	9.1	6.9	4.1	3.3	5.3	9	4	6	6	4	2	5	8	7	3
														10	10	10	10	10	10	10	10	10
	27.	10		99	99	99	99	98	98	98	98	98	10	07.	05.	05.	05.	05.	04.	04.	04.	04.
69	3	3	0	9.9	7.5	4.8	2.5	9.2	6.9	4.2	3.4	5.4	13	4	7	6	5	2	6	8	8	4
														10	10	10	10	10	10	10	10	10
	27.	10		10	99	99	99	98	98	98	98	98	10	07.	05.	05.	05.	05.	04.	04.	04.	04.
70	1	3	0	00	7.6	4.9	2.7	9.3	7.1	4.3	3.6	5.5	13	4	7	6	5	2	5	8	8	3
													10	10	10	10	10	10	10	10	10	10
	27.	10		99	99	99	99	98	98	98	98	98	12.	07.	05.	05.	05.	05.	04.	04.	04.	04.
71	3	3	0	9.9	7.5	4.7	2.5	9.1	6.8	4	3.2	5.1	9	3	6	5	3	1	4	6	6	2
													10	10	10	10	10		10	10	10	10
	27.	10		99	99	99	99	98	98	98	98	98	12.	07.	05.	05.	05.	10	04.	04.	04.	04.
72	9	4	0	9.7	7.2	4.5	2.2	8.8	6.5	3.7	2.9	4.9	9	2	5	5	2	05	3	5	5	1
													10	10	10	10	10		10	10	10	10
	28.	10		99	99	99	99	98	98	98	98	98	12.	07.	05.	05.	05.	10	04.	04.	04.	04.
73	1	5	0	9.6	7	4.3	2	8.6	6.3	3.5	2.7	4.8	9	2	5	4	3	05	4	6	6	2
														10	10	10	10	10	10	10	10	10
	27.	10		99	99	99	99	98	98	98	98	98	10	07.	05.	05.	05.	05.	04.	04.	04.	04.
74	6	4	0	9.8	7.3	4.5	2.3	9	6.7	4	3.3	5.4	13	4	7	6	4	1	6	8	8	4
				10									10	10	10	10	10	10	10	10	10	10
	26.	10		00.	99	99	99	98	98	98	98	98	12.	07.	05.	05.	05.	05.	04.	04.	04.	04.
75	6	2	0	1	7.6	5	2.7	9.4	7.2	4.4	3.6	5.6	9	4	7	6	4	2	5	8	7	3

													10	10	10	10	10	10	10	10	10	10	
	27.	10		99	99	99	99	98	98	98	98	98	12.	07.	05.	05.	05.	05.	04.	04.	04.	04.	
76	3	3	0	9.9	7.4	4.7	2.4	9.1	6.8	4.1	3.3	5.3	9	3	7	6	4	1	5	7	7	3	
													10	10	10	10	10	10	10	10	10	10	
	27.	10		99	99	99	99	98	98	98	98	98	12.	07.	05.	05.	05.	05.	04.	04.	04.	04.	
77	1	3	0	9.8	7.3	4.6	2.4	9	6.7	3.9	3.2	5.2	9	3	6	6	4	1	4	7	7	3	
													10	10	10	10	10	10	10	10	10	10	
	27.	10		99	99	99	99	98	98	98	98	98	12.	07.	05.	05.	05.	05.	04.	04.	04.	04.	
78	2	3	0	9.9	7.4	4.6	2.4	9.1	6.8	4	3.2	5.2	9	3	6	6	4	1	5	7	7	2	
													10	10	10	10	10	10	10	10	10	10	
	27.	10		99	99	99	99	98	98	98	98	98	12.	07.	05.	05.	05.	05.	04.	04.	04.	04.	
79	1	3	0	9.9	7.4	4.6	2.4	9.1	6.8	4	3.2	5.2	9	3	7	6	4	1	4	7	6	2	
													10	10	10	10	10	10	10	10	10	10	
		10		99	99	99	99	98	98	98	98	98	12.	07.	05.	05.	05.	05.	04.	04.	04.	04.	
80	27	3	0	9.8	7.3	4.6	2.3	9	6.7	3.9	3.2	5.2	9	3	7	6	4	1	5	7	7	3	
	27.	10		99	99	99	99	98	98	98	98	98	10	10	10	10	10	10	10	10	10	10	
	26	3.2		9.8	7.4	4.6	2.4	9.0	6.8	4.0	3.2	5.2	12.	07.	05.	05.	05.	05.	04.	04.	04.	04.	
	84	10		89	15	89	36	84	15	47	78	73	92	33	64	59	39	12	47	72	68	27	Av
	2	5	0	5	8	5	8	2	8	4	9	7	6	2	2	5	5	6	9	1	9	9	g
				20	20	20	20	20	20	20	20	20	21	21	21	21	20		20	20	20		
				88.	83.	77.	72.	65.	61.	55.	53.	57.	15.	03.	00.	00.	99.	20	97.	98.	98.	20	
				31	14	45	74	74	00	22	62	78	54	85	32	22	81	99.	89	40	33	97.	
				3	6	2	7	5	8	6	1	7	1	6	7	8	1	25	8	4	8	48	psf
		15																					
		1.3																					
		75																					FP
		5																					S
				-	-	-	-	-	-	-	-	-	0.7	0.3	0.2	0.1	0.1	0.1	0.1	0.1	0.1	0.1	
				0.2	0.4	0.6	0.8	1.0	1.2	1.4	1.5	1.3	46	10	14	87	64	44	32	20	10	05	
				40	52	50	12	84	20	62	06	76	19	79	32	72	74	18	89	80	72	32	
				83	89	6	41	13	73	63	17	37	8	3	7	1	4	5	8	4	6	5	Cp
			Al																				
		V_	p										P	P	P	P	P	P	P	P	P	P	
	q	ref	h	P 1	P 2	P 3	P 4	P 5	P 6	P 7	P 8	P 9	10	11	12	13	14	15	16	17	18	19	

count	[psf]	[mph]	a[deg]	[mbar]	[mbar]	[mbar]	[mbar]	[mbar]	[mbar]	[mbar]	[mbar]	[mbar]	[mbar]	[mbar]	[mbar]	[mbar]	[mbar]	[mbar]	[mbar]	[mbar]	[mbar]	[mbar]	[mbar]	[mbar]
1	0.1	7	0	10 15.9	10 16.2	10 16.1	10 15.9	10 16.1	10 15.7	10 16.1	10 15.8	10 16.1	10 16.1	10 16.2	10 15.8	10 16	10 16.2	10 16.2	10 15.6	10 16	10 16.1	10 15.8	1 mbar = 1 mph = 1 sq. ft =	2.0885433 1.466667 144	psf psf psi
2	0.1	7	0	10 15.9	10 16.2	10 16.1	10 15.9	10 16.1	10 15.7	10 16.1	10 15.8	10 16.1	10 16.1	10 16.2	10 15.8	10 16	10 16.2	10 16.2	10 15.6	10 16	10 16.1	10 15.8			
3	0.1	7	0	10 15.9	10 16.2	10 16.1	10 15.9	10 16.1	10 15.7	10 16	10 15.8	10 16.1	10 16.1	10 16.2	10 15.8	10 16	10 16.2	10 16.2	10 15.6	10 16	10 16.1	10 15.8			
4	0.1	6	0	10 15.9	10 16.2	10 16.1	10 15.9	10 16.1	10 15.7	10 16.1	10 15.8	10 16.1	10 16.1	10 16.2	10 15.7	10 16	10 16.2	10 16.2	10 15.6	10 16	10 16.1	10 15.8			
5	0.1	6	0	10 15.9	10 16.2	10 16.1	10 15.9	10 16.1	10 15.7	10 16.1	10 15.8	10 16.1	10 16.1	10 16.2	10 15.7	10 16	10 16.2	10 16.2	10 15.6	10 16	10 16.1	10 15.8			
6	0.1	7	0	10 15.9	10 16.2	10 16.1	10 15.9	10 16.1	10 15.7	10 16.1	10 15.8	10 16.1	10 16.1	10 16.2	10 15.7	10 16	10 16.2	10 16.2	10 15.6	10 16	10 16.1	10 15.8			
7	0.1	7	0	10 15.9	10 16.2	10 16.1	10 15.9	10 16.1	10 15.7	10 16.1	10 15.8	10 16.1	10 16.2	10 16.2	10 15.8	10 16	10 16.1	10 16.2	10 15.6	10 16	10 16.1	10 15.8			
8	0.1	7	0	10 15.9	10 16.2	10 16.1	10 15.9	10 16.1	10 15.7	10 16	10 15.8	10 16.1	10 16.2	10 16.2	10 15.7	10 16	10 16.2	10 16.2	10 15.6	10 16	10 16.1	10 15.8			
9	0.1	5	0	10 15.9	10 16.2	10 16.1	10 15.9	10 16.1	10 15.7	10 16	10 15.8	10 16.1	10 16.2	10 16.2	10 15.7	10 16	10 16.2	10 16.1	10 15.6	10 16	10 16.1	10 15.8			

				10	10	10	10	10	10		10	10	10	10	10		10	10	10		10	10	
				15.	16.	16.	15.	16.	15.	10	15.	16.	16.	16.	15.	10	16.	16.	15.	10	16.	15.	
10	0.1	7	0	9	2	1	9	1	7	16	8	1	2	2	7	16	2	2	6	16	1	8	
				10	10	10	10	10	10		10	10	10	10	10		10	10	10		10	10	
				15.	16.	16.	15.	16.	15.	10	15.	16.	16.	16.	15.	10	16.	16.	15.	10	16.	15.	
11	0.1	7	0	9	2	1	9	1	7	16	8	1	1	2	7	16	1	1	6	16	1	8	
				10	10	10	10	10	10		10	10	10	10	10		10	10	10		10	10	
				15.	16.	16.	15.	16.	15.	10	15.	16.	16.	16.	15.	10	16.	16.	15.	10	16.	15.	
12	0.1	7	0	9	2	1	9	1	7	16	8	1	2	2	7	16	1	1	6	16	1	8	
				10	10	10	10	10	10		10	10	10	10	10		10	10	10		10	10	
				15.	16.	16.	15.	16.	15.	10	15.	16.	16.	16.	15.	10	16.	16.	15.	10	16.	15.	
13	0.1	7	0	9	2	1	9	1	7	16	7	1	2	2	7	16	2	1	6	16	1	8	
				10	10	10	10	10	10		10	10	10	10	10		10	10	10		10	10	
				15.	16.	16.	15.	16.	15.	10	15.	16.	16.	16.	15.	10	16.	16.	15.	10	16.	15.	
14	0.1	6	0	9	2	1	9	1	7	16	8	1	2	2	8	16	2	1	6	16	1	8	
				10	10	10	10	10	10		10	10	10	10	10		10	10	10		10	10	
				15.	16.	16.	15.	16.	15.	10	15.	16.	16.	16.	15.	10	16.	16.	15.	10	16.	15.	
15	0.1	6	0	8	2	1	9	1	7	16	8	1	2	2	7	16	2	1	6	16	1	8	
				10	10	10	10	10	10		10	10	10	10	10	10	10	10	10		10	10	
				15.	16.	16.	15.	16.	15.	10	15.	16.	16.	16.	15.	16.	16.	16.	15.	10	16.	15.	
16	0.1	6	0	9	2	1	9	1	7	16	8	1	1	2	7	1	2	1	6	16	1	8	
				10	10	10	10	10	10		10	10	10	10	10		10	10	10		10	10	
				15.	16.	16.	15.	16.	15.	10	15.	16.	16.	16.	15.	10	16.	16.	15.	10	16.	15.	
17	0.1	7	0	9	2	1	8	1	7	16	8	1	2	2	7	16	2	1	6	16	1	8	
				10	10	10	10	10	10		10		10	10	10		10	10	10		10	10	
				15.	16.	16.	15.	16.	15.	10	15.	10	16.	16.	15.	10	16.	16.	15.	10	16.	15.	
18	0.1	6	0	9	2	1	8	1	7	16	8	16	2	2	8	16	2	1	6	16	1	8	
				10	10	10	10	10	10		10	10	10	10	10		10	10	10		10	10	
				15.	16.	16.	15.	16.	15.	10	15.	16.	16.	16.	15.	10	16.	16.	15.	10	16.	15.	
19	0.1	5	0	9	2	1	9	1	7	16	8	1	2	2	8	16	2	1	6	16	1	8	
				10	10	10	10	10	10		10	10	10	10	10		10	10	10		10	10	
				15.	16.	16.	15.	16.	15.	10	15.	16.	16.	16.	15.	10	16.	16.	15.	10	16.	15.	
20	0.1	7	0	9	2	1	9	1	7	16	8	1	2	2	7	16	1	1	6	16	1	8	
	0.1	6.5	0	10	10	10	10	10	10	10	10	10	10	10	10	10	10	10	10	10	10	10	Av

				15.895	16.2	16.1	15.89	16.1	15.7	16.03	15.795	16.095	16.18	16.2	15.735	16.005	16.18	16.145	15.6	16	16.1	15.8	g
				21	21	21		21	21	21	21	21	21	21	21	21	21	21	21		21	21	
				21.741	22.378	22.169	21.73	22.169	21.334	22.023	21.532	22.159	22.336	22.378	21.407	21.971	22.336	22.263	21.125	21.96	22.169	21.542	psf
		9.5333336																					FPS
				-3.07266	-2.86381	-1.92396	-3.33594	-3.07266	-1.2974	-2.55052	-3.28151	-3.28151	-0.25313	-1.71511	-2.44661	-3.07266	-1.50625	-2.23724	-3.17709	-3.17709	-3.17709	-2.34167	Cp
21	2.4	31	0	10 14.3	10 14.6	10 14.5	10 14.3	10 14.5	10 14.1	10 14.4	10 14.14	10 14.2	10 14.16	10 15.3	10 14.8	10 15.1	10 15.2	10 15.1	10 14.6	10 14.9	10 14.9	10 14.6	
22	2.4	30	0	10 14.3	10 14.6	10 14.4	10 14.3	10 14.4	10 14.1	10 14.5	10 14.14	10 14.2	10 14.16	10 15.3	10 14.8	10 15.1	10 15.2	10 15.1	10 14.5	10 14.9	10 14.9	10 14.6	
23	2.5	31	0	10 14.3	10 14.6	10 14.4	10 14.3	10 14.5	10 14.1	10 14.5	10 14.14	10 14.2	10 14.16	10 15.3	10 14.8	10 15.1	10 15.2	10 15.1	10 14.5	10 14.9	10 14.9	10 14.6	
24	2.3	30	0	10 14.3	10 14.6	10 14.4	10 14.3	10 14.4	10 14.1	10 14.5	10 14.14	10 14.2	10 14.16	10 15.3	10 14.8	10 15.1	10 15.2	10 15.1	10 14.5	10 14.9	10 14.9	10 14.6	
25	2.4	31	0	10 14.3	10 14.6	10 14.5	10 14.3	10 14.5	10 14.1	10 14.4	10 14.14	10 14.2	10 14.16	10 15.4	10 14.8	10 15.1	10 15.2	10 15.1	10 14.5	10 14.9	10 14.9	10 14.6	
26	2.5	31	0	10 14.3	10 14.5	10 14.4	10 14.3	10 14.4	10 14.1	10 14.4	10 14.14	10 14.2	10 14.16	10 15.3	10 14.8	10 15.1	10 15.2	10 15.1	10 14.5	10 14.9	10 14.9	10 14.6	

				10	10	10	10	10	10	10		10		10	10	10	10	10	10	10	10	10
				14.	14.	14.	14.	14.	14.	14.	10	14.	10	15.	14.	15.	15.	15.	14.	14.	14.	14.
27	2.4	31	0	3	6	5	3	5	1	5	14	2	16	3	8	1	1	1	5	9	9	6
				10	10	10	10	10	10	10		10		10	10	10	10	10	10	10	10	10
				14.	14.	14.	14.	14.	14.	14.	10	14.	10	15.	14.	15.	15.	15.	14.	14.	14.	14.
28	2.5	31	0	3	6	4	3	5	1	4	14	2	16	4	8	1	2	1	5	9	9	6
				10	10	10	10	10	10	10		10		10	10	10	10	10	10	10	10	10
				14.	14.	14.	14.	14.	14.	14.	10	14.	10	15.	14.	15.	15.	15.	14.	14.	14.	14.
29	2.5	31	0	3	6	4	3	5	1	4	14	2	16	4	8	1	2	1	5	9	9	6
				10	10	10	10	10	10	10		10		10	10		10	10	10	10	10	10
				14.	14.	14.	14.	14.	14.	14.	10	14.	10	15.	14.	10	15.	15.	14.	14.	14.	14.
30	2.5	31	0	3	6	5	3	5	1	5	14	2	16	4	8	15	1	1	6	9	9	6
				10	10	10	10	10	10	10		10		10	10	10	10	10	10	10	10	10
				14.	14.	14.	14.	14.	14.	14.	10	14.	10	15.	14.	15.	15.	15.	14.	14.	14.	14.
31	2.4	31	0	3	6	5	3	5	1	4	14	2	16	4	8	1	2	1	5	9	9	6
				10	10	10	10	10	10	10		10	10	10	10	10	10	10	10	10		10
				14.	14.	14.	14.	14.	14.	14.	10	14.	16.	15.	14.	15.	15.	15.	14.	14.	10	14.
32	2.5	31	0	3	6	4	3	4	1	5	14	2	1	4	9	1	2	1	6	9	15	6
				10	10	10	10	10	10	10		10		10	10	10	10	10	10	10		10
				14.	14.	14.	14.	14.	14.	14.	10	14.	10	15.	14.	15.	15.	15.	14.	14.	10	14.
33	2.6	32	0	3	6	5	3	5	1	5	14	2	16	4	8	1	2	1	6	9	15	6
				10	10	10	10	10	10	10		10	10	10	10	10	10	10	10	10		10
				14.	14.	14.	14.	14.	14.	14.	10	14.	16.	15.	14.	15.	15.	15.	14.	14.	10	14.
34	2.4	31	0	3	6	5	3	5	1	5	14	2	1	4	9	1	1	1	6	9	15	6
				10	10	10	10	10	10	10		10	10	10	10	10	10	10	10	10		10
				14.	14.	14.	14.	14.	14.	14.	10	14.	16.	15.	14.	15.	15.	15.	14.	14.	10	14.
35	2.3	30	0	3	6	5	3	5	1	5	14	2	1	4	8	1	2	1	6	9	15	6
				10	10	10	10	10	10	10		10	10	10	10	10	10	10	10	10		10
				14.	14.	14.	14.	14.	14.	14.	10	14.	16.	15.	14.	15.	15.	15.	14.	14.	10	14.
36	2.4	31	0	3	6	5	3	5	1	5	14	2	1	4	8	1	2	1	6	9	15	6
				10	10	10	10	10	10	10		10	10	10	10	10	10	10	10	10		10
				14.	14.	14.	14.	14.	14.	14.	10	14.	16.	15.	14.	15.	15.	15.	14.	14.	10	14.
37	2.5	31	0	3	6	5	3	5	1	5	14	2	1	4	8	1	2	1	6	9	15	6
38	2.4	31	0	10	10	10	10	10	10	10	10	10	10	10	10	10	10	10	10	10	10	10

				14.4	14.6	14.5	14.3	14.5	14.1	14.5	14	14.2	16	15.4	14.8	15.1	15.2	15.1	14.6	14.9	14.9	14.6	
				10	10	10	10	10	10	10		10		10	10	10	10	10	10	10	10	10	
39	2.4	31	0	14.3	14.6	14.5	14.3	14.5	14.1	14.5	10 14	14.2	10 16	15.4	14.9	15.1	15.1	15.1	14.6	14.9	14.9	14.6	
				10	10	10	10	10	10	10		10		10	10	10	10	10	10	10		10	
40	2.5	31	0	14.3	14.6	14.5	14.3	14.5	14.1	14.5	10 14	14.2	10 16	15.4	14.9	15.1	15.2	15.1	14.6	14.9	10 15	14.6	
				10	10	10							10			10			10		10		
	2.44	30.9	0	14.305	14.595	14.465	10 14.3	10 14.48	10 14.1	10 14.47	10 14	10 14.2	16.025	10 15.37	10 14.82	15.095	10 15.18	10 15.1	14.555	10 14.9	14.935	10 14.6	Avg
					21	21		21	21	21	21	21	21	21	21		21		21	21	21	21	
				21	19.02	18.754	21	18.786	17.992	18.765	17.783	18.201	22.012	20.644	19.496	21	20.248	21	18.942	19.663	19.736	19.036	
				18.42	6	4	18.41	6	2	5	3	1	2	4	6	20.07	8	20.08	2	3	6	6	psf
		45.3200 1																					FPS
				-0.5	-0.5	-0.5	-0.5	-0.5	-0.4	-0.4	-0.7	-0.7	0.815	0.178	0.075	0.054	0.041	0.027	-0.065	-0.112	-0.168	-0.164	
				27	32	19	40	53	63	80	11	97	96	27	56	16	32	15	67	75	39	11	
				89	17	33	73	57	69	81	92	52	9	8	3	4	4						Cp
				10	10	10	10	10		10			10	10	10	10	10	10	10	10	10	10	
	12.1			09.2	08.2	06.7	05.4	04.8	10 01	00.4	99 8.4	99 7.3	08.7	14.5	13.1	12.7	12.5	12.2	11.5	11.7	11.6	11.1	
41		69	0	10	10	10	10	10		10			10	10	10	10	10	10	10	10	10	10	
	11.9			09.2	08.2	06.7	05.4	04.8	10 01	00.4	99 8.3	99 7.3	08.7	14.5	13.1	12.7	12.5	12.2	11.5	11.7	11.6	11.1	
42		68	0	10	10	10	10	10		10			10	10	10	10	10	10	10	10	10	10	
	12.1			09.1	08.1	06.6	05.3	04.7	10 01	00.3	99 8.3	99 7.2	08.7	14.5	13.1	12.7	12.4	12.2	11.5	11.7	11.6	11.1	
43		69	0																				

				10	10	10	10	10	10	10			10	10	10	10	10	10	10	10	10	10
				09.	08.	06.	05.	04.	00.	00.	99	99	08.	14.	13.	12.	12.	12.	11.	11.	11.	11.
44	12	69	0	1	1	7	3	7	9	3	8.3	7.3	7	5	1	7	4	2	5	7	6	1
				10	10	10	10	10	10	10			10	10	10	10	10	10	10	10	10	
	11.			09.	08.	06.	05.	04.	00.	00.	99	99	08.	14.	13.	12.	12.	12.	11.	11.	11.	10
45	8	68	0	2	1	7	4	7	9	3	8.2	7.2	7	5	1	7	5	2	4	7	5	11
				10	10	10	10	10		10			10	10	10	10	10	10	10	10	10	10
	11.			09.	08.	06.	05.	04.	10	00.	99	99	08.	14.	13.	12.	12.	12.	11.	11.	11.	11.
46	9	68	0	1	2	7	4	8	01	4	8.3	7.2	7	5	1	7	5	2	5	7	6	1
				10	10	10	10	10		10			10	10	10	10	10	10	10	10	10	10
	12.			09.	08.	06.	05.	04.	10	00.	99	99	08.	14.	13.	12.	12.	12.	11.	11.	11.	11.
47	1	69	0	1	2	7	4	8	01	4	8.4	7.3	7	5	1	7	5	2	5	7	6	1
				10	10	10	10	10		10			10	10	10	10	10	10	10	10	10	10
	11.			09.	08.	06.	05.	04.	10	00.	99	99	08.	14.	13.	12.	12.	12.	11.	11.	11.	11.
48	4	67	0	2	2	7	5	8	01	4	8.4	7.3	7	5	1	7	4	2	5	7	6	1
				10	10	10	10	10		10			10	10	10	10	10	10	10	10	10	10
	11.			09.	08.	06.	05.	04.	10	00.	99	99	08.	14.	13.	12.	12.	12.	11.	11.	11.	11.
49	5	67	0	2	2	7	4	7	01	4	8.3	7.3	7	5	1	7	5	2	5	7	6	1
				10	10	10	10	10		10			10	10	10	10	10	10	10	10	10	10
	12.			09.	08.	06.	05.	04.	10	00.	99	99	08.	14.	13.	12.	12.	12.	11.	11.	11.	11.
50	2	69	0	2	2	8	4	8	01	4	8.4	7.4	7	5	1	7	5	2	5	7	6	1
				10	10	10	10	10	10	10			10	10	10	10	10	10	10	10	10	10
				09.	08.	06.	05.	04.	01.	00.	99	99	08.	14.	13.	12.	12.	12.	11.	11.	11.	11.
51	12	69	0	2	2	8	5	8	1	5	8.4	7.4	8	5	1	7	5	2	5	7	6	1
				10	10	10	10	10	10	10			10	10		10	10	10	10	10	10	
	12.			09.	08.	06.	05.	04.	00.	00.	99	99	08.	14.	10	12.	12.	12.	11.	11.	11.	10
52	3	69	0	1	1	7	4	7	9	3	8.2	7.1	6	5	13	7	4	1	4	7	5	11
				10	10	10	10	10	10	10			10	10	10	10	10	10	10	10	10	
	12.			09.	08.	06.	05.	04.	00.	00.	99	99	08.	14.	13.	12.	12.	12.	11.	11.	11.	10
53	2	69	0	1	1	6	2	6	8	1	8	7	6	5	1	7	4	1	4	6	5	11
						10	10	10	10				10	10	10	10	10	10	10	10	10	
				10	10	06.	05.	04.	00.	10	99	99	08.	14.	13.	12.	12.	12.	11.	11.	11.	10
54	12	68	0	09	08	6	2	5	7	00	8	6.9	6	5	1	7	4	1	4	6	5	11
55	12.	69	0	10	10	10	10	10	10	10	99	99	10	10	10	10	10	10	10	10	10	10

	1			09	08	06.5	05.2	04.5	00.7	00	7.9	6.9	08.5	14.5	13.1	12.7	12.4	12.1	11.4	11.6	11.5	11	
						10	10	10	10				10	10	10	10	10	10	10	10	10		
	12.2			10	10	06.5	05.1	04.5	00.7	10	99	99	08.6	14.5	13.1	12.7	12.4	12.1	11.4	11.6	11.5	10	
56		69	0	09	08					00	7.9	6.9										11	
				10		10	10	10	10	10			10	10	10	10	10	10	10	10	10		
	11.8			09.1	10	06.5	05.2	04.5	00.7	00.1	99	99	08.6	14.5	13.1	12.7	12.4	12.1	11.4	11.6	11.5	10	
57		68	0		08						8	7										11	
				10		10	10	10	10	10			10	10	10	10	10	10	10	10	10		
	11.9			09.1	10	06.6	05.2	04.6	00.7	00.1	99	99	08.6	14.5	13.1	12.7	12.4	12.1	11.4	11.7	11.5	10	
58		68	0		08						8	7										11	
				10	10	10	10	10	10	10			10	10	10	10	10	10	10	10	10	10	
	12.1			09.1	08.1	06.7	05.3	04.7	00.9	00.3	99	99	08.7	14.5	13.1	12.7	12.5	12.2	11.5	11.7	11.7	11.2	
59		69	0								8.3	7.3											
				10	10	10	10		10	10			10	10	10	10	10	10	10	10	10	10	
	11.7			09.3	08.3	06.9	05.7	10	01.3	00.7	99	99	08.8	14.5	13.1	12.8	12.5	12.3	11.5	11.8	11.6	11.1	
60		68	0					05			8.7	7.7											
					10		10		10						10	10					10	10	
	11.96	68.45		10	08.10	06.34	05.10	04.91	00.10	99	8.2	7.2	08.10	14.10	13.09	12.70	12.45	12.17	11.46	11.68	11.56	11.06	Av
			0	09.13	08.12	06.67	05.5	04.7	00.5	00.29	35	67	07.67	14.5	5	5	45	17	46	68	5	5	g
				21	21	21	20		20	20	20	20	21	21	21	21	21	21	21	21	21	21	
				07.61	05.51	02.47	99.70	20	90.45	89.14	84.85	82.69	06.65	18.82	15.89	15.07	14.54	13.96	12.47	12.93	12.69	11.65	
				2	3	4	7	98.36	4	9	7	6	1	7	3	8	6	1	8	8	7	3	psf
		10																					
		0.3																					
		93																					
		4																					FP
																							S
				-	-	-	-	-	-	-	-	-	-	0.6	0.5	0.3	0.3		0.2	0.2	0.1	0.1	
				0.2	0.4	0.6	0.8	1.0	1.5	1.7	2.1	2.3	0.3	80	10	89	27	0.2	42	11	73	45	
				14	41	70	77	23	99	77	00	33	21	56	37	93	96	79	43	01	48	55	
				9	82	49	33	96	99	16	96	99	38	5	5	2	6	09	4	4	5	6	Cp

				10										10	10	10	10	10	10	10	10	
	26.	10		00.	99	99	99	98	98	97	97	97	99	12.	09.	08.	07.	07.	06.	06.	05.	10
61	9	3	0	5	7.6	4.3	1.2	8.8	2.2	9.3	5.3	2.5	9	4	7	5	7	1	1	1	7	05
				10										10	10	10	10			10	10	10
	27.	10		00.	99	99	99	98	98	97	97	97	99	12.	09.	08.	07.	10	10	06.	05.	04.
62	2	3	0	6	7.7	4.4	1.4	8.9	2.2	9.3	5.2	2.5	9.1	4	7	5	7	07	06	1	7	9
				10										10	10	10	10		10		10	
	27.	10		00.	99	99	99	98	98	97	97	97	99	12.	09.	08.	07.	10	06.	10	05.	10
63	3	3	0	4	7.5	4.2	1.1	8.6	1.9	8.9	4.8	2	8.9	4	7	4	7	07	1	06	7	05
				10										10	10	10	10		10		10	
	26.	10		00.	99	99	99	98	98	97	97	97	99	12.	09.	08.	07.	10	06.	10	05.	10
64	8	2	0	5	7.6	4.4	1.3	8.8	2.1	9.2	5.1	2.4	9	4	7	4	7	07	1	06	7	05
				10										10	10	10	10		10	10	10	
	26.	10		00.	99	99	99	98	98	97	97	97	99	12.	09.	08.	07.	10	06.	06.	05.	10
65	7	2	0	5	7.7	4.4	1.3	8.8	2.2	9.2	5.2	2.5	9	4	7	4	7	07	1	1	7	05
				10										10	10	10	10				10	10
	26.	10		00.	99	99	99	98	98	97	97	97	99	12.	09.	08.	07.	10	10	10	05.	04.
66	6	2	0	5	7.6	4.3	1.2	8.7	2.1	9.2	5.1	2.3	8.9	3	7	4	6	07	06	06	6	9
				10										10	10	10	10				10	10
	27.	10		00.	99	99	99	98	98	97	97	97	99	12.	09.	08.	07.	10	10	10	05.	04.
67	4	4	0	4	7.5	4.2	1.1	8.6	1.9	8.9	4.8	2.1	8.8	3	7	4	6	07	06	06	7	9
				10										10	10	10	10	10	10	10	10	10
	27.	10		00.	99	99	99	98	98	97	97	97	99	12.	09.	08.	07.	06.	05.	05.	05.	04.
68	5	4	0	4	7.6	4.3	1.2	8.7	2	8.9	4.8	2	8.8	3	6	4	6	9	9	9	6	9
				10										10	10	10	10	10	10	10	10	10
	27.	10		00.	99	99	99	98	98	97	97	97	99	12.	09.	08.	07.	06.	05.	05.	05.	04.
69	4	3	0	4	7.5	4.2	1.1	8.6	2	9	4.9	2.1	8.8	3	6	3	6	9	9	9	6	9
				10										10	10	10	10	10	10	10	10	10
		10		00.	99	99	99	98	98	97	97	97	99	12.	09.	08.	07.	06.	05.	05.	05.	04.
70	27	3	0	3	7.5	4.2	1.1	8.5	1.9	8.9	4.8	2.1	8.8	3	6	3	6	9	9	9	6	9
				10										10	10	10	10	10			10	
	27.	10		00.	99	99	99	98	98	97	97	97	99	12.	09.	08.	07.	06.	10	10	05.	10
71	1	3	0	4	7.5	4.2	1.1	8.6	2	8.9	4.9	2.1	8.8	3	6	3	6	9	06	06	7	05
72	26.	10	0	10	99	99	99	98	98	97	97	97	99	10	10	10	10	10	10	10	10	10

	1	1		00.5	7.6	4.4	1.3	8.8	2.3	9.3	5.2	2.5	8.9	12.3	09.7	08.4	07.7	07	06.1	06	05.7	05
				10										10	10	10	10				10	10
	26.7	102	0	00.5	99 7.8	99 4.4	99 1.4	98 8.9	98 2.3	97 9.4	97 5.3	97 2.6	99 8.9	12.3	09.7	08.4	07.6	10 07	10 06	10 06	05.6	04.9
				10										10	10	10	10				10	10
74	26.3	101	0	00.4	99 7.6	99 4.3	99 1.2	98 8.8	98 2.2	97 9.2	97 5.1	97 2.4	99 8.8	12.3	09.7	08.4	07.6	10 07	10 06	10 06	05.6	04.9
				10										10	10	10	10				10	10
75	26.4	102	0	00.5	99 7.6	99 4.4	99 1.3	98 8.8	98 2.2	97 9.2	97 5.1	97 2.4	99 8.9	12.3	09.6	08.4	07.6	10 07	10 06	10 06	05.6	04.9
				10										10	10	10	10	10	10	10	10	10
76	27.5	104	0	00.4	99 7.6	99 4.3	99 1.2	98 8.7	98 2.1	97 9.1	97 5	97 2.1	99 8.8	12.3	09.6	08.3	07.6	06.9	05.9	05.9	05.5	04.9
				10										10	10	10	10	10	10	10	10	10
77	27.1	103	0	00.4	99 7.5	99 4.2	99 1	98 8.5	98 1.9	97 8.8	97 4.6	97 1.8	99 8.6	12.2	09.5	08.3	07.5	06.8	05.8	05.8	05.3	04.6
				10										10	10	10	10	10	10	10	10	10
78	27.6	104	0	00.1	99 7.1	99 3.7	99 0.6	98 8	98 1.4	97 8.1	97 3.9	97 1.1	99 8.4	12.2	09.4	08.2	07.4	06.7	05.7	05.6	05.3	04.6
														10	10	10	10	10	10	10	10	10
79	28	105	0	99 9.9	99 6.9	99 3.5	99 0.3	98 7.7	98 1.1	97 7.7	97 3.6	97 0.9	99 8.3	12.2	09.4	08.1	07.3	06.6	05.6	05.6	05.2	04.5
														10	10	10	10	10	10	10	10	10
80	27.1	103	0	10 00	99 7	99 3.6	99 0.5	98 8	98 1.3	97 8.1	97 4	97 1.1	99 8.4	12.2	09.5	08.1	07.4	06.6	05.7	05.7	05.3	04.6
														10		10		10	10			10
	27.03	102.85	0	10 00.38		99 4.195	99 1.095	98 8.59	98 1.965	97 8.93	97 4.835	97 2.075	99 8.795	12.305	10 09.62	08.345	10 07.59	06.915	05.945	10 05.93	10 05.57	04.865
				20	20	20	20	20	20	20	20	20	20	21	21	21	21	21		21	21	20
				89.33 7	83.32 2	76.41 9	69.94 5	64.71 3	50.87 7	44.53 8	35.98 5	30.22 1	86.02 7	14.24 3	08.63 5	05.97 2	04.39 5	02.98 6	21 00.96	00.92 8	00.17 7	98.70 4

	Avg
	psf

		150.8467																			FPS		
				-0.210774	-0.455443	-0.669896	-0.927009	-1.135117	-1.608037	-1.872333	-2.172551	-2.408033	-0.344445	0.689801	0.516013	0.394631	0.328738	0.276717	0.240495	0.208511	0.173106	0.144493	Cp		
count	q [psf]	V_ref [mph]	Alpha [deg]	P 1 [mbar]	P 2 [mbar]	P 3 [mbar]	P 4 [mbar]	P 5 [mbar]	P 6 [mbar]	P 7 [mbar]	P 8 [mbar]	P 9 [mbar]	P 10 [mbar]	P 11 [mbar]	P 12 [mbar]	P 13 [mbar]	P 14 [mbar]	P 15 [mbar]	P 16 [mbar]	P 17 [mbar]	P 18 [mbar]	P 19 [mbar]	1 mbar = 1 mph = 1 sq. ft =	2.088543 1.466667 144	psf psf psi n
1	0.1	6	0	10016	10016.2	10016.1	10015.9	10016.1	10015.7	10016	10015.8	10016.1	10016.2	10016.3	10015.8	10016	10016.2	10016.2	10015.7	10016.1	10016.1	10015.8			
2	0.1	6	0	10015.9	10016.2	10016.1	10015.9	10016.1	10015.7	10016.1	10015.8	10016.1	10016.2	10016.2	10015.8	10016.1	10016.2	10016.2	10015.7	10016.1	10016.1	10015.8			
3	0.1	7	0	10015.9	10016.2	10016.1	10015.9	10016.1	10015.7	10016.1	10015.8	10016.1	10016.2	10016.3	10015.8	10016	10016.2	10016.2	10015.7	10016.1	10016.1	10015.8			
4	0.1	6	0	10015.9	10016.2	10016.1	10015.9	10016.1	10015.7	10016.1	10015.8	10016.1	10016.2	10016.3	10015.8	10016	10016.2	10016.2	10015.7	10016.1	10016.1	10015.8			
5	0.1	7	0	10015.9	10016.2	10016.1	10015.9	10016.1	10015.7	10016.1	10015.8	10016.1	10016.2	10016.3	10015.8	10016.1	10016.2	10016.2	10015.7	10016.1	10016.1	10015.8			
6	0.1	7	0	10010	10010	10010	10010	10010	10010	10010	10010	10010	10010	10010	10010	10010	10010	10010	10010	10010	10010	10010			

				15.9	16.2	16.1	15.8	16.1	15.7	16	15.8	16.1	16.2	16.3	15.8	16.1	16.2	16.2	15.7	16.1	16.1	15.8
				10	10	10	10	10	10	10	10	10	10	10	10	10	10	10	10	10	10	10
7	0.2	8	0	15.9	16.2	16.1	15.9	16.1	15.7	16.1	15.8	16.1	16.2	16.3	15.8	16.1	16.2	16.2	15.7	16.1	16.1	15.8
					10	10	10	10	10	10	10	10	10	10	10	10	10	10	10	10	10	10
8	0.1	6	0	10 16	16.2	16.1	15.9	16.1	15.7	16.1	15.8	16.1	16.2	16.3	15.8	16.1	16.2	16.2	15.7	16.1	16.1	15.8
					10	10	10	10	10	10	10	10	10	10	10	10	10	10	10	10	10	10
9	0.1	7	0	10 16	16.2	16.1	15.9	16.1	15.7	16.1	15.8	16.1	16.2	16.3	15.8	16.1	16.2	16.2	15.7	16.1	16.1	15.8
				10	10	10	10	10	10	10	10	10	10	10	10	10	10	10	10	10	10	10
10	0.1	7	0	15.9	16.2	16.1	15.9	16.1	15.7	16.1	15.8	16.1	16.2	16.3	15.8	16.1	16.2	16.2	15.7	16.1	16.1	15.8
				10	10	10	10	10	10	10	10		10	10	10	10	10	10	10	10	10	10
11	0.1	6	0	15.9	16.2	16.1	15.9	16.1	15.7	16.1	15.8	16	16.2	16.3	15.8	16.1	16.2	16.2	15.7	16.1	16.1	15.8
					10	10	10	10	10	10	10	10	10	10	10		10	10	10	10	10	10
12	0.1	6	0	10 16	16.2	16.1	15.9	16.1	15.7	16.1	15.8	16.1	16.2	16.3	15.8	16	16.2	16.2	15.7	16.1	16.1	15.8
					10	10	10	10	10	10	10	10	10	10	10	10	10	10	10	10	10	10
13	0.1	6	0	10 16	16.2	16.1	15.9	16.1	15.7	16.1	15.8	16.1	16.2	16.3	15.8	16.1	16.2	16.2	15.7	16.1	16.1	15.8
					10	10	10	10	10	10	10	10	10	10	10		10	10	10	10	10	10
14	0.1	7	0	15.9	16.2	16.1	15.9	16.1	15.7	16.1	15.8	16.1	16.2	16.3	15.8	16	16.2	16.2	15.7	16.1	16.1	15.8
					10	10	10	10	10	10	10	10	10	10	10		10	10	10	10	10	10
15	0.1	7	0	15.9	16.2	16.1	15.9	16.1	15.7	16.1	15.8	16.1	16.2	16.3	15.8	16	16.2	16.2	15.7	16.1	16.1	15.8
					10	10	10	10	10	10	10	10	10	10	10	10	10	10	10	10	10	10
16	0.1	7	0	15.9	16.2	16.1	15.9	16.1	15.7	16.1	15.8	16.1	16.2	16.3	15.8	16	16.2	16.2	15.7	16.1	16.1	15.8
					10	10	10	10	10	10	10	10	10	10	10	10	10	10	10	10	10	10
17	0.1	7	0	15.	16.	16.	15.	16.	15.	16.	15.	16.	16.	16.	15.	16.	16.	16.	15.	16.	16.	15.

				9	2	1	9	1	7	1	8	1	2	3	8	1	2	2	7	1	1	8	
				10	10	10	10	10	10	10	10	10	10	10	10	10	10	10	10		10	10	
				15.	16.	16.	15.	16.	15.	16.	15.	16.	16.	16.	15.	16.	16.	16.	15.	10	16.	15.	
18	0.1	6	0	9	2	1	9	1	7	1	8	1	2	3	8	1	2	2	7	16	1	8	
				10	10	10	10	10	10	10	10	10	10	10	10		10	10	10	10	10	10	
				15.	16.	16.	15.	16.	15.	16.	15.	16.	16.	16.	15.	10	16.	16.	15.	16.	16.	15.	
19	0.1	6	0	9	2	1	9	1	7	1	8	1	2	3	8	16	2	1	7	1	1	8	
				10	10	10	10	10	10	10	10	10	10	10	10		10	10	10	10	10	10	
				15.	16.	16.	15.	16.	15.	16.	15.	16.	16.	16.	15.	10	16.	16.	15.	16.	16.	15.	
20	0.1	7	0	9	2	1	9	1	7	1	8	1	2	3	8	16	2	1	7	1	1	8	
				10			10					10		10		10				10			
				15.	10	10	15.	10	10	10	10	16.	10	16.	10	16.	10	10	10	16.	10	10	
	0.1			92	16.	16.	89	16.	15.	16.	15.	09	16.	29	15.	05	16.	16.	15.	09	16.	15.	Av
	05	6.6	0	5	2	1	5	1	7	09	8	5	2	5	8	5	2	19	7	5	1	8	g
				21	21	21	21	21	21	21	21	21	21	21	21	21	21	21	21	21	21	21	
				21.	22.	22.	21.	22.	21.	22.	21.	22.	22.	22.	21.	22.	22.	22.	21.	22.	22.	21.	
				80	37	16	74	16	33	14	54	15	37	57	54	07	37	35	33	15	16	54	
				3	8	9	1	9	4	8	2	9	8	6	2	5	8	7	4	9	9	2	psf
		9.6																					
		80																					
		00																					FP
		2																					S
					-	-	-	-			-	-	0.2	0.3	-	-	-		-	-	-	-	
				-	2.6	1.7	3.0	2.8	-	-	2.9	3.0	04	03	0.9	1.8	0.9	-	0.9	1.0	2.9	2.1	
				2.2	79	84	77	78	1.1	1.1	78	77	36	81	89	84	89	1.1	89	88	78	82	
				82	81	72	63	72	88	88	18	63	4	9	09	18	09	88	09	54	18	54	Cp
				10	10	10	10	10		10	10	10	10	10		10	10	10	10			10	
				14.	14.	14.	14.	14.	10	14.	14.	14.	15.	15.	10	15.	15.	15.	14.	10	10	14.	
21	2.4	30	0	2	5	4	2	4	14	4	1	1	8	7	15	2	3	2	6	15	15	5	
				10	10	10	10	10		10	10	10	10	10		10	10	10	10			10	
				14.	14.	14.	14.	14.	10	14.	14.	14.	15.	15.	10	15.	15.	15.	14.	10	10	14.	
22	2.2	30	0	3	6	4	2	4	14	4	1	1	8	7	15	2	3	2	6	15	15	6	
23	2.2	29	0	10	10	10	10	10	10	10	10	10	10	10	10	10	10	10	10	10	10	10	

				14.2	14.6	14.4	14.2	14.4	14	14.4	14.1	14.1	15.7	15.7	15	15.2	15.3	15.2	14.6	15	15	14.6
				10	10	10	10	10		10	10	10	10	10		10	10	10	10		10	10
24	2.3	30	0	14.3	14.6	14.4	14.2	14.4	10 14	14.4	14.1	14.1	15.8	15.7	10 15	15.2	15.3	15.2	14.6	10 15	14.9	14.6
				10	10	10	10	10		10	10	10	10	10		10	10	10	10			10
25	2.3	30	0	14.2	14.5	14.4	14.2	14.4	10 14	14.4	14.1	14.1	15.7	15.7	10 15	15.2	15.3	15.2	14.7	10 15	10 15	14.6
				10	10	10	10	10		10	10	10	10	10		10	10	10	10			10
26	2.4	31	0	14.3	14.6	14.4	14.2	14.4	10 14	14.4	14.1	14.1	15.8	15.6	10 15	15.2	15.3	15.1	14.6	10 15	10 15	14.6
				10	10	10	10	10		10	10	10	10	10		10	10	10	10			10
27	2.5	31	0	14.3	14.6	14.4	14.2	14.4	10 14	14.5	14.1	14.1	15.8	15.6	10 15	15.2	15.3	15.2	14.6	10 15	10 15	14.6
				10	10	10	10	10		10	10	10	10	10		10	10	10	10			10
28	2.3	30	0	14.2	14.6	14.4	14.2	14.4	10 14	14.4	14.1	14.1	15.8	15.7	10 15	15.2	15.3	15.2	14.7	10 15	10 15	14.6
				10	10	10	10	10		10	10	10	10	10		10	10	10	10			10
29	2.4	30	0	14.2	14.5	14.4	14.2	14.4	10 14	14.4	14.1	14.1	15.8	15.7	10 15	15.2	15.3	15.2	14.6	10 15	10 15	14.6
				10	10	10	10	10		10	10	10	10	10		10	10	10	10			10
30	2.3	30	0	14.3	14.6	14.4	14.2	14.4	10 14	14.4	14.1	14.1	15.8	15.6	10 15	15.2	15.3	15.2	14.6	10 15	10 15	14.6
				10	10	10	10	10		10	10		10	10		10	10	10	10			10
31	2.3	30	0	14.2	14.5	14.4	14.2	14.4	10 14	14.4	14.1	10 14	15.8	15.6	10 15	15.2	15.3	15.2	14.6	10 15	10 15	14.6
				10	10	10	10	10		10	10	10	10	10		10	10	10	10			10
32	2.4	31	0	14.2	14.5	14.4	14.2	14.4	10 14	14.4	14.1	14.1	15.8	15.6	10 15	15.2	15.3	15.2	14.6	10 15	10 15	14.6
				10	10	10	10	10		10	10	10	10	10		10	10	10	10			10
33	2.4	31	0	14.3	14.5	14.4	14.2	14.4	10 14	14.4	14.1	14.1	15.8	15.7	10 15	15.2	15.3	15.2	14.6	10 15	10 15	14.6
				10	10	10	10	10	10	10	10	10	10	10	10	10	10	10	10	10	10	10
34	2.3	30	0	14.2	14.6	14.4	14.2	14.4	14	14.4	14.1	14.1	15.7	15.7	15	15.2	15.3	15.2	14.6	15	15	14.6

				2	5	4	2	4		5	1	1	8	6		2	3	2	6			6	
				10	10	10	10	10		10	10	10	10	10	10	10	10	10	10			10	
				14.	14.	14.	14.	14.	10	14.	14.	14.	15.	15.	15.	15.	15.	15.	14.	10	10	14.	
35	2.4	31	0	2	5	4	2	4	14	5	1	1	8	7	1	2	3	2	6	15	15	6	
				10	10	10	10	10		10	10	10	10	10		10	10	10	10			10	
				14.	14.	14.	14.	14.	10	14.	14.	14.	15.	15.	10	15.	15.	15.	14.	10	10	14.	
36	2.4	30	0	2	5	4	2	4	14	4	1	1	8	7	15	2	3	2	6	15	15	6	
				10	10	10	10	10		10	10	10	10	10		10	10	10	10			10	
				14.	14.	14.	14.	14.	10	14.	14.	14.	15.	15.	10	15.	15.	15.	14.	10	10	14.	
37	2.4	30	0	2	6	4	2	4	14	4	1	1	8	7	15	2	3	1	6	15	15	6	
				10	10	10	10	10		10	10	10	10	10		10	10	10	10			10	
				14.	14.	14.	14.	14.	10	14.	14.	14.	15.	15.	10	15.	15.	15.	14.	10	10	14.	
38	2.4	30	0	3	6	5	2	4	14	4	1	1	8	7	15	2	3	2	6	15	15	6	
				10	10	10	10	10		10	10	10	10	10		10	10	10	10			10	
				14.	14.	14.	14.	14.	10	14.	14.	14.	15.	15.	10	15.	15.	15.	14.	10	10	14.	
39	2.3	30	0	3	5	4	2	4	14	4	1	1	8	7	15	2	3	2	6	15	15	6	
				10	10	10	10	10		10	10	10	10	10		10	10	10	10			10	
				14.	14.	14.	14.	14.	10	14.	14.	14.	15.	15.	10	15.	15.	15.	14.	10	10	14.	
40	2.3	30	0	2	5	4	2	4	14	4	1	1	8	7	15	2	3	2	6	15	15	6	
					10	10				10		10			10						10	10	
				10	14.	14.	10	10		14.	10	14.	10	10	15.	10	10	10	10		14.	14.	
	2.3	30.		14.	54	40	14.	14.	10	41	14.	09	15.	15.	00	15.	15.	15.	14.	10	99	59	Av
	45	2	0	24	5	5	2	4	14	5	1	5	79	67	5	2	3	19	61	15	5	5	g
				21	21	21	21	21	21		21	21	21	21	21	21	21	21	21	21	21	21	
				18.	18.	18.	18.	18.	17.	21	17.	17.	21.	21.	19.	20.	20.	20.	19.	19.	19.	19.	
				28	92	62	20	61	78	18.	99	98	52	27	88	28	49	26	05	87	86	02	
				4	1	9	1	8	3	65	2	1	2	1	2	9	8	8	7	2	1	6	psf
		44.																					
		29																					
		33																					FP
		4																					S
				-	-	-	-	-	-	-	-	-	0.5	0.4	0.2	0.1	0.1	0.0	-	-	-	-	
				0.6	0.6	0.6	0.6	0.6	0.6	0.5	0.6	0.9	99	12	02	09	09	11	0.0	0.0	0.1	0.2	
				47	38	34	92	87	12	89	92	63	21	18	88	36	36	39	59	68	62	15	Cp

				68	77	32	21	76	05	79	21	85	3			3	3	3	86	76	28	72
				10	10	10	10	10	10	10	10	10	10	10	10	10	10	10	10	10	10	10
	12.			06.	06.	06.	06.	06.	06.	06.	05.	04.	12.	13.	12.	12.	11.	11.	10.	10.	10.	09.
41	1	69	0	1	4	4	3	6	3	4	7	8	2	9	5	2	9	4	7	7	3	5
				10	10	10	10	10	10	10	10		10	10	10	10	10	10	10	10	10	10
	12.			06.	06.	06.	06.	06.	06.	06.	05.	10	12.	13.	12.	12.	11.	11.	10.	10.	10.	09.
42	3	69	0	2	4	5	5	8	4	5	9	05	4	8	5	1	8	5	6	7	3	5
				10	10	10	10	10	10	10			10	10	10	10	10	10	10	10	10	10
	11.			06.	06.	06.	06.	06.	06.	06.	10	10	12.	13.	12.	12.	11.	11.	10.	10.	10.	09.
43	8	68	0	3	6	6	6	8	5	6	06	05	4	8	5	1	9	4	6	7	4	5
				10	10	10	10	10	10	10			10	10	10	10	10	10	10	10	10	10
				06.	06.	06.	06.	06.	06.	06.	10	10	12.	13.	12.	12.	11.	11.	10.	10.	10.	09.
44	12	69	0	3	6	5	5	8	4	5	06	05	5	8	5	1	8	4	6	7	3	5
				10	10	10	10	10	10	10	10	10	10	10	10	10	10	10	10	10	10	10
	11.			06.	06.	06.	06.	06.	06.	06.	05.	04.	12.	13.	12.	12.	11.	11.	10.	10.	10.	09.
45	9	68	0	2	4	3	3	7	3	4	8	8	3	8	5	2	8	4	6	7	3	5
				10	10	10	10	10	10	10	10	10	10	10	10	10	10	10	10	10	10	10
	12.			06.	06.	06.	06.	06.	06.	06.	05.	04.	12.	13.	12.	12.	11.	11.	10.	10.	10.	09.
46	2	69	0	3	6	6	5	7	4	4	8	9	2	8	5	1	8	4	6	7	3	5
				10	10	10	10	10	10	10	10		10	10	10	10	10	10	10	10	10	10
	11.			06.	06.	06.	06.	06.	06.	06.	06.	10	13.	13.	12.	12.	11.	11.	10.	10.	10.	09.
47	7	68	0	1	4	4	4	7	4	5	2	05	1	5	3	1	7	4	6	6	5	7
				10			10	10	10	10	10	10	10		10	10	10	10	10	10	10	10
	11.			05.	10	10	06.	06.	06.	06.	05.	04.	11.	10	12.	12.	11.	11.	10.	10.	10.	09.
48	7	68	0	8	06	06	1	6	1	3	7	7	7	14	6	2	9	5	6	7	3	5
				10	10	10	10	10		10	10	10	10	10	10	10	10	10	10	10	10	10
	12.			05.	06.	06.	06.	06.	10	06.	05.	04.	11.	13.	12.	12.	11.	11.	10.	10.	10.	09.
49	3	69	0	9	2	2	1	4	06	2	6	7	8	8	5	1	7	4	4	5	1	3
				10	10	10	10	10	10		10	10	10	10	10		10	10	10	10		10
	12.			05.	05.	05.	05.	06.	05.	10	05.	04.	11.	13.	12.	10	11.	11.	10.	10.	10	09.
50	4	70	0	7	9	8	8	1	9	06	3	5	7	8	4	12	7	3	4	4	10	2
	12.			10	10	10	10	10	10	10	10	10	10	10	10	10	10	10	10	10	10	10
51	6	70	0	05.	05.	05.	05.	06.	05.	06	05.	04.	11.	13.	12.	12	11.	11.	10.	10.	10	09.

				6	9	9	9	3	9		4	5	7	8	4		7	3	4	4		2	
				10	10	10	10	10	10		10	10	10	10	10		10	10	10	10	10	10	
	13.			05.	05.	05.	05.	06.	05.	10	05.	04.	11.	13.	12.	10	11.	11.	10.	10.	09.	09.	
52	1	71	0	5	7	6	7	1	9	06	4	7	8	8	4	12	6	2	3	4	9	1	
				10	10	10	10	10	10		10	10	10	10	10	10	10	10	10	10	10		
	13.			05.	05.	05.	05.	06.	05.	10	05.	04.	11.	13.	12.	11.	11.	11.	10.	10.	09.	10	
53	3	72	0	3	7	7	8	1	8	06	3	5	8	7	3	9	6	1	3	3	9	09	
				10	10	10	10	10	10	10	10	10	10	10	10	10	10	10	10	10	10		
	13.			05.	05.	05.	05.	05.	05.	05.	05.	04.	11.	13.	12.	11.	11.	11.	10.	10.	09.	10	
54	2	72	0	3	6	6	5	8	5	6	2	4	6	7	3	9	5	1	2	3	8	09	
				10	10	10	10	10	10	10	10	10	10	10	10	10	10	10	10	10	10		
	13.			05.	05.	05.	05.	05.	05.	05.	04.	04.	11.	13.	12.	11.	11.	11.	10.	10.	09.	10	
55	2	72	0	1	3	4	4	7	4	5	9	2	5	7	3	9	5	1	2	2	8	09	
				10	10	10	10	10	10	10	10	10	10	10	10	10	10		10	10	10		
	13.			05.	05.	05.	05.	05.	05.	05.	04.	03.	11.	13.	12.	11.	11.	10	10.	10.	09.	10	
56	3	72	0	1	3	3	3	7	4	5	8	9	5	7	3	8	5	11	2	2	8	09	
				10	10	10	10		10	10	10	10	10	10	10	10	10		10	10	10	10	
	13.			05.	05.	05.	05.	10	05.	05.	04.	03.	11.	13.	12.	11.	11.	10	10.	10.	09.	08.	
57	2	72	0	2	5	6	6	06	6	7	9	9	4	7	3	8	4	11	2	2	8	9	
				10	10	10	10	10	10	10	10	10	10	10	10	10	10		10	10	10	10	
	13.			05.	05.	05.	04.	04.	04.	04.	04.	03.	11.	13.	12.	11.	11.	10	10.	10.	09.	08.	
58	7	73	0	2	4	3	8	7	6	9	5	9	6	8	3	8	5	11	2	2	7	9	
				10	10	10	10	10	10	10	10	10	10	10	10	10	10		10	10	10	10	
	13.			05.	05.	05.	04.	04.	04.	05.	04.	03.	11.	13.	12.	11.	11.	10	10.	10.	09.	08.	
59	4	72	0	2	4	1	7	8	4	1	4	7	5	8	3	8	5	11	1	2	8	9	
					10	10	10	10	10	10	10		10	10	10	10	10		10	10	10	10	
	13.			10	05.	05.	05.	05.	05.	05.	04.	10	11.	13.	12.	11.	11.	10	10.	10.	09.	08.	
60	2	72	0	05	2	3	3	8	4	5	9	04	6	7	2	8	4	11	1	2	8	9	
					10	10	10				10	10	10		10	10		10	10		10		
				10	05.	05.	05.	10	10	10	05.	04.	11.	10	12.	11.	10	11.	10.	10	10.	10	
	12.	70.		05.	92	90	85	06.	05.	05.	38	50	91	13.	39	99	11.	24	39	10.	05	09.	Av
	63	25	0	67	5	5	5	16	83	98	5	5	5	77	5	5	66	5	5	45	5	23	g
				21	21	21	21	21	21	21	20	20	21	21	21	21	21	21	21	21	21	21	
				00.	00.	00.	00.	01.	00.	01.	99.	97.	13.	17.	14.	13.	12.	12.	10.	10.	09.	07.	psf

				385	918	876	772	409	72	033	79	952	428	303	431	596	896	029	254	369	544	821	
		103.0334																					FPS
				-0.72309	-0.7297	-0.70903	-0.69415	-0.67596	-0.65033	-0.69002	-0.75534	-0.95046	0.284802	0.576669	0.4204	0.304646	0.232712	0.164087	0.106209	0.049159	-0.0327	-0.1129	Cp
61	27.4	103	0	1000.2	1000	996.6	992.1	987.7	982.7	975.1	967.2	960.2	979.5	1014.6	1011.8	1009.9	1008.8	1007.8	1006.6	1006.3	1005.7	1004.5	
62	27.5	104	0	1000.2	1000.2	997	992.3	987.8	982.8	975.4	967.4	960.3	979.3	1014.5	1011.8	1009.9	1008.8	1007.8	1006.6	1006.3	1005.6	1004.5	
63	26.5	102	0	1000.4	1000.3	997	992.4	987.9	983	975.5	967.8	960.8	979.8	1014.6	1011.8	1010	1008.8	1007.8	1006.6	1006.3	1005.7	1004.5	
64	27.5	104	0	1000.3	1000.2	997	992.4	987.9	983	975.4	967.6	960.6	979.9	1014.6	1011.8	1009.9	1008.8	1007.8	1006.6	1006.4	1005.7	1004.6	
65	26.4	102	0	1000.3	1000.3	997.1	992.5	988.1	983.2	975.8	968	960.9	979.3	1014.6	1011.8	1010	1008.9	1007.9	1006.6	1006.4	1005.7	1004.6	
66	27.4	103	0	1000.3	1000.2	996.9	992.3	987.9	982.8	975.4	967.4	960.4	979.4	1014.6	1011.8	1010	1008.8	1007.8	1006.6	1006.3	1005.6	1004.5	
67	26.6	102	0	1000.3	1000.2	997	992.4	987.9	982.8	975.3	967.3	960.1	979.2	1014.6	1011.8	1009.9	1008.7	1007.8	1006.5	1006.3	1005.6	1004.5	
68	28.4	105	0	1000.	1000.	996.8	992.2	987.7	982.7	975.3	967.4	960.4	979.4	1014.	1011.	1009.	1008.	1007.	1006.	1006.	1005.	1004.	

				2	1									6	8	9	9	8	7	4	8	6
				10	10									10	10	10	10	10	10	10	10	10
	26.	10		00.	00.	99	99	98	98	97	96	96	97	14.	11.	10.	08.	07.	06.	06.	05.	04.
69	2	1	0	7	4	7.2	2.7	8.3	3.5	6.1	8.5	1.5	9.9	6	9	1	9	9	8	5	8	6
				10	10									10	10	10	10	10	10	10	10	10
	26.	10		00.	00.	99	99	98	98	97	96	96	97	14.	11.	10.	08.	07.	06.	06.	05.	04.
70	6	2	0	5	4	7.2	2.7	8.2	3.2	5.8	8	1	9.7	6	9	1	9	9	7	5	8	7
				10	10									10	10		10	10	10	10	10	10
	27.	10		00.	00.	99	99	98	98	97	96	96	97	14.	11.	10	08.	07.	06.	06.	05.	04.
71	2	3	0	4	4	7.3	2.7	8.3	3.3	5.9	7.9	0.9	9.6	6	9	10	9	9	7	4	7	6
				10	10									10	10		10	10	10	10	10	10
	26.	10		00.	00.	99	99	98	98	97	96	96	97	14.	11.	10	08.	07.	06.	06.	05.	04.
72	1	1	0	3	3	7.3	2.7	8.2	3.2	5.8	8	1	9.5	6	9	10	9	9	7	5	8	7
				10	10									10	10		10	10	10	10	10	10
	26.	10		00.	00.	99	99	98	98	97	96	96	98	14.	11.	10	08.	07.	06.	06.	05.	04.
73	6	2	0	6	5	7.4	2.8	8.4	3.5	6.1	8.4	1.5	0.2	6	8	10	9	9	7	4	8	6
				10	10									10	10		10	10	10	10	10	10
	27.	10		00.	00.	99	99	98	98	97	96	96	97	14.	11.	10	08.	07.	06.	06.	05.	04.
74	1	3	0	3	3	7.2	2.6	8.1	3.1	5.6	7.7	0.7	9.6	6	9	10	9	9	7	4	8	6
				10	10									10	10		10	10	10	10	10	10
	27.	10		00.	00.	99	99	98	98	97	96	96	97	14.	11.	10	08.	07.	06.	06.	05.	04.
75	5	4	0	4	4	7.3	2.7	8.2	3.2	5.8	7.7	0.5	9.2	6	9	10	9	9	6	4	7	6
				10	10									10	10		10	10	10	10	10	10
	26.	10		00.	00.	99	99	98	98	97	96	96	97	14.	11.	10	08.	07.	06.	06.	05.	04.
76	2	1	0	3	4	7.6	2.7	8	3.1	5.6	7.8	0.8	9.6	6	8	10	8	9	6	4	7	5
				10	10									10	10		10	10	10	10	10	10
	26.	10		00.	00.	99	99	98	98	97	96	96	97	14.	11.	10	08.	07.	06.	06.	05.	04.
77	9	3	0	2	2	7.1	2.4	7.9	2.9	5.4	7.6	0.7	9.6	6	8	10	8	8	6	3	7	6
				10	10									10	10		10	10	10	10	10	10
	26.	10		00.	00.	99	99	98	98	97	96	96	98	14.	11.	10	08.	07.	06.	06.	05.	04.
78	9	3	0	3	2	7	2.4	8	3.1	5.7	8.2	1.4	0.2	6	8	10	9	9	8	5	9	8
				10	10									10	10		10	10	10	10	10	10
	26.	10		00.	00.	99	99	98	98	97	96	96	97	14.	11.	10	08.	07.	06.	06.	05.	04.
79	5	2	0	5	4	7.4	2.8	8.3	3.4	5.9	8.1	1.1	9.7	6	9	10	9	9	7	5	8	7

80	27.4	103	0	1000.8	999.9	996.3	992.3	988.2	983.4	976.1	968.4	961.4	979.7	1014.6	1011.9	1010.1	1009	1008	1006.8	1006.5	1005.9	1004.8							
	26.945	102.65	0	1000.375	1000.265	997.085	992.505	988.05	983.095	975.655	967.82	960.81	969.615	1014.595	1011.8421	1010.9921	1008.8621	1007.865	1006.6621	1006.4	1005.7421	1004.605	Avg							
				2089.327	2089.097	2082.455	2072.89	2063.585	2053.237	2037.687	2021.334	2006.693	2045.968	2019.026	2013.272	2009.408	2007.048	2104.97	2102.453	2101.91	2100.532	2098.161	psf							
		150.5534																					FPS							
				-0.218	-0.249	-0.484	-0.828	-1.189	-1.535	-2.143	-2.734	-3.301	-1.838	0.86518	0.68530	0.51865	0.42316	0.34619	0.29154	0.24038	0.18148	0.11985	Cp							
	q	V_ref	Alpha	P 1	P 2	P 3	P 4	P 5	P 6	P 7	P 8	P 9	P 10	P 11	P 12	P 13	P 14	P 15	P 16	P 17	P 18	P 19							
count	[psf]	[mph]	[deg]	[mbar]	[mbar]	[mbar]	[mbar]	[mbar]	[mbar]	[mbar]	[mbar]	[mbar]	[mbar]	[mbar]	[mbar]	[mbar]	[mbar]	[mbar]	[mbar]	[mbar]	[mbar]	[mbar]	[mbar]	1 mbar = 1 mph = 1 sq. ft	2.0885433	psf			
1	0.1	6	0	1015.9	1016.2	1016.1	1015.8	1016.1	1015.6	1016	1015.8	1016	1016.1	1016.2	1015.8	1016	1016.1	1016	1015.6	1016	1016.1	1015.8			1.4666667	fps			
2	0.1	6	0	1015.9	1016.2	1016.1	1015.9	1016.1	1015.6	1016	1015.8	1016	1016.1	1016.2	1015.8	1016	1016.1	1016	1015.6	1016	1016.1	1015.8			144	psi			

																								=	n
				10	10	10	10	10	10		10		10	10	10		10	10	10		10	10				
				15.	16.	16.	15.	16.	15.	10	15.	10	16.	16.	15.	10	16.	16.	15.	10	16.	15.				
3	0.1	7	0	9	2	1	9	1	6	16	8	16	1	2	8	16	1	1	6	16	1	8				
				10	10	10	10	10	10		10		10	10	10		10	10	10		10	10				
				15.	16.	16.	15.	16.	15.	10	15.	10	16.	16.	15.	10	16.	16.	15.	10	16.	15.				
4	0.1	7	0	9	2	1	9	1	6	16	8	16	1	2	8	16	1	1	6	16	1	8				
				10	10	10	10	10	10		10		10	10	10		10	10	10		10	10				
				15.	16.	16.	15.	16.	15.	10	15.	10	16.	16.	15.	10	16.	16.	15.	10	16.	15.				
5	0.1	6	0	9	2	1	9	1	6	16	8	16	1	2	8	16	2	1	6	16	1	8				
				10	10	10	10	10	10		10		10	10	10		10	10	10	10	10	10				
				15.	16.	16.	15.	16.	15.	10	15.	10	16.	16.	15.	10	16.	16.	15.	16.	16.	15.				
6	0.1	7	0	9	2	1	9	1	6	16	7	16	1	2	8	16	2	1	6	1	2	8				
				10	10		10	10	10		10		10	10	10		10	10	10		10	10				
				15.	16.	10	15.	16.	15.	10	15.	10	16.	16.	15.	10	16.	16.	15.	10	16.	15.				
7	0.1	7	0	9	2	16	9	1	6	16	8	16	1	2	8	16	2	1	6	16	1	8				
				10	10	10	10	10	10		10	10	10	10	10		10	10	10	10	10	10				
				15.	16.	16.	15.	16.	15.	10	15.	16.	16.	16.	15.	10	16.	16.	15.	16.	16.	15.				
8	0.1	7	0	9	2	1	9	1	6	16	8	1	1	2	8	16	2	1	6	1	1	8				
				10	10	10	10	10	10		10		10	10	10		10	10	10		10	10				
				15.	16.	16.	15.	16.	15.	10	15.	10	16.	16.	15.	10	16.	16.	15.	10	16.	15.				
9	0.1	7	0	9	2	1	9	1	6	16	8	16	1	2	8	16	2	1	6	16	2	8				
				10	10	10	10	10	10	10	10		10	10	10		10	10	10		10	10				
				15.	16.	16.	15.	16.	15.	16.	15.	10	16.	16.	15.	10	16.	16.	15.	10	16.	15.				
10	0.2	8	0	9	2	1	9	1	7	1	8	16	1	2	8	16	2	2	6	16	2	8				
				10	10	10	10	10	10		10	10	10	10	10		10	10	10		10	10				
				15.	16.	16.	15.	16.	15.	10	15.	16.	16.	16.	15.	10	16.	16.	15.	10	16.	15.				
11	0.1	7	0	9	1	1	8	1	6	16	8	1	1	2	8	16	2	2	6	16	2	8				
				10	10	10	10		10		10		10	10	10		10	10	10		10	10				
				15.	16.	16.	15.	10	15.	10	15.	10	16.	16.	15.	10	16.	16.	15.	10	16.	15.				
12	0.1	7	0	9	2	1	8	16	6	16	8	16	1	2	8	16	2	2	6	16	2	8				
				10	10	10	10		10		10		10	10	10		10	10	10		10	10				
				15.	16.	16.	15.	10	15.	10	15.	10	16.	16.	15.	10	16.	16.	15.	10	16.	15.				
13	0.1	7	0	9	2	1	8	16	6	16	8	16	1	2	8	16	2	2	6	16	1	8				

				10	10		10	10	10		10	10	10	10	10		10	10	10	10	10	10	
				15.	16.	10	15.	16.	15.	10	15.	16.	16.	16.	15.	10	16.	16.	15.	16.	16.	15.	
14	0.1	7	0	9	2	16	9	1	7	16	8	1	1	2	8	16	2	1	6	1	1	8	
				10	10	10	10	10	10		10		10	10	10		10	10	10		10	10	
				15.	16.	16.	15.	16.	15.	10	15.	10	16.	16.	15.	10	16.	16.	15.	10	16.	15.	
15	0.1	6	0	9	2	1	9	1	6	16	8	16	1	2	8	16	2	1	6	16	1	8	
				10	10	10	10	10	10	10	10		10	10	10		10	10	10		10	10	
				15.	16.	16.	15.	16.	15.	16.	15.	10	16.	16.	15.	10	16.	16.	15.	10	16.	15.	
16	0.1	7	0	9	2	1	9	1	6	1	8	16	1	2	8	16	2	1	6	16	1	8	
				10	10	10	10	10	10		10	10	10	10	10		10	10	10		10	10	
				15.	16.	16.	15.	16.	15.	10	15.	16.	16.	16.	15.	10	16.	16.	15.	10	16.	15.	
17	0.1	7	0	9	1	1	9	1	6	16	8	1	1	2	8	16	2	1	6	16	1	8	
				10	10	10	10	10	10		10	10	10	10	10		10	10	10		10	10	
				15.	16.	16.	15.	16.	15.	10	15.	16.	16.	16.	15.	10	16.	16.	15.	10	16.	15.	
18	0.1	8	0	9	2	1	9	1	7	16	8	1	1	2	8	16	2	1	6	16	1	8	
				10	10	10	10	10	10	10	10	10	10	10	10		10	10	10		10	10	
				15.	16.	16.	15.	16.	15.	16.	15.	16.	16.	16.	15.	10	16.	16.	15.	10	16.	15.	
19	0.1	7	0	9	2	1	9	1	7	1	8	1	1	2	8	16	2	2	6	16	1	8	
				10	10	10	10	10	10		10		10	10	10		10	10	10	10	10	10	
				15.	16.	16.	15.	16.	15.	10	15.	10	16.	16.	15.	10	16.	16.	15.	16.	16.	15.	
20	0.1	7	0	9	2	1	9	1	7	16	8	16	1	2	8	16	2	2	6	1	1	8	
									10	10	10										10		
				10	10	10	10	10	15.	16.	15.	10	10	10	10		10	10	10	10	16.	10	
	0.1			15.	16.	16.	15.	16.	62	01	79	16.	16.	16.	15.	10	16.	16.	15.	16.	12	15.	Av
	05	6.9	0	9	19	09	88	09	5	5	5	03	1	2	8	16	18	13	6	02	5	8	g
				21	21	21	21	21	21	21	21	21	21	21	21		21	21	21	21	21	21	
				21.	22.	22.	21.	22.	21.	21.	21.	22.	22.	22.	21.	21	22.	22.	21.	22.	22.	21.	
				75	35	14	70	14	17	99	53	02	16	37	54	21.	33	23	12	00	22	54	
				1	7	8	9	8	7	1	2	3	9	8	2	96	6	2	5	2	1	2	psf
		10.																					FP
		12																					S
				-	-	-	-	-	-	-	-	-	-	-	-	-	-	-	-	-	-	-	
				2.7	2.8	1.9	3.3	3.0	2.6	2.6	3.0	4.3	1.7	1.5	0.9	2.9	1.3	2.3	2.9	2.5	2.4	2.1	
				79	78	83	76	77	79	79	77	70	84	85	89	78	86	81	78	80	80	82	Cp

				27	72	63		63	81	81	63	54	72	82	09	18	91	45	18	36	91	54
				10	10	10		10	10	10		10	10	10	10	10	10	10	10			10
				14.	14.	14.	10	14.	13.	14.	10	14.	15.	15.	15.	15.	15.	15.	14.	10	10	14.
21	2.3	30	0	1	4	3	14	2	9	2	14	1	2	9	2	3	3	3	7	15	15	5
				10	10	10	10	10	10	10		10	10	10	10	10	10	10	10			10
				14.	14.	14.	14.	14.	13.	14.	10	14.	15.	15.	15.	15.	15.	15.	14.	10	10	14.
22	2.4	31	0	1	4	3	1	3	9	3	14	1	3	8	2	3	4	2	6	15	15	6
				10	10	10		10	10	10		10	10	10	10	10	10	10	10			10
				14.	14.	14.	10	14.	13.	14.	10	14.	15.	15.	15.	15.	15.	15.	14.	10	10	14.
23	2.5	31	0	1	3	2	14	2	8	2	14	1	2	8	2	3	3	2	7	15	15	5
				10	10	10		10	10	10		10	10	10	10	10	10	10	10		10	10
				14.	14.	14.	10	14.	13.	14.	10	14.	15.	15.	15.	15.	15.	15.	14.	10	14.	14.
24	2.3	30	0	1	4	2	14	2	9	2	14	1	2	9	2	3	4	2	7	15	9	6
				10	10	10		10	10	10		10	10	10	10	10	10	10	10			10
				14.	14.	14.	10	14.	13.	14.	10	14.	15.	15.	15.	15.	15.	15.	14.	10	10	14.
25	2.3	30	0	1	4	2	14	2	9	2	14	1	2	9	2	3	4	2	7	15	15	6
				10	10	10		10	10	10		10	10	10	10	10	10	10	10			10
				14.	14.	14.	10	14.	13.	14.	10	14.	15.	15.	15.	15.	15.	15.	14.	10	10	14.
26	2.4	31	0	1	3	2	14	2	9	2	14	1	2	9	2	3	4	2	7	15	15	6
				10	10	10		10	10	10		10	10	10	10	10	10	10	10			10
				14.	14.	14.	10	14.	13.	14.	10	14.	15.	15.	15.	15.	15.	15.	14.	10	10	14.
27	2.2	30	0	1	3	2	14	2	9	2	14	1	2	9	2	3	4	2	6	15	15	5
				10	10	10		10	10	10		10	10	10	10	10	10	10	10			10
				14.	14.	14.	10	14.	13.	14.	10	14.	15.	15.	15.	15.	15.	15.	14.	10	10	14.
28	2.4	31	0	1	4	2	14	3	9	2	14	1	2	8	2	3	4	2	6	15	15	5
				10	10	10		10	10	10	10		10	10	10	10	10	10	10		10	10
				14.	14.	14.	10	14.	13.	14.	13.	10	15.	15.	15.	15.	15.	15.	14.	10	14.	14.
29	2.5	31	0	1	3	2	14	2	8	2	9	14	2	9	3	3	4	2	6	15	9	6
					10	10	10	10	10	10	10		10	10	10	10	10	10	10		10	10
				10	14.	14.	13.	14.	13.	14.	13.	10	15.	15.	15.	15.	15.	15.	14.	10	14.	14.
30	2.3	30	0	14	3	1	9	1	8	1	9	14	2	9	2	3	4	2	6	15	9	5
				10	10	10	10	10	10	10	10	10	10	10	10	10	10	10	10	10	10	10
31	2.4	31	0	14	14.	14.	14	14.	13.	14.	14	14.	15.	15.	15.	15.	15.	15.	14.	15	15	14.

					3	2		2	8	2		1	2	9	3	3	4	2	7			6	
				10	10	10		10	10	10			10	10	10	10	10	10	10			10	
				14.	14.	14.	10	14.	13.	14.	10	10	15.	15.	15.	15.	15.	15.	14.	10	10	14.	
32	2.5	32	0	1	3	2	14	2	9	2	14	14	2	9	3	3	4	2	7	15	15	6	
				10	10	10		10	10	10		10	10	10	10	10	10	10	10			10	
				14.	14.	14.	10	14.	13.	14.	10	14.	15.	15.	15.	15.	15.	15.	14.	10	10	14.	
33	2.4	30	0	1	3	2	14	2	9	2	14	1	3	9	2	3	4	2	6	15	15	6	
				10	10	10		10	10	10			10	10	10	10	10	10	10			10	
				14.	14.	14.	10	14.	13.	14.	10	10	15.	15.	15.	15.	15.	15.	14.	10	10	14.	
34	2.4	31	0	1	4	2	14	2	8	2	14	14	2	9	3	3	4	2	6	15	15	5	
				10	10	10		10	10	10		10	10	10	10	10	10	10	10			10	
				14.	14.	14.	10	14.	13.	14.	10	14.	15.	15.	15.	15.	15.	15.	14.	10	10	14.	
35	2.4	31	0	1	3	2	14	2	8	2	14	1	3	9	2	3	3	2	6	15	15	6	
				10	10	10		10	10	10		10	10	10	10	10	10	10	10			10	
				14.	14.	14.	10	14.	13.	14.	10	14.	15.	15.	15.	15.	15.	15.	14.	10	10	14.	
36	2.4	31	0	1	3	2	14	2	9	2	14	1	2	9	3	3	4	2	6	15	15	6	
				10	10	10		10	10	10		10	10	10	10	10	10	10	10			10	
				14.	14.	14.	10	14.	13.	14.	10	14.	15.	15.	15.	15.	15.	15.	14.	10	10	14.	
37	2.3	30	0	1	3	2	14	2	9	2	14	1	3	8	2	3	3	2	6	15	15	6	
				10	10	10		10	10	10	10		10	10	10	10	10	10	10			10	
				14.	14.	14.	10	14.	13.	14.	13.	10	15.	15.	15.	15.	15.	15.	14.	10	10	14.	
38	2.4	31	0	1	3	2	14	2	8	2	9	14	2	9	2	3	4	3	7	15	15	5	
				10	10	10		10	10	10	10		10	10	10	10	10	10	10			10	
				14.	14.	14.	10	14.	13.	14.	13.	10	15.	15.	15.	15.	15.	15.	14.	10	10	14.	
39	2.6	32	0	1	3	2	14	2	8	1	9	14	2	9	2	4	4	3	7	15	15	6	
				10	10	10		10	10	10	10	10	10	10	10	10	10	10	10			10	
				14.	14.	14.	10	14.	13.	14.	14.	14.	15.	15.	15.	15.	15.	15.	14.	10	10	14.	
40	2.3	30	0	1	3	2	14	3	9	2	1	1	3	8	2	3	4	3	6	15	15	5	
						10				10	10		10	10	10	10			10		10		
				10	10	14.		10	10	14.	13.	10	15.	15.	15.	15.	10	10	14.		14.	10	
	2.3	30.		14.	14.	20	10	14.	13.	19	98	14.	22	87	22	30	15.	15.	64	10	98	14.	Av
	85	7	0	09	33	5	14	21	86	5	5	07	5	5	5	5	38	22	5	15	5	56	g
				21	21	21	21	21	21	21	21	21	21	21	21	21	21	21	21	21	21	21	
				17.	18.	18.	17.	18.	17.	18.	17.	17.	20.	21.	20.	20.	20.	20.	19.	19.	19.	18.	psf

				971	472	211	783	222	491	19	752	929	341	699	341	509	665	331	13	872	84	953	
		45.0266																					FPS
				-0.751	-0.799	-0.782	-0.838	-0.825	-0.707	-0.755	-0.764	-0.952	0.1116	0.6015	0.4089	0.2249	0.1943	0.0544	-0.011	-0.0508	-0.1515	-0.2598	Cp
41	11.6	67	0	10 06.4	10 06.7	10 06.7	10 06.5	10 06.7	10 06.2	10 06.5	10 06.2	10 06.2	10 11.6	10 14.2	10 12.8	10 12.3	10 12	10 11.4	10 10.6	10 10.5	10 10.1	10 09.3	
42	11.7	68	0	10 06.5	10 06.9	10 06.8	10 06.6	10 06.8	10 06.4	10 06.6	10 06.3	10 06.4	10 11.5	10 14.2	10 12.8	10 12.3	10 11.9	10 11.4	10 10.6	10 10.5	10 10.1	10 09.3	
43	11.7	68	0	10 06.5	10 06.8	10 06.7	10 06.5	10 06.7	10 06.3	10 06.5	10 06.2	10 06.3	10 11.6	10 14.2	10 12.8	10 12.3	10 11.9	10 11.4	10 10.5	10 10.5	10 10.1	10 09.2	
44	11.5	67	0	10 06.4	10 06.7	10 06.6	10 06.4	10 06.5	10 06.1	10 06.3	10 06.1	10 06.1	10 11.4	10 14.2	10 12.8	10 12.3	10 11.9	10 11.4	10 10.5	10 10.5	10 10.1	10 09.2	
45	11.7	68	0	10 06.5	10 06.8	10 06.7	10 06.6	10 06.8	10 06.3	10 06.6	10 06.3	10 06.3	10 11.6	10 14.2	10 12.8	10 12.3	10 11.9	10 11.4	10 10.6	10 10.5	10 10.1	10 09.3	
46	11.6	67	0	10 06.6	10 06.9	10 06.8	10 06.6	10 06.9	10 06.4	10 06.7	10 06.4	10 06.4	10 11.7	10 14.2	10 12.8	10 12.3	10 12	10 11.4	10 10.6	10 10.6	10 10.2	10 09.3	
47	11.8	68	0	10 06.8	10 07.0	10 06.9	10 06.7	10 06.9	10 06.4	10 06.7	10 06.4	10 06.4	10 11.7	10 14.1	10 12.7	10 12.3	10 11.9	10 11.4	10 10.5	10 10.5	10 10.1	10 09.2	
48	11.8	68	0	10 06.	10 06.	10 06.	10 06.	10 06.	10 06.	10 06.	10 06.	10 06.	10 11.	10 14.	10 12.	10 12.	10 11.	10 11.	10 10.	10 10.	10 10.	10 09.	

				5	8	7	6	8	4	6	4	4	7	2	7	3	9	4	5	5	1	2
				10	10	10	10	10	10	10	10	10	10	10	10	10	10	10	10	10	10	10
	11.			06.	06.	06.	06.	06.	06.	06.	06.	06.	11.	14.	12.	12.	11.	11.	10.	10.	10.	09.
49	8	68	0	6	8	7	5	7	2	5	3	3	6	2	7	3	9	4	5	5	1	2
				10	10	10	10	10	10	10	10	10	10	10	10	10	10	10	10	10	10	10
	11.			06.	06.	06.	06.	06.	06.	06.	06.	06.	11.	14.	12.	12.	11.	11.	10.	10.	10.	09.
50	6	67	0	5	8	7	5	7	2	4	1	2	5	2	8	3	9	4	6	5	1	2
				10	10	10	10	10	10	10	10	10	10	10	10	10	10	10	10	10		10
	11.			06.	06.	06.	06.	06.	06.	06.	06.	06.	11.	14.	12.	12.	11.	11.	10.	10.	10	09.
51	8	68	0	5	8	7	6	8	3	6	2	3	6	2	7	3	9	4	5	5	10	2
				10	10	10	10	10	10	10	10	10	10	10	10	10	10	10	10	10	10	10
	11.			06.	06.	06.	06.	06.	06.	06.	06.	06.	11.	14.	12.	12.	11.	11.	10.	10.	10.	09.
52	7	68	0	6	8	7	6	8	3	6	3	3	7	1	7	2	9	4	5	5	1	2
				10	10	10	10	10	10	10	10	10	10	10	10	10	10	10	10	10	10	10
	11.			06.	06.	06.	06.	06.	06.	06.	06.	06.	11.	14.	12.	12.	11.	11.	10.	10.	10.	09.
53	6	67	0	2	6	5	4	6	2	4	1	2	5	2	8	3	9	4	5	5	1	2
				10	10	10	10	10	10	10	10	10	10	10	10	10	10	10	10	10	10	10
	12.			06.	06.	06.	06.	06.	06.	06.	06.	06.	11.	14.	12.	12.	11.	11.	10.	10.	10.	09.
54	1	69	0	4	7	6	4	7	2	4	1	1	2	2	8	3	9	4	5	5	1	2
				10	10	10	10	10	10	10	10	10	10	10	10	10	10	10	10	10		10
	11.			06.	06.	06.	06.	06.	06.	06.	06.	06.	11.	14.	12.	12.	11.	11.	10.	10.	10	09.
55	8	68	0	2	6	5	3	5	1	4	1	1	6	2	8	3	9	4	5	4	10	2
				10	10	10	10	10	10	10	10	10	10	10	10	10	10	10	10	10	10	10
	11.			06.	06.	06.	06.	06.	06.	06.	06.	06.	11.	14.	12.	12.	11.	11.	10.	10.	10.	09.
56	7	68	0	5	8	6	5	8	3	5	2	2	6	2	7	3	9	4	5	5	1	2
				10	10	10	10	10	10	10		10	10	10	10	10	10	10	10	10		10
	11.			06.	06.	06.	06.	06.	06.	06.	10	06.	11.	14.	12.	12.	11.	11.	10.	10.	10	09.
57	5	67	0	6	9	8	5	6	1	3	06	1	4	2	8	3	9	4	5	5	10	2
				10	10	10	10	10	10	10	10	10	10	10	10	10	10	10	10	10		10
	11.			06.	06.	06.	06.	06.	06.	06.	06.	06.	11.	14.	12.	12.	11.	11.	10.	10.	10	09.
58	8	68	0	4	7	7	5	7	2	5	2	3	7	1	7	2	8	3	5	4	10	1
				10	10	10	10	10		10		10	10	10	10	10	10	10	10	10		10
	12.			06.	06.	06.	06.	06.	10	06.	10	06.	11.	14.	12.	12.	11.	11.	10.	10.	10	09.
59	2	69	0	4	6	6	3	5	06	3	06	1	5	2	7	2	8	3	5	4	10	1

				10	10	10	10	10	10	10	10	10	10	10	10	10	10	10	10	10		10	
	12.			06.	06.	06.	06.	06.	06.	06.	06.	06.	11.	14.	12.	12.	11.	11.	10.	10.	10	09.	
60	1	69	0	5	8	6	5	7	2	5	1	2	5	2	7	2	8	3	5	4	10	1	
					10		10			10		10		10	10		10	10	10	10	10	10	
	11.			10	06.	10	06.	10	10	06.	10	06.	10	14.	12.	10	11.	11.	10.	10.	10.	09.	
	755	67.		06.	77	06.	50	06.	06.	49	06.	24	11.	18	75	12.	89	38	52	48	07	20	Av
	5	85	0	48	5	68	5	71	24	5	2	5	56	5	5	28	5	5	5	5	5	5	g
				21	21	21	21	21	21	21	21	21	21	21	21	21	21	21	21	21	21	21	
				02.	02.	02.	02.	02.	01.	02.	01.	01.	12.	18.	15.	14.	13.	12.	10.	10.	09.	07.	
				077	693	495	129	558	576	109	492	586	687	169	183	191	387	321	525	442	585	768	psf
		99.																					
		51																					
		33																					FP
		6																					S
				-	-	-	-	-	-	-	-	-	0.1	0.6	0.4	0.3	0.2	0.1	0.0	-	-	-	
				0.7	0.7	0.6	0.7	0.7	0.7	0.7	0.7	0.7	168	18	41	03	17	26	62	0.0	0.1	0.2	
				07	07	98	04	02	00	24	41	86	491	892	219	523	351	738	776	154	061	0018	
				44	44	55	77	99	33	31	19	5											Cp
													10	10	10	10	10		10			10	
	27.	10		99	99	99	99	99	99	99	99	99	05.	11.	08.	07.	06.	10	03.	10	10	00.	
61	6	4	0	3.9	4.2	3.9	3.7	3.8	3.2	3.1	2.3	2.3	6	5	8	2	2	05	6	03	02	3	
													10	10	10	10	10		10	10		10	
	27.	10		99	99	99	99	99	99	99	99	99	05.	11.	08.	07.	06.	10	03.	03.	10	00.	
62	4	3	0	3.7	4.1	4	4	4.3	3.7	3.7	2.7	2.7	1	5	8	3	2	05	7	1	02	4	
													10	10	10	10	10		10	10		10	
	26.	10		99	99	99	99	99	99	99	99	99	05.	11.	08.	07.	06.	10	03.	03.	10	00.	
63	3	1	0	3.8	4.1	4.1	4	4.3	3.8	3.7	2.9	2.7	4	5	8	3	2	05	7	1	02	3	
													10	10	10	10	10		10		10	10	
	27.	10		99	99	99	99	99	99	99	99	99	05.	11.	08.	07.	06.	10	03.	10	01.	00.	
64	5	4	0	3.9	4.3	4.2	4.2	4.4	3.9	3.8	2.8	2.5	2	4	6	2	1	05	6	03	9	3	
	27.	10		99	99	99	99	99	99	99	99	99	10	10	10	10	10	10	10	10	10	10	
65	8	4	0	3.4	3.8	3.8	3.8	4.2	3.7	3.6	2.7	2.6	05.	11.	08.	07.	06	05	03.	02.	01.	00.	

													1	5	7	2			5	9	8	2
													10	10	10	10	10	10	10	10	10	10
	27.	10		99	99	99	99	99	99	99	99	99	04.	11.	08.	07.	05.	04.	03.	02.	01.	00.
66	9	4	0	3.7	3.9	3.8	3.8	4	3.4	3.2	2.1	1.8	9	4	6	2	9	8	4	8	7	1
													10	10	10	10		10	10	10	10	10
	28.	10		99	99	99	99	99	99	99	99	99	05.	11.	08.	07.	10	04.	03.	02.	01.	00.
67	1	5	0	3.4	3.7	3.7	3.7	4	3.7	3.6	2.7	2.4	4	4	6	1	06	8	4	8	7	1
													10	10	10	10		10	10	10	10	10
		10		99	99	99	99	99	99	99	99	99	05.	11.	08.	07.	10	04.	03.	02.	01.	00.
68	27	3	0	3.7	4	3.9	3.8	4.1	3.6	3.5	2.7	2.4	4	3	6	1	06	8	5	9	8	2
													10	10	10	10		10	10	10	10	10
	27.	10		99	99	99	99	99	99	99	99	99	05.	11.	08.	07.	10	04.	03.	02.	01.	00.
69	2	3	0	4.1	4.3	4.2	4.1	4.4	4	3.8	2.9	2.5	3	4	6	2	06	9	5	9	8	2
													10	10	10	10	10	10	10		10	10
	27.	10		99	99	99	99	99	99	99	99	99	04.	11.	08.	07.	06.	04.	03.	10	01.	00.
70	1	3	0	3.7	4	3.9	3.9	4.1	3.6	3.5	2.5	2	6	5	8	2	1	9	6	03	9	2
													10	10	10	10		10	10	10	10	10
	27.	10		99	99	99	99	99	99	99	99	99	05.	11.	08.	07.	10	04.	03.	02.	01.	00.
71	2	3	0	3.6	4	4	3.9	4.3	3.7	3.6	2.6	2.1	2	4	6	1	06	9	5	9	8	2
													10	10	10	10	10	10	10	10		10
	27.	10		99	99	99	99	99	99	99	99	99	05.	11.	08.	07.	06.	04.	03.	02.	10	00.
72	4	4	0	3.4	3.7	3.8	3.7	3.9	3.6	3.4	2.5	2.2	2	4	7	2	1	9	6	9	02	3
													10	10	10	10	10		10	10	10	10
	26.	10		99	99	99	99	99	99	99	99	99	05.	11.	08.	07.	06.	10	03.	03.	02.	00.
73	5	2	0	3.7	4.1	4.1	4	4.4	4.1	3.9	3	2.7	4	5	8	3	2	05	7	1	1	5
													10	10	10	10	10	10	10	10	10	10
	26.	10		99	99	99	99	99	99	99	99	99	05.	11.	08.	07.	06.	05.	03.	03.	01.	00.
74	9	3	0	4.1	4.4	4.3	4.3	4.5	4	3.9	2.9	2.6	3	5	7	3	2	1	7	1	9	3
													10	10	10	10	10	10	10	10	10	10
	26.	10		99	99	99	99	99	99	99	99	99	05.	11.	08.	07.	06.	05.	03.	03.	02.	00.
75	9	3	0	3.7	4.1	4.1	4.1	4.3	4	3.9	3	2.7	6	5	8	3	2	1	7	1	1	5
													10	10	10	10	10	10	10	10	10	10
	26.	10		99	99	99	99	99	99	99	99	99	05.	11.	08.	07.	06.	05.	03.	03.	02.	00.
76	6	2	0	4.2	4.5	4.5	4.4	4.8	4.3	4.2	3.1	3	5	5	9	4	3	1	8	2	2	5

													10	10	10	10	10	10	10	10	10	10	
	27.	10		99	99	99	99	99	99	99	99	99	04.	11.	08.	07.	06.	05.	03.	03.	02.	00.	
77	4	3	0	4.2	4.5	4.4	4.2	4.4	3.9	3.8	2.6	2.4	9	6	9	4	3	2	8	2	2	6	
													10	10	10	10	10	10	10	10	10	10	
	26.	10		99	99	99	99	99	99	99	99	99	05.	11.	08.	07.	06.	05.	03.	03.	02.	00.	
78	7	2	0	4.1	4.4	4.4	4.3	4.5	4	3.9	3	2.7	2	5	9	4	3	2	8	2	1	5	
													10	10	10	10	10	10	10			10	
	27.	10		99	99	99	99	99	99	99	99	99	05.	11.	08.	07.	06.	05.	03.	10	10	00.	
79	1	3	0	3.9	4.3	4.2	4	4.2	3.7	3.6	2.8	2.8	5	5	7	3	1	1	6	03	02	3	
													10	10	10	10	10	10	10		10	10	
	27.	10		99	99	99	99	99	99	99	99	99	05.	11.	08.	07.	06.	04.	03.	10	01.	00.	
80	2	3	0	3.9	4.3	4.2	4.1	4.3	3.9	3.8	2.9	2.7	5	3	6	2	1	9	6	03	9	3	
													10	10	10	10	10	10	10		10	10	
				99	99	99		99	99	99	99	99	05.	11.	08.	07.	06.	04.	03.	10	01.	00.	
	27.	10		3.8	4.1	4.0	99	4.2	3.7	3.6	2.7	2.4	26	45	72	24	12	98	61	03.	94	31	Av
	19	3.1	0	05	35	75	4	6	9	75	35	9	5	5	5	5	5	5	5	01	5	5	g
				20	20	20	20	20	20	20		20		21	21	21	21	20	20		20	20	
				75.	76.	76.	76.	76.	75.	75.	20	72.	20	12.	06.	03.	01.	98.	96.	20	92.	89.	
				60	29	16	01	55	57	33	73.	85	99.	46	76	67	33	95	09	94.	60	20	
				5	4	9	2	5	4	3	37	8	54	8	6	5	6	5	4	83	6	1	psf
		15																					
		1.2																					
		13																					FP
		4																					S
				-	-	-	-	-	-	-	-	-	0.1	0.6	0.4		0.2	0.1	0.0	-	-	-	
				0.7	0.7	0.7	0.6	0.6	0.6	0.7	0.7	0.8	56	25	48	0.3	18	30	64	0.0	0.1	0.2	
				11	09	02	97	92	91	30	87	28	97	53	86	12	42	86	03	13	02	01	
				78	09	56	57	57	42	21	05	92	8	7	7	14	8	2	5	16	65	74	Cp

2D Airfoil Calculations

% of Chord																			
Upper Surface										Lower Surface									
P1	P2	P3	P4	P5	P6	P7	P8	P9	P10	P11	P12	P13	P14	P15	P16	P17	P18	P19	

	MPH	0.8	0.7	0.6	0.5	0.4	0.3	0.2	0.1	0.075	0	0.075	0.1	0.2	0.3	0.4	0.5	0.6	0.7	0.8
AOA = -4	6	-0.42401	-0.51894	-0.43039	-0.61387	-0.80374	-0.71519	-0.71519	-0.05066		-1.37973	-0.32907	-0.61387	-0.89868	-0.70881	-0.89868	-0.89868	-0.80374	-0.89868	-0.13921
	30	-0.28283	-0.33235	-0.29634	-0.44037	-0.44938	-0.44938	-0.44488	-0.17481	-0.27081	-0.60 7	-0.76896	-0.66093	-0.71495	-0.11629	-0.15 68	-0.17 03	-0.10279	-0.08028	-0.04427
	68	-0.28432	-0.36839	-0.41375	-0.49893	-0.54981	-0.55203	-0.56973	-0.25224	-0.23 6	-0.63 6	-0.80314	-0.64716	-0.13277	-0.16485	-0.12503	-0.09073	-0.05644	-0.01772	-0.01 4
	102	-0.13207	-0.39119	-0.44192	-0.52973	-0.58553	-0.59411	-0.60465	-0.27 1	-0.24177 1	-0.61444 7	-0.89733	-0.74045	-0.25539	-0.19685	-0.14261	-0.10203	-0.06534	-0.03413	-0.00 9
AOA = 0	6	-0.97862	-1.41831	-1.08854	-1.52824	-2.51755	-1.41831	-1.19847	-1.63816	-1.96793	-0.12 061 3	-1.85801	-1.63816	-2.95724	-1.19847	-1.41831	-1.96793	-1.30839	-1.30839	-0.31908
	30	-0.42829	-0.49567	-0.44177	-0.51812	-0.50465	-0.61245	-0.76066	-0.60795	-0.23516	-0.88 771 3	-0.46423	-0.34745	-0.25762	-0.16779	-0.16 33	-0.16 33	-0.16 33	-0.14 982	-0.10 042
	68	-0.16304	-0.44368	-0.61172	-0.68 21	-0.77359	-0.86069	-0.98385	-0.80 79	-0.43312	-0.95 777 2	-0.23254	-0.16216	-0.05747	-0.01524	0.00 147 6	0.01 555 2	0.02 698 9	0.03 930 5	0.06 129 9
	102	-0.20811	-0.36961	-0.64228	-0.71835	-0.81 86	-0.90091	-1.03003	-0.84474	-0.45504	-0.96 528 2	-0.24751	-0.17807	-0.06378	-0.01931	0.00 097	0.01 463 2	0.02 711 5	0.03 803 7	0.05 949 2
AOA = 4	6	-2.60748	-2.51255	-1.65815	-2.79735	-2.70242	-1.08854	-1.84801	-2.79735	-2.70242	-0.24 053	-1.46828	-1.37334	-2.70242	-0.89868	-2.03788	-2.41762	-2.79735	-2.70242	-2.03788
	30	-0.18493	-0.43214	-0.90953	-1.02461	-1.04166	-1.03 74	-1.27609	-1.38691	-1.24199	-0.79 114 6	-0.21 146 8	-0.14 753 3	-0.08 786 1	-0.10 064 8	-0.06 228 7	-0.06 228 7	-0.06 228 7	-0.04 523 7	-0.02 392 6
	68	-	-	-	-	-	-	-	-	-	-0.74	-0.31	-0.21	-0.18	-0.17	-0.14	-0.14	-0.12	-0.11	-0.11

		0.22	0.41	0.56	0.87	1.03	1.14	1.38	1.43	1.31	784	740	552	750	816	930	081	807	279	364
		171	359	216	884	336	967	654	748	608	7	3	3	6	7	1	1	6	4	3
		-	-	-	-	-	-	-	-	-	0.74	0.31	0.21	0.18	0.16	0.14	0.13	0.12	0.11	0.10
	10	0.24	0.45	0.65	0.81	1.08	1.22	1.46	1.50	1.37	619	079	432	772	474	418	289	080	072	532
	2	083	289	06	241	413	073	263	617	637	8	3	7	1	4	5	8	4	6	5
		-	-	-	-	-	-	-	-	-	-	-	-	-	-	-	-	-	-	-
		3.07	2.86	1.92	3.38	3.07	1.29	2.55	3.28	3.28	0.25	1.71	2.44	3.07	1.50	2.23	3.17	3.17	3.17	2.34
	6	266	381	396	594	266	74	052	151	151	313	511	61	266	625	724	709	709	709	167
		-	-	-	-	-	-	-	-	-	0.81	0.17	0.07	0.05	0.04	-	-	-	-	-
		0.52	0.53	0.51	0.54	0.55	0.46	0.48	0.71	0.79	596	827	556	416	132	0.02	0.06	0.11	0.16	0.16
AOA = 8	30	789	217	933	073	357	369	081	192	752	9	8	3	4	4	715	567	275	839	411
		-	-	-	-	-	-	-	-	-	-	0.68	0.51	0.38	0.32		0.24	0.21	0.17	0.14
		0.21	0.44	0.67	0.87	1.02	1.59	1.77	2.10	2.33	0.32	056	037	993	796	0.27	243	101	348	555
	68	49	182	049	733	396	999	716	096	399	138	5	5	2	6	909	4	4	5	6
		-	-	-	-	-	-	-	-	-	-	0.68	0.51	0.39	0.32	0.27	0.24	0.20		
	10	0.21	0.45	0.69	0.92	1.13	1.60	1.87	2.17	2.40	0.34	980	601	463	873	671	049	851	0.17	0.14
	2	074	543	896	709	517	837	233	251	833	445	1	3	1	8	7	5	1	306	493
		-	-	-	-	-	-	-	-	-	0.20	0.30	-	-	-	-	-	-	-	-
		2.28	2.67	1.78	3.07	2.87	1.18	1.18	2.97	3.07	436	381	0.98	1.88	0.98	1.18	0.98	1.08	2.97	2.18
	6	2	981	472	763	872	8	8	818	763	4	9	909	418	909	8	909	854	818	254
		-	-	-	-	-	-	-	-	-	0.59			0.10	0.10	0.01	-	-	-	-
		0.64	0.63	0.63	0.69	0.68	0.61	0.58	0.69	0.96	921	0.41	0.20	936	936	139	0.05	0.06	0.16	0.21
AOA = 12	30	768	877	432	221	776	205	979	221	385	3	218	288	3	3	3	986	876	228	572
		-	-	-	-	-	-	-	-	-	0.28	0.57		0.30	0.23	0.16	0.10	0.04	-	-
		0.72	0.72	0.70	0.69	0.67	0.65	0.69	0.75	0.95	480	666	0.42	464	271	408	620	915	0.03	0.11
	68	309	97	903	415	596	033	002	534	046	2	9	04	6	2	7	9	9	27	29
		-	-	-	-	-	-	-	-	-	-	0.86	0.68	0.51	0.42	0.34	0.29	0.24		0.11
	10	0.21	0.24	0.48	0.82	1.18	1.53	2.14	2.73	3.30	1.83	551	530	865	331	619	154	038	0.18	985
	2	809	948	473	888	931	578	309	45	111	885	8	4	4	6	2	6	9	148	9
		-	-	-	-	-	-	-	-	-	-	-	-	-	-	-	-	-	-	-
		2.77	2.87	1.98	3.37	3.07	2.67	2.67	3.07	4.37	1.78	1.58	0.98	2.97	1.38	2.38	2.97	2.58	2.48	2.18
AOA = 16	6	927	872	363	6	763	981	981	763	054	472	582	909	818	691	145	818	036	091	254
		-	-	-	-	-	-	-	-	-	0.11	0.60	0.40	0.21	0.19	0.05	-	-	-	-
	30	0.75	0.79	0.78	0.83	0.82	0.70	0.75	0.76	0.95	116	155	890	624	435	424	0.01	0.05	0.15	0.22

	14	956	205	897	583	761	578	453	281	5	7	3	9	6	4	143	084	154	598
68	-0.70744	-0.70744	-0.69855	-0.70477	-0.70299	-0.70033	-0.72431	-0.74119	-0.7865	0.168491	0.618892	0.441219	0.303523	0.217351	0.126738	0.062776	-0.0154	-0.10601	-0.20018
102	-0.71178	-0.70909	-0.70256	-0.69757	-0.69257	-0.69142	-0.73021	-0.78705	-0.82892	0.156978	0.625537	0.448867	0.31214	0.218428	0.130862	0.064035	-0.01316	-0.10265	-0.20174

For V = 6 MPH

Angle of Attack (deg) / C_p

	% of Chord																		
	Upper Surface										Lower Surface								
Airfoil Station	**P1**	**P2**	**P3**	**P4**	**P5**	**P6**	**P7**	**P8**	**P9**	**P10**	**P11**	**P12**	**P13**	**P14**	**P15**	**P16**	**P17**	**P18**	**P19**
% of Chord	0.8	0.7	0.6	0.5	0.4	0.3	0.2	0.1	0.0075	0	0.0075	0.1	0.2	0.3	0.4	0.5	0.6	0.7	0.8
Distance from LE (in)	2.8	2.45	2.1	1.75	1.4	1.05	0.7	0.35	0.2625	0	0.2625	0.35	0.7	1.05	1.4	1.75	2.1	2.45	2.8
-4	-0.42401	-0.51894	0.430397	-0.61387	-0.80374	0.715199	0.715199	0.050662	1	1.379735	-0.32907	-0.61387	-0.89868	-0.70881	-0.89868	-0.89868	-0.80374	-0.89868	-0.13921
0	-0.97862	-1.41831	-1.08854	-1.52824	-2.51755	-1.41831	-1.19847	-1.63816	-1.96793	0.120613	-1.85801	-1.63816	-2.95724	-1.19847	-1.41831	-1.96793	-1.30839	-1.30839	-0.31908
4	-	-	-	-	-	-	-	-	-	0.2	-	-	-	-	-	-	-	-	-

		2.6	2.5	1.6	2.7	2.7	1.0	1.8	2.7	2.7	40	1.4	1.3	2.7	0.8	2.0	2.4	2.7	2.7	2.0
		07	12	58	97	02	88	48	97	02	53	68	73	02	98	37	17	97	02	37
		48	55	15	35	42	54	01	35	42		28	34	42	68	88	62	35	42	88
		-	-	-	-	-	-	-	-	-	-	-	-	-	-	-	-	-	-	-
		3.0	2.8	1.9	3.3	3.0	1.2	2.5	3.2	3.2	0.2	1.7	2.4	3.0	1.5	2.2	3.1	3.1	3.1	2.3
		72	63	23	85	72	97	50	81	81	53	15	46	72	06	37	77	77	77	41
	8	66	81	96	94	66	4	52	51	51	13	11	1	66	25	24	09	09	09	67
			-	-	-	-			-	-	0.2	0.3	-	-	-		-	-	-	-
		-	2.6	1.7	3.0	2.8	-	-	2.9	3.0	04	03	0.9	1.8	0.9	-	0.9	1.0	2.9	2.1
		2.2	79	84	77	78	1.1	1.1	78	77	36	81	89	84	89	1.1	89	88	78	82
	12	82	81	72	63	72	88	88	18	63	4	9	09	18	09	88	09	54	18	54
		-	-	-		-	-	-	-	-	-	-	-	-	-	-	-	-	-	-
		2.7	2.8	1.9	-	3.0	2.6	2.6	3.0	4.3	1.7	1.5	0.9	2.9	1.3	2.3	2.9	2.5	2.4	2.1
		79	78	83	3.3	77	79	79	77	70	84	85	89	78	86	81	78	80	80	82
	16	27	72	63	76	63	81	81	63	54	72	82	09	18	91	45	18	36	91	54

Angle of Attack (deg)		2-1	3-2	4-3	5-4	6-5	7-6	8-7	9-8	10-9	C_l upper	10-11	11-12	12-13	13-14	14-15	15-16	16-17	17-18	18-19	C_l lower	C_l total	
		0.0	0.0	0.0	0.0	0.0	-	-	-	-	-		-	-	-	-	-	-	-	-	-	-	-
		47	04	09	70	04	0.0	0.0	0.0	0.0	0.0	0.0	0.0	0.0	0.0	0.0	0.0	0.0	0.0	0.0	0.5	0.5	0.4
		14	42	17	88	42	71	38	13	89	76	39	11	75	80	80	89	85	85	51	20	96	44
	-4	7	7	4	1	7	52	29	13	24	13	4	79	63	37	37	87	12	12	89	77	9	64
		0.1	0.1	0.1	0.2	0.1	0.1	0.1	0.0	0.0	1.1	-	-	-	-	-	-	-	-	-	-	-	-
		19	25	30	02	96	30	41	45	69	62	0.0	0.0	0.2	0.2	0.1	0.1	0.1	0.1	0.0	1.2	0.0	2.3
		84	34	83	28	79	83	83	07	27	13	65	43	29	07	30	69	63	30	81	22	60	84
	0	7	3	9	9	3	9	1	6	4	2	15	7	77	79	84	31	82	84	37	59	46	72
		0.2	0.2	0.2	0.2	0.1	0.1	0.2	0.0	0.0	1.6	-	-	-	-	-	-	-	-	-	-	0.0	-
		56	08	22	74	89	46	32	68	92	92	0.0	0.0	0.2	0.1	0.1	0.2	0.2	0.2	0.2	1.6	84	3.2
		00	53	77	98	54	82	26	74	32	01	46	35	03	80	46	22	60	74	37	07	25	99
	4	2	5	5	8	8	8	8	7	1	2	04	52	79	05	83	77	75	99	01	76	4	77
		0.2	0.2	0.2	0.3	0.2	0.1	0.2	0.0	0.1	2.0	-	-	-	-	-	-	-	-	-	-	0.0	-
		96	39	65	22	18	92	91	82	32	41	0.0	0.0	0.2	0.2	0.1	0.2	0.3	0.3	0.2	1.9	41	4.0
	8	82	38	49	93	50	39	60	03	54	72	73	52	75	28	87	70	17	17	75	99	77	41

	3	8	5		3	6	2	8	9	4	81	02	94	95	17	72	71	71	94	95	1	68
12	0.248091	0.223227	0.243118	0.297818	0.203336	0.1188	0.208309	0.075698	0.107748	1.726143	0.019057	-0.00857	-0.14366	-0.14366	-0.10885	-0.10885	-0.10388	-0.20334	-0.25804	-1.05598	0.66345	-2.78594
16	0.2829	0.243118	0.267981	0.322681	0.287872	0.267981	0.287872	0.093102	0.230822	2.284331	-0.12264	-0.03219	-0.19836	-0.21825	-0.18842	-0.26798	-0.27793	-0.25306	-0.23317	-1.79576	0.48857	-4.08009

For V = 30 MPH

	% of Chord																		
	Upper Surface										Lower Surface								
Airfoil Station	**P1**	**P2**	**P3**	**P4**	**P5**	**P6**	**P7**	**P8**	**P9**	**P10**	**P11**	**P12**	**P13**	**P14**	**P15**	**P16**	**P17**	**P18**	**P19**
% of Chord	0.8	0.7	0.6	0.5	0.4	0.3	0.2	0.1	0.075	0	0.075	0.1	0.2	0.3	0.4	0.5	0.6	0.7	0.8
Distance from LE (in)	2.8	2.45	2.1	1.75	1.4	1.05	0.7	0.35	0.2625	0	0.2625	0.35	0.7	1.05	1.4	1.75	2.1	2.45	2.8
Angle of Attack (deg) -4	-0.28283	-0.33235	-0.29634	-0.44037	-0.44938	-0.44938	-0.44488	-0.17481	-0.27081	0.603897	-0.76896	-0.66093	-0.71495	-0.11629	-0.1568	-0.1703	-0.10279	-0.08028	-0.04427
0	-0.42829	-0.49567	-0.44177	-0.51812	-0.50465	-0.61245	-0.76066	-0.60795	-0.23516	0.887713	-0.46423	-0.34745	-0.25762	-0.16779	-0.1633	-0.1633	-0.1633	-0.14982	-0.10042

C_p

		-	-	-	-	-	-	-	-	-	0.7	0.2	0.1	0.0	0.1	0.0	0.0	0.0	0.0	0.0		
		0.1	0.4	0.9	1.0	1.0	1.0	1.2	1.3	1.2	91	11	47	87	00	62	62	62	45	23		
		84	32	09	24	41	37	76	86	41	14	46	53	86	64	28	28	28	23	92		
	4	93	14	53	61	66	4	09	91	99	6	8	3	1	8	7	7	7	7	6		
		-	-	-	-	-	-	-	-	-	0.8	0.1	0.0	0.0	0.0	-	-	-	-	-		
		0.5	0.5	0.5	0.5	0.5	0.4	0.4	0.7	0.7	15	78	75	54	41	0.0	0.0	0.1	0.1	0.1		
		27	32	19	40	53	63	80	11	97	96	27	56	16	32	27	65	12	68	64		
	8	89	17	33	73	57	69	81	92	52	9	8	3	4	4	15	67	75	39	11		
		-	-	-	-	-	-	-	-	-	0.5			0.1	0.1	0.0	-	-	-	-		
		0.6	0.6	0.6	0.6	0.6	0.6	0.5	0.6	0.9	99	0.4	0.2	09	09	11	0.0	0.0	0.1	0.2		
		47	38	34	92	87	12	89	92	63	21	12	02	36	36	39	59	68	62	15		
	12	68	77	32	21	76	05	79	21	85	3	18	88	3	3	3	86	76	28	72		
		-	-	-	-	-	-	-	-	-	0.1	0.6	0.4	0.2	0.1	0.0	-	-	-	-		
		0.7	0.7	0.7	0.8	0.8	0.7	0.7	0.7	0.9	11	01	08	16	94	54	0.0	0.0	0.1	0.2		
		51	99	82	38	25	07	55	64	52	16	55	90	24	35	24	11	50	51	25		
	16	4	56	05	97	83	61	78	53	81	5	7	3	9	6	4	43	84	54	98		

Angle of Attack (deg)	2-1	3-2	4-3	5-4	6-5	7-6	8-7	9-8	10-9	C_l upper	10-11	11-12	12-13	13-14	14-15	15-16	16-17	17-18	18-19	C_l lower	C_l total	
	0.0	0.0	0.0	0.0	0.0	0.0	0.0	-	-	0.2	-	-	-	-	-	-	-	-	-	-	0.0	-
	30	31	36	44	44	44	30	0.0	0.0	30	0.0	0.0	0.0	0.0	0.0	0.0	0.0	0.0	0.0	0.1	36	0.4
	75	43	83	48	93	71	98	01	32	14	06	17	68	41	13	16	13	09	06	93	68	23
-4	9	4	6	8	8	3	4	2	8	9	19	87	79	56	65	36	65	15	23	46	5	61
	0.0	0.0	0.0	0.0	0.0	0.0	0.0	0.0	-	0.3	0.0	-	-	-	-	-	-	-	-	-	0.2	-
	46	46	47	51	55	68	68	10	0.0	71	15	0.0	0.0	0.0	0.0	0.0	0.0	0.0	0.0	0.1	48	0.4
	19	87	99	13	85	65	43	53	24	21	88	10	30	21	16	16	16	15	12	23	04	94
0	8	2	5	9	5	5	1	9	47	2	1	15	25	27	55	33	33	66	51	17	3	38
	0.0	0.0	0.0	0.1	0.1	0.1		0.0	0.0	0.7	0.0	0.0		0.0	0.0	0.0	0.0	0.0	0.0	0.0		-
	30	67	96	03	03	15	0.1	32	16	00	37	04	0.0	09	08	06	06	05	03	92	0.7	0.6
	85	08	70	31	95	67	33	86	90	50	59	48	11	42	14	22	22	37	45	71	93	07
4	4	3	7	3	3	4	15	1	7	1	8	8	77	5	7	9	9	6	8	9	22	78
	0.0	0.0	0.0	0.0	0.0	0.0	0.0	0.0	-	0.3	0.0	0.0	0.0	0.0	0.0	-	-	-	-	0.0	0.3	-
8	53	52	53	54	50	47	59	18	0.0	89	37	03	06	04	00	0.0	0.0	0.0	0.0	08	97	0.3

	P1	P2	P3	P4	P5	P6	P7	P8	P9	P10	P11	P12	P13	P14	P15	P16	P17	P18	P19			
	003	575	003	715	863	225	637	868	0069	197	284	173	486	774	709	0464	0892	1406	1662	183	38	8101
12	0.064322	0.063655	0.066326	0.068998	0.06499	0.060092	0.06641	0.020701	0.013674	0.486859	0.037927	0.007688	0.015612	0.010936	0.006038	-0.00242	-0.00643	-0.01155	-0.0189	0.038895	0.525754	-0.44796
16	0.077548	0.079081	0.081051	0.08324	0.076672	0.07317	0.076016	0.021467	0.031562	0.599806	0.026727	0.012631	0.031258	0.02053	0.01243	0.002141	-0.00311	-0.01012	-0.01888	0.073607	0.673413	-0.5262

For V = 68 MPH

		% of Chord																		
		Upper Surface										Lower Surface								
	Airfoil Station	**P1**	**P2**	**P3**	**P4**	**P5**	**P6**	**P7**	**P8**	**P9**	**P10**	**P11**	**P12**	**P13**	**P14**	**P15**	**P16**	**P17**	**P18**	**P19**
	% of Chord	0.8	0.7	0.6	0.5	0.4	0.3	0.2	0.1	0.0075	0	0.0075	0.1	0.2	0.3	0.4	0.5	0.6	0.7	0.8
	Distance from LE (in)	2.8	2.45	2.1	1.75	1.4	1.05	0.7	0.35	0.2625	0	0.2625	0.35	0.7	1.05	1.4	1.75	2.1	2.45	2.8
Angle of Attack (deg)	-4	-0.28432	-0.36839	-0.41375	-0.49893	-0.54981	-0.55203	-0.56973	-0.25224	0.234496	0.638266	-0.80314	-0.64716	-0.13277	-0.16485	-0.12503	-0.09073	-0.05644	-0.01772	0.015464
	0	-0.16363	-0.44343	-0.61311	-0.68282	-0.77373	-0.86060	-0.98383	-0.80807	-0.43333	0.95777	-0.23232	-0.16262	-0.05757	-0.01515	0.00147	0.01555	0.02698	0.03930	0.06129

C_p

	04	68	72	1	59	69	85	9	12	2	54	16	47	24	6	2	9	5	9	
	-	-	-	-	-	-	-	-	-	0.7	0.3	0.2	0.1	0.1	0.1	0.1	0.1	0.1	0.1	
	0.2	0.4	0.5	0.8	1.0	1.1	1.3	1.4	1.3	47	17	15	87	78	49	40	28	12	13	
	21	13	62	78	33	49	86	37	16	84	40	52	50	16	30	81	07	79	64	
4	71	59	16	84	36	67	54	48	08	7	3	3	6	7	1	1	6	4	3	
	-	-	-	-	-	-	-	-	-	-	0.6	0.5	0.3	0.3		0.2	0.2	0.1	0.1	
	0.2	0.4	0.6	0.8	1.0	1.5	1.7	2.1	2.3	0.3	80	10	89	27	0.2	42	11	73	45	
	14	41	70	77	23	99	77	00	33	21	56	37	93	96	79	43	01	48	55	
8	9	82	49	33	96	99	16	96	99	38	5	5	2	6	09	4	4	5	6	
	-	-	-	-	-	-	-	-	-	0.2	0.5		0.3	0.2	0.1	0.1	0.0	-	-	
	0.7	0.7	0.7	0.6	0.6	0.6	0.6	0.7	0.9	84	76	0.4	04	32	64	06	49	0.0	0.1	
	23	29	09	94	75	50	90	55	50	80	66	20	64	71	08	20	15	32	12	
12	09	7	03	15	96	33	02	34	46	2	9	4	6	2	7	9	9	7	9	
	-	-	-	-	-	-	-	-	-	0.1	0.6	0.4	0.3	0.2	0.1	0.0	-	-	-	
	0.7	0.7	0.6	0.7	0.7	0.7	0.7	0.7	0.7	68	18	41	03	17	26	62	0.0	0.1	0.2	
	07	07	98	04	02	00	24	41	86	49	89	21	52	35	73	77	15	06	00	
16	44	44	55	77	99	33	31	19	5	1	2	9	3	1	8	6	4	01	18	

Angle of Attack (deg)	2-1	3-2	4-3	5-4	6-5	7-6	8-7	9-8	10-9	C_l upper	10-11	11-12	12-13	13-14	14-15	15-16	16-17	17-18	18-19	C_l lower	C_l total	
	0.0	0.0	0.0	0.0	0.0	0.0	0.0	0.0	-	0.2	-	-		-	-	-	-	-	-	-	0.1	-
	32	39	45	52	55	56	41	00	0.0	89	0.0	0.0	-	0.0	0.0	0.0	0.0	0.0	0.0	0.1	74	0.4
	63	10	63	43	09	08	09	22	32	58	06	18	0.0	14	14	10	07	03	00	14	93	04
-4	6	7	4	7	2	8	8	2	73	5	18	13	39	88	49	79	36	71	11	65	5	24
	0.0		0.0	0.0	0.0	0.0	0.0	0.0	-	0.4	0.0	-	-	-	-	0.0	0.0	0.0		0.0	0.4	-
	30	0.0	64	72	81	92	89	15	0.0	79	27	0.0	0.0	0.0	0.0	00	02	03	0.0	18	98	0.4
	33	52	69	78	71	22	58	51	19	94	19	04	10	03	00	85	12	31	05	28	22	61
0	6	77	1	4	4	7	8	3	67	8	6	93	98	64	69	1	7	5	03	1	8	67
	0.0	0.0			0.1	0.1	0.1	0.0	0.0	0.6	0.0	0.0	0.0	0.0	0.0	0.0	0.0	0.0	0.0	0.1	0.8	-
	31	48	0.0	0.0	09	26	41	34	21	81	39	06	20	18	16	14	13	12	11	52	33	0.5
	76	78	72	95	15	81	20	41	30	10	94	66	15	28	37	50	44	04	32	73	83	28
4	5	7	05	61	1	1	1	9	9	4	7	2	1	4	3	6	4	3	2	2	6	37
8	0.0	0.0	0.0	0.0	0.1	0.1	0.1	0.0	0.0	0.9	0.0	0.0	0.0	0.0	0.0	0.0	0.0	0.0	0.0	0.2	1.1	-

	P1	P2	P3	P4	P5	P6	P7	P8	P9	P10	P11	P12	P13	P14	P15	P16	P17	P18	P19			
	32836	55615	77391	95065	31197	68857	93906	55437	99576	0988	1347	14887	45015	35895	30353	26076	22672	19225	15952	23545	33425	0.68634
12	0.07264	0.071937	0.070159	0.068506	0.066315	0.067017	0.072268	0.021323	0.024962	0.535126	0.032305	0.012463	0.036252	0.026868	0.01984	0.013515	0.007768	0.000823	-0.00728	0.142555	0.677681	-0.39257
16	0.070744	0.070299	0.070166	0.070388	0.070166	0.071232	0.073275	0.019096	0.023175	0.538542	0.029527	0.013251	0.037237	0.026044	0.017204	0.009476	0.002369	-0.00607	-0.01531	0.113728	0.65227	-0.42481

For V = 102 MPH

	% of Chord																		
	Upper Surface										Lower Surface								
Airfoil Station	**P1**	**P2**	**P3**	**P4**	**P5**	**P6**	**P7**	**P8**	**P9**	**P10**	**P11**	**P12**	**P13**	**P14**	**P15**	**P16**	**P17**	**P18**	**P19**
% of Chord	0.8	0.7	0.6	0.5	0.4	0.3	0.2	0.1	0.0075	0	0.0075	0.1	0.2	0.3	0.4	0.5	0.6	0.7	0.8
Distance from LE (in)	2.8	2.45	2.1	1.75	1.4	1.05	0.7	0.35	0.2625	0	0.2625	0.35	0.7	1.05	1.4	1.75	2.1	2.45	2.8
(deg) -4	-0.13207	-0.39119	-0.44192	-0.52973	-0.58553	-0.59411	-0.60465	-0.271	0.241771	0.614447	-0.89733	-0.74045	-0.25539	-0.19685	-0.14261	-0.10203	-0.06534	-0.03413	0.006849
0	-	-	-	-	-	-	-	-	-	0.9	-	-	-	-	-	0.0	0.0	0.0	0.0

C_p

		0.2	0.3	0.6	0.7	0.8	0.9	1.0	0.8	0.4	65	0.2	0.1	0.0	0.0	0.0	14	27	38	59		
		08	69	42	18	18	00	30	44	55	28	47	78	63	19	00	63	11	03	49		
		11	61	28	35	6	91	03	74	04	2	51	07	78	31	97	2	5	7	2		
		-	-	-	-	-	-	-	-	-	0.7	0.3	0.2	0.1	0.1	0.1	0.1	0.1	0.1	0.1		
		0.2	0.4	0.6	0.8	1.0	1.2	1.4	1.5	1.3	46	10	14	87	64	44	32	20	10	05		
		40	52	50	12	84	20	62	06	76	19	79	32	72	74	18	89	80	72	32		
	4	83	89	6	41	13	73	63	17	37	8	3	7	1	4	5	8	4	6	5		
		-	-	-	-	-	-	-	-	-	-	0.6	0.5	0.3	0.3	0.2	0.2	0.2				
		0.2	0.4	0.6	0.9	1.1	1.6	1.8	2.1	2.4	0.3	89	16	94	28	76	40	08	0.1	0.1		
		10	55	98	27	35	08	72	72	08	44	80	01	63	73	71	49	51	73	44		
	8	74	43	96	09	17	37	33	51	33	45	1	3	1	8	7	5	1	06	93		
		-	-	-	-	-	-	-	-	-	-	0.8	0.6	0.5	0.4	0.3	0.2	0.2		0.1		
		0.2	0.2	0.4	0.8	1.1	1.5	2.1	2.7	3.3	1.8	65	85	18	23	46	91	40	0.1	19		
		18	49	84	28	89	35	43	34	01	38	51	30	65	31	19	54	38	81	85		
	12	09	48	73	88	31	78	09	5	11	85	8	4	4	6	2	6	9	48	9		
		-	-	-	-	-	-	-	-	-	0.1	0.6	0.4		0.2	0.1	0.0	-	-	-		
		0.7	0.7	0.7	0.6	0.6	0.6	0.7	0.7	0.8	56	25	48	0.3	18	30	64	0.0	0.1	0.2		
		11	09	02	97	92	91	30	87	28	97	53	86	12	42	86	03	13	02	01		
	16	78	09	56	57	57	42	21	05	92	8	7	7	14	8	2	5	16	65	74		

Angle of Attack (deg)	2-1	3-2	4-3	5-4	6-5	7-6	8-7	9-8	10-9	C_l upper	10-11	11-12	12-13	13-14	14-15	15-16	16-17	17-18	18-19	C_l lower	C_l total	
	0.0	0.0	0.0	0.0	0.0	0.0	0.0	0.0	-	0.3	-	-	-	-	-	-	-	-	-	-	0.1	-
	26	41	48	55	58	59	43	00	0.0	03	0.0	0.0	0.0	0.0	0.0	0.0	0.0	0.0	0.0	0.1	55	0.4
	16	65	58	76	98	93	78	36	32	12	10	20	49	22	16	12	08	04	01	47	72	50
-4	3	6	2	3	2	8	2	5	11	4	61	47	79	61	97	23	37	97	36	4	9	52
	0.0	0.0	0.0	0.0	0.0	0.0	0.0	0.0	-	0.4	0.0	-	-	-	-	0.0	0.0	0.0	0.0	0.0	0.5	-
	28	50	68	76	85	96	93	16	0.0	97	26	0.0	0.0	0.0	0.0	00	02	03	04	15	12	0.4
	88	59	03	84	97	54	73	24	19	73	91	05	12	04	01	68	08	25	87	24	97	82
0	6	4	1	7	6	7	8	7	13	3	6	32	09	15	01	3	7	8	6	1	4	49
	0.0	0.0	0.0	0.0	0.1	0.1	0.1	0.0	0.0	0.7	0.0	0.0	0.0	0.0	0.0	0.0	0.0	0.0	0.0	0.1	0.8	-
	34	55	73	94	15	34	48	36	23	15	39	06	20	17	15	13	12	11	10	48	63	0.5
4	68	17	15	82	24	16	44	03	63	35	63	56	10	62	44	85	68	57	80	29	64	67

		6	4		7	3	8		2	1	2	7	4	2	3	6	4	5	7	3	2	4	06
		0.0		0.0	0.1	0.1	0.1	0.2		0.1	0.9	0.0	0.0	0.0	0.0	0.0	0.0		0.0		0.2	1.1	-
		33	0.0	81	03	37	74	02	0.0	03	49	12	15	45	36	30	25	0.0	19	0.0	23	72	0.7
		30	57	30	11	17	03	24	57	22	38	95	07	53	16	27	86	22	07	15	28	67	26
	8	8	72	3	3	7	5	2	26	9	6	1	3	2	8	3	1	45	9	9	6	2	1
		0.0	0.0	0.0	0.1	0.1	0.1	0.2	0.0	0.1		-	0.0	0.0	0.0	0.0	0.0	0.0	0.0	0.0	0.2	1.2	-
		23	36	65	00	36	83	43	75	92	1.0	0.0	19	60	47	38	31	26	21	15	23	82	0.8
		37	71	68	90	25	94	87	44	74	58	36	38	19	09	47	88	59	09	06	30	25	35
	12	9	1	1	9	5	3	9	5	8	95	5	5	8	9	5	7	7	3	7	1	1	65
		0.0	0.0	0.0	0.0		0.0	0.0		0.0		0.0			0.0	0.0	0.0	0.0	-	-	0.1	0.6	-
		71	70	70	69	0.0	71	75	0.0	25	0.5	29	0.0	0.0	26	17	09	02	0.0	0.0	16	58	0.4
		04	58	00	50	69	08	86	20	19	42	34	13	38	52	46	74	54	05	15	09	77	26
	16	3	2	6	7	2	2	3	2	8	68	4	43	05	8	5	5	4	79	22	6	6	58

V = 6 MPH

Angle of Attack (deg)	C_l	q	c (ft)	L' (lbf)
-4	-0.597	0.104	0.292	-0.01813
0	-0.060	0.104	0.292	-0.00184
4	0.084	0.104	0.292	0.00256
8	0.042	0.104	0.292	0.001269
12	0.666	0.104	0.292	0.020245
16	0.489	0.104	0.292	0.014844

Dynamic Pressure

Angle of Attack (deg)	6 MPH	30 MPH	68 MPH	102 MPH	
-4	0.11	2.32	9.44	26.76	
0	0.10	2.33	11.87	26.77	
4	0.11	2.45	12.30	27.27	
8	0.10	2.44	11.97	27.04	
12	0.11	2.35	12.63	26.95	
16	0.11	2.39	11.76	27.19	
	0.10	2.38	11.66	26.99	Avg

V = 30 MPH

Angle of Attack (deg)				
-4	0.037	2.378	0.292	0.025438
0	0.248	2.378	0.292	0.172002
4	0.793	2.378	0.292	0.550049
8	0.397	2.378	0.292	0.275558
12	0.526	2.378	0.292	0.364578
16	0.673	2.378	0.292	0.46697

1 inch = 0.083333 ft

V = 68 MPH

Angle of Attack (deg)					
	-4	0.175	11.660	0.292	0.594924
	0	0.498	11.660	0.292	1.694392
	4	0.834	11.660	0.292	2.835738
	8	1.133	11.660	0.292	3.854591
	12	0.678	11.660	0.292	2.30468
	16	0.652	11.660	0.292	2.218262

V = 102 MPH

Angle of Attack (deg)					
	-4	0.156	26.995	0.292	1.226124
	0	0.513	26.995	0.292	4.03888
	4	0.864	26.995	0.292	6.799867
	8	1.173	26.995	0.292	9.232991
	12	1.282	26.995	0.292	10.09576
	16	0.659	26.995	0.292	5.186853

Appendix C

3D Wing Data

q [psf]	V_ref [mph]	Alpha [deg]	NF/SF [lbf]	AF/AF2 [lbf]	PM/YM [in-lbf]	Mc/4 [in-lbf]
0.1	6	-4	-0.03	-0.01	-0.01	0.052
0.1	5	-4	-0.02	0	-0.02	0.021

0.1	5	-4	-0.04	-0.02	-0.01	0.073	
0.1	7	-4	-0.05	0.01	0.01	0.114	
0.1	5	-4	0	0	-0.01	-0.010	
0.1	6	-4	-0.05	-0.02	-0.01	0.094	
0.1	6	-4	-0.03	0	-0.01	0.052	
0.1	6	-4	-0.02	0.01	-0.02	0.021	
0.1	6	-4	-0.02	0	-0.02	0.021	
0.1	5	-4	-0.03	0	-0.05	0.012	
0.1	6	-4	0	0	-0.04	-0.010	
0.1	6	-4	-0.05	0	-0.01	0.094	
0.1	5	-4	-0.04	0	-0.01	0.073	
0.1	6	-4	-0.03	0	-0.03	0.032	
0.1	6	-4	-0.02	0	0	0.041	
0.1	6	-4	-0.03	0	0.02	0.082	
0.1	5	-4	-0.03	-0.01	-0.03	0.032	
0.1	6	-4	-0.03	-0.01	-0.02	0.042	
0.1	5	-4	-0.04	-0.01	-0.03	0.053	
0.1	6	-4	-0.03	0	0	0.062	
0.1	5.7	-4	-0.0295	-0.003	-0.015	0.047639	Avg.
2.3	30	-4	0.13	0.02	0.07	-0.199	
2.4	31	-4	0.08	0.02	0.06	-0.106	
2.3	30	-4	0	0.01	-0.08	-0.080	
2.3	30	-4	0.02	0.02	-0.01	-0.051	
2.5	31	-4	0.12	0.03	0.08	-0.169	
2.3	30	-4	0.08	0.04	0.06	-0.106	
2.4	31	-4	0.04	0.05	-0.01	-0.093	
2.4	31	-4	0.04	0.04	0.02	-0.063	
2.5	31	-4	0.11	0.03	0.05	-0.178	
2.4	31	-4	0.07	0.03	0.02	-0.125	
2.5	31	-4	0.14	0.03	0.06	-0.230	

2.4	31	-4	0.11	0.02	0.04	-0.188	
2.5	31	-4	0.12	0.02	0.06	-0.189	
2.3	30	-4	0.1	0.02	0.05	-0.157	
2.5	31	-4	0.05	0.03	-0.03	-0.134	
2.5	31	-4	0.05	0.03	-0.02	-0.124	
2.5	31	-4	0.08	0.03	0.07	-0.096	
2.5	31	-4	0.14	0.03	0.08	-0.210	
2.4	30	-4	0.11	0.02	0.03	-0.198	
2.4	31	-4	0.04	0.02	-0.01	-0.093	
2.415	30.7	-4	0.0815	0.027	0.0295	-0.13941	Avg.
12.1	69	-4	0.39	0.14	0.05	-0.758	
12.2	69	-4	0.46	0.17	0.17	-0.783	
12.1	69	-4	0.35	0.13	0.02	-0.080	
12.1	69	-4	0.39	0.14	0.04	-0.768	
11.9	68	-4	0.22	0.16	-0.12	-0.576	
12.1	69	-4	0.51	0.15	0.16	-0.897	
11.9	68	-4	0.41	0.1	0.01	-0.840	
12.1	69	-4	0.33	0.14	-0.05	-0.734	
12	69	-4	0.47	0.12	0.12	-0.854	
12	69	-4	0.4	0.13	0.03	-0.799	
12.1	69	-4	0.43	0.16	0.11	-0.781	
12.3	69	-4	0.42	0.17	0.11	-0.760	
11.9	68	-4	0.39	0.09	0.05	-0.758	
12.2	69	-4	0.49	0.08	0.13	-0.886	
12	69	-4	0.51	0.13	0.15	-0.907	
11.9	68	-4	0.5	0.12	0.17	-0.866	
12.1	69	-4	0.43	0.11	0.1	-0.791	
11.9	68	-4	0.35	0.15	0.03	-0.695	
12.2	69	-4	0.44	0.13	0.1	-0.812	
11.9	68	-4	0.36	0.11	0.06	-0.686	

12.05	68.7	-4	0.4125	0.1315	0.072	-0.75164	Avg.
26.9	103	-4	1	0.14	0.13	-1.943	
26.8	102	-4	0.91	0.46	0.22	-1.666	
27.5	104	-4	1.04	0.08	0.28	-0.080	
26.9	103	-4	0.85	0.54	0.23	-1.532	
26.8	102	-4	1.06	0.13	0.29	-1.907	
26.7	102	-4	1.02	0.14	0.19	-1.924	
26.3	101	-4	1.05	0.21	0.32	-1.856	
27.3	103	-4	1.05	0.25	0.32	-1.856	
26.2	101	-4	0.97	0.27	0.26	-1.750	
26.3	101	-4	0.95	0.39	0.22	-1.749	
27.2	103	-4	0.95	0.51	0.3	-1.669	
26.1	101	-4	1.02	0.25	0.26	-1.854	
26.7	102	-4	0.99	0.25	0.31	-1.742	
26.5	102	-4	1.04	0.31	0.27	-1.885	
26.9	103	-4	0.93	0.28	0.34	-1.587	
26.3	101	-4	1.02	0.28	0.32	-1.794	
26.3	101	-4	1.03	0.21	0.33	-1.805	
26.9	103	-4	0.99	0.29	0.33	-1.722	
26.9	103	-4	0.97	0.42	0.21	-1.800	
27.3	103	-4	0.95	0.37	0.2	-1.769	
26.74	102.2	-4	0.9895	0.289	0.2665	-1.69447	Avg.

q [psf]	V_ref [mph]	Alpha [deg]	NF/SF [lbf]	AF/AF2 [lbf]	PM/YM [in-lbf]	Mc/4 [in-lbf]
0.1	6	0	0	0.03	-0.01	-0.010
0.1	5	0	0.01	0	0.01	-0.011
0.1	6	0	-0.01	-0.01	-0.02	-0.080
0.1	7	0	-0.01	0.01	0.02	0.041
0.1	6	0	-0.02	0.01	-0.01	0.031
0.1	6	0	0	0.01	0.01	0.010

0.1	6	0	-0.03	-0.01	0	0.062	
0.1	6	0	-0.03	0.01	-0.01	0.052	
0.1	7	0	0.02	0.01	0.01	-0.031	
0.1	7	0	0.01	0.01	0.02	-0.001	
0.1	6	0	0	-0.01	0.03	0.030	
0.1	7	0	-0.02	0.02	0	0.041	
0.1	6	0	0	0.01	0	0.000	
0.1	7	0	-0.02	0	0.01	0.051	
0.1	6	0	-0.01	0.01	0.02	0.041	
0.1	7	0	-0.01	0.01	-0.01	0.011	
0.1	6	0	-0.01	0.02	0.03	0.051	
0.1	7	0	0.01	0	0	-0.021	
0.1	6	0	-0.01	0.01	-0.01	0.011	
0.1	6	0	0	0	0.03	0.030	
0.1	6.3	0	-0.0065	0.007	0.006	0.015435	Avg.
2.4	31	0	0.23	0.04	0.3	-0.177	
2.3	30	0	0.2	0.02	0.22	-0.195	
2.3	30	0	0.19	0.02	0.18	-0.080	
2.3	30	0	0.24	0.01	0.28	-0.217	
2.3	30	0	0.23	0.04	0.26	-0.217	
2.3	30	0	0.23	0.03	0.26	-0.217	
2.4	30	0	0.2	0.04	0.21	-0.205	
2.3	30	0	0.2	0.05	0.2	-0.215	
2.3	30	0	0.22	0.04	0.24	-0.216	
2.4	30	0	0.25	0.03	0.28	-0.238	
2.3	30	0	0.27	0.01	0.29	-0.270	
2.4	31	0	0.21	0.03	0.2	-0.235	
2.3	30	0	0.19	0.03	0.2	-0.194	
2.4	31	0	0.23	0.04	0.24	-0.237	
2.4	31	0	0.28	0.04	0.28	-0.300	

2.3	30	0	0.27	0.02	0.25	-0.310	
2.3	30	0	0.22	0.01	0.22	-0.236	
2.4	30	0	0.24	0.03	0.26	-0.237	
2.5	31	0	0.27	0.05	0.26	-0.300	
2.3	30	0	0.22	0.01	0.19	-0.266	
2.345	30.25	0	0.2295	0.0295	0.241	-0.22795	Avg.
11.8	68	0	1.14	0.16	1.28	-1.083	
12	69	0	1.11	0.13	1.31	-0.990	
12.1	69	0	1.22	0.11	1.24	-0.080	
12.1	69	0	1.16	0.14	1.32	-1.084	
11.8	68	0	1.12	0.12	1.23	-1.091	
12.2	69	0	1.15	0.12	1.2	-1.183	
12	69	0	1.14	0.13	1.27	-1.093	
11.9	68	0	1.16	0.12	1.18	-1.224	
12.1	69	0	1.15	0.14	1.28	-1.103	
12.1	69	0	1.15	0.13	1.24	-1.143	
12.2	69	0	1.11	0.14	1.29	-1.010	
12	69	0	1.15	0.17	1.3	-1.083	
11.9	68	0	1.18	0.13	1.28	-1.166	
11.7	68	0	1.15	0.11	1.32	-1.063	
11.9	68	0	1.16	0.12	1.3	-1.104	
11.9	68	0	1.16	0.17	1.27	-1.134	
12.1	69	0	1.13	0.15	1.37	-0.972	
11.9	68	0	1.14	0.16	1.32	-1.043	
11.9	68	0	1.15	0.1	1.27	-1.113	
12.2	69	0	1.15	0.12	1.32	-1.063	
11.99	68.55	0	1.149	0.1335	1.2795	-1.04138	Avg.
27.2	103	-0.1	2.72	0.35	3.21	-2.427	
27.1	103	-0.1	2.98	0.23	3.36	-2.816	

26.9	103	-0.1	2.58	0.39	2.98	-0.080	
26.6	102	-0.1	2.47	0.42	3.03	-2.089	
27.1	103	-0.1	2.52	0.43	3.05	-2.173	
26.9	103	-0.1	2.69	0.26	3.18	-2.395	
27.1	103	-0.1	2.91	0.35	3.45	-2.581	
26.5	102	-0.1	2.68	0.29	3.2	-2.354	
27.6	104	-0.1	2.6	0.43	3.09	-2.299	
27.4	103	-0.1	2.62	0.48	3.21	-2.220	
27.3	103	-0.1	3.02	0.3	3.31	-2.949	
27.5	104	-0.1	2.79	0.32	3.36	-2.422	
26.5	102	-0.1	2.53	0.42	2.99	-2.253	
26.1	101	-0.1	2.48	0.37	3.01	-2.130	
26.9	103	-0.1	2.65	0.3	2.98	-2.512	
27.1	103	-0.1	2.7	0.32	3.24	-2.356	
26.9	103	-0.1	2.95	0.21	3.47	-2.644	
27.6	104	-0.1	3	0.21	3.41	-2.808	
27.1	103	-0.1	2.63	0.39	3.07	-2.381	
26.5	102	-0.1	2.54	0.42	3.12	-2.144	
26.995	102.85	-0.1	2.703	0.3445	3.186	-2.30162	Avg.
q	V_ref	Alpha	NF/SF	AF/AF2	PM/YM	Mc/4	
[psf]	[mph]	[deg]	[lbf]	[lbf]	[in-lbf]	[in-lbf]	
0.2	8	3.9	0	-0.01	0.02	0.020	
0.1	6	4	-0.01	-0.01	0.02	0.041	
0.1	7	3.9	-0.01	0	0.01	-0.080	
0.1	7	3.9	0	0.01	0.03	0.030	
0.1	6	4	-0.01	0.02	0.02	0.041	
0.1	5	4	-0.01	-0.01	-0.03	-0.009	
0.1	6	3.9	-0.01	-0.01	0.01	0.031	
0.1	5	3.9	-0.03	0	0	0.062	
0.1	7	4	-0.01	0.02	-0.01	0.011	
0.1	7	3.9	0.01	-0.01	0	-0.021	

0.1	6	3.9	0	0.01	0.01	0.010	
0.1	6	4	0	-0.01	-0.01	-0.010	
0.1	6	4	-0.02	0	-0.01	0.031	
0.1	6	4	-0.02	0.01	0	0.041	
0.1	7	3.9	-0.02	0	-0.01	0.031	
0.1	7	4	0	0.01	0.02	0.020	
0.1	6	3.9	0.01	0	0.02	-0.001	
0.1	8	4	0.01	0	0.02	-0.001	
0.2	8	3.9	0.01	0	0.04	0.019	
0.1	7	4	0.01	-0.02	0.03	0.009	
0.11	6.55	3.95	-0.005	0	0.009	0.013826	Avg.
2.3	30	4	0.34	0.01	0.43	-0.275	
2.3	30	4	0.27	0	0.45	-0.110	
2.4	31	4	0.42	0.01	0.53	-0.080	
2.4	30	4	0.36	-0.01	0.41	-0.336	
2.4	30	4	0.36	0.02	0.46	-0.286	
2.4	31	3.9	0.45	0.05	0.54	-0.393	
2.3	30	4	0.39	0.02	0.48	-0.328	
2.4	31	4	0.37	0.03	0.47	-0.297	
2.3	30	4	0.32	0.03	0.46	-0.203	
2.4	30	4	0.37	0	0.48	-0.287	
2.3	30	4	0.3	0.04	0.43	-0.192	
2.4	31	4	0.39	0.04	0.45	-0.358	
2.4	31	4	0.36	0.04	0.46	-0.286	
2.3	30	4	0.35	0.03	0.46	-0.265	
2.4	31	4	0.38	-0.01	0.48	-0.308	
2.4	31	3.9	0.29	0.03	0.42	-0.181	
2.5	31	4	0.35	0.04	0.5	-0.225	
2.3	30	4	0.37	0.01	0.47	-0.297	
2.4	31	4	0.41	0	0.5	-0.350	

2.5	32	4	0.39	0.03	0.55	-0.258	
2.375	30.55	3.99	0.362	0.0205	0.4715	-0.26572	Avg.
11.7	68	4	1.95	0	2.17	-1.871	
11.8	68	4	1.78	0.05	2.62	-1.069	
11.7	68	4	1.68	0.03	2.59	-0.080	
11.8	68	4	1.79	0.08	2.49	-1.220	
11.8	68	4	1.87	0.03	2.22	-1.656	
11.7	68	4	1.94	0.24	1.89	-2.131	
11.9	68	4	1.77	0.13	2.35	-1.318	
11.5	67	4	1.78	-0.02	2.22	-1.469	
11.8	68	4	1.72	0.09	2.79	-0.775	
11.7	68	4	1.89	0.05	2.34	-1.577	
11.6	67	4	1.79	0.05	2.62	-1.090	
11.8	68	4	1.76	0.22	2.58	-1.068	
12.1	69	4	1.96	0.17	2.19	-1.872	
12.1	69	4	1.88	0.11	2.38	-1.516	
12	69	4	1.87	0.12	2.38	-1.496	
11.7	68	4	1.8	0.23	2.1	-1.631	
11.9	68	4	1.73	0.08	2.7	-0.885	
12	68	4	1.81	0.25	2.22	-1.531	
11.8	68	4	1.87	0.18	2.16	-1.716	
11.8	68	4	1.85	0.05	2.42	-1.414	
11.81	68.05	4	1.8245	0.107	2.3715	-1.36919	Avg.
27	103	4	4.41	0.05	5.83	-3.310	
26.2	101	4	4.33	0.06	5.41	-3.564	
26.7	102	4	3.96	0.19	5.69	-0.080	
26.7	102	4	4.37	0.19	4.61	-4.447	
26.6	102	4	3.94	0.1	6.24	-1.926	
26.8	102	4	4.02	0.27	6.15	-2.181	

26.7	102	4	4.23	0.56	4.98	-3.787	
26.8	102	4	4.27	0.05	5.41	-3.440	
26.7	102	4	4.38	0.27	6.28	-2.798	
26.5	102	4	3.99	0.06	6.44	-1.829	
26	101	4	4.16	0.26	4.43	-4.192	
26	101	4	4.29	0.16	6.12	-2.771	
25.8	100	4	4.1	0.07	5.96	-2.537	
26.2	101	4	3.97	0.42	5.24	-2.988	
26	101	4	4.18	-0.12	6.01	-2.653	
26.6	102	4	4.14	0.22	5.08	-3.500	
26.2	101	4	4.25	0.23	5.54	-3.268	
26.6	102	4	4.28	0.24	5.54	-3.330	
26.6	102	4.1	4.02	0.1	5.93	-2.401	
26.3	101	4	4.55	0.41	4.98	-4.450	
26.45	101.6	4.005	4.192	0.1895	5.5935	-2.97257	Avg.
q	V_ref	Alpha	NF/SF	AF/AF2	PM/YM	Mc/4	
[psf]	[mph]	[deg]	[lbf]	[lbf]	[in-lbf]	[in-lbf]	
0.1	6	8	0.05	-0.01	0.01	-0.094	
0.1	6	8	0.03	0.01	-0.02	-0.082	
0.1	7	8	0.04	0.02	-0.06	-0.080	
0.1	6	8	0.03	0.02	-0.04	-0.102	
0.2	8	8	0.04	0	-0.01	-0.093	
0.1	7	8	0.03	0.01	0	-0.062	
0.2	8	8	0.04	0.02	0.01	-0.073	
0.1	7	8	0.04	0	0.03	-0.053	
0.1	7	8	0.03	0.02	-0.02	-0.082	
0.1	7	8	0.02	0.02	0.01	-0.031	
0.1	7	8	0.02	0.01	0	-0.041	
0.1	6	8	0.03	0.01	0	-0.062	
0.1	7	8	0	0	0	0.000	
0.1	7	8	0.03	0.02	-0.01	-0.072	

0.1	6	8	0.01	-0.01	-0.03	-0.051	
0.1	6	8	0.04	0.01	0.01	-0.073	
0.1	7	8	0.01	0.01	0	-0.021	
0.2	8	8	0.04	0.02	0.01	-0.073	
0.1	7	8	0.05	0.01	0.01	-0.094	
0.2	8	8	0.04	0.03	0.02	-0.063	
0.12	6.9	8	0.031	0.011	-0.004	-0.0651	Avg.
2.4	31	8	0.47	0.02	0.57	-0.404	
2.5	32	8	0.5	-0.03	0.63	-0.406	
2.4	31	8	0.48	0.04	0.58	-0.080	
2.5	31	8	0.48	0	0.63	-0.365	
2.4	31	8	0.47	-0.02	0.62	-0.354	
2.3	30	8	0.47	0	0.62	-0.354	
2.4	31	8	0.49	-0.01	0.62	-0.396	
2.4	31	8	0.47	0.01	0.61	-0.364	
2.4	31	8	0.46	0	0.58	-0.373	
2.5	31	8	0.49	-0.02	0.65	-0.366	
2.5	31	8	0.48	0.02	0.62	-0.375	
2.4	31	8	0.49	-0.01	0.57	-0.446	
2.4	30	8	0.46	-0.02	0.57	-0.383	
2.2	30	8	0.46	0	0.58	-0.373	
2.5	31	8	0.47	0	0.61	-0.364	
2.4	31	8	0.49	-0.02	0.64	-0.376	
2.4	31	8	0.5	-0.03	0.61	-0.426	
2.4	31	8	0.43	0.02	0.58	-0.311	
2.6	32	8	0.51	-0.01	0.6	-0.457	
2.4	31	8	0.49	0	0.63	-0.386	
2.42	30.95	8	0.478	-0.003	0.606	-0.36792	Avg.
12	69	8	2.34	-0.03	3.37	-1.480	

12.1	69	8	2.39	-0.19	3.04	-1.913	
12.1	69	8	2.28	0.16	3.38	-0.080	
11.8	68	8	2.43	-0.15	2.99	-2.046	
11.9	68	8	2.53	0.38	2.94	-2.303	
11.9	68	8	2.46	0.36	2.84	-2.258	
12.2	69	8	2.75	-0.22	2.65	-3.049	
11.9	68	8	2.31	0.29	3.42	-1.367	
11.8	68	8	2.3	0.26	3.37	-1.397	
11.8	68	8	2.26	-0.34	3.09	-1.594	
11.9	68	8	2.45	-0.2	3.14	-1.938	
12	68	8	2.24	0.25	3.27	-1.372	
12	68	8	2.28	0.3	3.38	-1.345	
12	69	8	2.5	-0.31	2.92	-2.261	
11.7	68	8	2.7	-0.22	2.6	-2.996	
11.7	68	8	2.3	0.4	3.19	-1.577	
12.1	69	8	2.37	0.24	3.3	-1.612	
12.1	69	8	2.28	0.23	3.59	-1.135	
11.9	68	8	2.37	0.02	3.25	-1.662	
11.9	68	8	2.48	0.33	2.92	-2.220	
11.94	68.35	8	2.401	0.078	3.1325	-1.78031	Avg.
27.3	103	8	5.53	0.01	7.23	-4.231	
26.1	101	8	6.03	0.06	6.83	-5.667	
26.2	101	8	5.49	0.07	6.04	-0.080	
26.9	103	8	6.17	0.22	7.2	-5.587	
26.9	103	8	6.21	-0.01	7.41	-5.460	
26.2	101	8	5.44	0	6.4	-4.874	
26.5	102	8	5.97	0.02	7.33	-5.043	
26	101	8	5.05	0.49	7.99	-2.476	
25.7	100	8	4.64	-0.51	7.58	-2.036	
26.3	101	8	5.84	0.5	6.44	-5.663	

26.6	102	8	5.7	-0.43	7.45	-4.363	
26.5	102	8	5.16	0.43	8.34	-2.354	
26.7	102	8	4.89	0.33	8.45	-1.685	
26.9	103	8	6.35	0.02	7.05	-6.110	
26.2	101	8	5.79	0.32	6.59	-5.410	
26.2	101	8	5.5	0.03	6.57	-4.829	
26.9	103	8	5.88	0.07	6.92	-5.266	
26.6	102	8	5.23	0.48	8.21	-2.629	
26.2	101	8	5.23	-0.05	8.31	-2.529	
26.6	102	8	5.41	0.61	8.45	-2.762	
26.475	101.75	8	5.5755	0.133	7.3395	-3.95282	Avg.
q	V_ref	Alpha	NF/SF	AF/AF2	PM/YM	Mc/4	
[psf]	[mph]	[deg]	[lbf]	[lbf]	[in-lbf]	[in-lbf]	
0.1	7	12	0.05	0.01	0.04	-0.064	
0.1	7	12	0.05	0.01	0.03	-0.074	
0.1	7	12	0.02	0.01	0.01	-0.080	
0.2	8	12	0.04	0.01	0.02	-0.063	
0.1	7	12	0.04	0.01	0	-0.083	
0.1	7	12	0.06	0.02	0.03	-0.094	
0.1	6	12	0.07	0.01	0	-0.145	
0.1	6	12	0.04	0.01	0	-0.083	
0.1	6	12	0.03	0	0	-0.062	
0.1	6	12	0.03	0	0.02	-0.042	
0.1	7	12	0.04	0	0.02	-0.063	
0.1	7	12	0.04	0.01	0.04	-0.043	
0.1	6	12	0.04	0.01	0.02	-0.063	
0.1	6	12	0.04	0.02	0.03	-0.053	
0.1	7	12	0.04	0.02	0.02	-0.063	
0.1	7	12	0.03	0.02	0.01	-0.052	
0.1	7	12	0.03	-0.01	0.02	-0.042	
0.1	6	12	0.03	0.02	0.03	-0.032	

0.1	7	12	0.02	0.01	0	-0.041	
0.1	7	12	0.04	0.01	0.03	-0.053	
0.105	6.7	12	0.039	0.01	0.0185	-0.06476	Avg.
2.5	31	12	0.54	0.06	0.62	-0.499	
2.4	31	12	0.59	0.06	0.58	-0.643	
2.6	32	12	0.55	-0.01	0.66	-0.080	
2.4	31	12	0.52	0.02	0.61	-0.468	
2.4	31	12	0.46	0.08	0.55	-0.403	
2.4	31	12	0.51	0.01	0.67	-0.387	
2.6	32	12	0.68	0	0.66	-0.749	
2.6	32	12	0.46	0.07	0.59	-0.363	
2.5	31	12	0.54	0.06	0.71	-0.409	
2.4	31	12	0.44	0.02	0.55	-0.362	
2.4	31	12	0.52	0.03	0.58	-0.498	
2.5	31	12	0.56	0.05	0.55	-0.611	
2.5	32	12	0.54	0.04	0.57	-0.549	
2.5	32	12	0.57	0	0.6	-0.581	
2.6	32	12	0.51	0.04	0.59	-0.467	
2.7	33	12	0.51	0.07	0.64	-0.417	
2.5	31	12	0.59	-0.01	0.55	-0.673	
2.5	31	12	0.44	0.05	0.59	-0.322	
2.6	32	12	0.51	0.08	0.62	-0.437	
2.4	31	12	0.53	0	0.62	-0.478	
2.5	31.45	12	0.5285	0.036	0.6055	-0.46982	Avg.
11.7	68	12	2.79	0.21	2.91	-2.872	
11.8	68	12	3.06	0.21	3.5	-2.842	
11.6	67	12	2.69	-0.01	2.49	-0.080	
12.1	69	12	2.81	0.11	2.99	-2.834	
11.7	68	12	3.31	0.22	3.18	-3.680	

11.8	68	12	2.54	0.21	3.05	-2.214	
12	68	12	2.66	0.02	3.41	-2.103	
11.8	68	12	3.24	0.14	3.09	-3.625	
11.7	68	12	2.95	0.1	2.68	-3.434	
11.8	68	12	2.34	0.03	3.24	-1.610	
12.1	69	12	2.78	0.21	3.03	-2.732	
11.8	68	12	3.12	-0.18	3.76	-2.706	
11.8	68	12	2.7	0.07	2.09	-3.506	
11.9	68	12	3.2	0.19	2.95	-3.682	
11.9	68	12	3.35	0.13	3.11	-3.833	
11.7	68	12	2.84	0.15	3.75	-2.136	
11.8	68	12	2.67	-0.04	3.74	-1.794	
11.7	68	12	2.8	0.2	3.58	-2.223	
12.3	69	12	3.06	0.12	3.68	-2.662	
11.8	68	12	2.72	0.22	2.88	-2.757	
11.84	68.1	12	2.8815	0.1155	3.1555	-2.66616	Avg.
26.7	102	11.9	6.79	-0.68	8.63	-5.442	
26.1	101	11.9	6.84	0.07	7.03	-7.146	
26	101	11.9	7.04	0.13	9.19	-0.080	
27.1	103	11.9	7.05	0.45	7.19	-7.421	
27.4	104	11.9	8.34	-0.44	8.33	-8.955	
26.2	101	11.9	7.37	1.2	8.41	-6.864	
27.2	103	11.9	7.51	0.94	9.72	-5.844	
26.3	102	11.9	6.63	-0.34	5.75	-7.991	
25.9	101	11.9	7.05	0	7.97	-6.641	
25.7	100	11.9	7.05	0.69	9.62	-4.991	
26.5	102	11.9	6.3	1.01	8.91	-4.147	
25.6	100	11.9	6.67	-0.27	7.34	-6.484	
27.9	104	11.9	6.91	0.27	8.96	-5.361	
26.9	103	11.9	7.22	-0.3	9.83	-5.133	

27.4	103	11.9	7.22	0.83	8.74	-6.223	
27.2	103	11.9	7.22	-1.14	8.51	-6.453	
28.6	106	11.9	7.53	0.35	9.14	-6.466	
26.4	102	11.9	6.59	-0.32	8.9	-4.758	
27.3	103	11.9	6.74	0.51	8.34	-5.629	
27	103	11.9	6.66	0.02	6.31	-7.493	
26.77	102.35	11.9	7.0365	0.149	8.341	-5.97613	Avg.
q	V_ref	Alpha	NF/SF	AF/AF2	PM/YM	Mc/4	
[psf]	[mph]	[deg]	[lbf]	[lbf]	[in-lbf]	[in-lbf]	
0.1	7	16	0.01	0.01	0.02	-0.001	
0.1	7	16	0.05	0.01	0.02	-0.084	
0.2	8	16	0.02	0.02	0.03	-0.080	
0.1	7	16	0.04	0.02	0.02	-0.063	
0.1	7	16	0.01	0.01	0	-0.021	
0.1	7	16	0.03	0.01	-0.01	-0.072	
0.2	8	16	0.03	0.01	0.03	-0.032	
0.1	7	16	0.02	0.01	0.03	-0.011	
0.1	8	16	0.03	0.02	0.02	-0.042	
0.1	7	16	0.03	0.01	0.01	-0.052	
0.1	7	16	0.03	0.01	0.01	-0.052	
0.1	7	16	0.03	0.02	0.03	-0.032	
0.1	7	16	0.04	0.01	0.04	-0.043	
0.2	8	16	0.01	0.01	0.01	-0.011	
0.1	7	16	0.03	0.01	0.01	-0.052	
0.1	6	16	0.03	0.01	0.03	-0.032	
0.1	7	16	0	0.01	0.03	0.030	
0.1	7	16	0.02	0.02	0.03	-0.011	
0.1	7	16	0	0.01	0.02	0.020	
0.1	7	16	0.01	0.01	0.01	-0.011	
0.115	7.15	16	0.0235	0.0125	0.0195	-0.03263	Avg.

2.5	31	16	0.61	0.01	0.66	-0.604	
2.2	30	16	0.56	0.03	0.55	-0.611	
2.3	30	16	0.59	-0.01	0.65	-0.080	
2.2	30	16	0.6	0	0.63	-0.614	
2.4	31	16	0.54	0.04	0.63	-0.489	
2.5	31	16	0.53	0.03	0.66	-0.438	
2.5	31	16	0.59	-0.03	0.62	-0.603	
2.3	30	16	0.61	0.01	0.67	-0.594	
2.3	30	16	0.48	0.05	0.54	-0.455	
2.4	31	16	0.53	0.04	0.6	-0.498	
2.5	32	16	0.57	0	0.7	-0.481	
2.4	30	16	0.53	0.01	0.59	-0.508	
2.5	31	16	0.59	0.04	0.63	-0.593	
2.3	30	16	0.54	0.04	0.62	-0.499	
2.4	31	16	0.56	-0.01	0.63	-0.531	
2.5	31	16	0.53	0	0.65	-0.448	
2.5	31	16	0.53	0.05	0.66	-0.438	
2.5	31	16	0.61	0	0.73	-0.534	
2.3	30	16	0.55	0.04	0.57	-0.570	
2.4	30	16	0.55	0.06	0.65	-0.490	
2.395	30.6	16	0.56	0.02	0.632	-0.50396	Avg.
11.5	67	15.9	2.66	0.08	3.24	-2.273	
11.9	68	15.9	2.72	0.11	3.11	-2.527	
11.9	68	15.9	2.74	0.09	3.17	-0.080	
11.9	68	15.9	2.75	0.07	3.19	-2.509	
12	69	15.9	2.83	0.06	3.39	-2.475	
11.8	68	15.9	2.67	0	3.17	-2.364	
11.8	68	15.9	2.74	0.08	3.2	-2.479	
11.9	68	15.9	2.41	0.1	2.97	-2.025	
11.6	67	15.9	2.66	0.07	3.05	-2.463	

11.8	68	15.9	2.61	0.1	3.06	-2.349	
12.1	69	15.9	2.61	0.02	3.1	-2.309	
11.9	68	15.9	2.55	0.16	3.17	-2.115	
12.1	69	15.9	2.87	0.01	3.16	-2.788	
12.1	69	15.9	2.81	0.09	3.15	-2.674	
12	69	15.9	2.72	0.05	3.31	-2.327	
12	69	15.9	2.64	0.1	3.3	-2.171	
12.1	69	15.9	2.82	0.01	3.19	-2.654	
11.8	68	15.9	2.73	0.05	3.19	-2.468	
12.1	69	15.9	3	0.18	3.49	-2.728	
11.9	68	15.9	2.82	0.07	3.49	-2.354	
11.91	68.3	15.9	2.718	0.075	3.205	-2.30662	Avg.
27.5	104	15.9	8.9	-0.36	11.71	-6.735	
26.7	102	15.9	10.3	0.29	10.21	-11.137	
28.3	105	15.9	10.96	-0.01	12.85	-0.080	
27.7	104	15.9	8.36	-0.45	12.11	-5.216	
26.5	102	15.9	9.25	-0.38	12.92	-6.251	
26.1	101	15.9	10.22	-1	12.05	-9.131	
26	101	15.9	10.05	-0.29	14.5	-6.329	
26	101	15.9	8.82	-0.91	8.26	-10.019	
28.6	106	15.9	10.63	-0.41	13.27	-8.761	
27.9	104	15.9	9.48	-0.44	8.34	-11.307	
27.9	104	15.9	11.09	-0.6	13.44	-9.544	
26.6	102	15.9	7.96	-0.27	11.35	-5.147	
26.8	102	15.9	11.27	-0.58	10.41	-12.947	
26.4	102	15.9	8.93	0.04	9.18	-9.327	
25.6	100	15.9	9.32	-0.53	10.72	-8.596	
26	101	15.9	9.01	0.44	12.93	-5.743	
26.4	102	15.9	8.62	-0.62	9.15	-8.715	
28.5	106	15.9	10.24	-0.81	8.94	-12.282	

28.1	105	15.9	11.83	0.54	10.78	-13.738	
27.3	103	15.9	11.34	0.28	12.51	-10.992	
27.045	102.85	15.9	9.829	-0.3035	11.2815	-8.59987	Avg.

3D Wing Calculations

Angle of Attack (deg) V = 6 MPH	q	NF/SF	AF/AF2	PM/YM		Sin	Cos	Tan
	[psf]	[lbf]	[lbf]	[in-lbf]	-4	-0.06976	0.99756	-0.06993
-4	0.1	-0.0295	-0.003	-0.015	-3	-0.05234	0.99863	-0.05241
0	0.1	-0.0065	0.007	0.006	-2	-0.03490	0.99939	-0.03492
4	0.11	-0.005	0	0.009	-1	-0.01745	0.99985	-0.01746
8	0.12	0.031	0.011	-0.004	0	0.00000	1.00000	0.00000
12	0.105	0.039	0.01	0.0185	1	0.01745	0.99985	0.01746
1	0.	0.0	0.0	0.0	2	0.034	0.9	0.0

Angle of Attack (deg) V = 6 MPH	Lift (lb)	Drag (lb)	C_L	C_D
-4	-0.02964	-0.00093	-1.23	-0.039
0	-0.0065	0.007	-0.27	0.292
4	-0.0499	-0.0035	-0.19	-0.013
8	0.029167	0.015207	1.01	0.528
12	0.036069	0.01789	1.43	0.710
1	0.0	0.0	0.	0.

Angle of Attack (deg)	6.5 MPH	30 MPH	68 MPH	102 MPH
-4	-0.03895	0.036659	0.035407	0.034165
0	0.291646	0.052413	0.046389	0.05317
4	-0.01321	0.080175	0.082557	0.075841
8	0.527993	0.109417	0.143553	0.142839
12	0.709871	0.241807	0.250571	0.250374
1	0.6	0.3	0.2	0.3

	6	115	235	125	195		90	9939	3492		6	19144	18493	669	670		6	69997	01965	87299	72422
								0.9986	0.0524											
						3	34	3	1											
								0.9975	0.0699											
V = 30 MPH							0.069	6	3	V = 30 MPH										
						4	76	0.9962	0.0874											
							0.087													
						5	16	0	9											
		2.41	0.0815		0.0295			0.9945	0.1051			0.0831	0.0212	0.14	0.03					
	-4	5	5	0.027	5	6	0.104	2	0		-4	85	49	4	7					
		2.34	0.229	0.029			53	0.9	0.1					0.4	0.05					
	0	5	5	5	0.241	7	0.121	925	227			0.2	0.0							
		2.		0.0	0.4		87	5	9		0	295	295	1	2					
		37	0.3	20	71			0.9	0.1			0.3	0.0	0.	0.					
Angle of Attack (deg)	4	5	62	5	5	8	0.139	902	495	Angle of Attack (deg)		596	457	6	08					
				-			17	7	4		4	88	03	3	0					
								0.9	0.1			0.4	0.0	0.	0.					
		2.	0.4	0.0	0.6		0.156	876	583			737	635	8	10					
	8	42	78	03	06	9	43	9	8		8	66	54	2	9					
			0.5		0.6			0.9	0.1			0.5	0.1	0.	0.					
	1	2.	28	0.0	05	1	0.173	848	763		1	094	450	8	24					
	2	5	5	36	5	0	65	1	3		2	66	95	5	2					
		2.						0.9	0.1			0.5	0.1	0.	0.					
	1	39	0.5	0.0	0.6	1	0.190	816	943		1	327	735	9	30					
	6	5	6	2	32	1	81	3	8		6	94	82	3	2					
								0.9	0.2											
						1	0.207	781	125											
						2	91	5	6											
V = 68 MPH						1	0.224	0.9	0.2	V = 68 MPH										
						3	95	743	308											

Angle of Attack (deg)										
								7	7	
								0.9	0.2	
						1	0.241	703	493	
						4	92	0	3	
		12	0.4	0.1				0.9	0.2	
		.0	12	31	0.0	1	0.258	659	679	
	-4	5	5	5	72	5	82	3	5	
		11		0.1	1.2			0.9	0.2	
		.9	1.1	33	79	1	0.275	612	867	
	0	9	49	5	5	6	64	6	5	
		11	1.8		2.3					
		.8	24	0.1	71					
	4	1	5	07	5					
		11			3.1					
		.9	2.4	0.0	32					
	8	4	01	78	5					
		11	2.8	0.1	3.1		Planfo	34.		
	1	.8	81	15	55		rm	562	in^	
	2	4	5	5	5		Area:	5	2	
		11						0.2		
	1	.9	2.7	0.0	3.2			400	ft^	
	6	1	18	75	05			17	2	

V =
102
MPH

Angle of Attack (deg)					
		26	0.9		0.2
		.7	89	0.2	66
	-4	4	5	89	5
		26		0.3	
		.9	2.7	44	3.1
	0	95	03	5	86
	4	26	4.1	0.1	5.5

Angle of Attack (deg)					
		0.4	0.1	0.	0.
		206	024	1	03
	-4	68	05	5	5
				0.	0.
		1.1	0.1	4	04
	0	49	335	0	6
		1.8	0.2	0.	0.
		125	340	6	08
	4	91	16	4	3
		2.3	0.4	0.	0.
		667	113	8	14
	8	78	95	3	4
		2.7	0.7	0.	0.
	1	945	120	9	25
	2	2	75	8	1
		2.5	0.8	0.	0.
	1	920	212	9	28
	6	37	76	1	7

V =
102
MPH

Angle of Attack (deg)					
		1.0	0.2	0.	0.
		072	192	1	03
	-4	49	72	6	4
				0.	0.
		2.7	0.3	4	05
	0	03	445	2	3
	4	4.1	0.4	0.	0.

		.4	92	89	93
		5		5	5
		26	5.5		7.3
		.4	75	0.1	39
	8	75	5	33	5
		26	7.0		
	1	.7	36	0.1	8.3
	2	7	5	49	41
				-	
		27		0.3	11.
	1	.0	9.8	03	28
	6	45	29	5	15

		685	814	6	07
		69	72	6	6
		5.5	0.9	0.	0.
		027	076	8	14
	8	29	65	7	3
		6.8	1.6	1.	0.
	1	517	087	0	25
	2	6	17	7	0
			2.4	1.	0.
	1	9.5	174	4	37
	6	319	93	7	2

V = 6 MPH

Angle of Attack (deg)	q [psf]	Mc/4 [in-lbf]	Mc/4 [ft-lbf]	M' lbf	$c_{m1/4}$
-4	0.1	0.048	0.004	0.0048	0.000041
0	0.1	0.015	0.001	0.0016	0.000013
4	0.11	0.014	0.001	0.0014	0.000013
8	0.12	-0.065	-0.005	-0.0066	-0.000067
12	0.105	-0.065	-0.005	-0.0066	-0.000059
16	0.115	-0.033	-0.003	-0.0033	-0.000032

V = 30 MPH

Angle of Attack (deg)					
-4	2.415	-0.139	-0.012	-0.0141	-0.002900
0	2.345	-0.228	-0.019	-0.0231	-0.004605
4	2.375	-0.266	-0.022	-0.0269	-

						0.005437
	8	2.42	-0.368	-0.031	-0.0373	-0.007670
	12	2.5	-0.470	-0.039	-0.0476	-0.010118
	16	2.395	-0.504	-0.042	-0.0510	-0.010398

V = 68 MPH

Angle of Attack (deg)						
	-4	12.05	-0.752	-0.063	-0.0761	-0.078025
	0	11.99	-1.041	-0.087	-0.1055	-0.107563
	4	11.81	-1.369	-0.114	-0.1387	-0.139299
	8	11.94	-1.780	-0.148	-0.1803	-0.183120
	12	11.84	-2.666	-0.222	-0.2700	-0.271941
	16	11.91	-2.307	-0.192	-0.2336	-0.236660

V = 102 MPH

Angle of Attack (deg)						
	-4	26.74	-0.991	-0.083	-0.1003	-0.228245
	0	26.995	-2.302	-0.192	-0.2331	-0.535245
	4	26.45	-2.973	-0.248	-0.3010	-0.677319
	8	26.475	-3.953	-0.329	-0.4003	-0.901529

	12	26.77	-5.976	-0.498	-0.6052	-1.378176
	16	27.045	-8.600	-0.717	-0.8709	-2.003621